

STATUS OF THESIS

Title of thesis

Synthesis of Optimal Enterprise Networks between Bio-refinery
and Petroleum Refinery

I

MAHMOUD AHMED MUSAAD ELHADI

hereby allow my thesis to be placed at the Information Resource Center (IRC) of
Universiti Teknologi PETRONAS (UTP) with the following conditions:

1. The thesis becomes the property of UTP thesis for academic purposes only.
2. This thesis is classified as

Confidential

Non-confidential

If this thesis is confidential, please state the reason:

The contents of the thesis will remain confidential for _____ years.

Remarks on disclosure:

Endorsed by

Signature of Author

Signature of Supervisor

Permanent address: Dep. of Chem.
Eng., Gazira University, Madani,

SUDAN

Name of Supervisor
Assoc. Prof. Dr. Shuhaimi Mahadzir

Date : 21-04-2014

Date : 21-04-2014

UNIVERSITI TEKNOLOGI PETRONAS
SYNTHESIS OF OPTIMAL ENTERPRISE NETWORKS BETWEEN BIO-
REFINERY AND PETROLEUM REFINERY

by

MAHMOUD AHMED MUSAAD ELHADI

The undersigned certify that they have read, and recommend to the Postgraduate Studies Programme for acceptance this thesis for the fulfillment of the requirements for the degree stated.

Signature:

Main Supervisor:

Assoc. Prof. Dr. Shuhaimi Mahadzir

Signature:

Co-Supervisor:

Dr. Usama Eldemerdash

Signature:

Head of Department:

Assoc. Prof. Dr. Suriati Bt Sufian

Date:

21-04-2014

SYNTHESIS OF OPTIMAL ENTERPRISE NETWORKS BETWEEN BIO-
REFINERY AND PETROLEUM REFINERY

by

MAHMOUD AHMED MUSAAD ELHADI

A Thesis

Submitted to the Postgraduate Studies Programme

as a Requirement for the Degree of

DOCTOR OF PHILOSOPHY
DEPARTMENT OF CHEMICAL ENGINEERING
UNIVERSITI TEKNOLOGI PETRONAS
BANDAR SERI ISKANDAR,
PERAK

APRIL 2014

DECLARATION OF THESIS

Title of thesis

Synthesis of Optimal Enterprise Networks between Bio-Refinery
and Petroleum Refinery

I MAHMOUD AHMED MUSAAD ELHADI

hereby declare that the thesis is based on my original work except for quotations and citations which have been duly acknowledged. I also declare that it has not been previously or concurrently submitted for any other degree at UTP or other institutions.

Witnessed by

Signature of Author

Signature of Supervisor

Permanent address: Dept of Chem
Eng, Gazira University, Madani,
SUDAN

Name of Supervisor
Assoc. Prof. Dr. Shuhaimi Mahadzir

Date : 21-04-2014

Date : 21-04-2014

DEDICATION

Dedicated to my parents,
my wonderful wife Sara
my loving son...Ahmed
and my loving daughter...Shaza

ACKNOWLEDGEMENTS

First and foremost, I would like to thank Allah, for without his consent, it would be impossible to achieve what had been done in this work. And I would like to thank my parents, my wife and all of my family members for their endless support, love and encouragement.

I would like to express my most sincere gratitude to my supervisor Assoc. Prof. Dr. Shuhaimi B Mahadzir and my co-supervisor Assoc. Prof. Dr. Usama Eldemerdash for their guidance, patience and supervision of this research work. Without their guidance, I believe this research would not have been completed. I genuinely appreciate all the discussions we had which did help me all the way through, for which I am extremely grateful.

Last not least, I want to thanks Universiti Tecknologi PETRONAS for the financial support through GA scheme.

ABSTRACT

The production of transportation fuels from the conversion of biomass into gasoline and diesel in a bio-refinery is an attractive, clean, carbon neutral and sustainable process. The economics of standalone bio-refinery can be improved via integration with an existing petroleum refinery, whereby bio-refinery intermediates can be upgraded using the existing petroleum refinery infrastructure. The current literature considered only limited materials integration between bio-refinery and petroleum refinery. In this work, an efficient mathematical modeling approach for synthesizing optimum enterprise networks between bio-refinery and petroleum refinery is proposed for the utilization of materials and hydrogen across the enterprise. Two different models are formulated and then integrated. Firstly, a superstructure-based MINLP model for the synthesis of an enterprise plant network was developed for the optimum utilization of materials between bio-refinery and petroleum refinery. Secondly, an integrated MINLP model comprising materials-processing and hydrogen management is developed for synthesizing an optimum hydrogen network to meet the requirement of the enterprise plant. The models performances were tested on a literature based case studies of pyrolysis-based bio-refinery, existing petroleum refinery and enterprise plant network superstructure between bio-refinery and petroleum refinery. The studies have shown that the enterprise plant is a more economically attractive solution than installing a new standalone bio-refinery. The optimum enterprise plant network achieved \$58 MM/y higher profit compared to the combined profits of the stand-alone bio-refinery and petroleum refinery plants. Furthermore, the optimum enterprise plant hydrogen network achieved 18.5% and 5% reduction in operating and capital costs, respectively. Linearization techniques are also developed to transform the integrated MINLP model into MILP model. The linearized MILP model achieved 92% and 85% savings in the number of iteration and CPU time, respectively, compared to the original MINLP model.

ABSTRAK

Pengeluaran bahan api pengangkutan dari pengubahan biomass ke dalam petrol dan diesel dalam bio- penapisan adalah menarik, bersih, karbon proses yang neutral dan mampan. Ekonomi daripada berdiri bio- penapisan boleh diperbaiki melalui integrasi dengan kilang penapis petroleum sedia ada, di mana perantaraan bio- penapisan boleh dinaik taraf dengan menggunakan infrastruktur penapisan petroleum yang sedia ada. Kesusasteraan semasa dianggap integrasi hanya bahan-bahan terhad antara bio- penapisan dan penapisan petroleum. Dalam karya ini, satu pendekatan pemodelan matematik berkesan untuk mensintesis rangkaian perusahaan optimum antara bio- kilang penapis dan kilang penapis petroleum adalah dicadangkan untuk penggunaan bahan dan hidrogen di seluruh perusahaan. Dua model yang berbeza digubal dan kemudian bersepadu. Pertama, model MINLP berdasarkan struktur - untuk sintesis rangkaian kilang perusahaan telah dibangunkan untuk penggunaan optimum bahan antara bio- penapisan dan penapisan petroleum. Yang kedua, model MINLP bersepadu yang terdiri daripada bahan-bahan pemprosesan dan hidrogen pengurusan dibangunkan untuk mensintesis rangkaian hidrogen optimum untuk memenuhi keperluan kilang perusahaan. Model persembahan telah diuji ke atas kajian kes kesusasteraan berasaskan berasaskan pirolisis - bio- penapisan, penapisan petroleum sedia ada dan perusahaan kilang rangkaian struktur antara bio- penapisan dan penapisan petroleum. Kajian telah menunjukkan bahawa tumbuhan perusahaan itu adalah penyelesaian yang lebih ekonomi yang menarik daripada memasang berdiri bio- penapisan baru. Optimum rangkaian kilang perusahaan mencapai \$ 58 MM / y keuntungan yang lebih tinggi berbanding dengan keuntungan gabungan bio- kilang penapis dan kilang penapis petroleum tumbuhan berdiri sendiri. Tambahan pula, perusahaan kilang rangkaian hidrogen optimum dicapai 18.5 % dan pengurangan 5% dalam operasi dan kos modal, masing-masing. Teknik pelelurusan juga dibangunkan untuk mengubah model MINLP bersepadu ke dalam model MILP. Model MILP dileluruskan mencapai 92% dan 85 % penjimatan dalam bilangan lelaran dan masa CPU, masing-masing, berbanding dengan model MINLP asal.

In compliance with the terms of the Copyright Act 1987 and the IP Policy of the university, the copyright of this thesis has been reassigned by the author to the legal entity of the university,

Institute of Technology PETRONAS Sdn Bhd.

Due acknowledgement shall always be made of the use of any material contained in, or derived from, this thesis.

© Mahmoud Ahmed Musaad Elhadi, 2014

Institute of Technology PETRONAS SdnBhd

All rights reserved.

TABLE OF CONTENT

ABSTRACT.....	vii
ABSTRAK.....	viii
LIST OF FIGURES.....	xiii
LIST OF TABLES	xv
CHAPTER 1 INTRODUCTION	1
1.1 Background.....	1
1.2 Bio-refinery.....	1
1.3 Overview of pyrolysis-based bio-refinery	3
1.4 Overview of Petroleum Refinery	4
1.5 Overview of Refinery Hydrogen Management.....	5
1.5.1 Hydrogen Producers	5
1.5.2 Hydrogen Consumers	6
1.5.3 Hydrogen Recovery.....	6
1.6 Bio-refinery and Petroleum Refinery Integration	6
1.7 Modeling of Enterprise Network	8
1.8 Problem Statement	9
1.9 Objectives	10
1.10 Research Contribution	10
1.11 Scope of study.....	10
1.12 Bio-refinery and petroleum refinery data	12
1.13 Organization of Thesis.....	13
CHAPTER 2 LITERATURE REVIEW	15
2.1 Introduction.....	15
2.2 Bio-oil Up-grading	15
2.3 The Environmental Impact of Bio-fuel Production	16
2.4 Integrating Bio-refinery into an Existing Petroleum Refinery	18
2.4.1 Processing Biomass-based Feedstock inside Petroleum Refinery Processing Units.....	18
2.4.2 Petroleum Refinery planning and optimization	20
2.5 Superstructure Modeling and Optimization.....	24

2.6 Hydrogen Management.....	26
2.7 Summary of Literature Review	31
CHAPTER 3 METHODOLOGY.....	34
3.1 Introduction	34
3.2 Superstructure Development	36
3.3 Modeling Materials-processing System.....	38
3.3.1 Sub-models Development	39
3.3.2 Master Model Development	43
3.3.2.1 General processing unit Model [42]	44
3.4 Development of the Integrated Model	49
3.4.1 Hydrogen Management Model.....	49
3.4.2 Integrated model	56
3.5 Model linearization	57
3.5.1 Materials-processing System Model Linearization	57
3.5.2 Linearization of Hydrogen Management Model	63
3.6 Mathematical Programming	64
3.7 Summary	67
CHAPTER 4 OPTIMIZATION USING MATERIALS-PROCESSING MODEL....	68
4.1 Introduction	68
4.2 Model Validation	68
4.3 Standalone plant optimization	70
4.4 Enterprise plant optimization	73
4.5 Sensitivity analysis	77
4.6 Summary	80
CHAPTER 5 INTEGRATED MODEL.....	81
5.1 Introduction	81
5.2 Model Validation	81
5.3 Standalone Plant Hydrogen Network Optimization	86
5.4 Enterprise Plant Hydrogen Network Optimization	93
5.5 Summary	97
CHAPTER 6 LINEARIZATION OF MODELS	98
6.1 Introduction	98

6.2 Computational Performance Analysis of the Materials-processing System	
Model	98
6.3 Computational performance analysis of the integrated model	100
6.4 Summary.....	102
CHAPTER 7 CONCLUSIONS AND FUTURE WORK	103
7.1 Conclusions.....	103
7.2 Future Work.....	104
REFERENCES	106
PUBLICATION LIST.....	116
APPENDIX A BIO-REFINERY PROCESSING UNITS	117
APPENDIX B PETROLEUM REFINERY PROCESSING UNITS	123
APPENDIX C ILLUSTRATIVE EXAMPLES	130
APPENDIX D PROCESSING UNITS' MODELS.....	136
APPENDIX E EQUIPMENT COST DETAILS	141
APPENDIX F GAMS CODE.....	149

LIST OF FIGURES

Figure 1.1: Conceptual bio-refinery [4].	2
Figure 1.2: Design case of pyrolysis-based bio-refinery [11].	3
Figure 1.3: Typical refinery flow diagram [16].	4
Figure 1.4: Superstructure representation of co-locating fast pyrolysis based bio-refinery into an existing petroleum refinery [11].	8
Figure 1.5: Petroleum refinery flowsheet used in this study [27].	12
Figure 3.1: System approach for the integration of the proposed bio-refinery into an existing petroleum refinery	35
Figure 3.2: The proposed superstructure for the integration of bio-refinery and existing petroleum refinery	37
Figure 3.3: TBP distillation curve of the crude oil used in this study [14].	39
Figure 3.4: Swing cuts of CDU fractions	41
Figure 3.5: General processing unit model [42].	44
Figure 3.6: Superstructure representation of a hydrogen network [19].	50
Figure 3.7: Simplified PSA flow diagram	54
Figure 3.8: Volume % accumulated at different cut temperature	58
Figure 3.9: °API as a function of Mid v% regions of CDU fractions	60
Figure 3.10: °API as a function of mid volume% of HN region.	60
Figure 3.11: General structure of GAMS representation.	65
Figure 4.1: Standalone fast-pyrolysis based bio-refinery [11].	72
Figure 4.2: Proposed enterprise plant network superstructure representation	74
Figure 4.3: Sensitivity analysis results: profit versus % retrofit cost reduction	77
Figure 4.4: Sensitivity analysis: profit versus % increasing and decreasing in final products prices.	80
Figure 5.1: Hydrogen distribution network [22]	82
Figure 5.2: MINLP based optimized hydrogen network	85
Figure 5.3: MINLP based optimized hydrogen network [22].	87
Figure 5.4: Optimized hydrogen network of stand-alone petroleum refinery.	89
Figure 5.5: Stand-alone bio-refinery – Optimized hydrogen distribution network.	92

Figure 5.6: Representative framework for retrofitting the standalone petroleum refinery hydrogen distribution network.....	94
Figure 5.7: Optimized hydrogen distribution network of the proposed enterprise plant	96
Figure 6.1: MILP based optimized hydrogen distribution network of the proposed enterprise pant.....	101

LIST OF TABLES

Table 1.1: Alaska crude oil assay [14].....	13
Table 1.2: Ultimate analysis of biomass [11]	13
Table 1.3: Bio-oil characterization [11].....	13
Table 2.1: Product prices, demands and quality specifications [27]	22
Table 2.2: Processing unit capacity [27].....	23
Table 2.3: The model used in this study and research gap	32
Table 3.1: Boiling range of typical crude oil fractions [15]	40
Table 3.2: Coefficients for CDU model equations (3.1) and (3.4).....	41
Table 3.3: The slope and intercept of the CDU model equations	58
Table 3.4: The slope and intercept of the CDU model equations: HN fraction.....	61
Table 4.1: Optimization results and comparison of petroleum refinery standalone plant	69
Table 4.2: Crude oil and final products prices [101].....	71
Table 4.3: Optimization results of the existing petroleum refinery stand-alone plant	71
Table 4.4: Optimization results of the bio-refinery stand-alone plant.....	72
Table 4.5: Optimization results of optimum enterprise network between bio-refinery and petroleum refinery.....	76
Table 4.6: Model results of the enterprise plant network between petroleum refinery and bio-refinery (Enterprise plant B).....	78
Table 4.7: CDU unit yields	79
Table 5.1: Hydrogen consumers' data [22].....	83
Table 5.2: Hydrogen producers' data [22].....	83
Table 5.3: Hydrogen consumption data of hydrogen consumers.....	84
Table 5.4: Optimized hydrogen networks costs breakdown.....	86
Table 5.5: Petroleum refinerystand-alone plant - Operating conditions of the processing units	88
Table 5.6: Petroleum refinery stand-alone plant – Data for hydrogen sources.....	88
Table 5.7: Petroleum refinery stand-alone plant – Data for makeup compressors	88
Table 5.8: Petroleum refinery stand-alone plant – Operating cost breakdown.....	90

Table 5.9: Stand-alone bio-refinery – Operating conditions of processing units	91
Table 5.10: Stand-alone bio-refinery – Data for hydrogen sources.....	91
Table 5.11: Stand-alone bio-refinery – data for makeup compressors	91
Table 5.12: Stand-alone bio-refinery – Costs breakdown.....	93
Table 5.13: Hydrogen network cost breakdown of enterprise and standalone plants .	97
Table 6.1: Comparison of computational performance between MINLP and MILP of materials-processing system model	99
Table 6.2: Comparison of computational Performance between MINLP and MILP of integrated model.....	102

NOMENCLATURES

B	Final blending units (b), $B \in I$
E	Processing unit (e) received external raw material, $E \in I$
I	Processing units (i) in the refinery, $i \in I$
W	Processing units (w) that must be installed to produce stable pyrolysis oil, $W \in I$
Z	Processing units (z) that must be installed in order to up-grade bio-refinery products into higher quality, $Z \in I$
Rt	Processing units (rt) that must be modified in order to process stable pyrolysis oil, $Rt \in I$
J	Processing units (j) that can send products to unit (i), $J \in I$
S	Product streams (s) of unit (i), $s \in S$
Ns	Streams (s) can sent from unit (j) to unit (i), $Ns \in S$
Ps	properties (ps) of stream (s)
PF	Properties (p) of feed to unit (i), $PF \in P$
Md	Processing unit (md) can received stream (s) from unit (i), $Md \in I$
Cf_i	Cost of external material (raw material) to processing unit (i)
Cx_i	Operating cost of processing unit i
Cp_i	Selling price of final product from blending pool
$TE_{CDU,s}^L$	Lower bound of the end point (cut) temperature of stream (s) from CDU unit
$TE_{CDU,s}^U$	Upper bound of the end point (cut) temperature of stream (s) from CDU unit
U_{max_i}	Maximum capacity of unit (i)
F_i	Volumetric flow rate of feed to unit (i), BPD
$FP_{i,p}$	Property (p) of feed to unit (i)
$V_{i,s}$	Volumetric flow rate of stream (s) from unit (i), BPD
$PV_{i,s,p}$	Property (p) of stream (s) from unit (i)
$XU_{i,x}$	Operating variable x of unit i

$V_{i,s,m}$	Volumetric flow rate of stream (s) splitted from product $V_{i,s}$ of unit (i) received by unit (m), BPD
y_t	Binary variable represent route selection for integrating bio-refinery into an existing petroleum refinery
y_d	Binary variable represent straight-line segment selection
H	Sources, $h \in H$
Q	Fuel system headers $q \in Q$
K	Exist compressors, $k \in K$
M	New purification units (PSA), $m \in M$
N	New compressors, $n \in N$
U	Processing units (hydrogen consumer), $u \in U$
UP,LP	Upper and lower bounds of pressure difference
UF,LF	Upper and lower bounds of flow rate
P	Pressure (psi), for u, k, q, h
$F_{max,k}$	Maximum compressor flow rate, for k
$UPwr$	Upper bound of compressor power
$y_{prod,m}$	Purity of PSA product streams
Rec	Recovery factor for PSA unit
C_{H2}	Operating cost of hydrogen production (\$/MMSCF)
C_{Elc}	Operating cost of electricity, compressors power (\$/KWh)
CRF	Operating credit of fuel gas, gained by heating (\$/MMBTU)
LHV	Low heating value of fuel gas
OD	Operating days per year
AF	Annualizing factor
a, b	Capital cost function constants, for n, m
F	Flow rate (MMSCFD)
y	Stream purity (hydrogen content %)
$cons_u$	Hydrogen consumption of processing unit (u)
R	Recycle streams
PG	Purge streams
PI	Inlet pressure of new compressors and PSA, for n, m

<i>PO</i>	Outlet pressure of new compressors and PSA, for <i>n, m</i>
<i>Pwr</i>	Compressor power
TAC	Total annual cost
<i>OC</i>	Operating cost
<i>Cap</i>	Capital cost of new compressors and PSA, for <i>n, m</i>
<i>X</i>	Existence of new equipments (NC and PSA)
<i>xf</i>	Existence of flow rate streams

ABBREVIATIONS

THN	Treated heavy naphtha
N	Naphtha from hydrotreating units
TDSL	Treated diesel
KDHT	Kerosene from diesel hydrotreating unit
LN FCC	Light naphtha from FCC
LCO FCC	Light cycle oil from FCC
HCO FCC	Heavy cycle oil from FCC
DOHT	Diesel from gas oil hydrotreater
LNHC	Light naphtha from hydrocracker
KHC	Kerosene from hydrotreater
DHC	Diesel from hydrotreater
DRDHT	Diesel from residual hydrotreater
LSFO	low sulfur fuel oil
RefBCR	Reformate from bio-refinery catalytic reforming unit
LTNBHC	Light naphtha from bio-refinery hydrocracking unit
DBHC	Diesel from bio-refinery hydrocracking unit

GASO	Petroleum refinery gasoline pool
GASOB	Bio-refinery gasoline pool
LSDSL	Petroleum refinery Low sulfur diesel pool
LSDSLB	Bio-refinery Low sulfur diesel pool
KERO	Kerosene pool
FOil	Fuel oil pool

CHAPTER 1

INTRODUCTION

1.1 Background

Energy drives human life and is essential for continued human development. Growing economies and increasing population will demand an increased energy supply in the coming years. All of the resources used for energy needs can be classified as either renewable or non-renewable. Non-renewable energy refers to energy sources such as fossil fuels that have finite availability and that cannot be practically replaced. In contrast, fuels from renewable energy resources can be replaced. This would include biomass, which can be planted, harvested and re-planted.

It is also important to note that the usages of non-renewable resources mainly contribute to the global climate change and become the cause of most air pollution. On the other hand, the renewable energy resources have no negative impact on the environment. For example, the CO₂ that is produced during the processing of biomass can be reabsorbed by the new growing plant generation. In this way the CO₂ cycle is balanced and fuels from biomass is therefore carbon neutral [1].

1.2 Bio-refinery

A bio-refinery is a chemical process facility that integrates biomass conversion processes and equipment to produce fuels, heat, power and chemicals. The bio-refinery concept is analogous to today's petroleum refinery that produces multiple fuels and other petroleum products [1, 2]. The IEA bio-energy Task 42 on bio-refineries has defined bio-refining as the sustainable processing of biomass into a spectrum of marketable products and energy [3]. The national renewable energy

laboratory (NREL) proposed a two-platform concept bio-refinery, which are the sugar platform and the thermochemical platform [2, 4]. Figure 1.1 shows a simplified illustration of a conceptual bio-refinery. Sugar platform breaks biomass down into different types of sugar components for fermentation into biogas, which is a mixture of methane and carbon dioxide. On the other hand, thermochemical platform utilizes heat energy to breakdown biomass into synthesis gas and pyrolysis oil through the process of gasification and fast pyrolysis, respectively. In the process of fast pyrolysis, biomass carbonaceous material thermally decomposes in the absence of oxygen to produce liquid bio-oil. Bio-oil is dark brown, free-flowing liquid that is rich in oxygenated hydrocarbons and contains about 25% water content, which is not easily separated [5]. Bio-oil may be used as burning oil in boilers or even as a transportation fuel after upgrading [6].

Malaysia as the world’s largest producer and exporter of palm oil has the opportunity to convert the palm oil waste into bio-oil using fast pyrolysis technology [7, 8]. The annual generation of palm oil waste in Malaysia stands at about 85 million tons in 2012 [9]. Converting this abundant quantity of waste palm oil into liquid bio-oil has

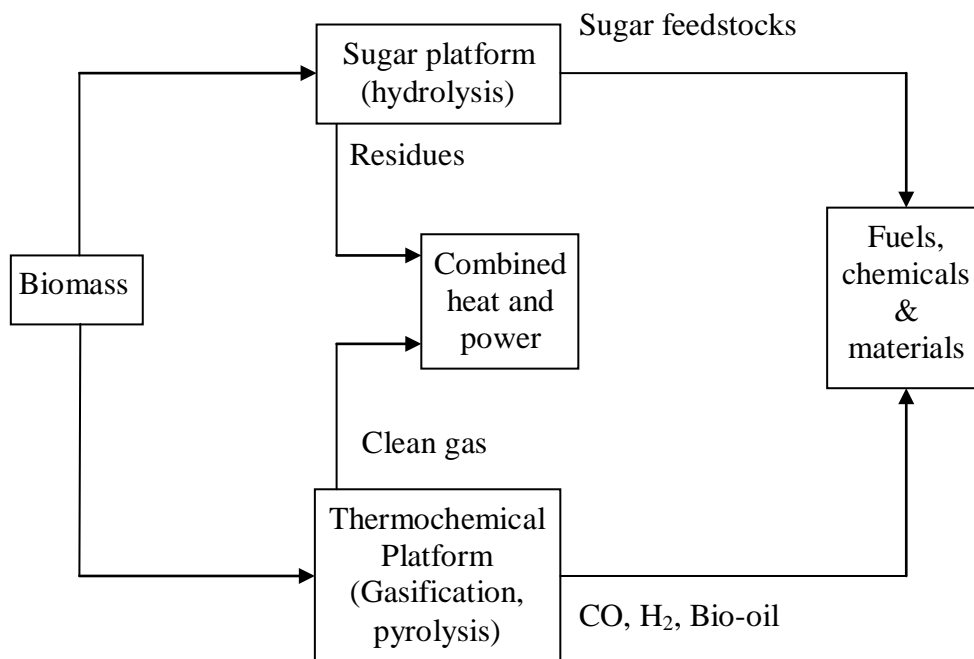


Figure 1.1: Conceptual bio-refinery [4].

the potential to substitute for 23.8 million tons/year of fuel oil leading to a CO₂ emissions reduction of about 76 million tons/year. This 76 million ton/year of CO₂ reduction is equivalent to more than 40% of 187 million tons/year of CO₂ emissions in 2005. Therefore, it carries the critical role of achieving Malaysia commitment to reduce 40% of CO₂ emissions in 2005 by 2025 as announced by the Prime Minister in Copenhagen 2009 [10].

1.3 Overview of pyrolysis-based bio-refinery

Jones et al. [11] developed a design case pyrolysis-based bio-refinery for converting biomass into gasoline and diesel fuels. The design case consists of feed pretreatment, fast pyrolysis reactor, two-stage hydrotreater, hydrocracker and hydrogen generation unit, as illustrated in Figure 1.2. This bio-refinery is designed with a capacity of 2150 metric tons/day of biomass feedstock. The feedstock is hybrid poplar wood chips delivered at 50% moisture content. This work refers to this bio-refinery as a new bio-refinery since it is not yet installed. The details of the bio-refinery processing units are shown in Appendix A. The yields of bio-refinery processing units are shown in Appendix D.

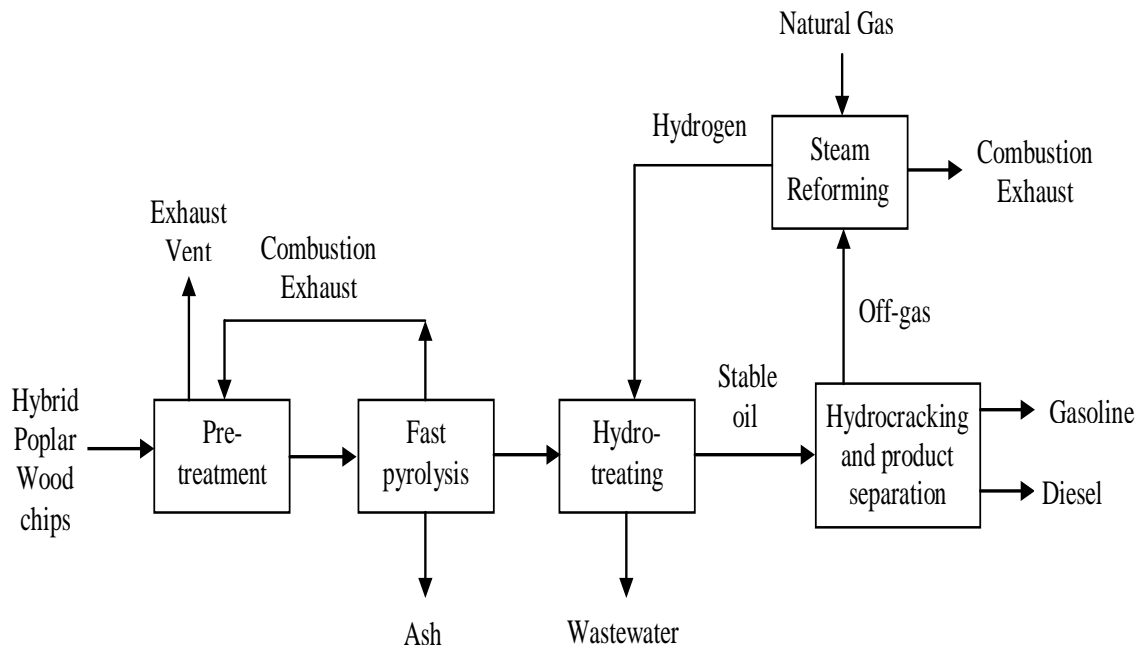


Figure 1.2: Design case of pyrolysis-based bio-refinery [11].

1.4 Overview of Petroleum Refinery

Before petroleum can be beneficially utilized, it must be refined into products with the desired properties. This occurs in petroleum refineries, where various physical and chemical methods are used to convert crude oil into a large array of useful petroleum products [12 - 17]. Figure 1.3 illustrates a typical petroleum refinery flow diagram. Petroleum refining begins with the atmospheric distillation column (ADU) and vacuum distillation column (VDU), which separate crude oil into several fractions

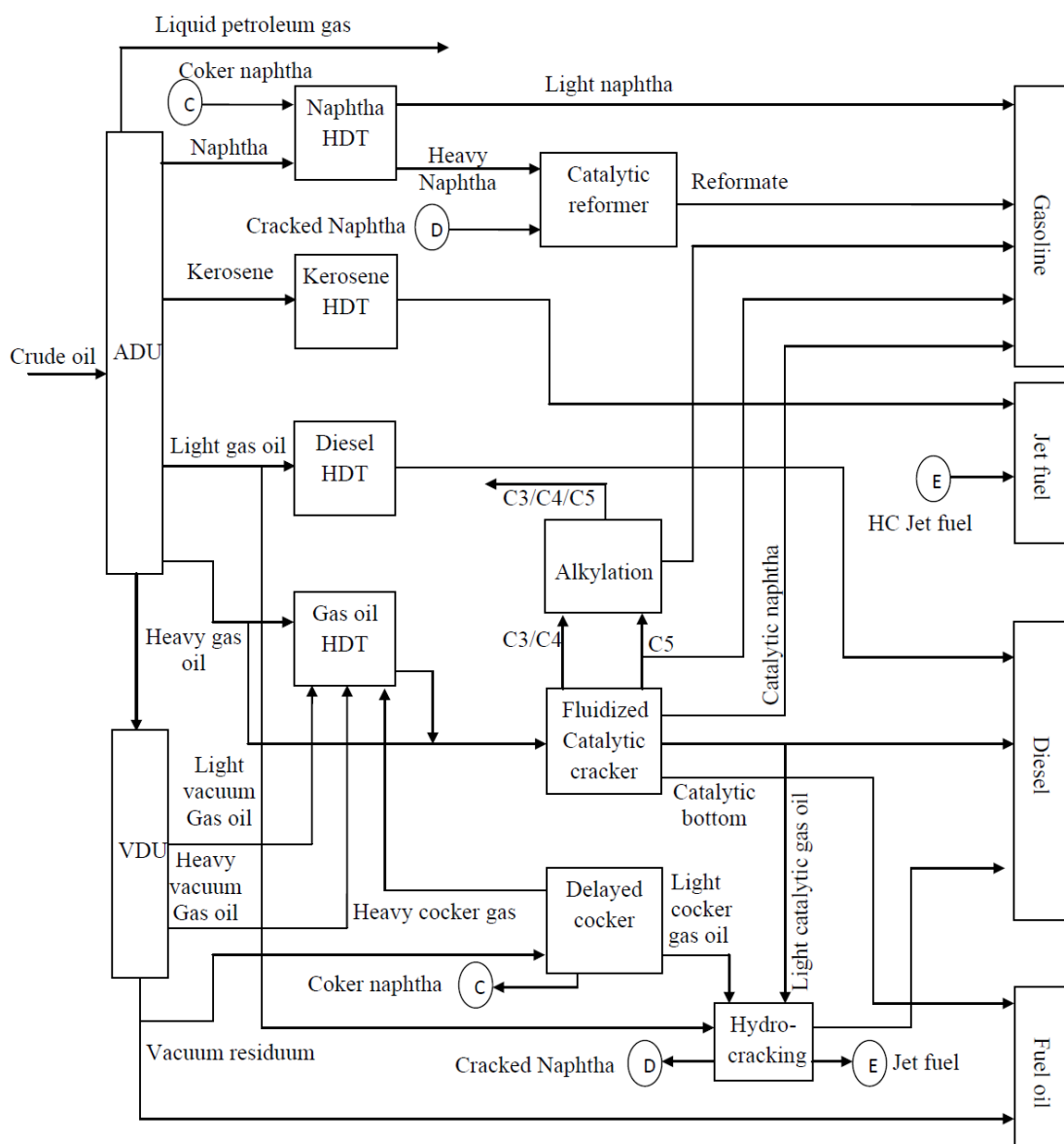


Figure 1.3: Typical refinery flow diagram [16].

such as Naphtha, Kerosene, Diesel, Vacuum gas oil and Residue. Most of these fractions are hydrotreated to remove undesirable constituents and improve product quality. Then, these products are converted into more usable products by changing the size and structure of the hydrocarbon molecules through cracking, reforming, and other conversion processes. Each petroleum refinery has its' own unique arrangement and combination, which are largely determined by the refinery location, desired products and economic considerations. There are most probably no two refineries that are identical. Refinery refining processes and operations can be classified into five basic areas, namely fractionation, conversion, hydrotreating, blending and supporting processes [12 - 17]. The details of the petroleum refinery processing units are shown in Appendix B.

1.5 Overview of Refinery Hydrogen Management

Refining industry is impacted by many factors that significantly increase hydrogen demand. First, stricter regulations on sulfur content in fuel increases the hydrogen demand in hydrotreating units. Second, processing of heavier crude oil and shrinking demand for heavy fuel is forcing the greater use of hydrocracking, hence increases the demand for hydrogen. On the other hand, stricter environmental regulations on the product specifications of low-aromatic gasoline have resulted in decreasing hydrogen produced by catalytic reformers. Hence, lowering the overall availability of hydrogen in the refinery. Therefore, it has been necessary for the petroleum refining industry to seek innovative approaches for dealing with the hydrogen balance issue [18, 19].

The hydrogen distribution system consists of three elements: hydrogen producers, hydrogen consumers and hydrogen recovery units. The interactions between these three elements define the performance of the hydrogen network in the refinery.

1.5.1 Hydrogen Producers

The primary sources of hydrogen in the refinery are hydrogen plants, catalytic reformers, and purchased hydrogen. The off gases from hydroprocessing units can be a secondary source if the hydrogen in these off gases can be used as a make-up for

other consumers or can be purified to upgrade its purity. Hydrogen plants produce hydrogen primarily by steam reforming of natural gas and hydrocarbons from off gases leaving hydroprocessing units. A Catalytic reformer is also a common unit in the petroleum refinery that produces hydrogen. During reforming of hydrocarbon molecules, a large amount of hydrogen is produced as a by-product at 70-90% purity that can be used in variety of refinery processes [20].

1.5.2 Hydrogen Consumers

Hydrotreaters and hydrocrackers are the major consumers of hydrogen in refinery. The hydrotreaters reaction consumes hydrogen in a series of reactions converting organic sulfur and nitrogen compounds to hydrogen sulfide and ammonia. Hydrocracking reactions convert heavier oils to diesel and naphtha range materials. All of these reactions increase the products' value and refinery's profit margin [21].

1.5.3 Hydrogen Recovery

Recovering hydrogen from the off gas streams of the hydroprocessing units is beneficial for the refinery because the cost of hydrogen recovery can be as low as 50% of the cost of producing hydrogen in a hydrogen plant [21]. The most common unit operations used for purifying hydrogen are pressure-swing adsorption (PSA) and membrane separation. Comparing to the membrane separation, PSA can achieve higher purity product and lower pressure drop. [22] All purification process takes in feed containing hydrogen and impurities and deliver two streams: a product stream which has high hydrogen purity and a residue with low hydrogen purity [22].

1.6 Bio-refinery and Petroleum Refinery Integration

Over the past decade, scientists have raised concerns about the sustainability of the traditional industries and how some practices may expose our future. Depletion of natural resources and greenhouse gas emissions have become a cause of concern [23, 24]. A bio-refinery can address some of these concerns because it involves the usage

of renewable resources such as biomass which is abundant, renewable and carbon neutral. Therefore, bio-refinery is regarded as an environmental-friendly alternative to produce fuels, energy and chemicals from biomass. However, the processing of biomass into transportation fuels in standalone bio-refinery processing plant is found to be unattractive economically. This is because it requires high-investment cost to be commercialized [25]. Therefore, there have been some industrial initiatives to develop a chain of process steps that will allow biomass feedstocks to be co-fed to a conventional petroleum refinery for the production of fuels and oxygenated chemicals [26]. The aim of this process is to save capital cost required for installing new up-grading unit to serve the bio-refinery as a standalone plant.

In 2009, the Pacific Northwest National Laboratory (PNNL) presented a new standalone bio-refinery plant design [11] that is capable of converting biomass into pyrolysis liquid followed by up-grading into transportation fuels, as illustrated in Figure 1.2. However, the bio-refinery's up-grading units consume large amount of hydrogen equivalent to about 7% of the total amount of pyrolysis oil products. The final bio-refinery's fuel products are also low quality characterized by the low octane number naphtha fraction and also low quality diesel fraction at low cetane number. The PNNL proposed a superstructure containing two options for the integration of a bio-refinery into an existing petroleum refinery, as shown in Figure 1.4. The superstructure can be defined as the representation that contains all feasible process options and all feasible interconnections that are candidates for an optimal design structure. From Figure 1.4, a stream of stable pyrolysis oil is fed to a petroleum refinery hydrocracking process to produce motor fuels. The off-gas from the bio-refinery's hydrotreaters is also transferred to the refinery, and in return the refinery returns hydrogen back to the hydrotreaters. This integration strategy resulted in a simple estimated savings of 37.9% in the bio-refinery initial investment cost [11]. The cost is estimated by just excluding bio-refinery hydrogen plant and hydrocracking unit from the bio-refinery initial investment cost after the integration.

Optimizing a superstructure containing many options of integrating bio-refinery and petroleum refinery may lead to optimal synthesis of an enterprise network design. In this work, the flowsheet of a conceptual bio-refinery is adopted from PNNL [11]

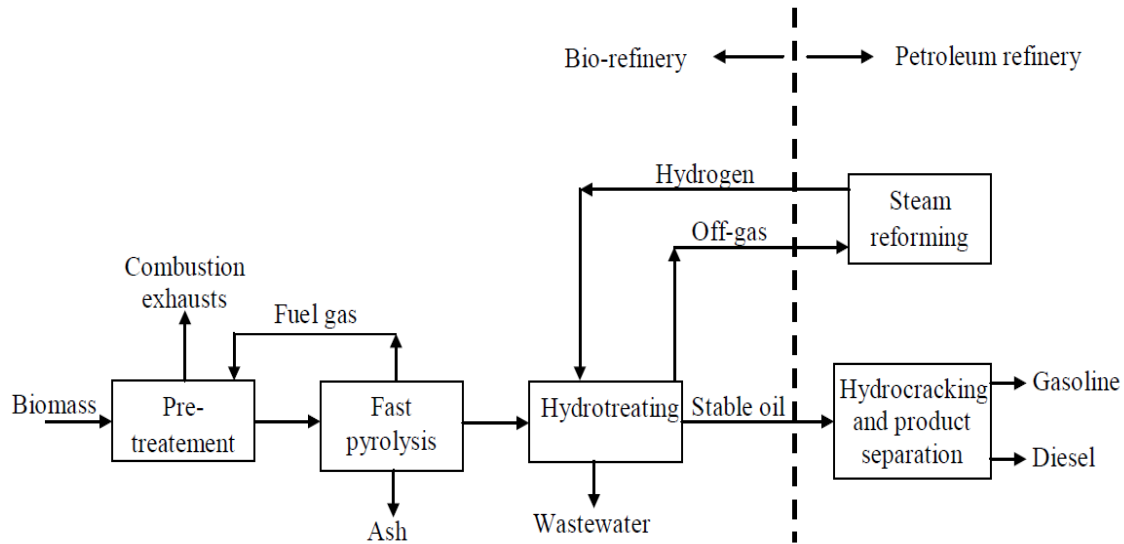


Figure 1.4: Superstructure representation of co-locating fast pyrolysis based bio-refinery into an existing petroleum refinery [11]

and the flowsheet of existing petroleum refinery is adopted from Elkamel et al. [27]. These flowsheets are only used in this study as basis case-study to demonstrate the feasibility of the mathematical programming model on the enterprise network.

1.7 Modeling of Enterprise Network

An enterprise network is the network that integrates two standalone processes or more. In this work, enterprise network refers to the network that integrates bio-refinery and petroleum refinery standalone plants. To synthesize optimal enterprise network, a superstructure that contains all feasible alternatives for the integration between bio-refinery and petroleum refinery needs to be set up and then modeled and optimized. The model should represent the streams entering and leaving the processing units of bio-refinery and petroleum refinery as well as the blending of intermediate streams to form the final products. The model constraints are mainly material balance over processing units, material balance around blending pools and hydrogen balance over processing units. Additionally, hydrogen balance over compressors and PSA units, capacity of processing units and capacity of compressors

and PSA units. As well as products demand, products quality specification and logic-based binary variables, which represent the existence of the new units as well as the synthesis of optimum enterprise network between bio-refinery and petroleum refinery. This study does not use rigorous process model, rather it uses simplified process correlations. This is because the goal is not to simulate any particular process unit or the performance of a specific catalyst, but to estimate yields and properties of processing units. For example, the yield from CDU is modeled as a function of cut temperature and the products properties are modeled as a function of mid volume %. The operating cost is modeled as a function of the quantity fed to the running unit. The capital cost is estimated using “n” exponent factor rule, which calculate the capital cost of processing unit in relations to the unit capacity.

1.8 Problem Statement

The production of transportation fuels from the conversion of biomass into gasoline and diesel in a bio-refinery is an attractive, clean, carbon neutral and sustainable process. The investment cost for the commercial application of a stand-alone bio-refinery can be reduced via integration with an existing petroleum refinery, whereby bio-refinery intermediates can be upgraded using the existing petroleum refinery infrastructure. The integration of bio-refinery and petroleum refinery is not an easy task. This is because petroleum refinery has complex operations with a large number of possible combinations in streams routing, blending compositions, products and utilities. These make the operation decision process an extremely complex problem. Therefore, the integration of bio-refinery into the petroleum refinery will further increase the complexity of the problem. Solving the problem will require a systematic approach to arrive at an optimum solution. Therefore, an efficient mathematical modeling approach is required to synthesize optimal enterprise networks between bio-refinery and petroleum refinery for the efficient utilization of materials and hydrogen across the enterprise.

1.9 Objectives

- To formulate a mathematical programming model based on a new concept of enterprise network between a pyrolysis based bio-refinery and a petroleum refinery.
- To investigate the sensitivity of optimum enterprise network solution to the changes of retrofit cost reduction and prices of final products.
- To develop a superstructure-based mathematical programming model for the synthesis of an enterprise hydrogen network.
- To improve the computational performance of the enterprise network model using linearization technique.

1.10 Research Contribution

- A systematic methodology comprising superstructure representation and mixed integer nonlinear programming (MINLP) formulation for the synthesis of an enterprise network has been developed for the optimum utilization of materials between a pyrolysis-based bio-refinery and petroleum refinery.
- An integrated model consisting of hydrogen management model and materials-processing system model has been developed for synthesizing an optimum hydrogen network to meet the hydrogen requirement of the enterprise plant.
- Linearization techniques have been developed to transform MINLP problem into mixed integer linear programming (MILP) problem that resulted in a superior computational efficiency.
- Integration of a new pyrolysis-based bio-refinery into petroleum refinery is shown to be more economically attractive than building a standalone bio-refinery.

1.11 Scope of study

This research mainly focuses on introducing a systematic methodology to synthesize optimal enterprise networks between a pyrolysis-based bio-refinery and petroleum

refinery for the efficient utilization of materials and hydrogen across the enterprise. The materials and hydrogen networks have been formulated as MINLP problems. The formulation comprises simplified processing unit's models and logic based binary variables. The processing unit's models are focused on the calculations of the products yields, properties and hydrogen consumption, while the logic based binary variables are introduced to synthesize optimal enterprise networks between bio-refinery and petroleum refinery as well as representing the existence of new equipment and the existence of gas flow from any hydrogen source to hydrogen sink. The CDU is modeled by fitting the crude oil assay data using polynomial regression, while the other processing units that process pure crude oil based feedstock are modeled using simplified process correlations. The processing unit that process biomass based feed stock are modeled using linear yields. The investment cost of the processing units is modeled as a function of the inlet flow rate of the processing unit. Solving an MINLP problem requires a large amount of computational effort and might result in inconsistency in the solution quality. Therefore, new linearization techniques have been introduced to transform MINLP problems into MILP problems which are easy to solve.

Sensitivity analysis with respect to the prices of the final products and retrofit cost of petroleum refinery processing units has been considered to analyze the impact on the synthesis of optimal enterprise network between bio-refinery and petroleum refinery.

The following general assumptions are related to the models.

- i. Hydrogen streams are represented by a binary mixture of hydrogen and methane.
- ii. The retrofit cost of modifying the existing petroleum refinery processing unit to process bio-refinery intermediate product is assumed to be equal to the cost of a small petroleum refinery processing units dedicated to process bio-refinery intermediate products.

The benefit of integration between a bio-refinery and a petroleum refinery is the potential to reduce the initial investment cost of bio-refinery by utilizing the existing process infrastructure of an existing petroleum refinery. Furthermore, the petroleum

refinery can save some operating cost by sharing the off-gas streams vented from bio-refinery pressure swing adsorption (PSA) unit.

1.12 Bio-refinery and petroleum refinery data

The goal of this work is to synthesize optimum enterprise networks between a new bio-refinery and an existing petroleum refinery for the efficient utilization of materials and hydrogen across the enterprise. The petroleum refinery flowsheet is adopted from the work done by Elkamel et al. [27] and shown in Figure 1.5. This refinery flowsheet is assumed to be representing an existing petroleum refinery. Table 1.1 shows an assay of the crude oil used in this study. The flowsheet of the new bio-refinery is adopted from PNNL [11]. The ultimate analysis of bio-refinery feedstock is shown in Table 1.2 and the characterization of the bio-oil product is shown in Table 1.3.

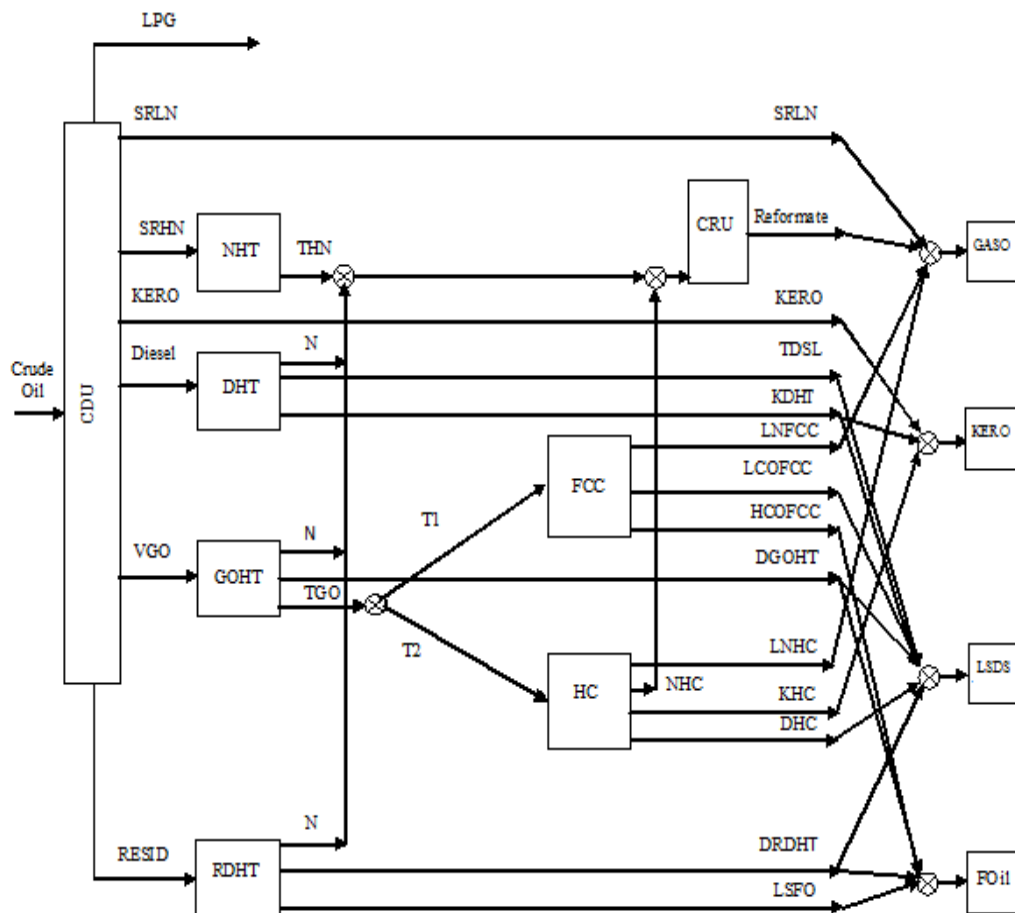


Figure 1.5: Petroleum refinery flowsheet used in this study [27].

Table 1.1: Alaska crude oil assay [14]

Cut T (°F)	160	220	300	360	450	525	650	1050	1300
Yield%	2.78	2.86	5.29	5.09	9.37	7.82	12.57	35.99	17.28
API	79.4	57.4	54.5	48.1	41.1	35.3	29.1	20.2	6
S%	0.002	0.0026	0.0064	0.038	0.19	0.4	0.64	1.21	2.93
N2%	0	0	0	0.003	0.002	0.0057	0.0221	0.166	0.657

Table 1.2: Ultimate analysis of biomass [11]

component	wt%, dry basis
Carbon	50.60
Hydrogen	6.08
Oxygen	40.75
Nitrogen	0.61
Sulfur	0.02
Chlorine	0.01
Ash	1.93

Table 1.3: Bio-oil characterization [11]

composition	wt%
Water	21
Carbon	58
Hydrogen	6
Oxygen	36

1.13 Organization of Thesis

The organization of this thesis is as follows:

Chapter 1 provides an overview of pyrolysis-based bio-refinery, petroleum refinery and hydrogen management, as well as providing the motivation for this study.

Besides, it states the problem statement, objectives of study, research contributions, scope of study and organization of the thesis.

Chapter 2 presents a review of previous studies related to the thesis topics: petroleum refinery, pyrolysis-based bio-refinery and hydrogen management.

Chapter 3 describes the development of the superstructure representation for the synthesizing of an enterprise network between pyrolysis based bio-refinery and petroleum refinery. This chapter also presents the development of enterprise networks models namely, materials-processing system model and hydrogen management model. In addition, this chapter presented new linearization techniques to improve the computational performance of the MINLP models.

Chapter 4 focuses on the application of the materials-processing system model using literature based case studies. In this chapter the performance of the enterprise plant is investigated and compared to the performance of the standalone plants.

Chapter 5 describes the application of the integrated model using literature based case studies. In this chapter the performance of the enterprise plant hydrogen network is investigated and compared to the performance of the standalone plants hydrogen networks.

Chapter 6 addresses on the computational performance of the MINLP and MILP of the materials-processing system model and the integrated model.

Chapter 7 gives the conclusions gained from this research and exploring the potential areas for future work.

CHAPTER 2

LITERATURE REVIEW

2.1 Introduction

The initial interest in green energy from biomass followed the sudden spike of crude oil price during OPEC energy crisis in the 1970s. Many of the original ideas to address the energy crisis then were not commercially pursued because of the subsequent decline in oil prices after mid-1980's [28, 29]. Recently however, with the increasing attention to global warming due to green house gas (GHG) emissions, the interest in biomass energy has gained momentum again.

Biomass provides naturally abundant resources that are low-cost, renewable and sustainable. It has an incredible potential to not only fulfill the energy and chemical needs of society, but also minimizes environmental impact [30, 31]. The reason is biomass energy is carbon neutral.

The common way to capture energy from biomass is to burn it to produce heat. However, the most efficient and cleaner way to use biomass is to convert it into liquid or gases fuels in a bio-refinery [32].

2.2 Bio-oil Up-grading

Bio-oil is a complex mixture of oxygenated compounds that is not miscible with any conventional hydrocarbon-base fuel [33]. In addition, bio-oil is unstable for long-term storage due to the potential oxygenation which leads to polymerization and significant increase of viscosity. Bio-oil can be stabilized and converted to a conventional hydrocarbon fuel by removing the oxygen through hydrotreating [11]. Hydrotreating to remove impurities such as sulfur and nitrogen from hydrocarbons is a common and

well established refinery process. The application of this technology for bio-oil upgrading was found to produce heavy tar product due to the polymerization of bio-oil at high temperature condition. The heavy tar production leads to plugging of the reactor system and fouling of the catalyst bed with a coke-like product [34]. To improve the properties of bio-oil and achieve higher liquid yield, a two-stage hydrotreatment process was proposed [34]. In the first stage, bio-oil is stabilized by removing the oxygen containing compounds in a low temperature reactor operating at a range of 150 – 280 °C to prevent polymerization. The stabilized oil is further hydrotreated in the second stage at high temperature between 350 – 400 °C, where the primary reactants are converted to a mixture of hydrocarbon products. The application of this technology resulted in less than 2% oxygen in the treated pyrolysis oil [11]. The treated pyrolysis oil can be further processed into conventional fuels in standalone bio-refinery or sent to existing conversion units in a petroleum refinery. Xu et al. [35] presented a two-step catalytic hydrodeoxygenation (HDO) for the translation of fast pyrolysis oil into transportation grade hydrocarbon liquid fuels. At the first mild HDO step, various organic solvents such as tetraline, decalin, diesel and diesel/isopropanol were employed to promote HDO of bio-oil to overcome coke formation using noble catalyst (Ru/C) under mild conditions (300 °C, 10 MPa). At the second deep HDO step, conventional hydrogenation setup and catalyst (NiMo/Al₂O₃) were used under severe conditions (400 °C, 13 MPa) for obtaining hydrocarbon fuel. Results show that the phenomenon of coke formation is effectively eliminated, and the properties of products have been significantly improved, such as oxygen content decreases from 48% to 0.5 wt% and high heating value increases from 17 to 46 MJ kg⁻¹.

2.3 The Environmental Impact of Bio-fuel Production

A recent study by the United Nation's food and agriculture organization (FAO) has revealed that different bio-fuels vary widely in their greenhouse gas balances when compared with gasoline. Depending on the methods used to produce the feedstock and to process the bio-fuels, some crops can even generate more greenhouse gases than do fossil fuels. For example, second-generation bio-fuels offer 70 – 90%

emissions reduction compared with fossil diesel and gasoline [36]. In addition to greenhouse-gas emissions, production and use of bio-fuels affect air quality, water quality, water use, and biodiversity [37 - 40]. For example, biodiesel and ethanol production results in organically contaminated wastewater that, if released untreated, could increase excessive richness of nutrients of surface water-bodies, which causes death of animal life from lack of oxygen. Therefore, environmental tradeoff becomes necessary to select the best type of biomass to be utilized. The environmental tradeoff can be determined using the technique of life-cycle analysis (LCA), which is an analytical tool to calculate greenhouse gas balance.

Hsu [41] performed LCA for the production of gasoline and diesel from forest residue biomass via fast pyrolysis followed by hydroprocessing. The gasoline and diesel produced are estimated to have greenhouse gas (GHG) emissions of CO₂ equivalent of 117 g km⁻¹ and 98 g km⁻¹, respectively, and net energy value of 1.09 MJ km⁻¹ and 0.92 MJ km⁻¹, respectively. Both the CO₂ equivalent and net energy value refer to emission generated and energy consumed by a light-duty passenger vehicle travel a distance of 1 km on engine run by fuels generated from biomass pyrolysis oil. In his work, Monte Carlo uncertainty analysis with respect to the parameters include in pyrolysis processes such as different bio-oil, water, char, ash, and gas yields as well as oil and gas amounts resulting from hydroprocessing was performed. All values from the uncertainty analysis were found to be having lower GHG emissions and higher net energy value than conventional gasoline in 2005.

Han [42] conducted a well-to-wheels (WTW) analysis for pyrolysis-based gasoline and compared it with petroleum gasoline. WTW analysis is an LCA applied to transportation fuels for use in vehicles covering feedstock recovery and transportation, fuel production and transportation, and fuel consumption by vehicles. For example, the WTW pathway for pyrolysis-based gasoline and diesel includes fertilizer production, biomass collection and transportation, pyrolysis of biomass, hydrotreating and upgrading of pyrolysis oil to gasoline and diesel, and transportation and distribution of gasoline and diesel to refueling stations (pump) as well as fuel consumption during vehicle operation. The WTW analysis shows that, the reforming of fuel gas/natural gas for H₂ production reduces WTW GHG emissions of pyrolysis-

based gasoline by 60% compared to petroleum gasoline. While, the reforming of pyrolysis oil for H₂ production increases the WTW GHG emissions reduction of pyrolysis-based gasoline up to 112% due to the carbon credit gain from biomass utilization. However, the reforming of pyrolysis oil for H₂ production reduces liquid fuel yield. Thus, the hydrogen source causes a trade-off between GHG reduction and fuel yields.

2.4 Integrating Bio-refinery into an Existing Petroleum Refinery

Despite the great prospects bio-refinery offers for enhancing energy security and mitigating environmental concerns, the commercial application of bio-refinery is an issue. A bio-refinery requires huge investment that makes installation of a new stand-alone plant unattractive economically. Seeking for economics improvement, BIOCOP proposed a chain of process steps to allow a range of biomass feedstocks to be co-fed to a conventional petroleum refinery to produce fuel and other oxygenated chemicals [26]. Bio-refinery can be located next or inside the existing petroleum refinery [43]. In this way, the required process utilities and product distribution network are already available. Using this concept, it is neither necessary to build a whole new bio-refinery nor to invest in new re-fuelling stations or car engines [43].

2.4.1 Processing Biomass-based Feedstock inside Petroleum Refinery Processing Units

The co-processing of up-graded bio-oil into standard refinery unit can be considered as one of the possible process options for producing bio-fuels. Samolada et al. [44] proposed co-feeding hydrotreated biomass flash pyrolysis liquid heavy fraction (HBFPL) with light cycle oil (LCO) (15/85 w/w) as fluidized catalytic cracking (FCC) process feedstock. Less than 1 wt% of coke on ReUSY catalyst and gasoline yields (23-25 wt%) were obtained. Commercial ReUSY catalysts with a Re₂O₃ content of 0.6 wt%, characterized by a narrow pore size distribution ($D = 36\text{\AA}$), were found to be more appropriate for this application. The produced bio-gasoline quality

was comparable with that obtained from vacuum gas oil (VGO) cracking route. It is characterized by a high research octane number value of 96. Lappas et al. [25] extended Samolada study by blending HBFPL/LCO mix with conventional VGO (2.25/12.75/85) and co-feeding them into FCC unit. The authors found that the presence of bio-oil in VGO reduces the cracking ability of the feedstock. Thus, at the same C/O ratio the conversion was reduced by 1 wt% when the HBFPL was present.

Gabriella et al. [45] found that the co-processing of 20 wt% hydrodeoxygenated pyrolysis oil (HDO-oil) mixed with 80 wt% VGO as FCC feedstock has no effect on the standard FCC catalyst activity. The production yields of gasoline and LCO from this co-processing are comparable to those corresponding to the cracking of VGO. Furthermore, bottom fraction yields are slightly lower, dry gas and coke yields are higher and liquefied petroleum gas (LPG) yield is lower. Mercader et al. [46] co-processed 20 wt% hydrodeoxygenated pyrolysis oil (HDO-oil) with 80 wt% Long Residue as FCC feedstock. Near normal FCC yield of gasoline (44–46 wt.%) and LCO (23–25 wt.%) were obtained without an excessive increase of undesired coke and dry gas. Noticeably, the much higher coke yields obtained from the catalytic cracking of undiluted HDO-oil showed the importance of co-processing using a refinery feed as diluents and hydrogen transfer source.

Agblevor et al. [47] developed a fractional catalytic pyrolysis process to convert biomass feedstocks into a product termed biocrude oils. The main characteristics of biocrude oils are that, they are low viscosity liquids that are storable at ambient conditions without any significant increases in viscosity and distillable at both atmospheric pressure and under vacuum without char or solid formation. The biocrude oils are blended with standard gas oil 15/85 wt% as FCC feedstock. At 70% conversion for standard gas oil and the biocrude oil/gas oil blend, the product gasoline yield was 44 wt%, LCO 17 wt%, HCO 13 wt%, and LPG 16 wt%. Furthermore, the coke yield for the standard gas oil was 7.06 wt% compared to 6.64–6.81 wt% for the blends, which means that the biocrude oil/gas oil blends has a potential as a feedstock to reduce FCC coke formation.

Marker et al. [48] reported that hydrocracking of hydrotreated pyrolytic lignin using nickel-molybdenum catalyst resulted in an overall oxygen removal of 96%, as well as very high level of conversion to gasoline. It is possible that some revamping of petroleum refinery equipment will be needed to accommodate the processing of stable biomass pyrolysis oil. The cost of revamping a hydrocracking unit is estimated by assuming that the incurred cost would not be greater than a small hydrocracker dedicated to process stable pyrolysis oil [11]. However, there are few cases in which refinery hydrotreating and hydrocracking units are designed with stainless steel because they are processing high naphthenic acid crudes [48]. These units could be compatible for processing stable pyrolysis oil.

2.4.2 Petroleum Refinery planning and optimization

Petroleum refinery processes crude oil into refined higher value products such as gasoline, jet fuel, diesel, heating oil and liquefied petroleum gas. The selection of crude oils is one of the most important aspects for petroleum refineries that process different crude oil mixtures. In addition to feedstock selection, process conditions such as cut-point temperatures and reaction severity also affect the refinery operations. Another aspect to be considered in refinery operations is product blending, which must be optimized subject to product demand quantity and quality specifications [49, 50]. It is common in refinery production planning to decide on products blending in order to maximize the sales revenue while maintaining an adequate level of products quality and quantity [51].

Symonds [52] used the method of linear programming (LP) to solve a gasoline-blending optimization problem. The objective function was to maximize the profit subject to constraints of final products requirement, availability of intermediate products, processing unit's capacities and quality balance for final products specifications. The model was coded as a matrix form and solved using the simplex method. The model application was demonstrated on an actual refinery processing and gasoline blending problem. The model results showed that the profit was increased proportional to increasing final products requirement and increasing capacity of reforming unit as well as relaxing the quality specification of the final

products. LP has found wide acceptance as a planning tool in the petroleum refining industry. For example, LP is used to analyze the allocation of CO₂ emissions associated with petroleum refineries to evaluate the environmental impacts of individual automotive fuels [53, 54]. Furthermore, LP is used to analyze the impact of changes in product specifications and environmental pressures on the refining industry [55]. In addition, LP is used as per Gomes et al [56] to evaluate the possibility of changing the design of the refining scheme as a function of the GHG emissions estimated for the lifetime of the complexes during their design stage. Hassan et al. [57] develop an LP model for solving petroleum refinery blending problem. Their objective function was to maximize naphtha productivity. The developed model yielded better overall Naphtha productivity for the petroleum refinery studied, as compared to results obtained by the commercial software.

One of the first contributions to consider nonlinearity in production planning is that of Moro et al. [58]. In their model, a general refinery topology is used to build a non-linear refinery planning model. The refinery process unit models comprise blending relations and process equations. Also, the unit variables must satisfy bound constraints which consist of product specifications, maximum and minimum unit feed flow rates and limits on operating variables. The model was coded into general algebraic modeling system (GAMS) and solved using CONOPT solver. The model was illustrated using an existing petroleum refinery of diesel production. The optimization results were compared to the current situation, where no computer algorithm was used and the stream allocation was made based on experience with the aid of manual calculations. Considering market demand and specification, the optimization algorithm was able to maximize the production of more valuable products, while satisfy the demand and specification of the low valuable products.

Zhang and Zhu [59] presented a decomposition strategy for overall petroleum refinery optimization. The approach was based on the resolution of the overall refinery model into a master model and sub-models. The master model determined interactions among the processes of site level, while the sub-models optimized the individual processes. The results from these sub-models are fed back into the master model for further optimization. This procedure terminates when a convergence

criteria is met. Alhajri et al. [49] presented a nonlinear programming model for refinery planning that combines the processing unit models with the blending correlations and optimizes the operating variables of each individual unit. The model is also able to evaluate properties of the final products to meet market specifications and demands.

Elkamel et al. [27] proposed a MINLP model for the production planning of refinery processes to achieve maximum operational profit while reducing CO₂ emissions to a given target through the use of different CO₂ mitigation options. The options are flow-rate balancing, fuel switching and installation of a CO₂ capture process. The model was demonstrated on a representative case study of petroleum refinery. The products prices, demand and quality specifications are used as shown in Table 2.1 and the maximum capacities of processing units are used as shown in Table 2.2. The model was found to be able to evaluate several mitigation options simultaneously with maximizing the profit of the petroleum refinery. For CO₂ emissions reduction greater than 30%, the CO₂ capture is found to be a promising option. This is because it can achieve up to 90% reduction. The flow rate balancing and fuel switching are found to be able to achieve up to 5% and 30%, respectively.

Table 2.1: Product prices, demands and quality specifications [27]

Final	Price (\$/bbl)	Demand (bbl/day)	Property	Specification
Gasoline	88.2	$\geq 25,000$	SG	≤ 0.8
			SUL%	≤ 0.05
			RON	≥ 89
			RVP	≤ 9
jet fuel	72.7	$\geq 25,000$	SG	≤ 0.85
			SUL%	≤ 0.25
			SP	≥ 20
Diesel	66.0	$\geq 25,000$	SG	≤ 0.87
			SUL%	≤ 0.5
			CN	≥ 45
Fuel oil	39.5	$\geq 18,000$	SG	≤ 1.0
			SUL%	≤ 1.0

Table 2.2: Processing unit capacity [27]

Processing unit	Maximum capacity (bbl/day)
CDU	100,000
CRU	20,000
HCU	25,000
FCCU	25,000

Al-Qahtani and Elkamel [60] presented a mixed-integer programming model for designing an integration and coordination policy among multiple refineries and a petrochemical network to improve their coordination and synergy. The objective function was to minimize the annualized cost over a given time horizon among the refineries and maximize the added value of the petrochemical network. The main feature of their work is the development of a methodology for simultaneous analysis of process network integration within a multisite refinery and petrochemical system. Their approach provides appropriate planning across the petroleum refining and petrochemical industry and achieves an optimal production strategy by allowing appropriate trade-offs between the refinery and the downstream petrochemical markets. Three large-scale refinery networks and a PVC petrochemical complex were integrated to illustrate the performance of the proposed model and to show the economic potential and trade-offs involved in the optimization of the network. The proposed methodology not only devises the integration network in the refineries and synthesizes the petrochemical industry, but also provides refinery expansion requirements, production levels, and blending levels. Elkamel et al. [19] introduced an integrated refinery planning model that simultaneously solve for the optimal refinery hydrogen management strategy and operational planning. The integrated model consists of two main building blocks comprising a set of non-linear processing units' models and a hydrogen balance framework. The integration of these blocks resulted in MINLP model. The model was illustrated on representative case study of petroleum refinery. The results showed that an additional annual profit equivalent to \$7 million could be achieved with a one-time investment of \$13 million in a new purification unit.

Aguilar et al. [61] developed refinery simulation and planning superstructure that was able to determine the most appropriate process scheme for upgrading vacuum residue. The superstructure used delayed coking, visbreaking and gasification processing units as candidates for upgrading vacuum residue. The objective function was to maximize the profitability of the entire refinery. The superstructure was formulated as NLP model and solved using a generalized reduced gradient method. To obtain the initial values for the optimization model, a refinery scheme simulation was done using the formulated model with a convergence criteria based on the error between calculated and desired flow rates of light cycle oil and heavy cycle oil while keeping constant the operating conditions of the vacuum residue upgrading processes. To optimize the superstructure, variables ranging from 0 to 1.0 were defined for delayed coking and visbreaking. The gasification was considered to be existence to cover all of the required hydrogen. When the optimization of the refinery superstructure was performed considering the possibility of using the three process alternatives, the greatest profitability was obtained employing only delayed coking and gasification.

The literature reviewed seeks such systematic methodology for the integration of bio-refinery into existing petroleum refinery. Most of the works are only focusing on the co-processing of bio-oil inside a single petroleum refinery processing unit such as FCC and HC. Thus, the aim of this work is to address this gap.

2.5 Superstructure Modeling and Optimization

Current chemical process synthesis methodologies can be classified into two categories, namely sequential-conceptual methods and superstructure optimization-based methods. The sequential methods are based on the existence of a natural hierarchy among the engineering decisions to be made in order to obtain a fully defined process structure [62]. Specific conceptual tools have been developed to support the design of process system. For example, Linnhoff et al [63] introduced the concept of synthesizing heat exchanger network and proposed systematic composite representation to identify targets for minimum energy consumption. El-Halwagi and Manousiouthakis [64] introduced the concept of synthesizing mass exchange

networks and proposed systematic composite representations to identify targets for the maximum extent of mass exchange among process streams and minimum usage of external lean streams. On the other hand, in superstructure optimization-based methods, an initial process structure will be proposed, including all potentially useful unit operations and all relevant interconnections between them. Then, the superstructure is formulated into a mathematical model. The model typically will include logic-based binary variables to represent the existence or non-existence of every unit in the superstructure. The model solution will indicate which of the initially considered units and interconnections are to be kept as well as the values of the optimal operational conditions [62]. A variety of methodologies have been developed for the generation of superstructures in the design of specific plant subsystems, such as separation network [65 - 67]. The aim of separation network is to configure a separation network for generating the desired products from the given feeds under the constraints imposed. Another example for the generation of superstructure is heat exchanger network design [68, 69], whereby the aim is to finding a network design that minimizes the total annualized cost, i.e. the investment cost in units and the operating cost in terms of utility consumption. Also, alternative methodologies for designing enterprise network between many plants sharing the same site have been proposed. For example, Al-Qahtani and Elkamel [55] presented a superstructure-based mathematical programming model for designing an enterprise network between multiple refineries and a petrochemical network to improve their coordination and synergy.

The superstructure formulation may lead to a complex MINLP model especially when realistic unit operation models are used. One of the common techniques to reduce the complexity of the MINLP model is to transform it into MILP problem by employing linearization techniques [45, 70 - 72]. There are many linearization techniques presented in the literature to relax non-linear problem. The linearization techniques depend highly on the type of non-linear function to be linearized. For example the non-linear relationship between dependent and independent variables can be relaxed by applying a series of straight-line segments [73, 74]. The bilinear term, which is the form of multiplying two different variables, can be relaxed using the

technique proposed by Quesada and Grossmann [75] into four linear inequalities constraints. These constraints were developed based on the lower and upper bounds over the variables present in the bilinear term. This technique is used extensively in the literature. For example, it used for linearizing the bilinear terms resulted from the material balance of crude oil scheduling problem [76] as well as linearizing the hydrogen balance of refinery hydrogen network problem [45, 70 - 72]. In refinery hydrogen network, the equations used to model the power of a new compressor are highly non-linear because it comprises three variables, namely suction pressure, discharge pressure and compressor inlet flow rate. These variables are modeled in such way that the discharge pressure is divided by suction pressure and then multiplied with the inlet flow rate. Due to the difficulty of linearizing this equation, many researchers assumed fixing the suction and discharge pressures of the new compressor [45, 70 - 72]. As results, they only calculated the power of the new compressor as a function of a single variable, namely compressor inlet flow rate.

2.6 Hydrogen Management

Various methodologies have been developed over the years to improve hydrogen utilization in the petroleum refining industry. The methodologies fall into two general categories. The first category utilizes graphical methods while the second category uses mathematical method. For the graphical method, Towler et al. [77] proposed a systematic approach to study hydrogen networks based on the analysis of cost and value composite curves. The composite curves visualize the difference between the hydrogen recovery cost from off-gases and the product value added by hydrogen in consuming units, which represents the driving force for re-use of off-gas streams. Alves and Towler [20] proposed a graphical targeting approach to identify the hydrogen pinch and the minimum fresh hydrogen requirement. The method defines sources and sinks of hydrogen that allow effective extraction of the important data of the hydrogen distribution problem. The target that is calculated is independent of the distribution system design. This is because the targeting method assumed that any stream containing hydrogen can be send to any consumer regardless of stream pressure. El-Halwagi et al. [64] developed a rigorous graphical targeting approach to

minimize the fresh resource consumption. The method provides insightful information on the minimum usage of fresh resources, the minimum discharge of waste, and the maximum recycle and reuse of process streams. In addition the method provides preliminary network to feature maximum mass exchange in the first stage of synthesis. The preliminary network is then improved in the second stage to develop a final cost effective configuration to satisfy the assigned exchange obligations. Thereafter, a linear transshipment model is also established for automatic synthesis of mass exchanger networks [78].

Foo and Manan [79] developed a numerical targeting method called gas cascade analysis (GCA) for targeting the minimum flow rate of utility gas network. The GCA method enables quick and accurate identification of the minimum flow rate targets, pinch-point location(s), and resource allocation targets for a utility gas network. The GCA method was successfully used to determine the minimum flow rate targets for nitrogen, oxygen, and hydrogen utility gas networks prior to detailed design. Ng et al. [80] proposed a pinch based automated targeting techniques for the resource conservation problem. This technique is based on mass exchange network synthesis [64]. It is conceptually similar to the algebraic targeting technique of cascade analysis [81, 82]. This technique provides flexibility in changing the objective function. For example, it can be used to target the minimum total cost of resource conservation network prior to detailed network design. Shariati et al. [83] developed an automated targeting approach to determine the minimum fresh hydrogen consumption in a petrochemical complex. This approach is developed by modifying the automated targeting technique presented by Ng et al. [80] to consider the pressure swing adsorption (PSA) units. The PSA product stream is assumed to be the main source of fresh hydrogen. Consequently, its relative sink (PSA feed) and source (PSA residue) are varied according to the obtained target. The model is illustrated using a real petrochemical complex and the results showed 16.7% reduction in fresh hydrogen consumption.

Despite the great role of graphical methods for targeting minimum hydrogen consumption of refinery hydrogen network, it cannot take into account pressure constraints, which is significant concern in the refinery hydrogen network. Thus, the

developments of mathematical approaches have become necessary. For mathematical method, Hallale and Liu [22] introduced an efficient mathematical method for refineries to optimize its' hydrogen network by maximizing the amount of hydrogen recovered throughout the refinery. The method account fully for pressure constraints as well as the existing equipment and are suited for revamping real industrial systems. This work has demonstrated via the case studies how payback time, maximum capital budgets and total annual cost can all be considered. Furthermore, it demonstrated how debottlenecking objectives can be achieved. In addition, it demonstrated how correct placement of new compressors avoids unnecessary usage of compression power, leading to a decrease in the pollution associated with electricity generation. Liu and Zhang [70] proposed a systematic methodology for the selection of purification processes and their integration in hydrogen network. In this method, a superstructure that considers hydrogen saving, compression costs and capital investment as well as the scenarios of a single purification process and a hybrid system was built. Then, the superstructure is formulated as MINLP model. The model is demonstrated using a Petro-Canada industrial example presented by Peramanu et al. [84]. The optimized superstructure achieved 42.4% and 27.5% reduction in hydrogen requirement and operating costs, respectively, on the expense of investing 8.5 MUS\$ in a new membrane unit.

Khajehpour et al. [85] introduced the concept of reduced superstructure for solving MINLP hydrogen management model. The superstructure is reduced by heuristic rules, based on engineering judgment. The optimization is performed using generic algorithm (GA) technique with an objective function of minimizing the total amount of purge hydrogen to the fuel system. The savings in hydrogen consumption were achieved without any new equipment addition to the plant and just by adjusting process parameters. The application of this method to an existing petroleum refinery hydrogen network achieved 22.6% reduction in hydrogen production. Liao et al. [86] propose a systematic methodology for refinery hydrogen network retrofit design. The method focuses on the placement of hydrogen purifiers such as PSA and membrane separation units as well as new compressors during retrofit design. The objective function was formulated in term of total annualized cost (TAC) to trade-off between

operating and capital costs. The application of this method to an existing petroleum refinery hydrogen network achieved a reduction of 22.8% in total annual cost. Kumar et al. [18] analyzed the characteristic of linear programming (LP), nonlinear programming (NLP), mixed-integer linear programming (MILP) and mixed-integer nonlinear programming (MINLP) for optimizing refinery hydrogen network. The MILP is modeled by fixing the suction and discharge pressures of the new compressor, which may reduce the degree of freedom in the optimization problem and may not lead to optimum and practical solution. Overall, MILP and MINLP techniques are found to be better than LP technique in providing less complex and more realistic refinery system. This is because MILP and MINLP techniques are able to account many complexities of real refinery system such as pressure constraints, source and sinks constraints, compressor flow rate recycle and purity constraints as well as flow combinations.

Ahmad et al. [87] developed a novel approach for the design of flexible hydrogen networks that can remain optimally operable under multiple periods of operation. The proposed method takes into account pressure differences, maximum capacity of existing equipment, and optimal placement of new equipment such as compressors. The novelty of this method was the ability to account the variations of operating conditions of hydrogen consuming processes, which was assumed to be constant in all of the previous work of modeling hydrogen network. Yunqiang et al. [88] presents a novel approach for modeling and implementing multi-objective optimization for hydrogen network in refineries. The optimization includes minimization of operating cost and minimization of investment cost of equipment. Most of the studies employ single-objective optimization method to optimize the hydrogen network. The optimization of hydrogen network using single-objective could minimize operating cost and investment cost simultaneously. In this case the operating cost will be reduced on the expense of increasing investment cost. The new approach of multi-objective optimization can find the compromise solution to balance the two objectives. Through the optimization based on the evaluation function method, optimal solutions denoted as Pareto set (Pareto curve) can be obtained. When one point on the set is moved to another, one objective function can be improved, while

another function becomes worse. Hence, within the Pareto set, neither solution dominates. Both give the optimal solution for the two objective functions. The decision makers have to use additional information, such as the market quotation, the financial situation, and the corresponding decision variable values, to select an operating point (preferred solution) from the entire Pareto set for operation [89, 90].

Zhang et al. [45] compared the performance of the sequential and the simultaneous optimization technique for integrating refinery hydrogen distribution system and utility system with material processing system. All the three systems were formulated as MINLP models. Linearization techniques were then used to transform these models into MILP to facilitate the models solution. The models were demonstrated using a simplified petroleum refinery case study. The models results showed that, the application of simultaneous optimization technique for hydrogen distribution system, utility system and material processing system could achieve better refinery margin than the application the sequential optimization technique, where material processing is optimized first, then hydrogen network and utility system. Elkamel et al. [19] introduced a systematic method for integrating a hydrogen management strategy within a rigorous refinery planning model. The authors proposed an MINLP model that was able to explore further hydrogen availability, which is otherwise hidden and prevented refineries from achieving their maximum production and profit.

Tahouni et al. [91] proposed a superstructure based mathematical model for hydrogen management in petrochemical complexes. The superstructure consists of all hydrogen sources and sinks and connections between them. The modification in this superstructure compared to conventional ones is incorporating compressor and PSA unit connected to a catalytic reforming unit. The superstructure is formulated as NLP model. The application of this method on an industrial petrochemical complexes resulted in about 16.7 % reduction in hydrogen consumption. Zhou et al. [92] presented an MINLP model for the synthesis of refinery hydrogen networks. The model accounts fully for both the economic and the environmental aspect of the hydrogen network. The economic efficiency of the network is assessed using TAC, while the environmental performance is assessed by the total CO₂ emission of the

network. Two types of fresh fuels, light and heavy are investigated in the case studies. Single-objective and multi-objective optimization mathematical programming models were solved for the optimization of the systems with light and heavy CO₂ emission fuels, respectively. The results showed that the selections of purification technologies as well as fuel types were key issues in the sustainable hydrogen network integration.

Most of the works in the literatures have addressed hydrogen management within a single petroleum refinery. It is better to expand the scope of hydrogen management to the integration between bio-refinery and petroleum refinery. This is in order to maximize the hydrogen recovery within the integrated plant and reduced costs.

2.7 Summary of Literature Review

Most of the work for the processing of up-graded pyrolysis oil in petroleum refinery was done on a single petroleum refinery processing unit such as FCC and HC. Thus, optimizing many options for synthesizing optimal enterprise network between bio-refinery and petroleum refinery based on a superstructure may result in optimum routes for processing bio-refinery intermediates inside petroleum refinery.

The up-grading of pyrolysis oil into transportation fuels consume large amount of hydrogen in hydrotreating and hydrocracking processes. Currently, there is no methodology that has been applied to manage bio-refinery hydrogen network as stand-alone or being integrated to other petroleum refinery processes. The application of the existing hydrogen network optimization methodologies may lead to a significant reduction in the size of bio-refinery hydrogen plant.

Most of the developed models of petroleum refinery hydrogen networks are MINLPs, which require a large amount of computational efforts. Many researchers are working on transforming this MINLP problem into MILP problem. The nonlinearity in the hydrogen network model is due to the bilinear terms and the equation of modeling the power of the new compressor. The bilinear terms are relaxed into four inequality constraints based on the lower and upper bounds over the variables present in the bilinear term. The equation of modeling the power of the new

compressor was relaxed by assumed fixing the suction and discharge pressures of the new compressor. The pressure assumption will reduce the degree of freedom in the optimization problem and may not lead to optimum and practical solution. Therefore, there is a need to develop a new linearization technique to allow the variation of the inlet flow rate and discharge pressures of the new compressor.

Table 2.3 summarizes the models used in this study as well as the research gap that need to be addressed.

Table 2.3: The model used in this study and research gap

Literature	Models/method used	Research gap
1. Alhajri et al. [44]	CDU model Blending model	The CDU model is based on fitting the crude oil assay using polynomial. Linearizing this model using linear regression is not appropriate. Thus, a new linearization technique that could track the polynomial function is required. The blending model is non-linear because of the multiplication of two variables, namely the stream flow rate and its property. Thus, this model needs to be linearized.
2. Bird. [93]	Simplified process correlations	The nature of these correlations is non-linear. Thus, new linearization techniques based on mid volume fraction of CDU products need to be developed.
3. Jones et al. [11]	Simulation of standalone bio-refinery	A yield model need to be developed based on the simulation provided by Jones et al. [11]. This in order to integrate this model with refinery model.
4. Jones et al. [11]	Superstructure for co-	Jones et al. [11] present a simplified superstructure to demonstrate the co-location

	locating bio-refinery and petroleum refinery	of bio-refinery and petroleum refinery. This superstructure is simple and used only for demonstration purpose. Thus, a detailed superstructure that contains all feasible options for the integration between bio-refinery and petroleum refinery need to be developed and then modeled and optimized to synthesis optimum enterprise network between bio-refinery and petroleum refinery.
5. Elkamel et al. [19]	Integrated model of hydrogen network and refinery planning	This model is developed for standalone petroleum refinery. The scope of this model needs to be expanded to 1/ the standalone bio-refinery 2/ the enterprise plant of bio-refinery and petroleum refinery.
6. Kumar et al. [18]	MILP model for refinery hydrogen network	Kumar et al. [18] linearized refinery hydrogen network model by fixing the suction and discharge pressure of the new compressor. A new linearization technique that could allow the variation of the discharge pressure of the new compressor may lead to optimal and practical solution to refinery hydrogen network.

CHAPTER 3

METHODOLOGY

3.1 Introduction

This chapter presents the development of formulation for process synthesis of proposed optimal enterprise networks between a pyrolysis-based bio-refinery and an existing petroleum refinery. Figure 3.1 summarizes four main phases in the system approach, namely superstructure framework, materials-processing model, integrated model for hydrogen management and models linearization.

A superstructure framework features a number of feasible options for the integration of pyrolysis-based bio-refinery and existing petroleum refinery. These options will be mathematically screened and optimized to produce a solution for an optimum enterprise network between bio-refinery and petroleum refinery.

The materials-processing system model is developed to synthesize optimum enterprise network among the options presented in the superstructure. Sub-models for the entire units of bio-refinery and petroleum refinery are developed along with a master model that represents the whole integration options of the enterprise. The objective of this model is to synthesize optimum enterprise network that provides maximum profit while satisfying the existing petroleum refinery product demand and quality specifications.

The development of hydrogen management model is to provide the best strategy for synthesizing optimum hydrogen network to meet the hydrogen requirement of the enterprise plants at lowest cost. The hydrogen management model is solved simultaneously with the materials-processing system model and is referred as the integrated model. The materials-processing system and hydrogen management models are then linearized to improve their computational performance.

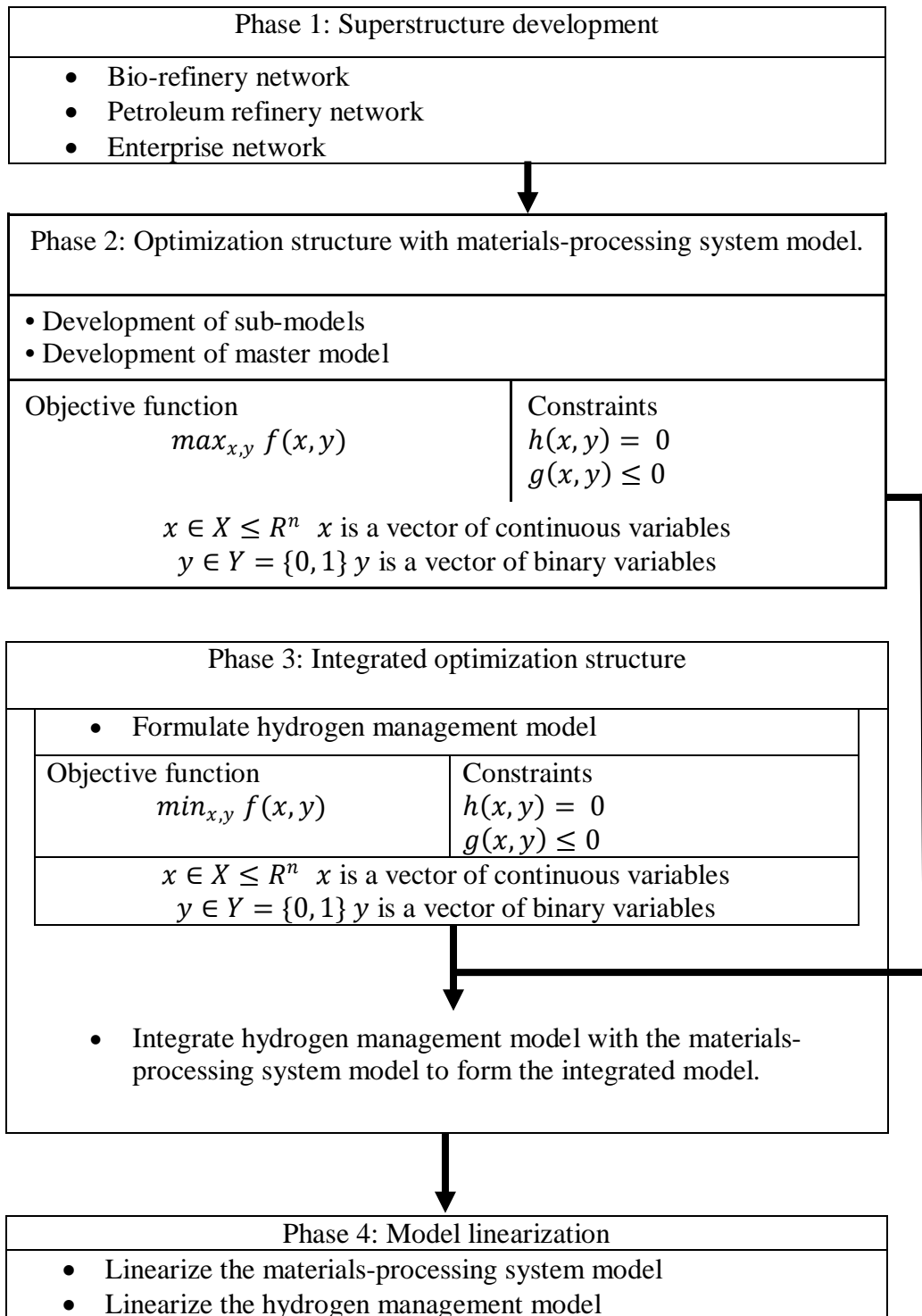


Figure 3.1: System approach for the integration of the proposed bio-refinery into an existing petroleum refinery

3.2 Superstructure Development

The superstructure for the integration of a new bio-refinery and existing petroleum refinery is shown in Figure 3.2. The existing flowsheet for petroleum refinery was adopted from [27], which consists of a crude distillation unit (CDU) to process single or mixed crude oils. Different fractions of petroleum products are withdrawn from the CDU, including LPG, straight run light naphtha (SRLN), straight run heavy naphtha (SRHN), kerosene (KERO), Diesel, vacuum gas oil (VGO), and residue (RESID). The SRLN stream is sent to a gasoline blending pool. The SRHN stream is hydrotreated in a naphtha hydrotreater (NHT) and fed to a catalytic reforming unit (CRU) to produce reformate for gasoline blending. The KERO stream is fed directly to a kerosene pool. The Diesel stream, after being hydrotreated in a diesel hydrotreater (DHT), is sent to a diesel blending pool. The VGO stream is hydrotreated in a gas oil hydrotreater (GOHT). Hydrotreated vacuum gas oil (TGO) may be further converted to gasoline and diesel blendstocks in a fluid catalytic cracking unit (FCC) and/or a hydrocracking unit (HC). The RESID stream from the bottom of the CDU is hydrotreated in a residue hydrotreater (RDHT) and then sent to a fuel oil product pool.

The flowsheet of a new bio-refinery is adapted from Pacific Northwest National Laboratory [11]. The flowsheet consists of a fast pyrolysis unit (PYR) that converts biomass into pyrolysis oil (py-oil), a two-stage hydrotreater unit (HDT) for production of treated pyrolysis oil (Tpy-oil) and a debutanizer unit (Dc4) for production of stable pyrolysis oil (St-oil). For the proposed integration of the new bio-refinery into an existing petroleum refinery, the St-oil stream carries the option to be fed into refinery FCC (stream S1) or be sent into naphtha splitter (NS) stream S2. With this option, S1 is mixed with TGO from GOHT unit before entering FCC unit. Gabriella et al. [58] proposed an optimum blend ratio S1:TGO at 20/80 wt. In addition, when stream S2 is fed to NS, the superstructure generates another option for the recovered naphtha (LTN) either to be up-graded into reformate in the bio-refinery catalytic reforming unit (BCR) or the CRU in existing petroleum refinery. This is because the recovered naphtha is characterized by its low octane number [11, 94]. In each case, the reformate is finally sent to a gasoline pool for product blending. The heavy stream

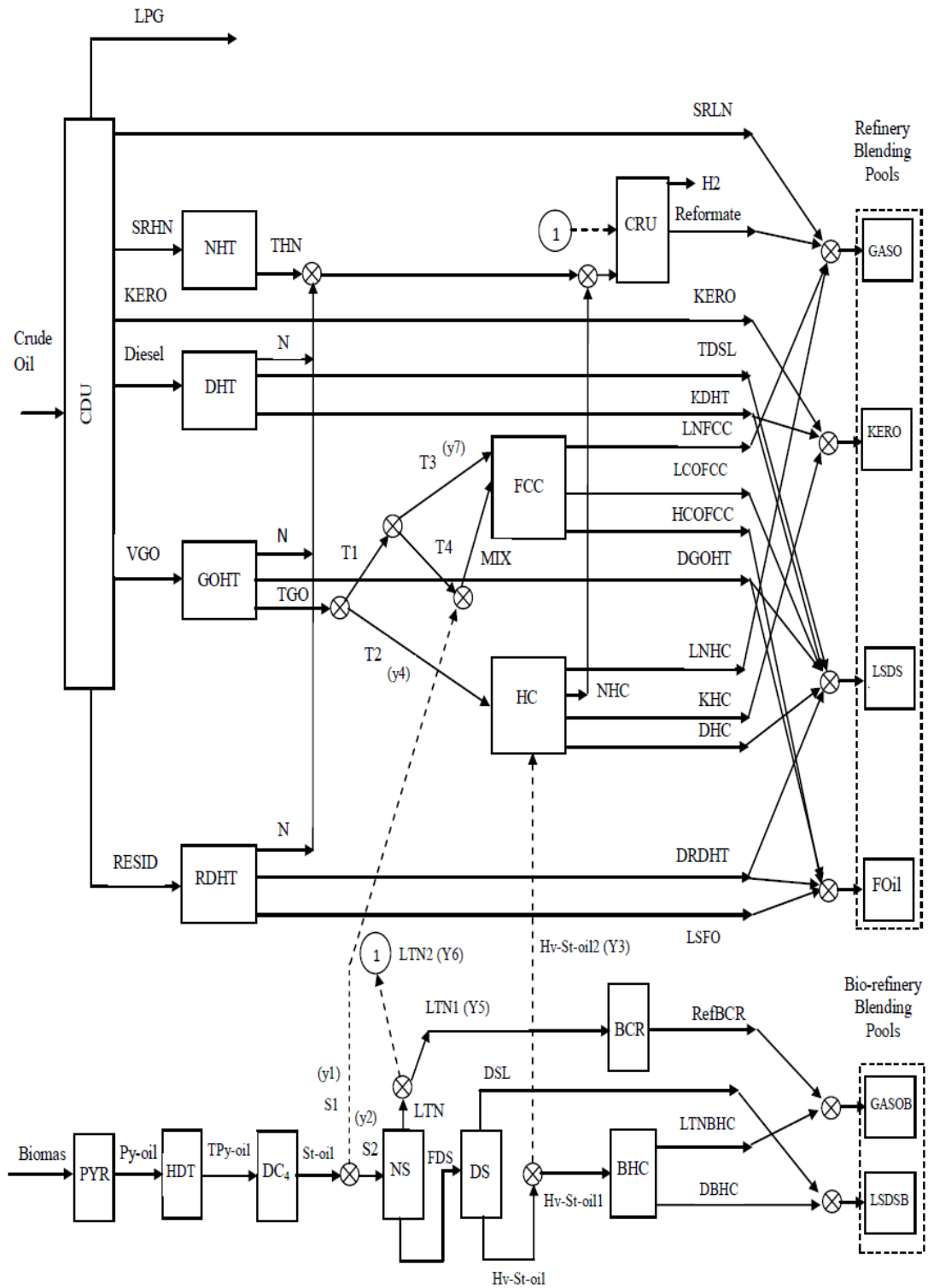


Figure 3.2: The proposed superstructure for the integration of bio-refinery and existing petroleum refinery

(FDS) from NS is further fed to a diesel splitter (DS) unit. The recovered diesel (DSL) is sent to a diesel pool while the heavy stream (Hv-st-oil) becomes an optional feed stock to either bio-refinery hydrocracker (BHC) or the existing HC in petroleum refinery [11]. The hydrocracker converts Hv-st-oil into naphtha and diesel range products. The naphtha is sent to gasoline pool, while the diesel is sent to diesel pool. For the integration of bio-refinery into an existing petroleum refinery, the bio-refinery's final products will only utilize the existing petroleum refinery blending pools.

To synthesize optimum enterprise network between bio-refinery and petroleum refinery, logic based binary variables constraints need to be introduced. The logic based binary variables constraints comprising binary variables and logic. The binary variables identify whether a feature exists or not, while the logic determine the number of features to be selected. These types of constraints allow the optimizer to select the optimum routes for processing bio-refinery streams inside petroleum refinery. In addition, the inlet flow rate to petroleum refinery FCC unit also needs to be modeled using logic based binary variables constraints. The reason is because FCC can only accept either pure VGO or a mixture of bio-oil and VGO at 20/80 wt% ratio [58]. At this ratio, the conversion of the VGO/HDO-oil over standard FCC catalyst gives comparable results to that of the pure VGO cracking [58].

3.3 Modeling Materials-processing System

Materials-processing system can be defined as the series of processing unit operations that transforms industrial materials from a raw-material state into finished products. The model formulation of materials-processing system to synthesize optimum enterprise network between a new pyrolysis-based bio-refinery and an existing petroleum refinery starts by developing sub-model for each processing unit. Then, a master model is formulated to determine the interactions among sub-model processing units and synthesize optimum enterprise network between bio-refinery and petroleum refinery.

3.3.1 Sub-models Development

CDU Model

CDU is a processing unit through which the whole crude oil entering a petroleum refinery is processed. Crude oil should be characterized before being fed to the CDU. The common method for characterizing crude oil is True Boiling Point (TBP) curve. The TBP curve is developed as a part of the crude assay in order to determine the liquid volume percent of the crude oil that is fractionated relative to temperature at atmospheric pressure [15]. Figure 3.3 shows the TBP curve for a heavy sour crude used in this study [14]. The TBP curve shows the liquid volume percent of the crude oil under study that evaporates relative to a specific temperature. Table 3.1 shows the fractions produced in the CDU from the crude and its boiling range [15].

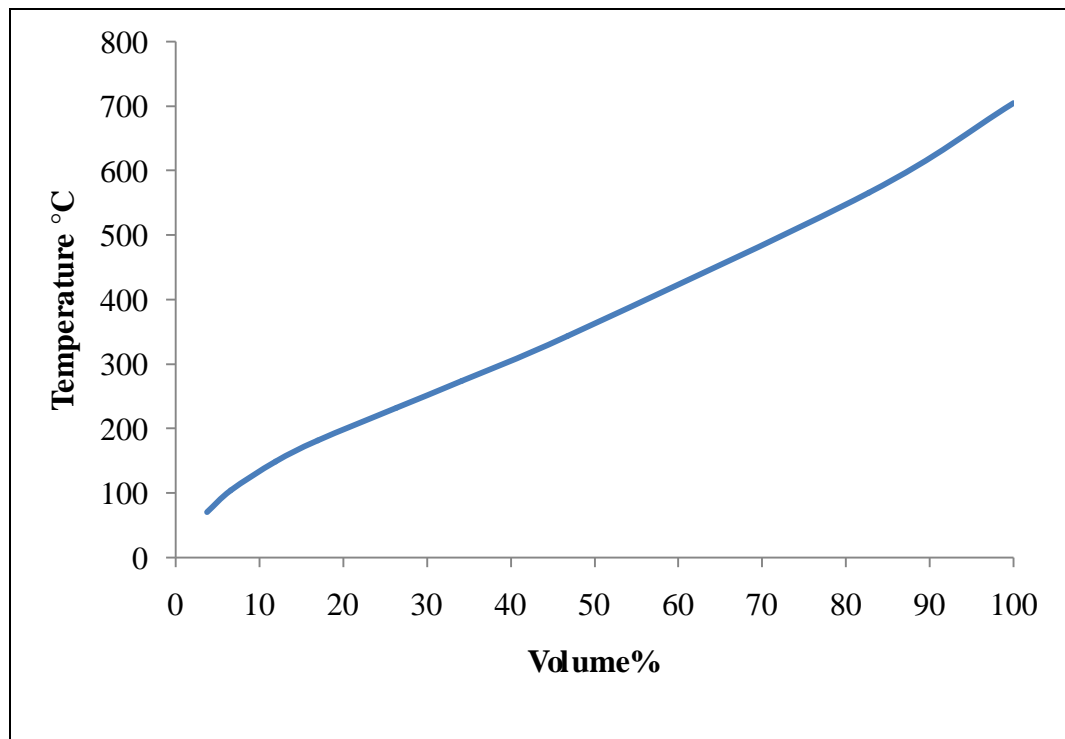


Figure 3.3: TBP distillation curve of the crude oil used in this study [14]

Table 3.1: Boiling range of typical crude oil fractions [15]

Fraction	TBP –Boiling range (°C)
SRLN	32.2 – 104.4
SRHN	82.2 – 193.3
Kerosene	165.6 – 271.1
Diesel	215.6 – 332.2
VGO	321.1 – 565.6
Residue	510 +

The products from CDU are fractions s ($s \in S_{CDU} = \text{LPG, SRLN, SRHN, Kero, Diesel, VGO and RESID}$). In addition, the operating variables of the CDU is the cut-point temperature (TE_{CDU}) for fraction s . The CDU model is described as follows:

$$\text{Cut}_s = \sum_{g=0}^4 a_g (TE_{CDU,s})^g \quad \forall s \in S_{CDU} \quad (3.1)$$

Cut_s represent the volume percent of all fractions s , except the residue product of the CDU unit. The cuts are represented as a polynomial function in $TE_{CDU,s}$. The coefficients of the polynomial of the CDU equation (a_g) are listed in Table 3.2. A fourth order polynomial is used to fit the data in order to use it conveniently in the model ($g = 0, \dots, 4$). $TE_{CDU,s}$ is equivalent to the end point temperatures (EP). EP is the actual terminal temperature of a fraction produced commercially. For every product from the CDU, the $TE_{CDU,s}$ has an upper and a lower bound, which is called the swing cut. The swing cut is the range between the initial boiling point (IBP) of a desired fraction and the end boiling point (EBP) of the previous one. Figure 3.4 shows a part of the distillation curve of a crude oil, in which Naphtha (Naph), kerosene (Kero), and diesel (Dies) are separated as distillates. Accordingly, the related Naph, Kero and Dies cut-points are shown as vertical dotted lines. The swing-cut Naph/Kero and Kero/Dies can be cut into either of the adjacent distillates. The reason is because these swing-cuts are bounded by IBP of Kero and EBP of Naph and IBP of Dies and EBP of Kero for Naph/Kero and Kero/Dies swing-cuts, respectively.

Table 3.2: Coefficients for CDU model equations (3.1) and (3.4)

Parameter	Cut _s	$PV_{CDU,s,API}$	$PV_{CDU,s,Sul\%}$	$PV_{CDU,s,N\%}$
a ₀	4.03844	81.852	5.0542E-02	-8.8508E-04
a ₁	-4.72479E-02	-3.7798	-2.0350E-02	3.0519E-04
a ₂	3.24907E-04	0.11338	1.8488E-03	-2.3044E-05
a ₃	-2.84207E-07	-1.5451E-03	-3.2565E-05	4.6110E-07
a ₄	8.14775E-11	7.1982E-06	2.0295E-07	6.7530E-09

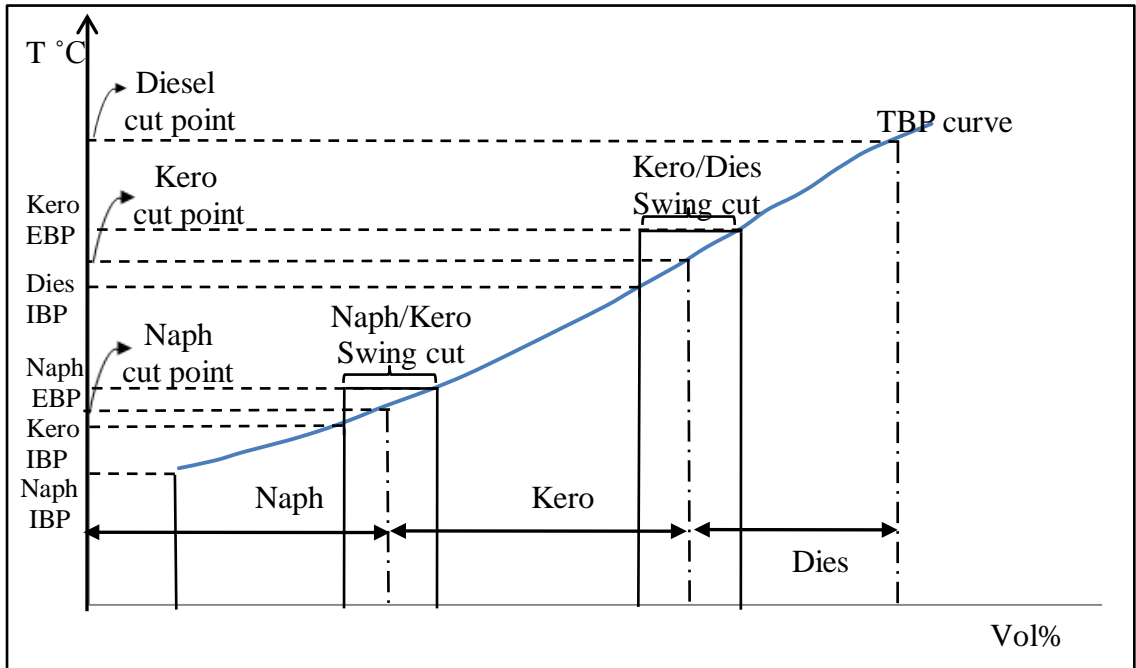


Figure 3.4: Swing cuts of CDU fractions

RESID is the final cut of the crude fractions that make up the balance of the cumulative fraction vaporized to 100%.

Each product volumetric flow rate is calculated by subtracting its volume percent vaporized from the previous cut and multiply the result with the volumetric flow rate of the crude feed to the CDU [44]. This is expressed using Equation (3.2).

$$V_{CDU,s} = F_{CDU} * \left(\frac{Cut_s - Cut_{s-1}}{100} \right) \quad s \in S_{CDU} \quad (3.2)$$

$V_{CDU,s}$ represents the volume flow rate of all the products (s) from the CDU and FCDU is the crude oil feed to CDU. See Appendix C, example C1, for an illustration of swing-cut model.

To find the properties of the CDU outlet streams from the CDU such as °API, % sulphur and % nitrogen, then a percentage of the middle volume is required. The %middle volume is the average between the volume% accumulated from the previous cut and volume% accumulated from current cut. This is given by equation (3.3).

$$MidV_{CDU,s} = \frac{Cut_{s-1} + Cut_s}{2} \quad s \in S_{CDU} \quad (3.3)$$

The properties of the CDU products can now be expressed as polynomial functions in each product mid-volume percent vaporized as shown in Equation 3.4.

$$PV_{CDU,s,p} = \sum_{g=0}^4 a_g MidV_s^g \quad s \in S_{CDU}, p \in P_s \quad (3.4)$$

$PV_{CDU,s,p}$ represents different properties (p) for each product (s) from the CDU unit. P_s is the set of all the properties calculated for the specified stream (s).

Hydrotreating Units Sub-models

Hydrotreaters are reaction units that operate under mild condition (temperature of 400 °C and below; hydrogen pressure of 40 bar and below) to remove impurities such as sulfur and nitrogen from the petroleum products. The products yields and properties of petroleum refinery hydrotreating units (NHT, DHT, and VGOHT) are estimated using empirical correlations [14, 93]. These correlations are derived from a number of different crudes. The objective of these correlations is not to simulate any particular process unit or the performance of a specific catalyst, but to estimate yields and properties that a typical process unit would achieve in commercial operation [93]. These correlations have been used extensively in the literature for modeling refinery processing units [14, 95]. See Appendix C, example C2, for an illustration of hydrotreating units sub-models.

Upgrading Units Sub-models

Petroleum refinery up-grading units are reactors that operate under more severe condition to hydro-crack, catalytic-crack and reform petroleum fractions into more valuable products. The products yields and properties of petroleum refinery up-grading units (HC, FCC, CR) are linear correlations as reported from the literature [58, 96].

Bio-refinery Units Sub-models

The bio-refinery units' sub-models include the fast pyrolysis, two-stage hydrotreating unit, product separators and up-grading units. The product yields of the entire bio-refinery processing units are yield function of the process flow rate [11, 58]. The properties of the entire bio-refinery processing units are adopted from the literatures [11, 94]. The sub-models for the petroleum refinery and the bio-refinery are shown in Appendix D.

3.3.2 Master Model Development

A master model is required to manage the connection of the units in the entire enterprise network and provide logical constraints for synthesizing the optimum enterprise network. The objective function in the master model is to maximize total profit Ψ of the enterprise, viz.

$$\text{Max } \Psi = \sum_{i \in B} C p_i - \sum_{i \in E} C f_i - \sum_{i \in I} C x_i - \sum_{i \in W} C \gamma_i - \sum_{i \in Z} C \beta_i - \sum_{i \in R_t} C \alpha_i \quad (3.5)$$

Equation (3.5) expresses the overall enterprise profit as revenues from bio-refinery and petroleum refinery blended products minus Costs. The components of costs are made up of feedstock cost ($C f_i$), operating cost ($C x_i$), bio-refinery investment costs ($C \gamma_i$ and $C \beta_i$) and existing petroleum refinery retrofit cost ($C \alpha_i$). In Equation (3.5), index B represents the set of blending units for the final products and their sales price ($C p_i$). The cost of feedstock purchased from external sources ($C f_i$) is defined under set E for all units receiving feedstock from outside of the enterprise. The operations cost for each processing unit in the enterprise ($C x_i$) is defined under set I ($i \in I$). The

operations cost is usually expressed as a function of the quantity fed to a running unit. The bio-refinery investment cost ($C\gamma_i$) is defined under set W for all basic units that must be installed to produce the stable pyrolysis oil while the investment cost of the bio-refinery upgrading units ($C\beta_i$) is defined under set Z for all units that must be installed in order to up-grade bio-refinery products into higher quality. The retrofit cost of the existing petroleum refinery ($C\alpha_i$) is defined under set R_t for all units that must be modified in order to process stable pyrolysis oil.

3.3.2.1 General processing unit Model [42]

A general processing unit as shown in Figure (3.5) illustrates the mathematical representation of the streams entering and leaving a processing unit i ($i \in I$). The general processing unit model is adapted from the work done by Alhajri et al. [44]. The model consists of the following sets of constraints:

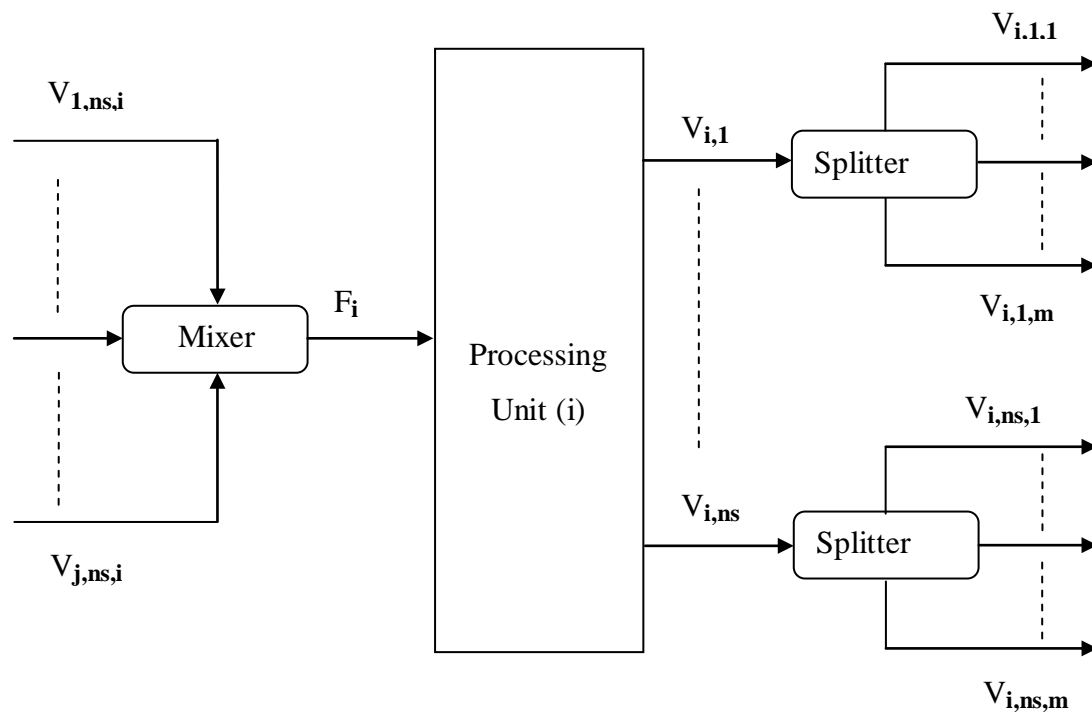


Figure 3.5: General processing unit model [42]

Feed Flow Rate of Processing Unit [44].

The feed flow rate of the processing unit is

$$F_i = \sum_{j \in J} \sum_{s \in N_s} V_{j,s,i} \quad \forall \{i \in I\} \quad (3.6)$$

The feed flow rate F_i for any processing unit ($i \in I$, I is the defined set for all the units in the enterprise) is the summation of all flow rates $V_{j,s,i}$ of the possible streams s that can be received by unit i from unit j ($j \in J$). Index J is defined as the set of all units that can send streams to unit i and N_s is defined as the set of all streams s that can be sent from unit j ($j \in J$) to unit ($i \in I$).

Feed Properties of Processing Units [44].

The properties of feed entering process unit i is described as.

$$FP_{i,p} = f(V_{j,s,i}, PV_{j,s,p}) \quad \forall \{i \in I\}; \{ps \in PF_i\} \quad (3.7)$$

Properties ps of the feed to unit i are represented by $FP_{i,p}$. The set of all feed properties ps to unit i is PF_i . The properties are functions of the quantities ($V_{j,s,i}$) and properties ($PV_{j,s,p}$) of all streams s from unit j ($j \in J$).

Product Flow Rates of Processing Units [44].

The following relation describes the product flow rates of the processing units.

$$V_{i,s} = f(F_i, FP_{i,p}, XU_{i,x}) \quad \forall \{i \in I\}; \{s \in S_i\}; \{x \in X\} \quad (3.8)$$

The flow rate of products $V_{i,s}$ from unit i for stream s ($s \in S_i$, S_i is the defined set of all streams produced from unit i) is a function of the unit i feed quantity (F_i) and feed property ($FP_{i,p}$) as well as the operating variables $XU_{i,x}$ ($x \in X$, X is the defined set of all operating variables). Equation (3.8) is valid for the unit that processes pure crude oil based feedstock. The other units, which process biomass feedstock, operate with linear yield correlation. This means that the function $f(F_i, FP_{i,p}, XU_{i,x})$ is replaced by a constant parameter multiplied by the feed flow rate (F_i).

Product Properties of Processing Units [44].

The following relation describes the properties of products from processing unit i .

$$PV_{i,s,ps} = f(FP_{i,p}, XU_{i,x}) \quad \forall \{i \in I\}; \{s \in S_i\}; \{ps \in PS_i\} \quad (3.9)$$

$PV_{i,s,p}$ is property ps for product stream s from unit i , which is a function of the feed properties and the operating variables of unit i ($ps \in PS_i$, PS_i is the defined set of the properties of all streams produced from unit i). Equation (3.9) is mainly used to estimate properties of the products from processing units that processes crude oil based feedstock. While for the units that process biomass based feedstock, the products properties are considered to be constant values.

Processing Unit Capacity [44].

The processing unit capacity is given as.

$$F_i \leq U_{\max_i} \quad \forall \{i \in I\} \quad (3.10)$$

The feed of processing unit i cannot exceed its maximum capacity, which is represented by U_{\max_i} .

Splitter [44].

For a stream s from unit i to be split into many streams, either as a final product or feed to other processing units, the model is described by:

$$V_{i,s} = \sum_{md \in MD} V_{i,s,md} \quad \forall \{i \in I\}; \{s \in S_i\} \quad (3.11)$$

The product stream s from unit i is represented by $V_{i,s}$ ($s \in S_i$) can be sent to different destinations md defined by streams $V_{i,s,md}$ ($md \in MD$, MD is defined as the set of the units or final products pool blending that can receive the splitted streams).

Integrating bio-refinery into petroleum refinery

The integration of bio-refinery into existing petroleum refinery is modeled using exclusive or logic constraint as follows.

$$\sum_{t=1}^T y_t = 1 \quad (3.12)$$

This constraint allows the model to select only one route among a number of routes, T, for the processing of bio-refinery intermediates inside the existing petroleum. The binary variable, y_t , are assigned (0-1) to represent the selected routes.

Capital cost calculations

The capital costs of bio-refinery processing units are taken from Jones et al. [11]. The “n” exponent factor rule [97] is used to calculate the capital cost of processing unit in relations to the unit capacity. The capital cost calculations are shown in Appendix E.

$$costB = cost A \left(\frac{size B}{size A} \right)^n \quad (3.13)$$

In this study, the retrofit cost of the existing petroleum refinery processing units are assumed to be equal to the cost of installing a new unit dedicated to up-grade bio-refinery intermediate product [11]. Therefore, Equation (3.13) is used to calculate the optimum retrofit cost of petroleum refinery processing units at their optimum capacities.

Blending models

Enterprise processes do not produce final products directly. Rather, intermediate products are blended together in order to meet quality specifications as required in the fuel market. Additive properties like sulfur and specific gravity of the blended products are estimated as follows:

$$P_{blend} = \frac{\sum_{s=1}^S q_s * p_s}{\sum_{s=1}^S q_s} \quad (3.14)$$

In Equation (3.14), P_{blend} is the desired property of the product, p_s is the value of the property of stream s and q_s is the mass or volume flow rate of stream s contributing to the total amount of the demanded product. The term q_s represents mass flow Rate for mass blending based and volume flowrate for volumetric blending based.

For other properties like octane number and Reid vapor pressure, which are non-additives, a blending index for each property is used. The blending index is calculated according to Equation (3.15). In Equation (3.15), BI_p represents the blending index for the desired property of the product, $IN_{p,s}$ is the index for a property p of stream s , and q_s is either mass or volume flow rate of stream s contributing to the total amount of the demanded product.

$$BI_p = \frac{\sum_{s=1}^S q_s * IN_{p,s}}{\sum_{s=1}^n q_s} \quad (3.15)$$

Equations (3.16) and (3.17) express the upper and lower bound on specifications constraints for all products that either blends by mass or volume

$$\sum_s Pr_s * q_s \geq Spec_{pr,p} * V_p \quad (3.16)$$

$$\sum_s Pr_s * q_s \leq Spec_{pr,p} * V_p \quad (3.17)$$

The term Pr_s represents the value of the property or the property index of stream s , q_s is either the mass or volume flow rate of stream s , $Spec_{pr,p}$ is the property specification of the final product and V_p is the volume or mass of the final product.

Equations (3.1 – 3.17) represent materials-processing system model. This model can be described as MINLP problem because it contains discrete variables and non-linear functions. The discrete variables are used to model the synthesis of the enterprise network between bio-refinery and petroleum refinery as expressed by Equation (3.12). The non-linearity is due to the non-linear correlation of modeling CDU as expressed by Equations (3.1) and (3.4), the non-linear correlations of modeling petroleum refinery hydrotreating units as shown in Appendix D, the non-linear equation of calculating capital cost as expressed by Equation (3.13) and the bilinear terms in the blending model as expressed by Equations (3.14), (3.15), (3.16) and (3.17).

3.4 Development of the Integrated Model

This section presents the development of a hydrogen management model, which is integrated with the materials-processing system modeled in section 3.3. The model is able to simultaneously synthesize optimum enterprise plant network between bio-refinery and petroleum refinery and synthesize optimum hydrogen network to meet the hydrogen requirement of the enterprise plant.

3.4.1 Hydrogen Management Model

The hydrogen management model is adopted from the work done by Elkamel et al. [19] and Hallale and Liu. [22]. Figure 3.6 shows the hydrogen network superstructure representation containing all possible alternatives for a potential hydrogen network. The superstructure consists of three parts; inlet hydrogen streams (Sources), different unit operations, and outlet streams (Fuel system). The set of inlet streams represents different hydrogen streams ($h = 1, 2, \dots, H$) that provide the network with its requirements of hydrogen. Every inlet stream is distributed over all the unit-operations and fuel system. The set of unit operations consist of enterprise hydrogen consumers, compressors and pressure swing adsorption (PSA) units. Hydrogen streams may flow between the different units (u, k, n, m) or delivered to the fuel system (q). The fuel system (q) is the final destination for unutilized hydrogen in the hydrogen network.

Flow assignment in hydrogen network [19]

The gas flow rate from any source to sink is defined by a binary variable $xf_{\mu\varphi}$ that allows the flow if the source pressure P_μ is greater than or equal to the sink pressure P_φ . This is can be introduced into the model using the following logic constraints.

$$UP(xf_{\mu\varphi} - 1) \leq (P_\mu - P_\varphi) \leq xf_{\mu\varphi} UP - \alpha \quad \forall \mu\varphi; \begin{matrix} \mu \in h, u, k, n, m \\ \varphi \in u, k, n, m, q \end{matrix} \quad (3.18)$$

$$F_{\mu\varphi} \leq xf_{\mu\varphi} UF \quad \forall \mu\varphi; \begin{matrix} \mu \in h, u, k, n, m \\ \varphi \in u, k, n, m, q \end{matrix} \quad (3.19)$$

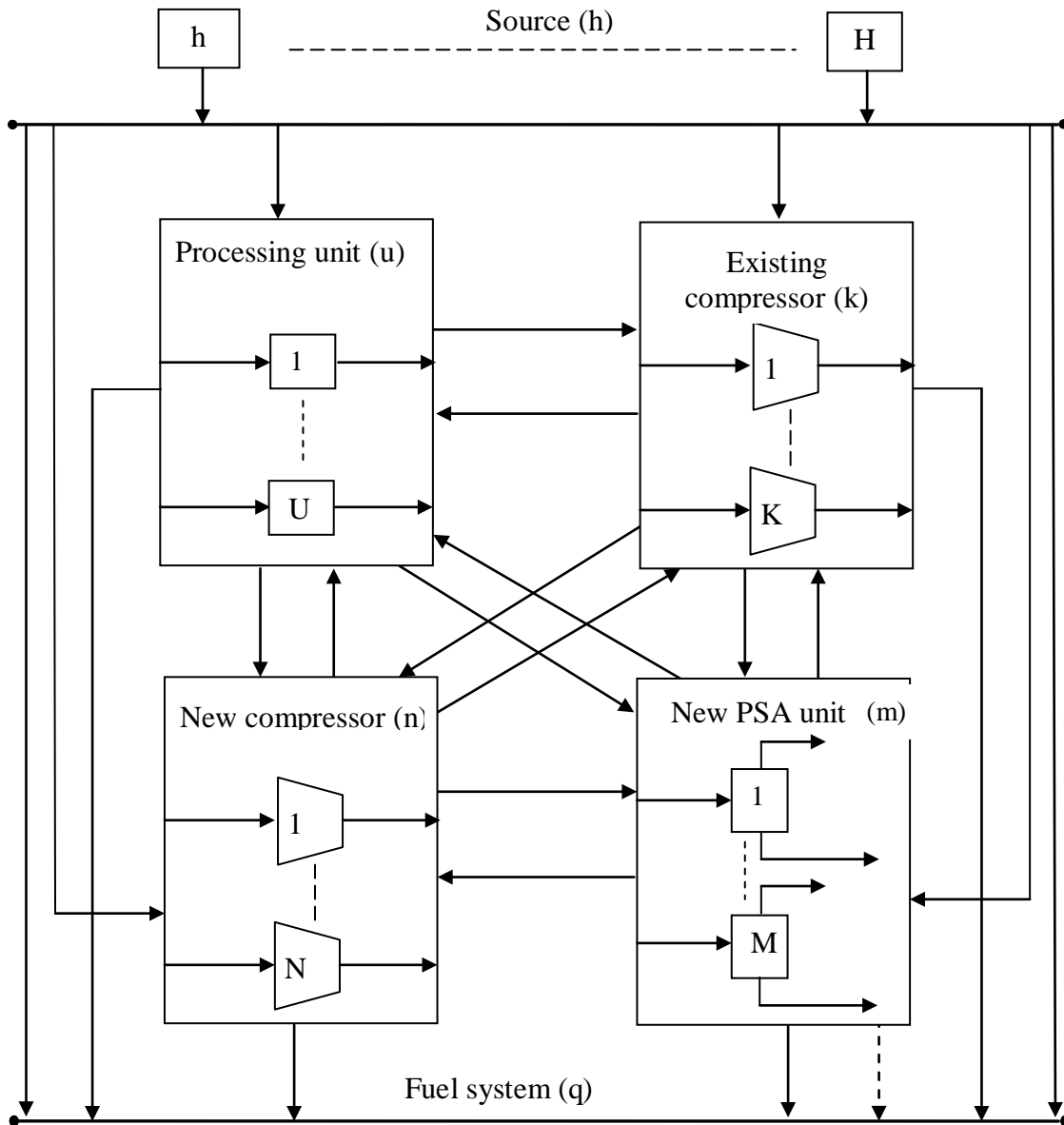


Figure 3.6: Superstructure representation of a hydrogen network [19]

In Equations 3.18 and 3.19, UP and UF represent the upper pressure difference bound and the upper flow rate bound. The term α in Equation 3.18 is a small value number to satisfy the logic constraints. The term μ represents the whole sources of hydrogen in the network. This include hydrogen from hydrogen plant and catalytic reforming unit h , the off-gases existing the processing units u , the high-pressure hydrogen exiting the existing compressors k , the high-pressure hydrogen exiting the new compressors n and the purified hydrogen exiting the purification units m . The term φ

represents the whole sinks of hydrogen in the network. This include the entrance of the processing unit u , the entrance of the existing compressors k , the entrance of the new compressors n , the entrance of the purification unit m and the fuel system q .

For sources and sinks with known pressure such as existing compressors, processing units, hydrogen plant and fuel system, the flow rates between them are fixed to zero when the pressure of source is less than the pressure of sink. Alternatively, the flow rates are equal to one when pressure of source is greater than or equal to the pressure of sink. This is in order to reduce the number of binary variables in the model, hence reduce the complexity of the model.

The total amount of gas sent to the sinks $\sum_{\varphi} F_{\mu,\varphi}$ must equal to the amount available from the source $F_{source,h}$ [22].

$$F_{source,h} = \sum_{\varphi} F_{h,\varphi} \quad (3.20)$$

Fuel system q is the final destination of the unutilized hydrogen in the network. The flow rate of gas $F_{sink,q}$ and purity of hydrogen $F_{sink,q}y_{sink,q}$ entering the fuel system can be modeled using equations (3.21) and (3.22), respectively [22].

$$F_{sink,q} = \sum_{\mu} F_{\mu,q} \quad (3.21)$$

$$F_{sink,q}y_{sink,q} = \sum_{\mu} F_{\mu,q}y_{\mu,q} \quad (3.22)$$

The processing units such as hydrotreaters and hydrocrackers are the only consumers of hydrogen in the hydrogen network. The amount of hydrogen consumed in these processing units can be expressed using Equation (3.23) where, $cons_u$ is the quantity of hydrogen consumed in the processing unit, $F_{sink,u}y_{sink,u}$ is the amount of hydrogen at the inlet of the processing unit, $F_{source,u}y_{source,u}$ is the amount of hydrogen at the outlet of the processing unit.

$$cons_u = F_{sink,u}y_{sink,u} - F_{source,u}y_{source,u} \quad (3.23)$$

The link between the hydrogen management model and materials-processing system model developed in section (3.3) is expressed by the variable $cons_u$ [19]. The

materials-processing system model is responsible for calculating $cons_u$, while the hydrogen management model is responsible for optimizing the hydrogen network in order to meet $cons_u$ with optimum cost.

The purity of the gas entering the processing unit $y_{sink,u}$ and the purity of the gas leaving the processing unit $y_{source,u}$ are assumed as constant parameters [19]. Processing unit works as both sinks and sources. In order to maintain the operation condition of the processing unit the amount of gas fed $F_{sink,u}$ as well as the hydrogen $F_{sink,u}y_{sink,u}$ at the inlet of the unit are kept constant. R_u is the recycle gas to the same unit u [22].

$$F_{sink,u} = \sum_{\mu} F_{\mu,u} + R_u \quad (3.24)$$

$$F_{sink,u}y_{sink,u} = \sum_{\mu} F_{\mu,u}y_{\mu} + R_u y_{source,u} \quad (3.25)$$

The gas leaving the outlet of the processing unit can be recycled back to the same unit (R_u) or purge to the other processing unit and fuels system ($PG_{u,\varphi}$).

$$F_{source,u} = R_u + PG_{u,\varphi} \quad (3.26)$$

The compressors are used in the hydrogen network to satisfy the pressure requirement of the consumers. The flow rate of gas and pure hydrogen entering the compressor must equal the flow rate leaving the compressor as expressed in Equations (3.27) to (3.30) [22]. As many hydrogen sources will be mixed before entering a compressor, the hydrogen purity as well as flow rate of compressor will be considered as optimization variables.

$$F_{in,k} = F_{out,k} \quad (3.27)$$

$$F_{in,k} = \sum_{\mu} F_{\mu,k} \quad (3.28)$$

$$F_{out,k} = \sum_{\varphi} F_{k,\varphi} \quad (3.29)$$

$$F_{in,k}y_k = \sum_{\mu} F_{\mu,k}y_{\mu,k} = \sum_{\varphi} F_{k,\varphi}y_{k,\varphi} \quad (3.30)$$

The existing compressors are designed with specific capacities. Therefore, the gas flow rate entering the compressor is lower than or equal to its maximum capacity.

$$F_{in,k} \leq F_{max,k} \quad (3.31)$$

The power of the existing compressor Pwr_k is adopted from the model by Elkamel et al. [19]. Equation (3.32) shows PI and PO as the suction and discharge pressure, respectively, while $F_{in,k}$ is the compressor inlet flow rate.

$$Pwr_k = 160.376 \left[\left(\frac{PO_k}{PI_k} \right)^{0.1857} - 1 \right] F_{in,k} \quad (3.32)$$

Equations (3.27) and (3.30) are valid for modeling a new compressor (n). The existence of the new compressors is modeled using binary variable X_n . Based on the preceding binary variable X_n , the new compressor inlet flow rate $F_{in,n}$ can be expressed using Equation (3.33) between the lower bound LF and upper bound UF.

$$X_n LF \leq F_{in,n} \leq X_n UF \quad (3.33)$$

For the new compressor, a minimum pressure difference (LPNC) between the inlet and the outlet must be satisfied [19]. This is represented using Equation (3.34). Since the new compressor has not yet been built, no maximum flow rate limit will be applied other than manufacturers' limitations.

$$UP(X_n - 1) + LPNC \leq (PO_n - PI_n) \leq X_n UP + LPNC - \alpha \quad (3.34)$$

The power of the new compressor can be calculated using Equations (3.35) – (3.37). Pwr_n and $UPwr$ are the power of the new compressor and the upper bound of the power of the new compressor, respectively [19].

$$Pwr_n - 160.376 \left[\left(\frac{PO_n}{PI_n} \right)^{0.1857} - 1 \right] F_{in,n} \leq (1 - X_n) UPwr \quad (3.35)$$

$$Pwr_n - 160.376 \left[\left(\frac{PO_n}{PI_n} \right)^{0.1857} - 1 \right] F_{in,n} \geq (X_n - 1) UPwr \quad (3.36)$$

$$Pwr_n - X_n UPwr \leq 0 \quad (3.37)$$

As illustrated in Figure 3.7, a purifier, such as pressure swing adsorption (PSA), can be modeled as one sink (feed stream) and two sources (the product stream and residue stream). By specifying the products purity, $y_{\text{prod},m}$, and hydrogen recovery, Rec , of the purifier m , the product flow rate $F_{\text{prod},m}$, residue stream flow rate $F_{\text{resid},m}$ and residue stream purity $y_{\text{resid},m}$ can be calculated using Equations (3.38) to (3.42). $F_{\text{in},m}$ and $y_{\text{in},m}$ are the gas flow rate and purity at the inlet of the purifier, respectively [22].

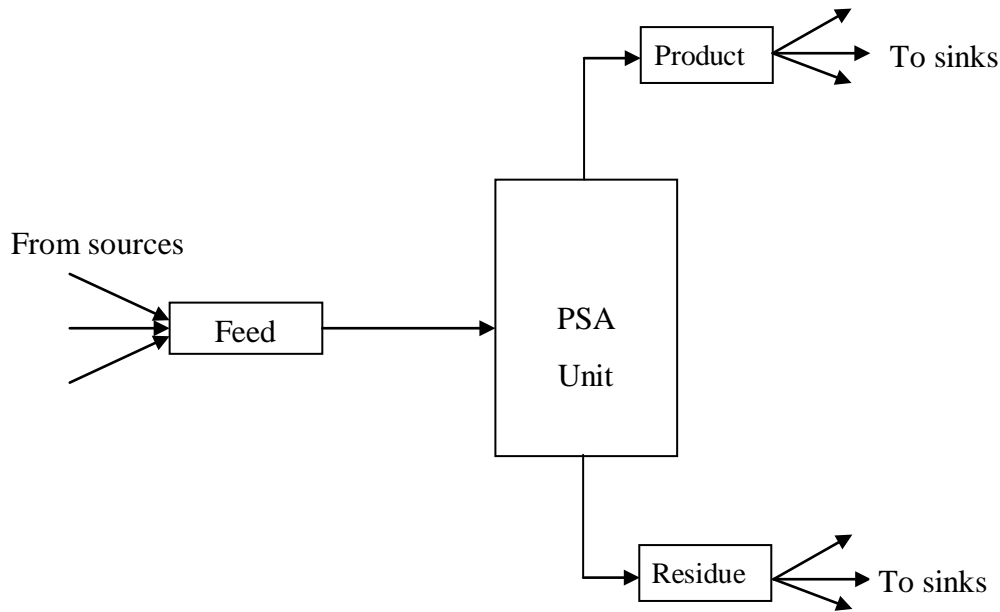


Figure 3.7: Simplified PSA flow diagram

$$F_{\text{in},m} = \sum_{\delta} F_{\delta,m} \quad \forall \delta \in h, u, k, n \quad (3.38)$$

$$y_{\text{in},m} = \frac{\sum_{\delta} F_{\delta,m} y_{\delta}}{\sum_{\delta} F_{\delta,m}} \quad \forall \delta \in h, u, k, n \quad (3.39)$$

$$F_{\text{prod},m} = \frac{\text{Rec} * F_{\text{in},m} * y_{\text{in},m}}{y_{\text{prod},m}} \quad (3.40)$$

$$F_{\text{resid},m} = F_{\text{in},m} - F_{\text{prod},m} \quad (3.41)$$

$$y_{\text{resid},m} = \frac{F_{\text{in},m} * y_{\text{in},m} (1 - \text{Rec})}{F_{\text{resid},m}} \quad (3.42)$$

The PSA unit can send its' product stream ($F_{\text{prod},m}$) to the sinks, where the residue stream ($F_{\text{resid},m}$) is sent to the fuel gas system in the integrated plant.

$$F_{prod,m} = \sum_{\varphi} F_{m,\varphi} \quad (3.43)$$

$$F_{resid,m} = \sum_m F_{m,q} \quad (3.44)$$

The existence of the new purifiers is modeled using binary variable X_m . Based on the preceding binary variable X_m , the new purifier inlet flow rate $F_{in,m}$ can be expressed between the lower bound LF and upper bound UF as shown in Equation (3.45).

$$X_m LF \leq F_{in,m} \leq X_m UF \quad (3.45)$$

The objective function is formulated in terms of total annual cost (TAC), which consists of operating costs and annualized capital cost. The operating costs are made up of the hydrogen costs plus the cost of electricity used in compression work minus the fuel credit created by burning the fuel gas. The capital costs are made up of the investment costs of new compressors, purifiers and pipes. Thus, the objective function is defined as:

$$TAC = (OC_{H_2} + OC_{Elc} - CR_{Fuel}) + AF * (\sum Cap_n + \sum Cap_m + C_{pipes}) \quad (3.46)$$

Hydrogen cost OC_{H_2} is calculated as a function of hydrogen plant flow rate $F_{H_2 plant}$ multiplied by hydrogen production cost unit C_{H_2} and operating days per year OD .

$$OC_{H_2} = F_{H_2 plant} * C_{H_2} * OD \quad (3.47)$$

Electricity cost OC_{Elc} is calculated as a function of the power required to operate the existing and new compressors $[\sum_k Pwr_k + \sum_n Pwr_n]$ multiplied by unit cost of electricity C_{Elc} and operating days per year OD .

$$OC_{Elc} = [\sum_k Pwr_k + \sum_n Pwr_n] * C_{Elc} * OD \quad (3.48)$$

The fuel credit CR_{Fuel} is calculated as function of heat value LHV for hydrogen and methane, unit cost of fuel gas CRF and operating days per year OD . $y_{sink,q}$ is the purity of hydrogen in fuel gas.

$$CR_{Fuel} = OD * CRF * F_{sink,q} (LHV_{H_2} y_{sink,q} + LHV_{CH_4} (1 - y_{sink,q})) \quad (3.49)$$

The annualizing factor (AF) is calculated using Equation (3.50), where i is the annual interest rate and n is the number of years [74].

$$AF = \frac{i(1+i)^n}{(1+i)^n - 1} \quad (3.50)$$

The capital cost of the new compressor Cap_n is calculated as a function of its power as shown in Equation (3.51). The coefficients a_n and b_n are constants at 150 and 1.91, respectively [19].

$$Cap_n = a_n + b_n Pwr_n \quad (3.51)$$

The capital cost of the new purification unit Cap_m is calculated as a function of its inlet flow rate as shown in Equation (3.52). The coefficients a_m and b_m are constants as 503.8 and 347.4 [19].

$$Cap_m = a_m + b_m * F_{in,m} \quad (3.52)$$

The capital cost of the pipe lines C_{pipes} is assumed to equal to 15% of the summation of the capital cost of the new compressors and purification units [18].

The nature of hydrogen management model as represented by Equations 3.18 – 3.52 is an MINLP. The reason is because the model combines discrete variables and non-linear functions. The discrete variables are used to model the existence of the new equipment as well as the pressure differences between the new units and the rest of the network. The non-linearity is due to the bilinear terms in Equations (3.22), (3.25), (3.30), (3.39), (3.42) and (3.49). In addition, the new compressor power expressed by equations (3.35) and (3.36) are also non-linear.

3.4.2 Integrated model

The hydrogen management model is integrated with the materials-processing system model developed in section (3.3) to form the integrated model. The objective function for the integrated model can now be formulated as profit function Ψ .

$$\text{Max } \Psi = \text{TEP} - \text{TAC} \quad (3.53)$$

where TEP is the total enterprise profit as per Equation 3.5 and TAC is the total annual cost as per Equation 3.46.

3.5 Model linearization

The materials-processing system model and hydrogen management model developed in sections 3.3 and 3.41, respectively, were formulated as MINLP. Solving an MINLP model directly requires large computational efforts and may sometimes result in inconsistency in solution quality and time.

This section presents the development of linearization techniques for both the materials-processing system model and hydrogen management model. As a result, the models are transformed into MILP which requires lower computational efforts as well as CPU time.

3.5.1 Materials-processing System Model Linearization

Linearization of CDU model

The CDU model is linearized by fitting the TBP curve using linear regression as shown in Figure 3.8. The volume% is set as a dependent variable and cut temperature is set as an independent variable in order to use it in the model for calculating volume % of each product based on its cut temperature. The coefficient of determination (R^2) for the linear fit is 0.996, which reflect the validity of the regression line for representing the relationship between Volume % and cut temperature. The regression line equation is written in a general form using notations as explained in section 3.3.1.

$$\text{cut}_s = \sum_{g=0}^1 a_g (\text{TE}_{\text{CDU},s})^g \quad \forall s \in S_{\text{CDU}} \quad (3.54)$$

The slope and intercept of the CDU Equation (3.54) are listed in Tables (3.3). For example, the kerosene cut can be calculated as:

$$V\%_{KERO} = -9.826 + 0.159T_{CDU,KERO}$$

Table 3.3 also presents the coefficients for the linear property models for each of the CDU products.

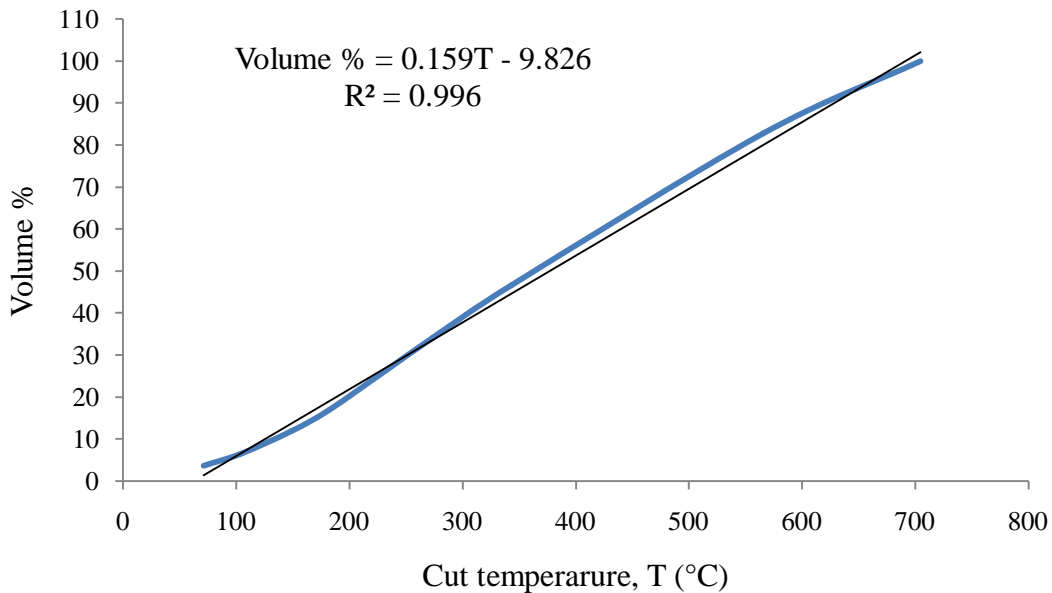


Figure 3.8: Volume % accumulated at different cut temperature

Table 3.3: The slope and intercept of the CDU model equations

Parameter	Cut				
	LN	KERO	DIES	VGO	RSD
a_0	- 9.826	- 9.826	- 9.826	- 9.826	- 9.826
a_1	0.159	0.159	0.159	0.159	0.159
	API				
	LN	KERO	DIES	VGO	RSD
a_0	98.61	61.41	56.55	44.03	48.37
a_1	-8.45	-0.90	-0.67	-0.37	-0.44
	N%				
	LN	KERO	DIES	VGO	RSD
a_0	-	-0.0024	-0.013	-0.191	-0.982
a_1	-	0.0002	0.0006	0.005	0.017
	S%				
	LN	KERO	DIES	VGO	RSD
a_0	0.0015	-0.28	-0.342	-0.258	-2.86
a_1	0.0002	0.0217	0.0243	0.0216	0.0627

Linearization of CDU Products properties versus Mid Volume% curves

The CDU product properties as a linear function of the Mid v% are also fitted using linear regression. To improve the representation, the Mid v% range of the crude oil is divided into regions based on Mid v% ranges of crude oil fractions. This means for every crude oil fraction, the Mid v% has an upper and a lower bound corresponding to its swing cut temperature.

The relation between °API and Mid v% crude oil is fitted as stand-alone region using linear regression as shown in Figure 3.9. The entire regions give good representation. However, for the HN region, which resulted in poor representation as indicated by R² value 0.805, a series of straight-line segment is used to improve the linear models as shown in Figure 3.10. Integer variables can be used in the model to ensure that only one of the straight-line segments is chosen at a time.

This procedure is carried out for linearizing the relationship between mid volume% and nitrogen content as well as mid volume% and sulphur content. Then, the properties of CDU fractions can be written in a general form as shown in equation 3.55.

$$PV_{CDU,s,p} = \sum_{g=0}^1 a_{k,p,s} (MidV)_s^g \quad s \in S_{CDU}, p \in P_s \quad (3.55)$$

$PV_{CDU,s,p}$ represents different properties p for each product s from the CDU unit. P_s is the set of all the properties calculated for the specified stream s . The slope and intercept of the CDU Equation 3.55 are listed in Tables 3.3.

For calculating °API and sulfur content at HN region, integer variable y_d ($d \in D$, D is the number of segments) are introduced into the model to choose only one segment at a time. This is given by Equation 3.56. The slope and intercept of the CDU Equation 3.56 are listed in Tables 3.4. In Table 3.4, a_{01} and a_{11} represent the intercept and slope of the first straight-line segment equation while a_{02} and a_{12} represent the intercept and slope of the second straight-line segment equation for °API and %sulfur properties.

$$PV_{HN,API} = \sum_{d=1}^D \sum_{g=0}^1 a_{g,API,HN,d} (MidV)_{API,HN,d}^g * y_d \quad (3.56)$$

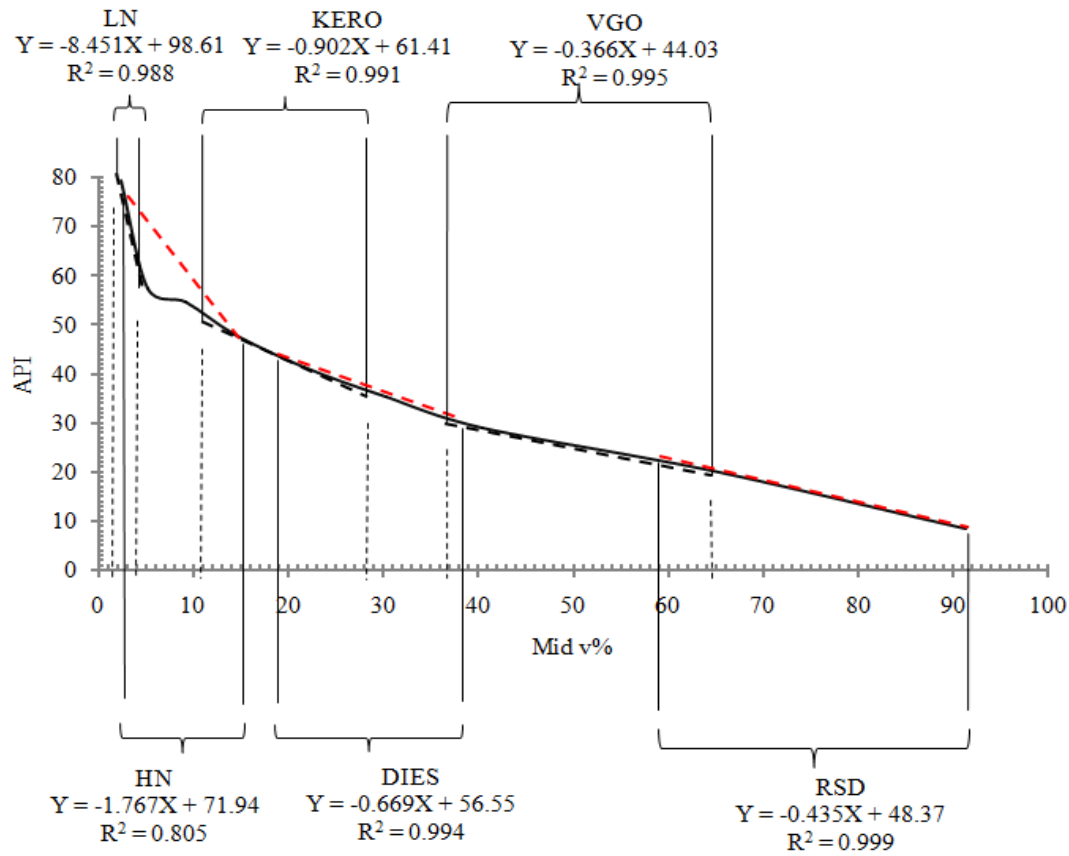


Figure 3.9: °API as a function of Mid v% regions of CDU fractions

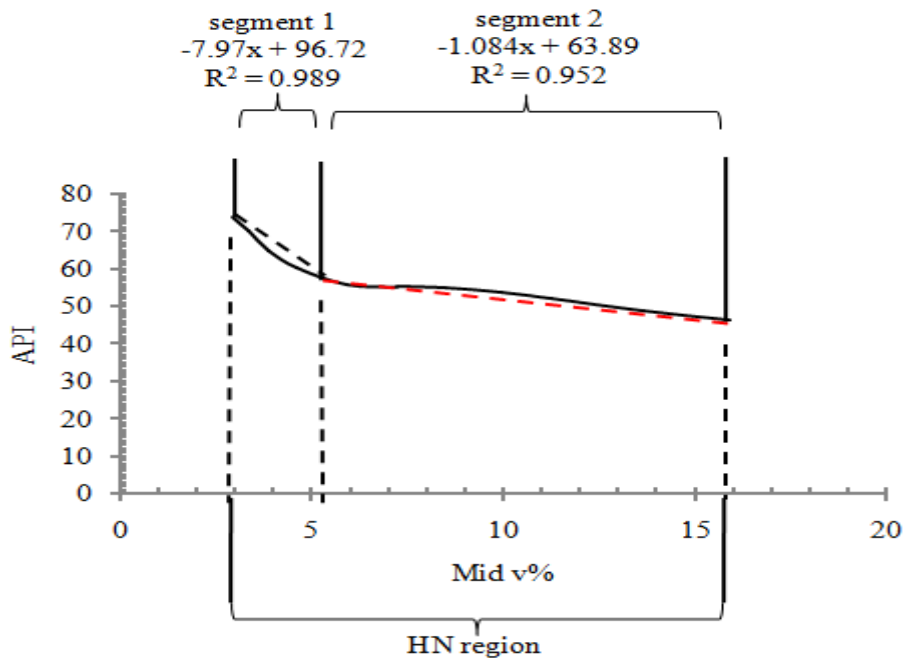


Figure 3.10: °API as a function of mid volume% of HN region

As shown in Equation (3.56), the introduction of the integer variable (y_d) resulted in non-linear function due to the multiplication of the integer variable y_d with the variable MidV. The linearizing of Equation (3.56) can be performed by first defining a new variable C_d for the multiplication of the variable MidV and the integer variable y_d as shown in equation (3.57).

$$C_d = \text{MidV}_d * y_d \quad (3.57)$$

Then, the non-linear term ($\text{MidV}_d * y_d$) can be linearized by adding the following constraints into the model.

$$0 \leq C_d \leq \text{MidV}_d \quad (3.58)$$

$$\text{MidV}_d - \text{MidV}_d^{up} (1 - y_d) \leq C_d \leq \text{MidV}_d^{up} y_d \quad (3.59)$$

Table 3.4: The slope and intercept of the CDU model equations: HN fraction

Parameter	°API	%sulfur
a ₀₁	96.72	-0.008
a ₁₁	-7.97	0.001
a ₀₂	63.89	-0.163
a ₁₂	-1.08	0.013

Where MidV_d^{up} is a maximum upper bound on MidV_d . Then, an exclusive-or logic constraint is used to select only one segment at a time from a number of segments (D). This is represented using Equation (3.60).

$$\sum_{d=1}^D y_d = 1 \quad (3.60)$$

See Appendix C, examples C3 and C4, for an illustration of straight-line segment series models.

Linearization of Refinery Hydrotreating Units Models

The refinery hydrotreating units models are developed with the aid of HPI correlations [93]. The models are written in such way that, the dependent variable (product yields or properties) is modeled as a function of independent variables

(properties of streams entering the processing unit). Therefore, a set of dependents and independents variable is generated based on mid volume% range of each products coming from the CDU unit and it is destination is the petroleum refinery hydrotreating unit. Then, the data set is fitted using multiple linear regressions in order to use it in the model for calculating products yield and properties of the processing units. This is can be written in a general form as follows.

For the generated data set $\{y_i, x_{i1}, x_{i2} \dots \dots, x_{ip}\}_{i=1}^n$, where n is the data set of mid volume% range of each crude oil fraction. The relationship between the dependent variable y_i and the p-vector of independent variables x_i is modeled using multiple linear regressions. Thus the model takes the following form [98].

$$y_i = \beta_1 x_{i1} + \beta_2 x_{i2} + \dots + \beta_p x_{ip} + \varepsilon_i = x_i^T \beta + \varepsilon_i \quad i = 1, 2, 3 \dots \dots n \quad (3.61)$$

The values of the coefficients β which fit equation (3.61) are calculated using spreadsheet based on the following matrix form [99].

$$\beta = (X^T X)^{-1} X^T Y \quad (3.62)$$

Linearization of Bilinear Terms

Bilinear term refers to the status of multiplying two variables. For example, if (q) and (p) are variables. Its multiplication ($q * p$) is defined as a bilinear term. This bilinear term can be relaxed using the following set of inequality constraints [75].

$$qp \geq q^{low} \cdot p + q \cdot p^{low} - q^{low} \cdot p^{low} \quad (3.63)$$

$$qp \geq q^{up} \cdot p + q \cdot p^{up} - q^{up} \cdot p^{up} \quad (3.64)$$

$$qp \leq q^{low} \cdot p + q \cdot p^{up} - q^{low} \cdot p^{up} \quad (3.65)$$

$$qp \leq q^{up} \cdot p + q \cdot p^{low} - q^{up} \cdot p^{low} \quad (3.66)$$

In the linearized Equations (3.63) through (3.66), qp is new variable defined to represent the multiplication of the bilinear variables q and p . q^{low} , q^{up} , p^{low} and p^{up} represents the lower and upper pounds of the q and p variables, respectively.

Linearization of Capital cost Model

The “n” exponent factor rule for estimation of capital cost is linearized by consideration of a linear function of a base cost. The non-linear relation in Equation (3.13) is segmented by employing a series of straight-line. Integer variable y_h is used to model the selection of straight line segments. The linear cost term is expressed as:

$$\text{cost B} = \text{costA} \left[\sum_{h=1}^H \sum_{g=0}^1 a_{g,h} * \left(\frac{\text{size B}}{\text{size A}} \right)_h^g * y_h \right] \quad (3.67)$$

where, $h \in H$ is the number of straight line segment while g is the degree of polynomial.

An exclusive-or logic constraint is used to ensure that only one of the straight-line segments is chosen at a time. This is represented using the following equations.

$$\sum_{h=1}^H y_h = 1 \quad (3.68)$$

The multiplication of the non-linear term $\left(\frac{\text{size B}}{\text{size A}} \right)_h^g * y_h$ in equation (3.67) can be linearized using the same techniques used for linearizing equation (3.57).

3.5.2 Linearization of Hydrogen Management Model

The new compressor power Equations (3.35) and (3.36) are non-linear because the suction pressure PI_n , discharge pressure PO_n and feed flow rate $F_{in,n}$ are variables. A common technique to linearize these equations is by assuming fixed suction and discharge pressures, hence making the power equation as a linear function of the flow rate only [45, 70 - 72]. In this work, the new compressor power equations are linearized by fixing the suction pressure PI_n to be the lowest pressure amongst all inlet sources feeding the new compressor. In practice, this is possible by throttling sources stream at higher pressure through let-down valves. Consequently, the new compressor is able to receive all pressure sources in the network. Then, the pressure ratios between the pressures of sinks in entire network and the suction pressure of the new compressor PI_n are calculated. Each pressure ratio is assumed to be representing

a new compressor. The number of the new compressors in the network is modeled using logic constraint, as shown in Equation 3.69. The term θ is the number of the new compressors allowed in the network. Equation 3.70 is used to set the discharge pressure of the new compressor PO_n to zero when X_n is equal to zero, where X_n is a binary variable to represent the existence of the new compressor, UPO_n is the upper bound of the discharge pressure of the new compressor.

$$\sum_n X_n \leq \theta \quad (3.69)$$

$$PO_n - X_n UPO_n \leq 0 \quad (3.70)$$

After knowing the pressure ration of each of the compressor, the power of the new compressor can be expressed as a function of inlet flow rate using equations 3.71 and 3.72. Pwr_n is the power of the new compressor. $UPwr$ is the upper bound of the power of the new compressor. X_n is a binary variable to represent the existence of the new compressor. γ_n is a constant. This constant depends of the suction and discharge pressure of the new compressor.

$$Pwr_n - UPwr(1 - X_n) \leq \gamma_n F_n \quad (3.71)$$

$$Pwr_n - UPwr(X_n - 1) \geq \gamma_n F_n \quad (3.72)$$

The main feature of this technique is that it provides more degree of freedom for the optimizer to choose appropriate compressors among different compressors with different discharge pressures.

See Appendix C, example C5, for an illustration of the linearized model of calculating the power of the new compressor.

3.6 Mathematical Programming

The mathematical programming models developed in this chapter are coded into general algebraic modeling system (GAMS) and shown in Appendix F. GAMS is a high-level modeling system that provides a flexible framework for formulating and

solving linear, nonlinear, mixed integer linear and nonlinear optimization problems [100]. It comprises language compiler and a stable of integrated high-performance solvers. Figure 3.11 shows the general structure of GAMS, which describes the basic steps towards optimization problem formulation. As shown in Figure 3.14, Data can be represented in form of Sets, Parameters, Tables and Scalar. After setting the data, user must specify all the variables and equations representing the objective function and constrains. After all Data has been entered and the model developed, the user must choose either to minimize or maximize the objective function, as well as choosing the solver required to solve the optimization problem.

GAMS processes the input file in two stages, namely compilation and execution. In the compilation stage, the compiler will check for syntax errors and ensure that an appropriate solver is used. When the compiler finds errors, the errors will be written in the output file before GAMS terminates. The user must modify the input file

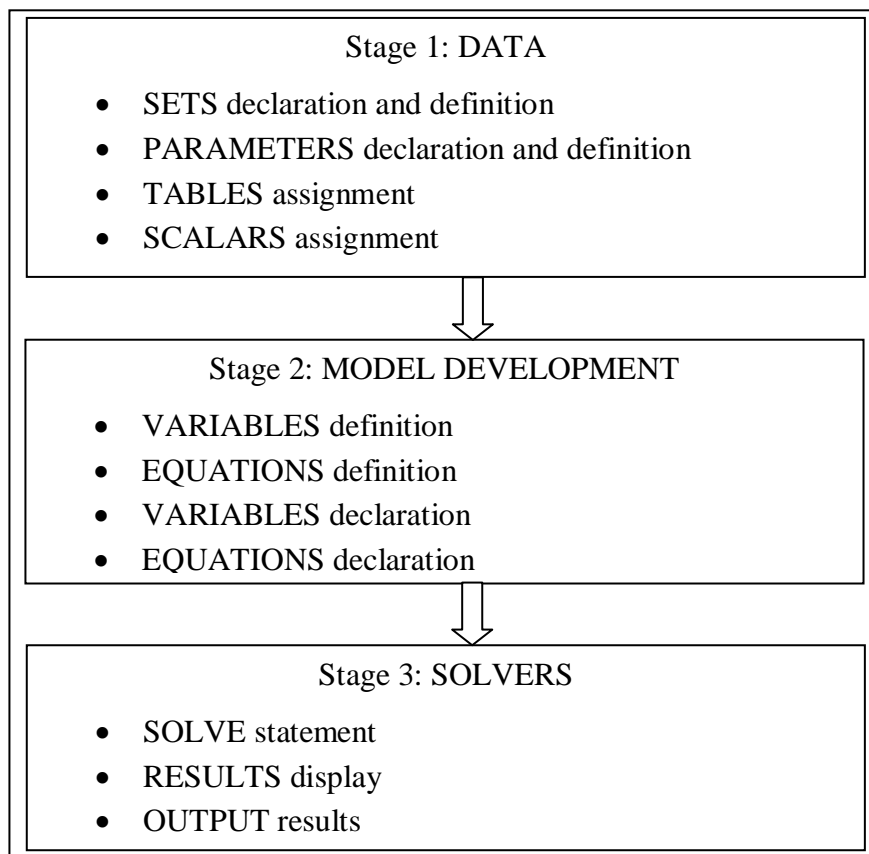


Figure 3.11: General structure of GAMS representation

accordingly. Once the compilation is done successfully, then GAMS will process to the execution stage. At execution stage GAMS will carry out the optimization processes based on the selected solver. The solver declared by the user must be applicable to the formulation. For instance, an MILP solver cannot be used to solve an MINLP problem.

GAMS LP and MILP solver

The common solver for LP and MILP is BDMLP. BDMLP comes as standard package with any GAMS system; it is part of the GAMS/BASE module. BDMILP solver uses simplex algorithm for solving LP problems and branch-and-bound algorithm for solving MIP problems. The MIP part of GAMS/BDMLP provides free access to a MIP solver that supports all types of discrete variables supported by GAMS.

GAMS NLP solvers

Nonlinear models created with GAMS must be solved with a nonlinear programming algorithm. Currently, there are three standard NLP algorithms available in GAMS: CONOPT, MINOS and SNOPT. CONOPT solver is available in two versions, the old CONOPT and the new CONOPT2. The algorithm used in GAMS/CONOPT is based on generalized reduced gradient (GRG) algorithm. The similarity among all the NLP solvers is that their developed algorithm attempt to find a local optimum. However, the algorithms in CONOPT, MINOS, and SNOPT are all based on fairly different mathematical algorithms and behave differently on most models. This means that CONOPT may perform better for some models while MINOS or SNOPT may also superior for some other models. Even CONOPT and CONOPT2 behave differently; the new CONOPT2 is best for most models, but there are a small number of models that are best solved with the older CONOPT. There are some rules of thumb used to choose the appropriate solvers. For example, GAMS/CONOPT2 is well suited for models with very nonlinear constraints. Besides, CONOPT2 solver can quickly find a first solution that is particularly with few degrees of freedom. On the other hand, if the model contains little nonlinearity outside the objective function, then either MINOS or SNOPT are probably the best solver.

GAMS MINLP solver

The common solver for MINLP problem that involve linear binary or integer variables and linear and nonlinear continuous variables is DICOPT. DICOPT solver is based on the extensions of the outer-approximation algorithm for the equality relaxation strategy. The MINLP algorithm inside DICOPT solves a series of NLP and MIP sub-problems. These sub-problems can be solved using any NLP or MIP solver that runs under GAMS. Although the algorithm has provisions to handle non-convexities, it does not necessarily obtain the global optimum

3.7 Summary

In this chapter, a superstructure framework is developed for enterprise plant network synthesis that integrates a new stand-alone pyrolysis-based bio-refinery into an existing stand-alone petroleum refinery. The superstructure is modeled based on materials-processing system as an MINLP. The objective of the developed model is to synthesize optimum enterprise network among the different options presented in the superstructure.

In order to meet the hydrogen demand of the enterprise plant, an MINLP hydrogen management model is formulated and integrated with materials-processing system model to form an integrated model. The objective of the integrated model is to simultaneously synthesize optimum enterprise network between bio-refinery and petroleum refinery and synthesize optimum hydrogen network to meet the enterprise hydrogen demand.

The optimization of MINLP problems requires large computation efforts and may results in inconsistency in model solution and time required. Therefore, the computations of the MINLP materials-processing system model and MINLP hydrogen management model are improved by developing linearization techniques. This is in order to transform the MINLP models into MILP models, which require less computational efforts and shorter time to converge.

CHAPTER 4

OPTIMIZATION USING MATERIALS-PROCESSING MODEL

4.1 Introduction

This chapter illustrates case studies to demonstrate the materials-processing system model for synthesizing optimum enterprise network between a new pyrolysis-based bio-refinery and an existing petroleum refinery. The aim of synthesizing the enterprise network is to systematically integrate a new pyrolysis-based bio-refinery into an existing petroleum refinery. The synthesis of the enterprise plant network is investigated and compared based on two options of operational scenarios. These options are stand-alone plants and enterprise plant. The stand alone plants bio-refinery and petroleum refinery are formulated as linear programming (LP) and non-linear programming (NLP) models, respectively. On the other hand, the enterprise plant is formulated using logic-based MINLP model to synthesize an optimal enterprise network for the processing of bio-refinery intermediates inside a petroleum refinery. The models are coded into GAMS and solved using BDMLP, CONOPT and DICOPT solvers for LP, NLP and MINLP models, respectively.

4.2 Model Validation

In this study, the materials-processing system model is demonstrated using the petroleum refinery standalone plant shown in Figure 1.5. The refinery flow sheet is adopted from Elkamel et al. [27] with a basis of 100,000 bbl/d crude oil feedstock at 26.4°API and crude oil price of 46.79 \$US/bbl (2008 price). The products prices and demand as well as their specifications are adopted from Table 2.1. The maximum capacities of petroleum refinery processing units are adopted from Table 2.2. The

model is implemented into GAMS and solved with CONOPT solver. The model optimizes all intermediates and final product streams across the petroleum refinery subject to constraints of processing units sub-models, connectivity, processing unit capacity and final products demand and quality specifications. The CDU is modeled using Equations 3.1 to 3.4, while the other processing units are modeled using the sub-models shown in Appendix D. The connectivity is modeled using Equations 3.6 and 3.11. The processing unit capacity is modeled using Equation 3.10. The final products demand and quality specifications are modeled using Equations 3.14 to 3.17. The objective function is set in term of profit and expressed by subtracting feedstock and operating costs from the revenue. The optimization of this problem satisfied the blending pools final products demand and quality specifications and resulted in a maximum profit of \$763MM/yr. Table 4.1 summarizes the optimization results for each blending pool product stream flow rate and properties. The results of this optimization are validated against Elkamel et al. [27]. As shown in Table 4.1, the deviation between the current results and the work done by Elkamel et al. [27] were

Table 4.1: Optimization results and comparison of petroleum refinery standalone plant

Blending pool	Elkamel et al. [94]	This study	Deviation (%)
Gasoline (bbl/day)	28,420	29,749	4.68
SG	0.795	0.757	4.78
SUL%	0.003	0.003	0
RON	91.5	93.0	1.64
RVP (psi)	8.9	8.6	3.37
Jet fuel (bbl/day)	25,850	25,017	3.22
SG	0.835	0.803	3.83
SUL%	0.2	0.191	4.50
SP	20.8	20.11	3.32
Diesel (bbl/day)	25,550	25,000	2.15
SG	0.86	0.872	1.16
SUL%	0.07	0.073	4.29
CN	52	49.9	4.04
Fuel oil (bbl/day)	18,805	18,729	0.40
SG	1	1	0
SUL%	0.2	0.203	1.50
Profit (\$MM/yr)	740	763	3.11

found to be less than 5%. Nevertheless, these minor percentage differences in the results validate the capability and flexibility of the materials-processing system model formulation to model the complexity of petroleum refinery operations, hence enterprise operations.

4.3 Standalone plant optimization

The standalone petroleum refinery shown in Figure 1.5 illustrates a typical representation of an existing petroleum refinery. This refinery is optimized with an objective function of maximizing the profit subjected to constraints of processing units sub-models, connectivity, processing unit capacity and final products demand and quality specifications. The CDU is modeled using Equations 3.1 to 3.4, while the other units are modeled using the sub-models shown in Appendix D. The connectivity is modeled using Equations 3.6 and 3.11. The processing unit capacity is modeled using Equation 3.10. The final products demand and quality specifications are modeled using Equations 3.14 to 3.17. The objective function is expressed by subtracting feedstock and operating costs from the revenue. The crude oil and final products prices are updated to June 2013 prices and shown in Table 4.2. The model is implemented into GAMS and solved with CONOPT solver. Table 4.3 shows the optimization results for each blending pool. The results are summarized in terms of blending pool final product quantity and properties. As shown in Table 4.3, the optimization satisfied the blending pools final products demand and quality specifications with a total profit of \$457MM/yr. For example, the gasoline pool meets the gasoline quantity demand and SG, SUL%, RON and RVP properties specification.

In order to demonstrate the model performance on standalone bio-refinery, the standalone pyrolysis-based bio-refinery shown in Figure 4.1 is used in this study. A 2,150 ton/day of wood chip biomass [11] is used as feedstock. The purchase price for the biomass feedstock is \$83/metric ton [102]. The bio-refinery processing units capital costs are indexed to 2011 US dollars [103]. The details of capital cost calculations are shown in Appendix E. The objective function is to maximize the overall bio-refinery profit subject to constraints of processing units sub-models,

connectivity, processing unit capacity and final products demand and quality specifications. The bio-refinery processing units are modeled using bio-refinery sub-models shown in Appendix D. The connectivity is modeled using Equations 3.6 and 3.11. The processing unit capacity is modeled using Equation 3.10. The final products

Table 4.2: Crude oil and final products prices [101]

Component	Price \$/bbl
Crude oil	92.02
Gasoline	133.64
Kerosene (jet fuel)	119.45
Diesel	119.28
Fuel oil	76.10

Table 4.3: Optimization results of the existing petroleum refinery stand-alone plant

Blending pool	Optimization Results
Gasoline (bbl/day)	26,595
SG	0.750
SUL%	0.004
RON	90.0
RVP (psi)	8.50
Jet fuel (bbl/day)	28,156
SG	0.802
SUL%	0.183
SP	20.0
Diesel (bbl/day)	25,216
SG	0.871
SUL%	0.076
CN	50.01
Fuel oil (bbl/day)	18,720
SG	1
SUL%	0.203
Profit (\$MM/yr)	457

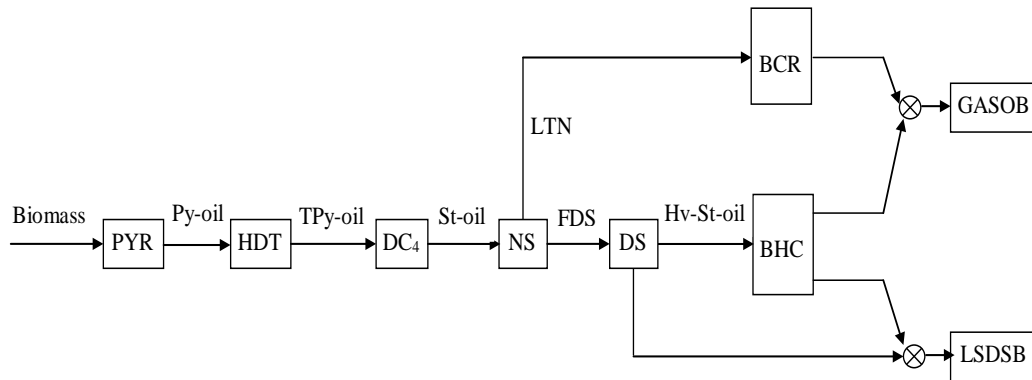


Figure 4.1: Standalone fast-pyrolysis based bio-refinery [11].

demand and quality specifications are modeled using Equations 3.14 to 3.17. The profit is expressed by subtracting feedstock and operating costs from revenue. The model is coded into GAMS and solved using BDMLP solver. Table 4.4 shows the optimization results for each blending pool final product stream flow rates and properties. The values in the last column of Table 4.4 show that the optimum product specifications are within the desired values except for the SG of Diesel, which is set at

Table 4.4: Optimization results of the bio-refinery stand-alone plant

Blending pool	Product stream	Flow rate (Bbl/day)	Final product (Bbl/day)	Product property	Property value
Gasoline	RefBCR	1500	2357	SG	0.738
	LTNBHC	857		SUL%	0.0002
				RON	91.9
				RVP (psi)	7.85
Diesel	DBHC	36	362	SG	0.87
	DSL	326		SUL%	0.01
				CN	47.3
Unblended product	DSL	2644	2644	SG SUL%	0.874 0.011

the limit. This is because, the diesel form diesel splitter (DSL) is characterized by its higher SG of 0.874 [11, 94]. As a result, the model allowed only 11% of DSL amount to be blended into the diesel pool. The unblended diesel will be sold as fuel oil since its specifications are in compliance with the specifications of the fuel oil pool as shown in Table 2.1. This optimization achieved maximum profit of \$76 MM/year, hence a payback period of 4.6 years against 347 MM\$ investment cost. The combined profit of standalone bio-refinery and petroleum refinery is \$533 MM/year.

4.4 Enterprise plant optimization

The superstructure shown in Figure 4.2 is used in this study to demonstrate the application of the materials-processing system model in synthesizing optimum enterprise network for integrating a new bio-refinery into existing petroleum refinery. 100,000 bbl/day of crude oil with 26.4°API (92.02\$US/bbl) is used as feedstock for the existing petroleum refinery and 2150 ton/day of wood chip biomass [11] is used as feedstock for the bio-refinery. The biomass feedstock is purchased at \$83/metric ton [102]. The enterprise capital costs are indexed to 2011 US dollars [103]. The details of capital cost calculations are shown in Appendix E. The capital cost comprises bio-refinery processing units' costs and petroleum refinery FCC, HC and CRU retrofit costs. The retrofit cost of modifying the existing petroleum refinery processing unit to process bio-refinery intermediate product is assumed to be equal to the cost of a small petroleum refinery processing units dedicated to process bio-refinery intermediate products [11]. The capital cost of installing a new bio-refinery and retrofitting the existing petroleum refinery is implemented in the model and amortized for 20 years at interest rate of 10%. The integration of the bio-refinery into an existing oil refinery is modeled using binary variables as per equation 3.12. The objective is to synthesize optimal enterprise plant network that is able to maximize the enterprise plant profit as per Equation 3.5 subjected to constraints of processing units' sub-models, connectivity, processing unit capacity, final products demand and quality specifications, logic-based binary variable and capital cost. The CDU is modeled using Equations 3.1 to 3.4, while the other processing units are modeled using the sub-models shown Appendix D. The connectivity is modeled using Equations 3.6 and 3.1

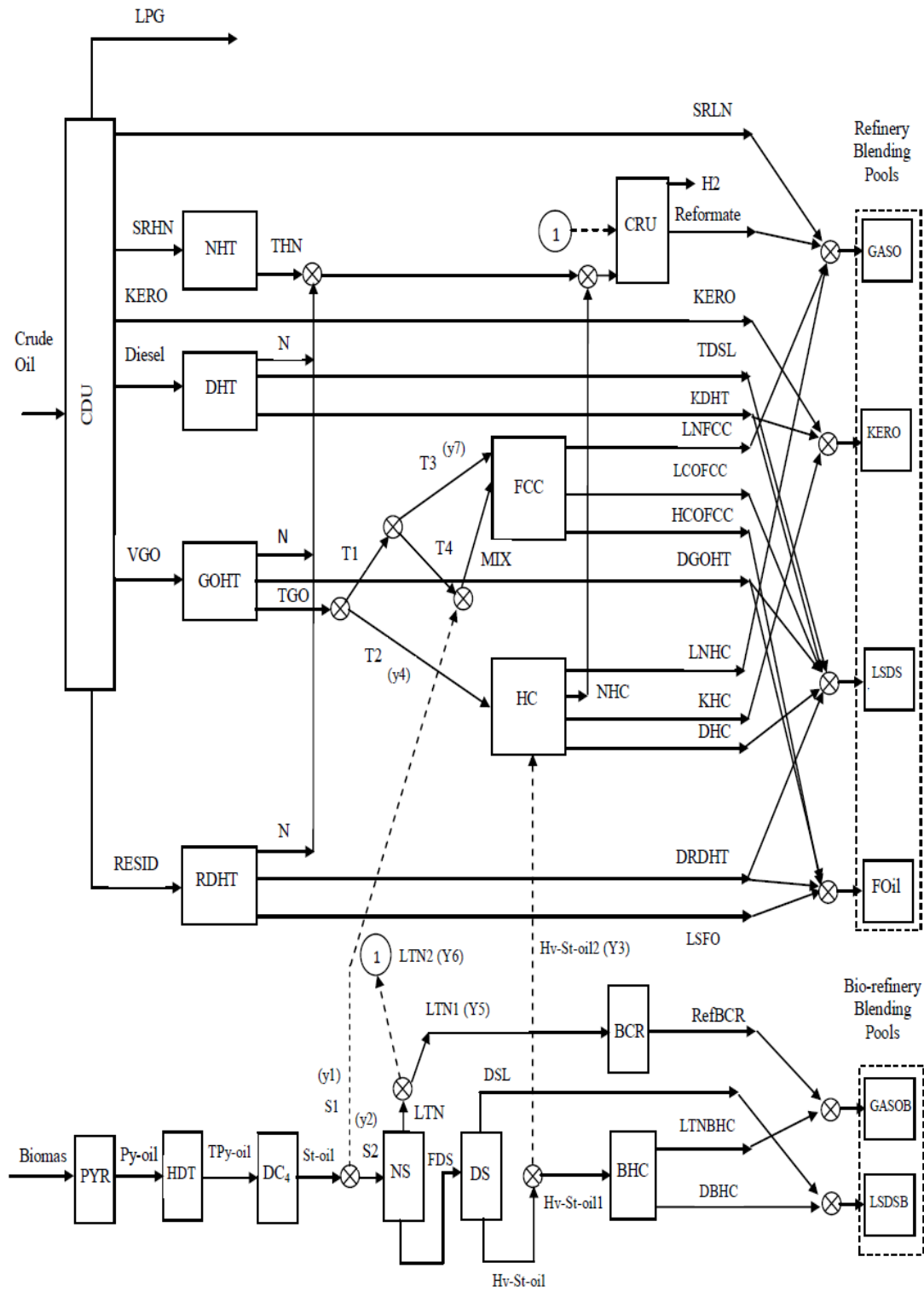


Figure 4.2: Proposed enterprise plant network superstructure representation

The processing unit capacity is modeled using Equation 3.10. The final products demand and quality specifications are modeled using Equations 3.14 to 3.17. The logic-based binary variables for integrating bio-refinery into an existing petroleum refinery are modeled using Equation 3.12. The optimization model considers linearization of capital cost estimation, Equation 3.13, using the technique developed in section 3.5.1 (Equations 3.67 and 3.68). The nature of the model is MINLP due to other nonlinear functions and discrete variables. The model is coded into GAMS and solved using DICOPT solver. Table 4.5 shows the model solutions in the context of blending pools final products and its properties, retrofit cost, capital cost and binary variables of enterprise plant network synthesis. These results show that, the optimal enterprise network meets the existing petroleum refinery products demand and specifications with a total profit of \$551MM/year. The integer variables shown in Table 4.5 indicate that the existing petroleum refinery blending pools are selected by the bio-refinery ($Y2 = Y4 = Y5 = Y7 = 1$) rather than sharing the existing petroleum refinery up-grading units ($Y1 = Y3 = Y6 = 0$).

The superstructure of enterprise plant network shown in Figure 4.2 is optimized again by fixing the binary variables values to the optimum enterprise network values shown in Table 4.5. Furthermore, the objective function is expressed in terms of revenue, raw materials costs and operating cost in order to be compatible with the objective functions of the standalone plants. As a result, the objective function improved to \$591 MM/year.

The net increase in the existing petroleum refinery profit as a result of integrating bio-refinery into existing petroleum refinery is defined as the difference between the profit of the enterprise plant (\$591 MM/year) and that of the existing petroleum refinery (\$457MM/yr). By relating this difference in the profit to the capital investment cost incurred by the enterprise plant after the proposed integration, it was found that, the bio-refinery payback period on the capital investment is 2.6 years. The new payback time is 43% lower compared to the payback period of standalone bio-refinery plant. In addition, the enterprise profit increases by 11% (\$58 MM/year) compared to the combined profits of the stand-alone plants.

Table 4.5: Optimization results of optimum enterprise network between bio-refinery and petroleum refinery

Final product	Flow rate (Bbl/day)	Product property	Property value
Gasoline	27500	SG	0.751
		SUL%	0.003
		RON	90.0
		RVP (psi)	8.70
Jet fuel	30,040	SG	0.823
		SUL%	0.180
		SP	20.40
Diesel	28,008	SG	0.869
		SUL%	0.040
		CN	50.90
Fuel oil	18,557	SG	1.0
		SUL%	0.20
Integer variables			
	Y1=	0	
	Y2=	1	
	Y3=	0	
	Y4=	1	
	Y5=	1	
	Y6=	0	
	Y7=	1	
Retrofit cost (MM \$)		0	
Bio-refinery capital cost (MM \$)		347	
Total capital cost (MM \$)	= (347 + 0) =	347	

4.5 Sensitivity analysis

This section presents the sensitivity analysis with respect to the prices of the final products and the retrofit cost of existing petroleum refinery units to process intermediate products from a new bio-refinery into an existing petroleum refinery. The impact of retrofit cost on the profit of the enterprise plant is first examined. Secondly, the impact of the selling prices of the final products on the profit of the enterprise plant is also evaluated.

The sensitivity of the profit of the enterprise plant is analyzed between 0 and 100% of retrofit cost reduction. The results of the sensitivity analysis are presented in Figure 4.3. Enterprise plant A refers to the optimum enterprise plant network resulted from solving the MINLP model. For enterprise plant A, no retrofit cost reduction is implemented. In this case the integration is only on product blending pool. As shown in Table 4.5, the integer variables Y1, Y3 and Y6 for enterprise plant A are all zeros. Enterprise plant B, however, provides an enterprise plant option where the entire st-oil from DC4 is forced to be processed using petroleum refinery FCC unit. This is in order to trade-off between this option and the enterprise plant A. Y1 and Y2 are fixed as parameters as shown in Table 4.6. Figure 4.3 shows that the profit of the enterprise

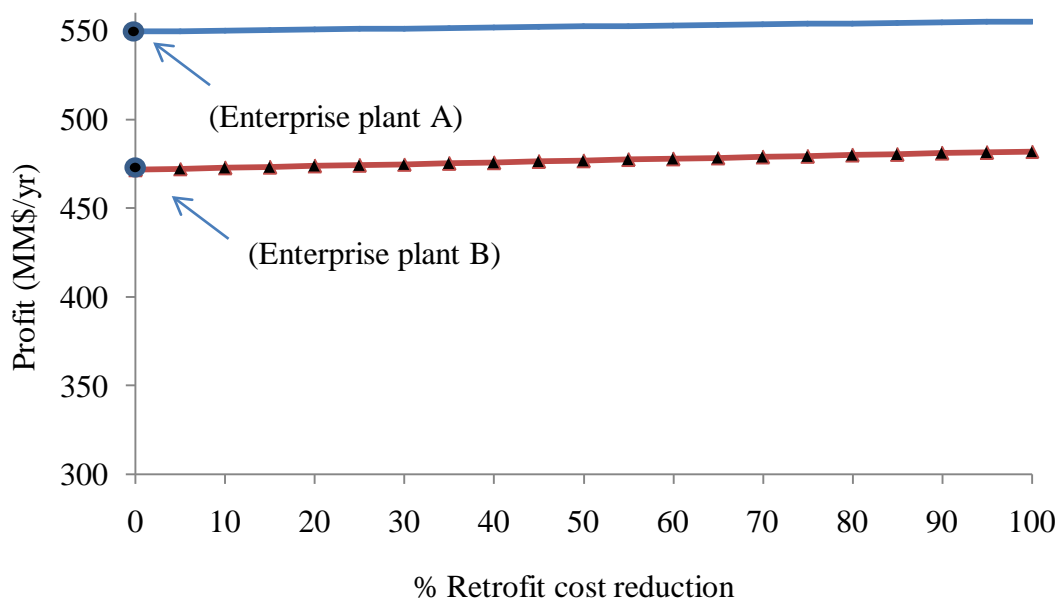


Figure 4.3: Sensitivity analysis results: profit versus % retrofit cost reduction

Table 4.6: Model results of the enterprise plant network between petroleum refinery and bio-refinery (Enterprise plant B)

Final product	Flowrate (Bbl/day)	Product property	Property value
Gasoline	27,454	SG	0.745
		SUL%	0.005
		RON	89
		RVP (psi)	8.41
Jet fuel	31,190	SG	0.810
		SUL%	0.181
		SP	20.04
Diesel	25,000	SG	0.869
		SUL%	0.095
		CN	48.07
Fuel oil	18,845	SG	1
		SUL%	0.211
Integer parameters			
	Y1=	1	
	Y2=	0	
Retrofit cost (MM\$)		87	
Bio-refinery capital cost (MM\$)		288	
Total capital cost (MM\$)		375	

plants A and B increases proportionally to the retrofit cost reduction. The enterprise plant A offers higher profit comparing to the enterprise plant B. This is because the total capital cost of the enterprise plant A is 7.5% lower than the total capital cost of enterprise plant B. Furthermore, the FCC restriction of processing the stable pyrolysis oil in the enterprise plant B affects the products yields from the CDU. Hence the total revenue from selling the final products of the enterprise plant B is 1.8% lower comparing to the revenue from enterprise plant A. As shown in Table 4.7, the optimization increases the yield of VGO of the enterprise plant B by 19.9% comparing to the enterprise plant A. This is in order to provide sufficient amount of

VGO to meet the restriction of processing the entire stable pyrolysis oil using the existing petroleum refinery FCC unit [58]. As a result of increasing VGO yield, the optimization modified the yields of the other products to satisfy the material balance. The kerosene yield increases 15% to substitute for the kerosene coming for HC unit, which is not included in synthesis of enterprise plant B. Furthermore, the heavy naphtha yield and diesel yield are reduced by 74% and 40%, respectively. This is because FCC can provide enough amount of gasoline and diesel to satisfy the demand of gasoline and diesel. From synthesis configuration point of view, the retrofit cost reduction leads to modification of the enterprise plant A by sending the split naphtha to the existing petroleum refinery's CRU rather than being processed in the bio-refinery's BCR while the enterprise plant B remained unchanged.

Table 4.7: CDU unit yields

Fractions	Enterprise plant A	Enterprise plant B
	Yield (%)	Yield (%)
SRLN	5.6	5.6
SRHN	7.8	2
DIES	11.7	7
KERO	19	21.9
VGO	37.7	45.2
RSD	17.3	17.3

The effect of the final products selling prices on the enterprise plant profit is analyzed between 10% decreasing a 10% increasing in the selling prices of final products. Figure 4.4 shows the results of the sensitivity analysis. These results are compatible with sensitivity analysis results presented in Figure 4.3 in that, the optimum enterprise plant for providing higher profit is the enterprise plant A.

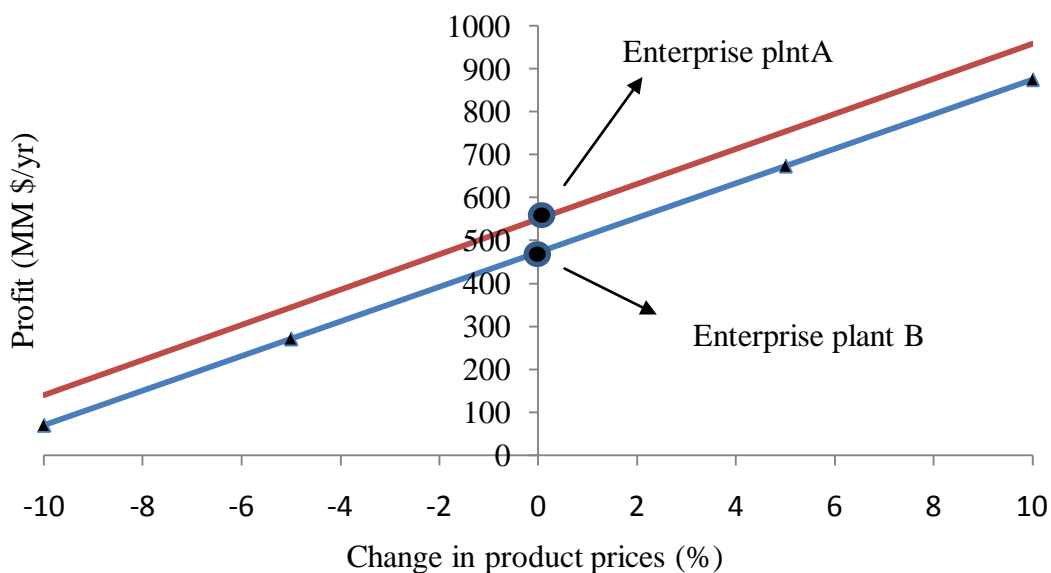


Figure 4.4: Sensitivity analysis: profit versus % increasing and decreasing in final products prices

4.6 Summary

In this chapter, the performance of the materials-processing system model is illustrated on standalone bio-refinery and petroleum refinery as well as an enterprise plant comprising bio-refinery and petroleum refinery. The model results show that, the optimal enterprise plant achieved 11% (\$58 MM/year) higher profit compared to the combined profits of the stand-alone bio-refinery and petroleum refinery plants. As a result, the integrated bio-refinery payback time reduced by 43% compared to the standalone bio-refinery plant operation. Thus, the synthesis of enterprise plant network between bio-refinery and an existing petroleum refinery can be considered as a cost-effective technique for producing affordable renewable transportation fuels.

The results of the sensitivity analysis further show that the effect of petroleum refinery retrofit cost reduction and/or changes in the selling prices of the final products is only notable on the objective function and not on the synthesis of the optimum enterprise network. In all cases, the enterprise plant A was the optimum one.

CHAPTER 5

INTEGRATED MODEL

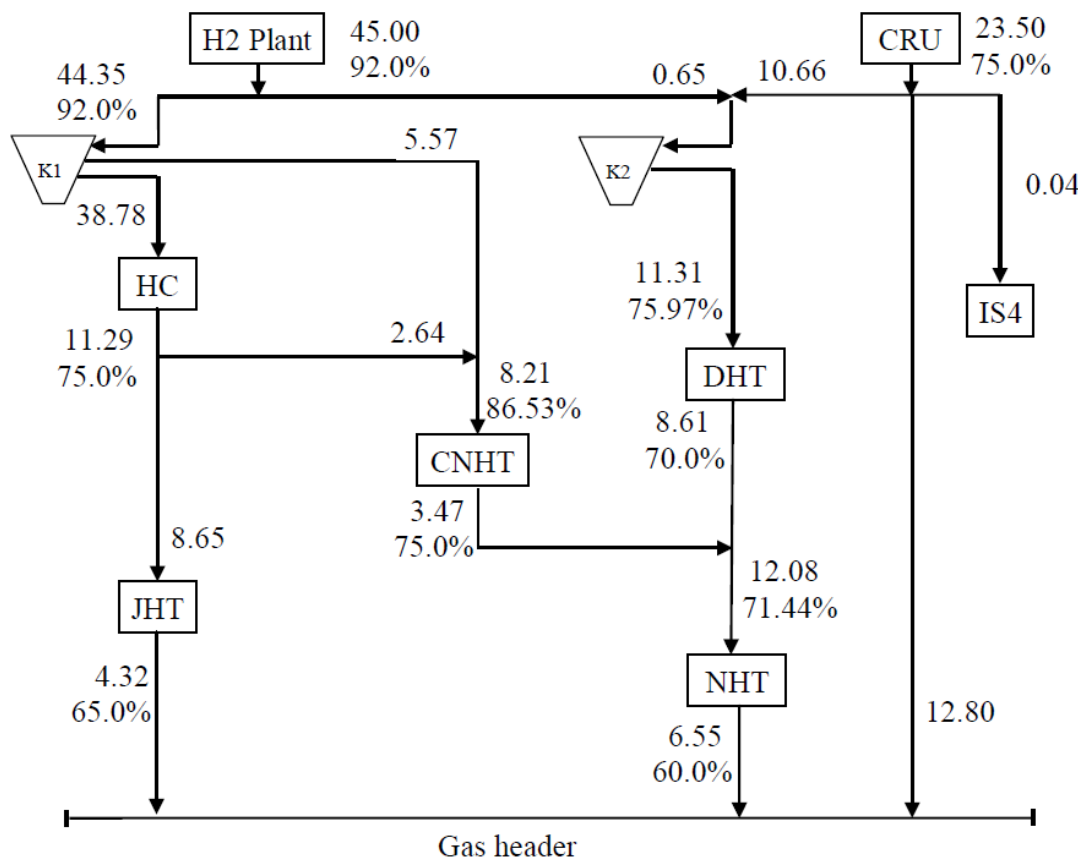
5.1 Introduction

This chapter illustrates case studies to demonstrate the integrated model for enterprise plant hydrogen network synthesis between a new bio-refinery and an existing petroleum refinery. The synthesis of the enterprise plant hydrogen network is investigated and compared based on two options. These options are hydrogen network for stand-alone plants and hydrogen network for enterprise plant. The standalone bio-refinery and petroleum refinery hydrogen networks are formulated as NLP problems. Consequently, the integrated models combining materials-processing system model and hydrogen management model are also formulated as NLPs. On the other hand, the enterprise plant hydrogen network is formulated using logic-based MINLP problem. Accordingly, the formulation of the integrated model for the enterprise plant is an MINLP problem. The objective of the integrated MINLP model is to simultaneously synthesize optimum enterprise network between bio-refinery and petroleum refinery and synthesize optimum hydrogen network to meet the hydrogen requirement of the enterprise plant. The models are coded into GAMS and solved using CONOPT and DICOPT solvers for NLP and MINLP problems, respectively.

5.2 Model Validation

In order to validate the integrated model formulation, the hydrogen network shown in Figure 5.1 is used [22]. As shown in Figure 5.1, hydrogen is supplied from a hydrogen plant (H₂ plant) and a catalytic reforming unit (CRU). Currently, 45 MMscfd of hydrogen at purity of 92% and 23.5 MMscfd of hydrogen at purity of 75%

are produced in the H2 plant and CRU, respectively. Hydrogen is consumed by hydrocracker (HC), diesel hydrotreater (DHT), jet fuel hydrotreater (JHT), cracked naphtha hydrotreater (CNHT), naphtha hydrotreater (NHT) and isomerization plant (IS4). There are two make-up compressors in the system, K1 and K2, and all consumers except isomerisation plant have internal recycle compressors. The network recycle compressors are not shown in Figure 5.1. Table 5.1 shows the flow rate, purity and pressure data for each of the hydrogen consumer's make-up, purge and recycle streams. The current flow rate, maximum flow rate, purity and pressure data for all hydrogen producers are shown in Table 5.2. The temperature data of hydrogen network streams are only needed for calculating the power of the compressor. In this study, the temperature at the inlet of the compressor is assumed to be constant at 520°R [19]. The operating cost data are adopted from Elkamel et al. [19] as follow:



- Flowrate: MMscfd
- Purity: %

Figure 5.1: Hydrogen distribution network [22]

Table 5.1: Hydrogen consumers' data [22]

Process unit	Make-up			Purge			Recycle
	F _m MMscfd	Y _m %H2	Pressure psia	F _p MMscfd	Y _p %H2	Pressure psia	F _R MMscfd
DHT	11.31	75.97	600	8.61	70.00	400	1.56
CNHT	8.21	86.53	500	3.47	75.00	350	36.75
JHT	8.65	75.00	500	4.32	65.00	350	3.6
NHT	12.08	71.44	300	6.55	60.00	200	3.59
IS4	0.04	75.00	300	-	-	-	-
HC	38.78	92.00	2000	11.29	75.00	1200	85.7

Table 5.2: Hydrogen producers' data [22]

Process unit	Flow MMscfd	Max. flow MMscfd	Purity %	Pressure psi
H2 plant	45	50	92	300
CRU	23.5	23.5	75	300

the operating cost of hydrogen is 2,000 \$/MMSCF, the electricity cost is 0.03 \$/KWh and the heat energy gained by burning the fuel gas is 2.5 \$/MMBTU.

Hallale and Liu [22] illustrated a future scenario, where fuel specifications change due to new environmental regulations. As a result, the HC and CNHT units capacities in Figure 5.1 will need to be increased by 40%. The existing hydrogen plant has a maximum capacity of 50 MMscfd and will not be able to cope with significant increase in hydrogen demand. To meet the new hydrogen requirement, the hydrogen network in Figure 5.1 is optimized using the integrated model. Since only a hydrogen network data is available, the amount of hydrogen consumed by hydrogen consumers $cons(u)$ are set in the integrated model, Equation 3.23, as parameter. Table 5.3 shows the values of $cons(u)$. These values are calculated based on the data presented in Table 5.1. At 40% increasing in the capacities of HC and CNHT, the $cons(u)$ of HC and CNHT are 38.094 and 6.303, respectively. The values of hydrogen consumption shown in Table 5.3 are assumed to be representing the optimum values of $cons(u)$ resulted from the materials-processing system model solution. As a result, the objective function of the integrated model as per Equation 3.53 is formulated only in

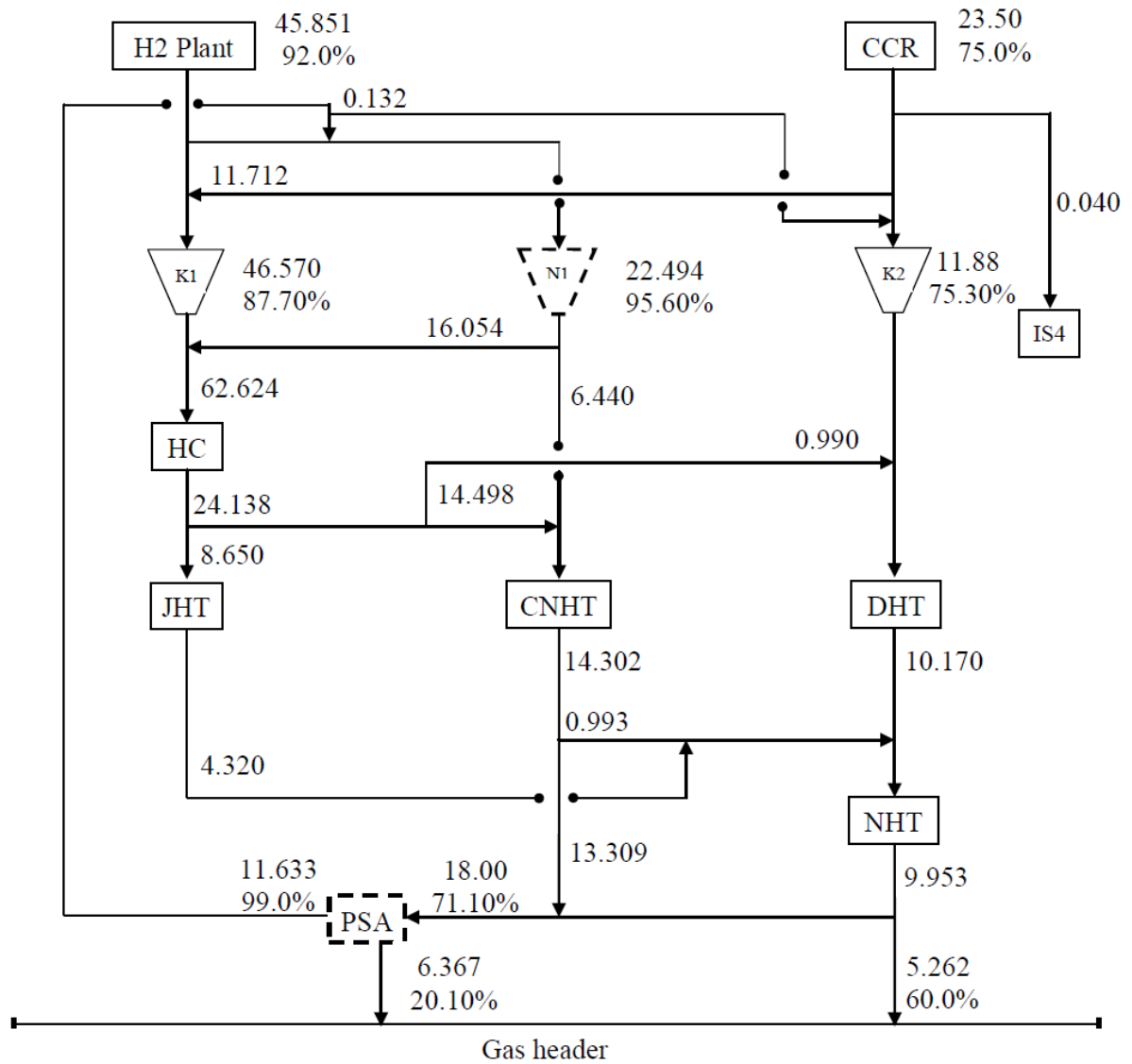
Table 5.3: Hydrogen consumption data of hydrogen consumers

Processing unit	DHT	CNHT	JHT	NHT	IS4	HC
H2 consumption (cons(u)), MMscfd	2.565	4.502	3.679	4.699	0.03	27.210

terms of TAC of hydrogen management model. The objective function is optimized subject to constraints of flow assignment, source and fuel system, hydrogen consumers, existing compressors, new compressors and new PSA units. The flow assignment is modeled using Equations 3.18 and 3.19. The source and fuel system are modeled using Equations 3.20 to 3.22. The hydrogen consumers are modeled using Equations 3.23 to 3.26. The existing compressors are modeled using Equations 3.27 to 3.32. The new compressors and PSA units are modeled using Equations 3.27, 3.30 and 3.33 to 3.45. Capital costs are to be annualized over 2 years with a 5% interest rate as proposed by Hallale and Liu [22]. The piping cost is assumed to be 15% of the summation of the new compressors and purification units capital costs [18]. The model is coded into GAMS as an MINLP and solved using DICOPT solver. Figure 5.2 shows the hydrogen network resulted from the optimization of the integrated model. The optimized network meets the 40% increased hydrogen requirement of HC and CNHT by introducing a new compressor N1 and a new PSA unit. As a result, the TAC for the optimized hydrogen network is \$34.4 million per year. The operating and capital costs break downs are given in Table 5.4. The operating cost is calculated by the summation of hydrogen, electricity and fuel gas costs. The negative sign of fuel gas denotes the value created by burning the fuel. The capital cost comprising the new compressor N1, PSA unit and piping costs.

The same network in Figure 5.1 was optimized using the model developed by Hallale and Liu [22]. Figure 5.3 shows their optimized network. This network follows the same instruction of the presented work in introducing a new compressor and PSA unit to meet the hydrogen requirement. The operating and capital costs break downs of Hallale's network are given in Table 5.4. By comparing the results in Figure 5.2 and Figure 5.3, the difference in the hydrogen requirement between Hallale's network and the presented network is about 2%. This minor difference in hydrogen requirement validates the capability of the formulation in this work for modeling the hydrogen network. Furthermore, the presented network used 4.4% lower total annual

cost comparing to Hallale's network. The reason is because Hallale's network used a new compressor with a capacity that was 85% larger than the capacity used in this work.



- Flowrate: MMscfd
- Purity: %

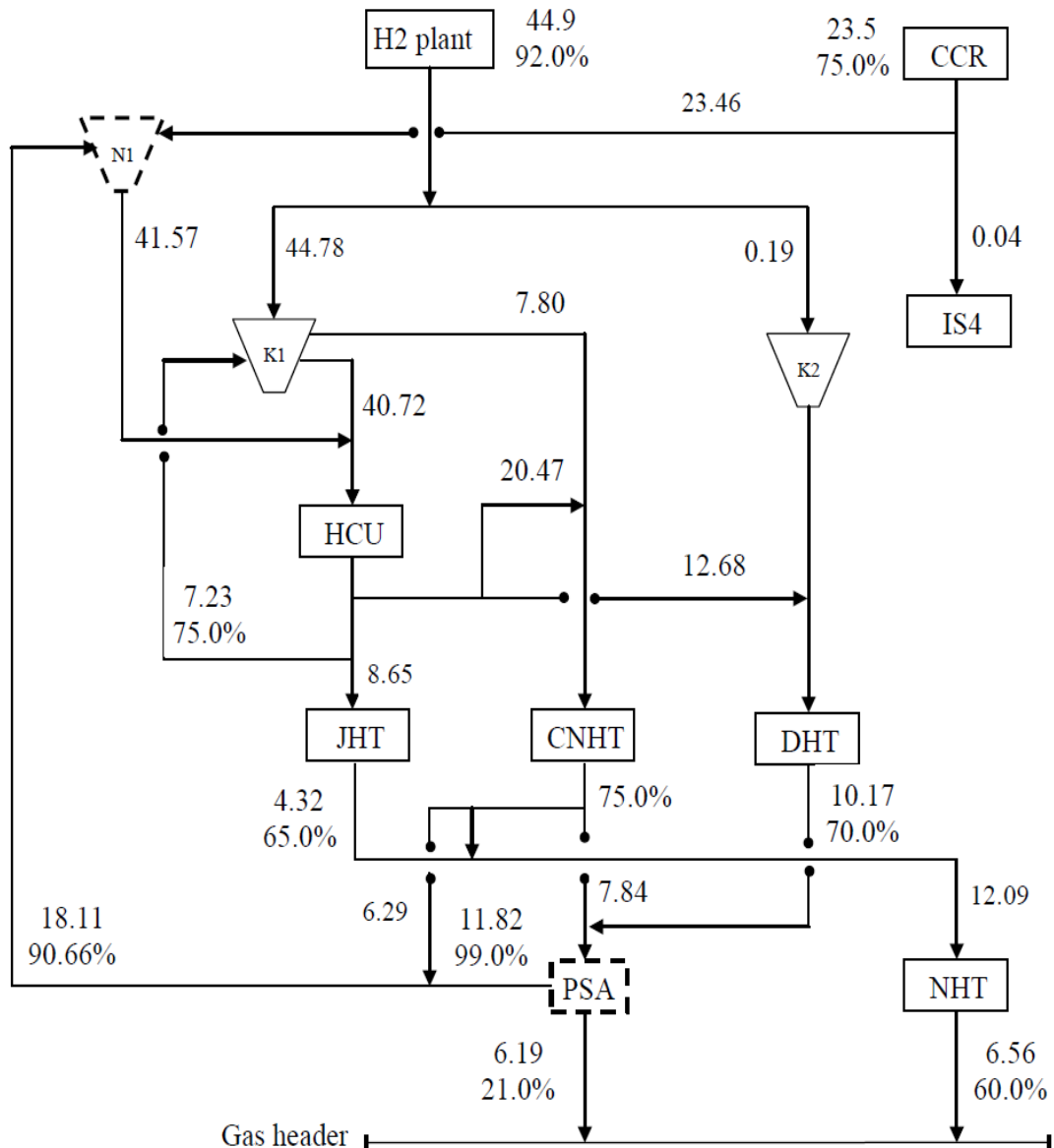
Figure 5.2: MINLP based optimized hydrogen network

Table 5.4: Optimized hydrogen networks costs breakdown

	Hallale and liu. [22]	This study
Operating cost (million \$/year)		
Hydrogen	32.80	33.47
Electricity	3.04	1.90
Fuel gas	-8.93	-7.07
Total operating cost	26.90	28.30
Capital cost (Million \$)		
Compressor	9.04	3.02
PSA	6.76	6.76
piping	1.20	1.47
Total capital cost	17	11.25
TAC (Million \$/yr)	36	34.4

5.3 Standalone Plant Hydrogen Network Optimization

In order to demonstrate the performance of the integrated model on stand-alone petroleum refinery, the materials-processing system model as per Figure 1.5 is adopted. For the hydrogen management model, the capacity of hydrogen producers and the operating conditions of the hydrogen consumers are adapted from Elkamel et al. [19]. The hydrogen sources in the refinery are the hydrogen plant, with a maximum production capacity of 80 MMscfd, and the catalytic reformer, with a maximum production capacity of 17.7 MMscfd. The purities of the hydrogen produced by the hydrogen plant and the catalytic reformer are 95.0% and 80.0%, respectively. The hydrogen sinks in the refinery are the processing units, which are the hydrocracker (HC), the gas oil hydrotreater (GOHT), the residue hydrotreater (RHT), the diesel hydrotreater (DHT), and the naphtha hydrotreater (NHT). The operating conditions of processing units such as inlet and outlet pressures, inlet and outlet hydrogen purities and hydrogen consumption percentage have to be met as described in Table 5.5. All the processing units have internal recycle compressors. The maximum flow rate, purity and pressure data of hydrogen producers are given in Table 5.6. There are three makeup compressors to deliver the fresh hydrogen to the



- Flowrate: MMscfd
- Purity: %

Figure 5.3: MINLP based optimized hydrogen network [22]

hydrogen consumers. The capacity and operating conditions of these compressors are adopted as per Elkamet et al. [19]. The suction pressure, discharge pressure and maximum capacity of the compressors are provided in Table 5.7. The compressors K1 and K2 are designed with higher discharge pressure of 2,000 psi to be able deliver gas into HC unit. This is because HC unit is the major hydrogen consumer in the network. Furthermore, the inlet pressure to the HC unit should be higher than or equal 2,000

psi. The compressor K3 meets the pressure requirement of all consumers except HC unit. The refinery fuel gas header operates at lowest pressure (200 psi) so that it can receive excess fuel gas streams from the hydrogen network. The objective function for this problem is formulated as profit in term of raw material cost, operating cost and hydrogen network operating cost subtracted from revenues. This objective function is optimized subject to constraints of processing units sub-models, connectivity, processing unit capacity and final products demand and quality specifications as well as gas flow, source and fuel system, hydrogen consumers and existing compressors. The CDU output is represented by Equations 3.1 to 3.4, while the other processing units are models using the sub-models shown Appendix D. Connectivity is modeled using Equations 3.6 and 3.11. Processing unit capacity is

Table 5.5: Petroleum refinery stand-alone plant - Operating conditions of the processing units

Processing unit	Inlet pressure psi	Inlet purity %	Outlet pressure psi	Outlet purity %	% H2 consumption
HC	2,000	86.7	1,200	80	39.88
GOHT	500	83.6	350	75	39.99
RHT	600	82.6	400	75	40.02
DHT	500	74.9	350	70	40.03
NHT	300	72.7	200	65	40.03

Table 5.6: Petroleum refinery stand-alone plant – Data for hydrogen sources

Processing unit	Maximum flow MMscfd	Purity %	Pressure psi
HP	80	95	300
REF	17.7	80	300

Table 5.7: Petroleum refinery stand-alone plant – Data for makeup compressors

compressor	Section pressure psi	Discharge pressure psi	Maximum capacity MMscfd
K1	300	2,000	31.5
K2	300	2,000	31.5
K3	300	600	31.5

modeled using Equation 3.10. The final products demand and quality specifications are modeled using Equations 3.14 to 3.17. The flow assignment is modeled using Equations 3.18 and 3.19. The source and fuel system are modeled using Equations 3.20 to 3.22. The hydrogen consumers are modeled using Equations 3.23 to 3.26. The existing compressors are modeled using Equations 3.27 to 3.32. The model is coded into GAMS as NLP and solved using CONOPT solver. Figure 5.4 shows the solution of the optimal hydrogen network resulted from the integrated model formulation on a standalone petroleum refinery. The operating cost breakdown is shown in Table 5.8. The operating cost was calculated as per Equation 3.46 by subtracting the fuel gas cost from the combined costs of hydrogen production and electricity power used in

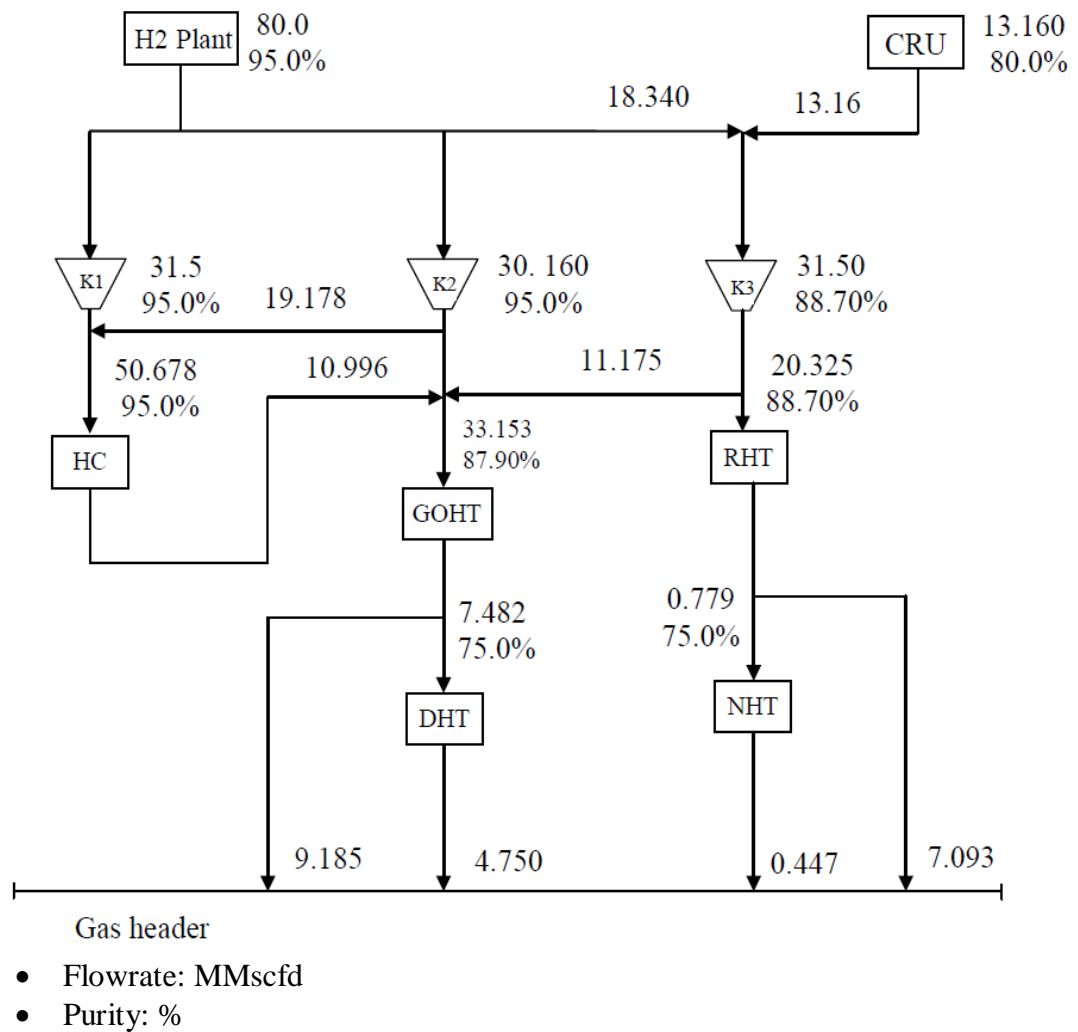


Figure 5.4: Optimized hydrogen network of stand-alone petroleum refinery.

Table 5.8: Petroleum refinery stand-alone plant – Operating cost breakdown

Operating cost	Thousands \$/day
Hydrogen production	160.0
Electricity	4.6
Fuel gas	-23.7
Total operating cost	140.9

compression work. The network in Figure 5.4 is assumed to be illustrating a typical representation of the standalone petroleum refinery hydrogen network. In section 5.4 later, this network shall be used as a base case for demonstrating the performance of the integrated model on the enterprise plant.

To demonstrate the performance of the integrated model on stand-alone bio-refinery plant, the materials-processing system model as per Figure 4.1 is adopted. The operating condition of hydrogen producers and consumers are adapted from Jones et al. [11]. The hydrogen sources in the bio-refinery are hydrogen plant and the catalytic reformer with maximum capacities of 32.5 MMscfd and 1.7 MMscfd and purities of 99% and 80% for H₂ plant and CRU, respectively. The hydrogen consumers in the bio-refinery are two-stage hydrotreating unit (BHDT) and hydrocracking unit (BHC). The operating conditions of the hydrogen consumers such as inlet and outlet pressures, inlet and outlet hydrogen purities and hydrogen consumption rate have to be met as described in Table 5.9. All the consumers have internal recycle compressors. The hydrogen flow rate, purity, and pressure data of all hydrogen producers are given in Table 5.10. There are one PSA unit to recover the off-gases hydrogen and two makeup compressors to deliver the fresh hydrogen to the consumer processes. The suction pressure, discharge pressure and maximum capacity of the compressors are adopted from Jones et al. [11] and shown in Table 5.11. The bio-refinery fuel gas header operates at lowest pressure (200 psi) so that it can receive excess fuel gas stream from hydrogen network. The objective function is formulated in terms of raw material cost, operating cost and hydrogen network total annual cost subtracted from revenues. This objective function is optimized subject to constraints of processing units sub-models, connectivity, processing unit capacity and final

products demand and quality specifications as well as flow assignment, source and fuel system, hydrogen consumers, existing compressors and existing PSA units. The processing units are modeled using the bio-refinery sub-models shown in Appendix D. The Connectivity is modeled using Equations 3.6 and 3.11. Processing unit capacity is modeled using Equation 3.10. The final products demand and quality specifications are modeled using Equations 3.14 to 3.17. The gas flow assignment is modeled using Equations 3.18 and 3.19. The source and fuel system are modeled using Equations 3.20 to 3.22. The hydrogen consumers are modeled using Equations 3.23 to 3.26. The existing compressors and PSA units are modeled using Equations 3.27 to 3.32 and 3.38 to 3.44, respectively. For a new bio-refinery, all the hydrogen network equipment like hydrogen plant, compressors and PSA unit will incur capital cost, which is annualized over 20 years with a 10% interest rate. The piping cost is assumed to be 15% of the summation of the new compressors and purification units capital costs [18]. The model is coded into GAMS as NLP and solved using CONOPT

Table 5.9: Stand-alone bio-refinery – Operating conditions of processing units

Processing unit	Inlet pressure psi	Inlet purity %	Outlet pressure psi	Outlet purity %	hydrogen consumption rate (%)
BHDT	2,515	99	715	19.49	59.68
BHC	1,315	95.84	1,270	92.70	40.67

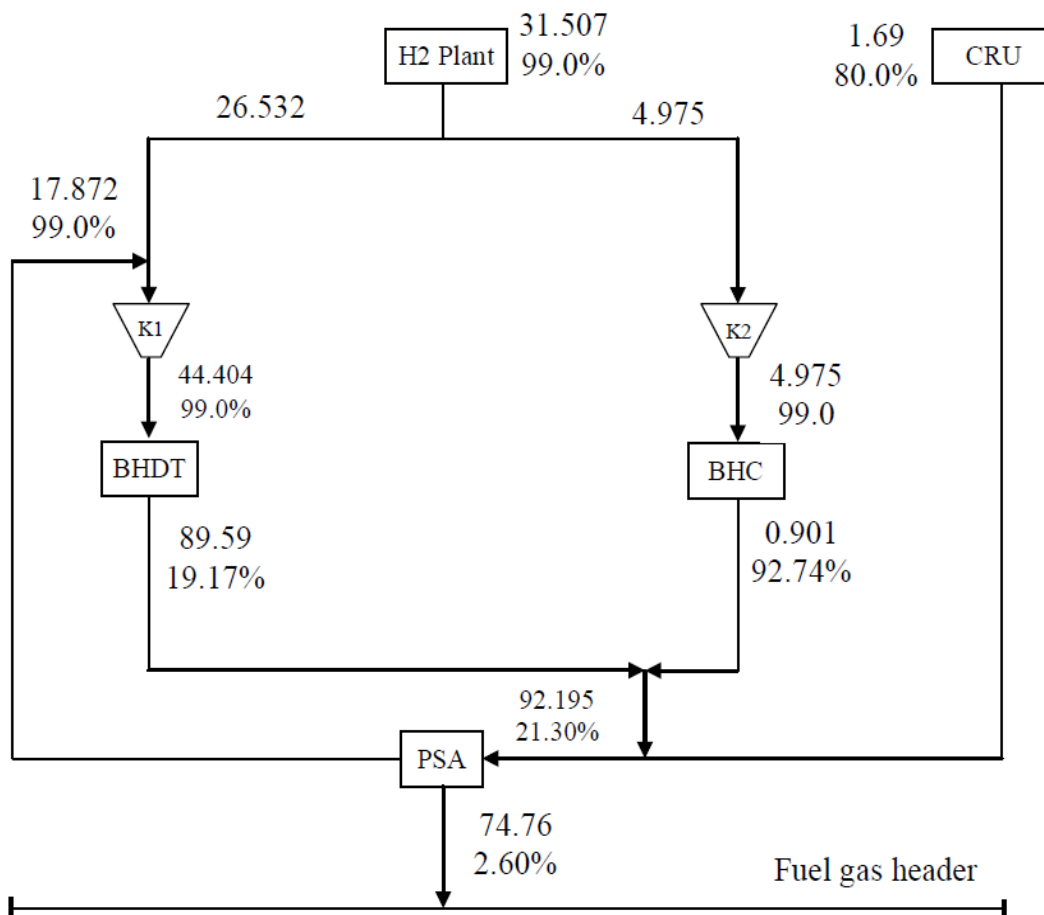
Table 5.10: Stand-alone bio-refinery – Data for hydrogen sources

Processing unit	Flow MMscfd	Purity %	Pressure psi
HP	32.5	95	315
REF	1.7	80	315

Table 5.11: Stand-alone bio-refinery – data for makeup compressors

compressor	Section pressure psi	Discharge pressure psi	Flow MMscfd	Maximum capacity MMscfd
K1	315	2,515	44.40	45
K2	315	1,315	4.98	5

solver. Figure 5.5 shows the optimum hydrogen network resulted from the solution of integrated model formulation on standalone bio-refinery. Due to the higher purity of 99% at the inlet of BHDT reactor, the gas at the outlet cannot be recycled to the inlet of this reactor. As a result, the flow rate at the outlet of the reactor is higher than the flowrate at the inlet of the reactor. Table 5.12 shows the cost breakdown of the hydrogen network. The operating cost is calculated as per Equation 3.46 by subtracting fuel cost from the combined costs of hydrogen production and electricity required for compression work. The negative sign of the total operating cost indicated that this network has a potential to provide fuel gas amount more than its requirement.



- Flowrate: MMscfd
- Purity: %

Figure 5.5: Stand-alone bio-refinery – Optimized hydrogen distribution network

Table 5.12: Stand-alone bio-refinery – Costs breakdown

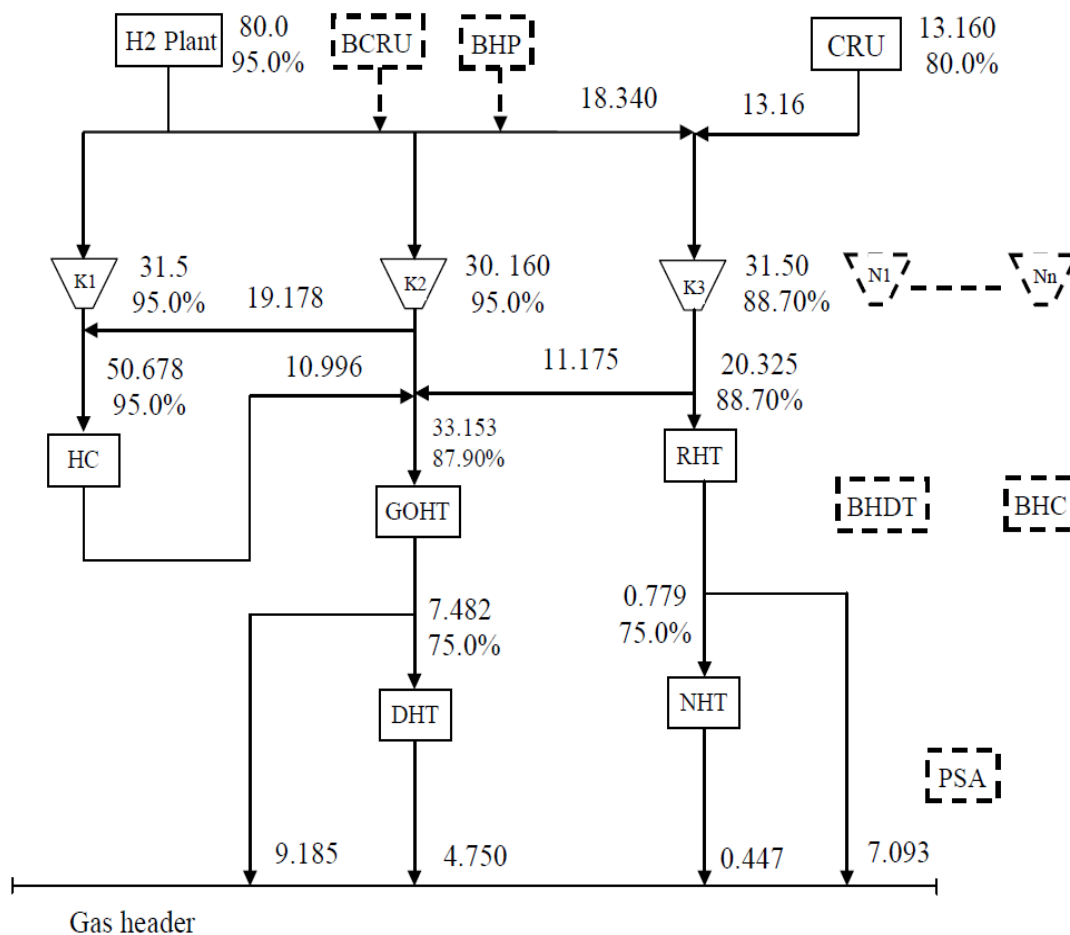
Operating cost	Thousand \$/d
Hydrogen production	75.62
Electricity	2.64
Fuel gas	179.24
Total operating cost	-100.98
Capital cost	Million \$
Compressors	6.64
Compressors	0.59
PSA	32.53
Piping	5.96
Hydrogen plant	93.51
Total capital cost	139.23
Total annual cost (TAC)	-20.50 Million \$/yr

Thus, the excess fuel gas credit is added to the total annual cost. This credit exceeds the total annual cost by 20.5 Million \$/yr. These costs will be added to the hydrogen network cost of standalone petroleum refinery. This is in order to compare the costs of the combined standalone plants' hydrogen networks with the cost of enterprise plant' hydrogen network.

5.4 Enterprise Plant Hydrogen Network Optimization

To demonstrate the performance of the integrated model on the enterprise plant of bio-refinery and petroleum refinery, the materials-processing system as per Figure 4.2 is adopted. Figure 5.6 shows a framework representation for retrofitting the existing hydrogen network of standalone petroleum refinery to meet the hydrogen requirement of the enterprise plant. For the existing hydrogen network of the standalone petroleum refinery, the operating conditions of processing unit, hydrogen source data and makeup compressor data are adopted from section 5.3, Tables 5.5, 5.6 and 5.7,

respectively. This network needs to be retrofitted in order to share its hydrogen with the bio-refinery consumers, BHDT and BHC. The operating conditions of the bio-refinery consumers are adopted from Table 5.9 in section 5.3. Binary variables are required to model the existence or non existence of new equipment such as new compressors (N) and new purification units (PSA). This framework can receive makeup hydrogen from the new bio-refinery hydrogen plant (BHP) and catalytic reforming unit (BCRU). The flow rate, purity and pressures of the new bio-refinery BHP and BCRU are adopted from section 5.3, Table 5.10. The objective function is formulated as per Equation 3.53 to maximize the total enterprise plant profit. This objective function is optimized subject to constraints of processing units' sub-models,

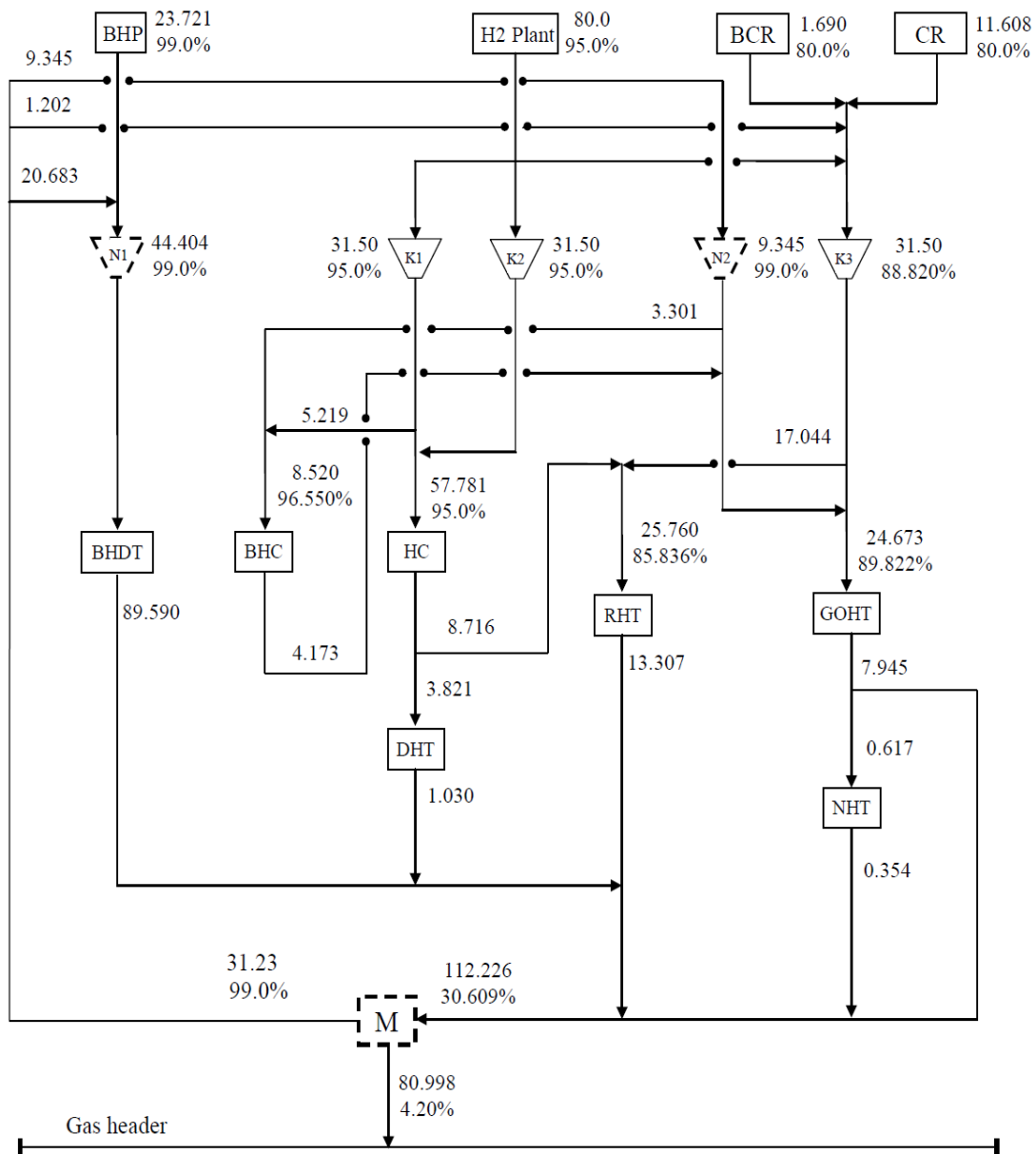


- Flowrate: MMscfd
- Purity: %

Figure 5.6: Representative framework for retrofitting the standalone petroleum refinery hydrogen distribution network

connectivity, processing unit capacity, products demand and quality specifications, logic-based binary variables and capital cost as well as flow assignment, source and fuel system, hydrogen consumers, existing compressors, new compressors and new PSA units. The CDU is modeled using Equations 3.1 to 3.4, while the other processing units are modeled using the sub-models shown Appendix D. The connectivity is modeled using Equations 3.6 and 3.11. The processing unit capacity is modeled using Equation 3.10. The final products demand and quality specifications are modeled using Equations 3.14 to 3.17. The logic-based binary variables for integrating bio-refinery into an existing petroleum refinery are modeled using Equation 3.12. The capital cost is modeled using Equations 3.67 and 3.68. The flow assignment is modeled using Equations 3.18 and 3.19. The source and fuel system are modeled using Equations 3.20 to 3.22. The hydrogen consumers are modeled using Equations 3.23 to 3.26. The existing compressors are modeled using Equations 3.27 to 3.32. The new compressors and PSA units are modeled using Equations 3.27, 3.30 and 3.33 to 3.45. Capital costs are to be annualized over 20 years with a 10% interest rate. The piping cost is assumed to be 15% of the summation of the new compressors and purification units capital costs [18]. The optimization performed on this problem resulted in a total enterprise profit of \$555 MM/yr. It was found that the optimum enterprise network is similar to the solution of the materials-processing system, in which the integration of bio-refinery into an existing petroleum refinery is done only on products blending pool ($Y_2 = Y_4 = Y_5 = Y_7 = 1$; $Y_1 = Y_3 = Y_6 = 0$). Figure 5.7 shows the retrofitted hydrogen network. This network meets the hydrogen requirement of the enterprise plant through introduction of a new PSA unit and two new compressors. Additionally 23.72 MMscfd and 1.69 MMscfd of hydrogen is imported from the bio-refinery hydrogen plant and catalytic reformer. This network achieved 25% reduction in hydrogen requirement compared to the total of the hydrogen requirement of the stand-alone plants. Table 5.13 shows the hydrogen network costs breakdown of the enterprise plant and the summation of standalone plants. Comparing to the total standalone plants hydrogen network cost, the hydrogen network of the enterprise plant achieved reductions in the operating cost and capital cost equivalent to 18.5% and 5%, respectively. Consequently, it reduces the total

annual cost by 11% comparing to the summation of stand-alone plants hydrogen networks costs.



- Flowrate: MMscfd
- Purity: %

Figure 5.7: Optimized hydrogen distribution network of the proposed enterprise plant

Table 5.13: Hydrogen network cost breakdown of enterprise and standalone plants

	Enterprise plant	Standalone petroleum refinery and bio-refinery
Operating cost (Thousand \$/day)		
Hydrogen	216.93	235.62
Electricity	8.14	7.24
Fuel gas	192.52	202.92
Total operating cost	32.55	39.94
Capital cost (Million \$)		
Compressors	7.86	7.23
PSA	39.49	32.53
pipng	7.10	5.96
Hydrogen plant	77.76	93.51
Total capital cost	132.21	139.23
TAC (Million \$/yr)	27.41	30.93

5.5 Summary

In this chapter, the integrated model of hydrogen management and materials-processing system is demonstrated on standalone bio-refinery and petroleum refinery plants as well as an enterprise plant between bio-refinery and petroleum refinery. The case study results validate the applicability of the integrated model for the synthesis of an optimum enterprise network between bio-refinery and petroleum refinery. The integrated model has also been shown to provide the best strategy for retrofitting the existing hydrogen network of standalone petroleum refinery to meet the hydrogen requirement of the enterprise plant. In addition, the model results showed that the retrofitted network achieved 18.5% and 5%, reductions in the operating cost and capital cost, respectively, comparing to the summation of stand-alone plants hydrogen networks costs. Therefore, the synthesis of an enterprise hydrogen network between the new bio-refinery and existing petroleum refinery can be considered as a cost-effective technique to improve the hydrogen utilization in the enterprise plant.

CHAPTER 6

LINEARIZATION OF MODELS

6.1 Introduction

MINLP models, being in general very difficult to solve, require large computational efforts and might result in inconsistency in solution quality and CPU time. Therefore, the MINLP models of materials-processing system and hydrogen management developed in this work have been linearized into MILP models using the linearization techniques developed in section 3.5. This is because MILP models can be solved with less computational effort [104].

This chapter analyses the performance of the linearized MILP materials-processing system and hydrogen management models. The solutions of these models are compared to the original MINLP models solutions in order to highlight the quality and efficiency of the linearized models. The MILP models are coded into GAMS and solved using DICOPT solver. The models are run on Intel Core2 Duo@ 2 GHZ and 1GB RAM.

6.2 Computational Performance Analysis of the Materials-processing System

Model

The superstructure shown in Figure 4.2 is used to demonstrate the performance of the linearized materials-processing system model in synthesizing optimum enterprise network between bio-refinery and petroleum refinery. The objective function is to maximize the enterprise profit as per Equation 3.5 and is subjected to constraints of processing units sub-models, connectivity, processing unit capacity, logic-based binary variables, capital cost and final products demand and quality specifications. To

formulate the problem as MILP, all the non-linear constraints such as CDU sub-model, petroleum refinery hydrotreating units sub-models, capital cost and final products demand and quality specifications are linearized using the technique developed in section 3.5. The CDU is modeled using Equations 3.54 to 3.60 and refinery hydrotreating units are modeled using Equations 3.61 and 3.62. The capital cost is modeled using Equations 3.67 and 3.68. The final products quality specifications are modeled using Equations 3.63 to 3.66. The model is coded into GAMS and solved using BDMLP solver. The optimization performed on this problem meets the blending pool final products demand and quality specifications and results in a total profit of \$540 MM/yr. This profit is 2% lower than the MINLP model solution of the same problem in section 4.4. Furthermore, it was found that the optimum enterprise network is in agreement with the solution of the MINLP model in that the integration is only on product blending pool.

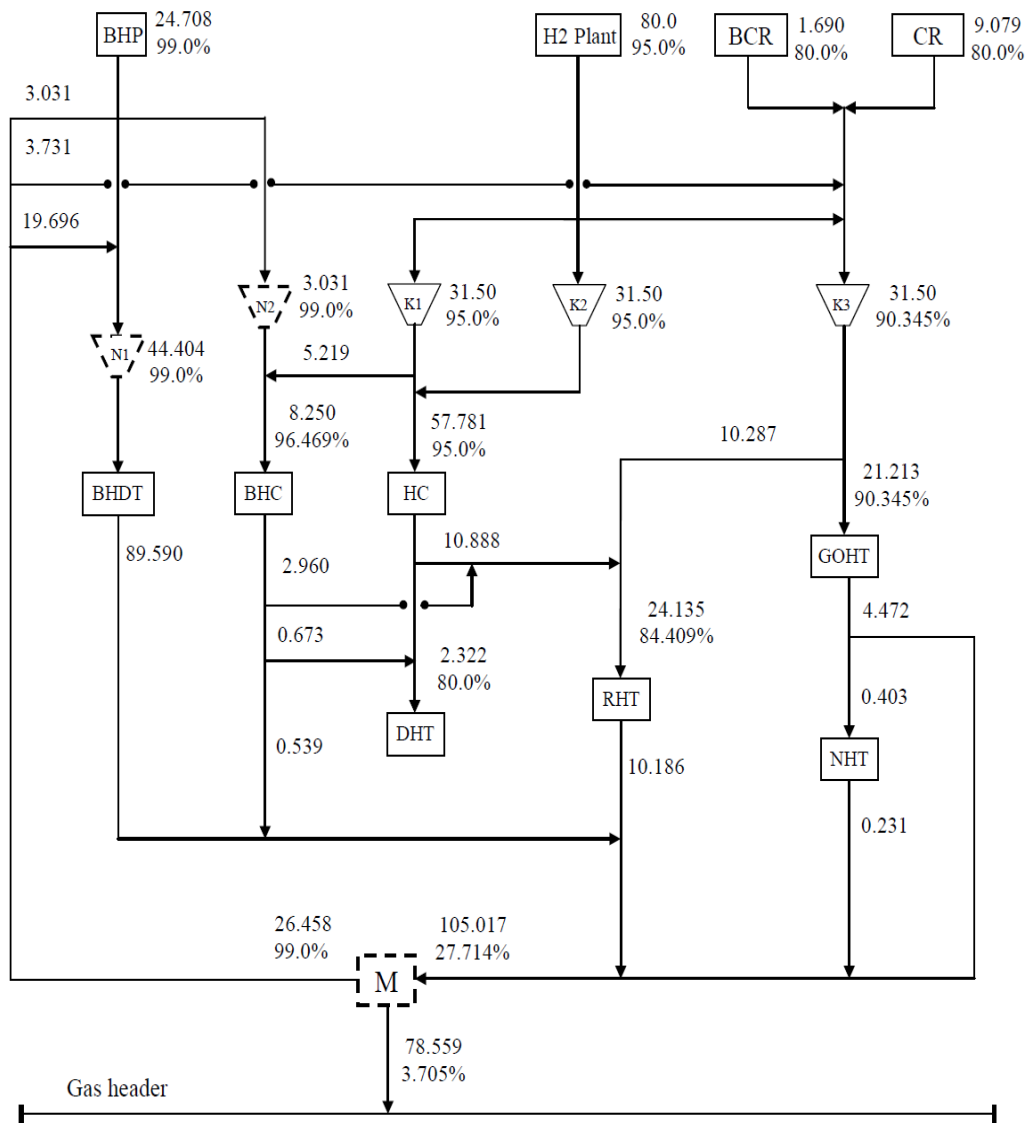
Table 6.1 summarizes the computational performance of MILP and MINLP models. In terms of problem size, the MILP model uses slightly more continuous and discrete variables than the MINLP model. The increasing in the number of variables originates from the definition of new variables for linearization purpose. However, the number of iterations used by MILP model is about 84% lower than MINLP model. In addition, the CPU time used by MILP model is about 95% lower than the MINLP model. The superior computational performance highlights the efficiency of the linearized model.

Table 6.1: Comparison of computational performance between MINLP and MILP of materials-processing system model

	MINLP	MILP
Number of variables	337	343
Number of discrete variables	31	34
Number of iterations	1570	247
CPU time (Sec)	1.7	0.08

6.3 Computational performance analysis of the integrated model

To demonstrate the performance of the linearized integrated model, which combined materials-processing system model and hydrogen management model, the superstructure shown in Figure 4.2 as well as the framework shown in Figure 5.6 are studied. The objective function is formulated in terms of maximizing the total enterprise plant profit while minimizing the total annual cost of hydrogen network as per Equation 3.53. This objective function is optimized subject to constraints of processing units sub-models, connectivity, processing unit capacity, logic-based binary variables, capital cost and final products demand and quality specifications as well as flow assignment, source and fuel system, hydrogen consumers, existing compressors, new compressors and new PSA units. To formulate the problem as MILP all non-linear constraints such as CDU sub-model, petroleum refinery hydrotreating units sub-models, capital cost, final products quality specifications, hydrogen network bilinear terms and new compressor power equations are linearized using the techniques developed in section 3.5. The CDU is modeled using Equations 3.54 to 3.60 and refinery hydrotreating units are modeled using Equations 3.61 and 3.62. The capital cost is modeled using Equations 3.67 and 3.68. The final products quality specifications are modeled using Equations 3.63 to 3.66. The hydrogen network bilinear terms in Equations 3.22, 3.25, 3.30, 3.39, 3.42 and 3.49 are linearized using Equations 3.63 to 3.66. The new compressor power equations are modeled using Equations 3.69 to 3.72. The model is coded into GAMS and solved using BDMLP solver. The optimization performed on this problem is simultaneously solved for materials-processing system model and hydrogen management model and resulted in a total profit of \$534 MM/yr. This profit is 3.8% lower than the MINLP model solution of the same problem. Furthermore, the optimum enterprise network between bio-refinery and petroleum refinery was agreeing with the network resulted from solving the integrated MINLP model. In addition, the strategy used for retrofitting hydrogen network was found to be similar to that resulted from MINLP model solution in meeting the hydrogen requirement by introducing a new PSA unit and two compressors as well as importing hydrogen from the bio-refinery hydrogen plant and catalytic reforming unit, as shown in Figure 6.1. These results prove the



- Flowrate: MMscfd
- Purity: %

Figure 6.1: MILP based optimized hydrogen distribution network of the proposed enterprise pant.

quality of the linearized integrated model for representing the non-linear behavior of the original MINLP model.

Table 6.2 summarizes the computational performance of MINLP and MILP of the integrated model in the context of number of continuous variables, number of discrete variables, number of iterations and CPU time. The MILP model uses slightly more variables than the MINLP model. The increasing in the number of variable is caused

by the definition of new variables for linearization purpose. In spite of this, the MILP model requires number of iteration and CPU time that are 92% and 85% lower than that of the MINLP model.

Table 6.2: Comparison of computational Performance between MINLP and MILP of integrated model

	MINLP	MILP
Number of continuous variables	534	586
Number of discrete variables	68	71
Number of iterations	43,747	3,638
CPU time (Sec)	11.99	1.75

6.4 Summary

In this chapter the linearized materials-processing system and integrated models are demonstrated on enterprise network superstructure between a new bio-refinery and an existing petroleum refinery. Furthermore, the computational performance of these models is compared to the original MINLP models. The results highlighted that, the solutions generated from the linearized models are superior to the solutions generated from the MINLP models. The MILP models required less CPU time and less number of iterations to converge comparing to the MINLP models. Furthermore, the minor differences in the objective function of the MINLP and MILP models solutions prove the accuracy of the developed linearization technique for representing the non-linear behavior of the MINLP models.

CHAPTER 7

CONCLUSIONS AND FUTURE WORK

This chapter presents the conclusions and future work based on the results obtained from this work. The chapter initially discusses the significant outcome of this work. The next section proposes the directions for improving and extending the future work.

7.1 Conclusions

- In this work, a superstructure-based materials-processing system model has been developed to synthesize optimum enterprise network between a new pyrolysis-based bio-refinery and an existing petroleum refinery. The mathematical model has been demonstrated using case studies of pyrolysis-based bio-refinery, existing petroleum refinery and enterprise plant network superstructure between bio-refinery and petroleum refinery. The results from the case studies have shown that the enterprise plant is a more economically attractive solution than installing a new bio-refinery and a petroleum refinery as standalone plants. The optimum enterprise plant network in this work has been shown to achieve 11% higher profit compared to the combined profits of the stand-alone bio-refinery and petroleum refinery plants.
- Sensitivity analysis with respect to the final product prices and retrofit cost of the existing petroleum refinery units on the synthesis of optimum enterprise network between bio-refinery and petroleum refinery has been performed. The results of the sensitivity analysis indicated that the effect of changing petroleum refinery retrofit cost and/or varying in the selling prices of the final products is only notable on the objective function. Variation of retrofit cost and selling price do not show evidence of changing the

synthesis of the optimum enterprise plant network. In all cases, the enterprise plant network A, where the bio-refinery only utilizes the existing petroleum refinery blending pool, was the optimum one.

- An integrated model for the simultaneous solution of materials-processing system and hydrogen management has been developed to synthesize an optimum enterprise hydrogen network between bio-refinery and petroleum refinery. The mathematical model has been demonstrated using case studies of pyrolysis-based bio-refinery, existing petroleum refinery and enterprise plant network superstructure between bio-refinery and petroleum refinery. The model was found to be capable of attaining the objective of materials-processing system in synthesizing optimum enterprise network between bio-refinery and petroleum refinery. Furthermore, the model has synthesized an optimum hydrogen network to meet the hydrogen requirement of the enterprise plant. This network has achieved 25% and 11% reduction in hydrogen requirement and total capital costs, respectively, compared to the combined performance of the stand-alone plants.
- Complex MINLP models of enterprise network namely, materials-processing system and hydrogen management have been linearized into MILP models. The case studies solved for MINLP based optimization of materials processing system and hydrogen network were adopted to demonstrate the performance of the linearized MILP models. MILP models achieved better computational performance in terms of number of iteration and CPU time as compared to the original MINLP models. The integrated MILP model achieved 92% and 85% reduction in the number of iterations and CPU time compare to the original MINLP model.

7.2 Future Work

Alhajri et al. [105] presented an overall integrated model for the simultaneous solution of the refinery planning, hydrogen management, and CO₂ abatement problems. The model addresses the optimum CO₂ strategy selection through integration of refinery planning with the hydrogen network and CO₂ emissions. The

options that considered for emissions reduction are flow rate balancing, fuel switching and installation of a CO₂ capture process. Adapting this model can extend our work to integrate CO₂ mitigations options model with the materials-processing system and hydrogen management models as a tool for synthesizing optimum enterprise network between bio-refinery and petroleum refinery.

REFERENCES

- [1] J. Clark and F. Deswarte, *Introduction to Chemicals from Biomass*, John Wiley and Sons Ltd: UK, 2008.
- [2] A. Demirbas, "Bio-refineries: Current Activities and Future Development," *Energy Conversion and Management*, vol. 50, pp. 2782 – 2801, 2009.
- [3] J. Henning, "Advanced Biofuels in a Biorefinery Approach," *Forest and Landscape Working Papers No. 70-2012*, Copenhagen, Denmark, 2012.
- [4] D. Elliott, "Biofuels Research Opportunities in Thermochemical Conversion of Biomass," *First Annual TIMBR Conference on Cellulosic Biofuels*, Massachusetts, 2008.
- [5] M. Dinesh, U. Charles and H. Philip, "Pyrolysis of Wood/Biomass for Bio-oil: A Critical Review," *Energy Fuels*, vol. 20., no. 3, pp. 848 – 889, 2006.
- [6] A. Bridgwater, "Renewable Fuels and Chemical by Thermal Processing of Biomass," *Chemical Engineering Journal*, vol. 91., no. (2-3), pp. 87 – 102, 2003.
- [7] N. Abdullah, H. Gerhauser and A. Bridgwater, "Bio-oil from Fast Pyrolysis of Oil Palm Empty Fruit Bunches," *Journal of Physical Science*, vol. 18, no. 1, pp. 57–74, 2007.
- [8] K. Khor, K. Lim and Z. Zainal, "Characterization of Bio-Oil: A By-Product from Slow Pyrolysis of Oil Palm Empty Fruit Bunches," *American Journal of Applied Sciences*, vol. 6., no. 9, pp. 1647-1652, 2009.
- [9] GPA, "Integrated Palm Oil Biomass Technology Solutions by Malaysia's Global Green Synergy" GPA Report no: GPA-BM-1-020512, 2012
- [10] Y. Leong, S. Mustapa and A. Hashim, "Climate Change Challenges on CO₂ Emission Reduction for Developing Countries: A Case for Malaysia's Agenda for Action," *The International Journal of Climate Change: Impacts and Responses*, vol. 2., no. 4, pp. 9 – 26, 2011.
- [11] S.B. Jones, J.E. Holladay, C. Valkenburg, D.J. Stevens, C. Walton, C. Kinchin et al., "Production of Gasoline and Diesel from Biomass via Fast Pyrolysis, Hydrotreating and Hydrocracking: A Design Case" *United States Department of Energy*, PNNL-18284 Rev. 1. DE-AC05-76RL01830, 2009.

- [12] R. Meyers, Handbook of Petroleum Refining Processes, McGraw-Hill, New York, 2004.
- [13] D. Jones, Elements of Petroleum Processing, John Wiley and Sons Ltd: UK, 1995.
- [14] M. Ba-Shammakh, “An Optimization Approach for Integrating Planning and CO₂ Mitigation in the Power and Refinery Sectors,” PhD thesis: Waterloo, Ontario, Canada, 2007.
- [15] J. Gary, and G. Handwerk, Petroleum Refining: Technology and Economics, Marcel Inc: New York, 2001.
- [16] G. Kevin, Fundamentals of Petroleum Refining, Course No. O-3001 www.PDHengineer.com (Last access 1/7/2013)
- [17] N. Charles, Occupational Safety and Health Administration (OSHA) Technical Manual, United States Department of Labor, Washington, 1999.
- [18] A. Kumar, G. Gautami and S. Khanam, “Hydrogen Distribution in the Refinery using Mathematical Modeling,” Energy, vol. 35, pp. 3763 – 3772, 2010.
- [19] A. Elkamel, I. Alhajri, A. Almansoori and Y. Saif, “Integration of Hydrogen Management in Refinery Planning with Rigorous Process Models and Product Quality Specifications,” International Journal of Process Systems Engineering, vol. 1., no. (3-4), pp. 302 – 330, 2011.
- [20] J. Alves and G. Towler, “Analysis of Refinery Hydrogen Distribution Systems,” Industrial and Engineering Chemistry Research, vol. 41, pp. 5759 – 5769, 2002.
- [21] R. Huycke and A. Zagoria, “Refinery Hydrogen Management – The Big Picture,” Hydrocarbon Processing, vol. 2, pp. 41 – 46, 2003.
- [22] N. Hallale and F. Liu, “Refinery Hydrogen Management for Clean Fuels Production,” Advances in Environmental Research, vol. 6, pp. 81–98, 2001.
- [23] I. Mintzer and P. Schwartz, “U.S. Energy Scenarios for the 21st Century,” Pew Center on Global Climate Change, Arlington, 2003.
- [24] R. Benjamin, “Retrofitting Analysis of Integrated Bio-refineries,” MSc thesis: Texas A&M University, USA, 2005.
- [25] A. Lappas S. Bezergianni and I. Vasalos, “Production of Biofuels via Co-processing in Conventional Refining Processes,” Catalyst Today, vol. 145, pp. 55 – 62, 2009.

- [26] BIOCOUP, “Co-processing of Upgraded Bio-liquids in Standard Refinery Units,” Final Activity Report, 2012.
- [27] A. Elkamel, M. Ba-Shammakh, P. Douglas and E. Croiset, “An Optimization Approach for Integrating Planning and CO₂ Emission Reduction in the Petroleum Refining Industry” *Ind. Eng. Chem. Res.*, vol. 47., no. 3, pp. 760 – 776, 2008.
- [28] P. Shukla, “Biomass Energy Future for India,” International Workshop of Science and Technology for a Modern Biomass Civilization, Brazil, 1997.
- [29] J. Shang and J. Su, “Development Strategy Research of China’s Rural Biomass Energy Based on SWOT Model,” *World Rural Observations*, vol. 1., no. 1, pp. 55 – 62, 2009.
- [30] Y. Xu, M. Hanna and L. Isom, “Green Chemicals from Renewable Agricultural Biomass - A Mini Review,” *The Open Agriculture Journal*, vol. 2, pp. 54 – 61, 2008.
- [31] A. Murtala, N. Shawal and H. Usman, “Biomass as a Renewable Source of Chemicals for Industrial Applications,” *International Journal of Engineering Science and Technology*, vol. 4., no. 2, pp. 721 – 730, 2012.
- [32] D. Macqueen and S. Korhaliller, *Bundles of Energy: The Case for Renewable Biomass Energy*, International Institute for Environment and Development, London, 2011.
- [33] S. Zhang, Y. Yan and R. Zhengwei, “Upgrading of Liquid Fuel from the Pyrolysis of Biomass,” *Bioresource Technology*, vol 96, pp. 545 – 550, 2005.
- [34] D. Elliott, “Historical Developments in Hydroprocessing Bio-oils,” *Energy and Fuels*, vol. 21., no. 3, pp. 1792 – 1815, 2007.
- [35] X. Xu, C. Zhang, Y. Liu, Y. Zhai and R. Zhang, “Two-step Catalytic Hydrodeoxygenation of Fast Pyrolysis Oil to Hydrocarbon Liquid Fuels,” *Chemosphere*, vol. 93, pp. 652–660, 2013.
- [36] FAO, *Biofuels: Prospects, Risks and Opportunities*, United Nation Food and Agriculture Organization, Rome, 2008.
- [37] E. Gnansounou, L. Panichelli, A. Panichelli and J. Villegas, *Accounting for Indirect Land-use Changes in GHG Balances of Biofuels: Review of Current*

- Approaches, École Polytechnique Fédérale de Lausanne, Working paper, REF. 437.101, 2008.
- [38] D. Sawyer, “Climate Change, Biofuels and Eco-Social Impacts in the Brazilian Amazon and Cerrado,” *Philosophical Transactions of the Royal Society B: Biological Sciences*, vol. 363, pp. 1747 – 1750, 2008.
- [39] H. Dale, L. Kline, J. Wiens and J. Fargione, *Biofuels: Implications for Land Use and Biodiversity*, Biofuels and Sustainability Reports, the Ecological Society of America, 2010.
- [40] G. Timilsina and A. Shrestha, “How Much Hope Should We Have For Biofuels?,” *Energy*, vol. 36, pp. 2055 – 2069, 2011.
- [41] D. Hsu, “Life Cycle Assessment of Gasoline and Diesel Produced via Fast Pyrolysis and Hydroprocessing,” *Biomass and Bioenergy*, vol. 45, pp. 41 – 47, 2012.
- [42] J. Han, A. Elgowainy, J. Dunn and M. Wang, “Life Cycle Analysis of Fuel Production from Fast Pyrolysis of Biomass,” *Bioresource Technology*, vol. 133, pp. 421- 428, 2013.
- [43] D. M. Mercader, “Pyrolysis Oil Upgrading for Co-processing in Standard Refinery Units,” PhD thesis: University of Twente, Enschede, The Netherlands, 2010.
- [44] M. Samolada, W. Baldauf and A. Vasalos, “Production of a Bio-gasoline by Upgrading Biomass Flash Pyrolysis Liquids via Hydrogen Processing and Catalytic Cracking,” *Fuel*, vol. 77., no. 14, pp. 1667 – 1675, 1998.
- [45] F. Gabriella, T. Nicolas, T. Guy, C. Andre, S. Yves and M. Claude, “Biomass Derived Feedstock Co-processing with Vacuum Gas Oil for Second-generation Fuel Production in FCC Units,” *Applied Catalyst B: Environmental*, vol. 96., no. 3-4, pp. 476 – 485, 2010.
- [46] D. M. Mercader M. Groeneveld S. Kersten N. Wayb, “Production of Advanced Biofuels: Co-processing of Upgraded Pyrolysis Oil in Standard Refinery Units,” *Applied Catalysis B: Environmental*, vol. 96, pp. 57 – 66, 2010.
- [47] F. Agblevor, O. Mante, R. McClung and S. Oyama, “Co-processing of Standard Gas Oil and Biocrude Oil to Hydrocarbon Fuels,” *Biomass and Bioenergy*, vol. 45, pp. 130 – 137, 2012.

- [48] T. Marker et al, Opportunities for Biorenewables in Oil Refineries, UOP report No DE-FG36-05GO15085, 2005.
- [49] I. Alhajri, A. Elkamel, T. Albahri and P.L. Douglas, “A Nonlinear Programming Model for Refinery Planning and Optimization with Rigorous Process Models and Products Quality Specifications,” *International Journal of Oil, Gas and Coal Technology*, vol. 1., no. 3, pp. 283 – 307, 2008.
- [50] J. Zhang, X. Zhu and G. Towler, “A Simultaneous Optimization Strategy for Overall Integration in Refinery Planning,” *Ind. Eng. Chem. Res.*, vol. 40, pp. 2640 – 2653, 2001.
- [51] R. Julija, T. Loreta, R. Ice and M. Liljana, “Optimization of Refinery Products Blending,” *Bulletin of the Chemists and Technologists of Macedonia*, vol. 18., no. 2, pp. 171-178, 1999.
- [52] G. Symonds, “Linear Programming Solves Gasoline Refining and Blending Problems,” *Industrial and Engineering Chemistry*, vol. 48., no. 3, pp. 394 – 401, 1956.
- [53] A. Tehrani, “Allocation of CO₂ Emissions in Petroleum Refineries to Petroleum Joint Products: A Linear Programming Model for Practical Application,” *Energy Economy*, vol. 29, pp. 974 – 997, 2007.
- [54] D. Babusiaux, A. Pierru, “Modeling and Allocation of CO₂ Emissions in a Multi Product Industry: The Case of Oil Refining,” *Applied Energy*, vol. 84, pp. 828–841, 2007.
- [55] N. Tehrani and V. Saint-Antonin, “Impact of Tightening the Sulfur Specifications on the Automotive Fuels’ CO₂ Contribution: A French Refinery Case Study,” *Energy Policy*, vol. 6, pp. 2449 – 2459, 2007.
- [56] G. Gomes, A. Szklo and R. Schaeffer, “The Impact of CO₂ Taxation on the Configuration of New Refineries: An Application to Brazil,” *Energy Policy*, vol. 37, pp. 5519 – 5529, 2009.
- [57] M. Hassan, A. Kandeil and A. Elkhayat, “Improving Oil Refinery Productivity through Enhanced Crude Blending using Linear Programming Modeling,” *Asian Journal of Scientific Research*, vol. 4., no. 2, pp. 95 – 113, 2011.

- [58] L. Moro, A. Zanin and J. Pinto, "A Planning Model for Refinery Diesel Production," *Computer and Chemical Engineering*, vol. 22, pp. 1039 – 1042, 1998.
- [59] N. Zhang and X. Zhu, "A Novel Modelling and Decomposition Strategy for Overall Refinery Optimization," *Comput. Chem. Eng.*, vol. 24, pp. 1543 – 1548, 2000.
- [60] K. Al-Qahtani and A. Elkamel, "Multisite Refinery and Petrochemical Network Design: Optimal Integration and Coordination," *Ind. Eng. Chem. Res.*, vol. 48., no. 2, pp. 814 – 826, 2009.
- [61] A. Aguilar, A. Jorge and T. Fernando, "Simulation and Planning of a Petroleum Refinery based on Carbon Rejection Processes," *Fuel*, vol. 100, pp. 80 – 90, 2012.
- [62] C. Henao and C. Maravelias, "Surrogate-based Superstructure Optimization Framework," *AIChE Journal*, vol. 57., No. 5, pp. 1216 – 1232, 2011.
- [63] B. Linnhoff, D. Townsend, D. Boland, G. Hewitt, B. Thomas, A. Guy and R. Marsland, *A User Guide on Process Integration for the Efficient Use of Energy*, UK: Institution of Chemical Engineers, Rugby, 1994.
- [64] M. El-Halwagi and V. Manousiouthakis, "Synthesis of Mass Exchange Networks," *AIChE J*, no. 35, pp. 1233–1244, 1989.
- [65] M. Bauer and J. Stichlmair, "Superstructures for the Mixed Integer Optimization of Nonideal and Azeotropic Distillation Processes," *Comput. Chem. Eng.*, vol. 20, pp. 25 –30, 1996.
- [66] M. Barttfield, P. Aguirre and I. Grossmann, "A Decomposition Method for Synthesizing Complex Column Configurations using Tray-by-Tray GDP Models," *Comput. Chem. Eng.*, vol. 28, pp. 2165–2188, 2004.
- [67] I. Heckl, Z. Kovacs, F. Friedler, L. Fanc and J. Liuc, "Algorithmic Synthesis of an Optimal Separation Network Comprising Separators of Different Classes," *Chem. Eng. Process*, vol 46, pp. 656 – 665, 2007.
- [68] S. Papoulias and I. Grossmann, "A Structural Optimization Approach in Process Synthesis, 2. Heat-recovery Networks," *Comput. Chem. Eng.*, vol. 7, pp. 707 – 721, 1983.

- [69] Sorsak and Z. Kravanja, "Simultaneous MINLP Synthesis of Heat Exchanger Networks Comprising Different Exchanger Types," *Comput. Chem. Eng.*, vol. 26, pp. 599 – 615, 2002.
- [70] F. Liu and N. Zhang, "Strategy of Purifier Selection and Integration in Hydrogen Networks," *Chemical Engineering Research and Design*, vol. 82, pp. 1315 – 1330, 2004.
- [71] Y. Jiao, H. Su and W. Hou, "Improved Optimization Methods for Refinery Hydrogen Network and their Applications," *Control Engineering Practice*, vol. 20, pp. 1075 – 1093, 2012.
- [72] Y. Jiao, H. Su, W. Hou and P. Li, "Design and Optimization of Flexible Hydrogen Systems in Refineries," *Ind. Eng. Chem. Res.*, vol. 52, pp. 4113 – 4131, 2013.
- [73] P. Varbanov, S. Doyle and R. Smith, "Modelling and Optimisation of Utility Systems," *Trans IChemE*, vol. 82., no 5, pp. 561 – 578, 2004.
- [74] R. Smith, *Chemical Process Design and Integration*, John Wiley and Sons Ltd, UK, 2005.
- [75] I. Quesada and I. Grossmann, "Global Optimization of Bilinear Process Networks with Multicomponent Flows," *Comput. Chem. Eng.*, vol. 19., no. 12, pp. 1219 – 1242, 1995.
- [76] Li, W. K.; Hui, C. W.; Hua, B.; Tong, Z. X. Scheduling Crude Oil Unloading, Storage and Processing. *Ind. Eng. Chem. Res.*, 2002, 41 (26), 6723–6734.
- [77] G. Towler, R. Mann, A. Serriere and Gabaude, "Refinery Hydrogen Management: Cost Analysis of Chemically-integrated Facilities," *Ind. Eng. Chem. Res.*, vol. 35., no. 7, pp. 2378 – 2388, 1996.
- [78] M. El-Halwagi, and V. Manousiouthakis, "Automatic Synthesis of Mass Exchange Networks with Single Component Targets," *Chemical Engineering Science*, vol. 45, pp. 2813-2831, 1990.
- [79] D. Foo, and Z. Mannan, "Setting the Minimum Utility Gas Flowrate Targets using Cascade Analysis Technique," *Ind. Eng. Chem. Res.*, vol. 45, pp. 5986–5995, 2006.

- [80] D. Ng, D. Foo and R. Tan, “Automated Targeting Technique for Single-impurity Resource Conservation Networks. Part 1: Direct Reuse/Recycle,” *Ind. Eng. Chem. Res.*, vol. 48, pp. 7637 – 7646, 2009.
- [81] Z. Manan, Y. Tan and D. Foo, “Targeting the Minimum Water Flow Rate Using Water Cascade Analysis Technique,” *AIChE J*, vol. 50, pp. 3169 – 3183, 2004.
- [82] D. Foo, Z. Manan and Y. Tan, “Use Cascade Analysis to Optimize Water Networks,” *Chem. Eng. Progress*, vol. 102, pp. 45–52, 2006.
- [83] M. Shariati, N. Tahouni and M. Panjeshahi, “Investigation of Different Approaches for Hydrogen Management in Petrochemical Complexes,” *International Journal of Hydrogen Energy*, vol. 38, pp. 3257 – 3267, 2013.
- [84] S. Peramanu, B. Cox and B. Pruden, “Economics of Hydrogen Recovery Processed for the Purification of Hydroprocessor Purge and Off-gases,” *International Journal of Hydrogen Energy*, vol. 24, pp. 405 – 424, 1999.
- [85] M. Khajepour, F. Farhadi and M. Pishvaie, “Reduced Superstructure Solution of MINLP Problem in Refinery Hydrogen Management,” *International Journal of Hydrogen Energy*, vol. 34, pp. 9233 - 9238, 2009.
- [86] Z. Liao, J. Wang, Y. Yang and G. Rong, “Integrating Purifiers in Refinery Hydrogen Networks: A Retrofit Case Study,” *Journal of Cleaner Production*, vol. 18, pp. 233 – 241, 2010.
- [87] M. Ahmad, N. Zhang and M. Jobson, “Modeling and Optimization for Design of Hydrogen Networks for Multi-period Operation,” *Journal of Cleaner Production*, vol. 18, pp. 889 – 899, 2010.
- [88] J. Yunqiang, S. Hongye, L. Zuwei and H. Weifeng, “Modeling and Multi-Objective Optimization of Refinery Hydrogen Network,” *Chinese Journal of Chemical Engineering*, vol. 19, pp. 990 — 998, 2011.
- [89] S. Mu, H. Su, Y. Gu and J. Chu, “Multi-objective Optimization of Industrial Purified Terephthalic Acid (PTA) Oxidation Process”, *Chinese Journal of Chemical Engineering*, vol. 11, pp. 536 – 541, 2003.
- [90] S. Mu, H. Su, Y. Gu and J. Chu, “Scalable Multi-objective Optimization of Industrial Purified Terephthalic Acid (PTA) Oxidation Process”, *Compu. and Chem. Eng.*, vol 28, pp. 2219 – 2231, 2004.

- [91] N. Tahouni, M. Shariati and M. Panjeshahi, “Comprehensive Modeling of Hydrogen Network in Petrochemical Complexes,” *Chemical Engineering Transactions*, vol. 29, pp. 1093 – 1098, 2012.
- [92] L. Zhou, Z. Liao, J. Wang, B. Jiang, Y. Yang and D. Hui, “Optimal Design of Sustainable Hydrogen Networks,” *International Journal of Hydrogen Energy*, vol. 38, pp. 2937 – 2950, 2013.
- [93] C. Baird, *Petroleum Refining Process Correlations*, HPI Consultant, 1987.
- [94] W. Baldauf, U. Balfanz and M. Rupp, “Upgrading of Flash Pyrolysis Oil and Utilization in Refineries,” *Biomass Bioenergy*, vol. 7., no. 1-6, pp. 237 – 244, 1994.
- [95] N. Zhang, “Novel Modelling and Decomposition for Overall Refinery Optimization and Debottlenecking,” PhD Thesis: University of Manchester Institute of Science and Technology, UK, 2000.
- [96] S. Parkash, *Refining Processes Handbook*, Elsevier, USA, 2003.
- [97] M. Peters and K. Timmerhaus, *Plant Design and Economics for Chemical Engineers*, McGraw-Hill, Singapore, 1990.
- [98] A. Sharma, *Text Book of Correlations and Regression*, Discovery Publishing House, India, 2005.
- [99] T. Edgar and D. Himmelblau, *Optimization of Chemical Processes*, McGraw-hill Companies, New York, 2001.
- [100] A. Brooke, D. Kendrick, A. Meeraus, and R. Ramesh, *GAMS – A User’s Guide: Tutorial by Richard E R*, GAMS Development Corporation, Washington, USA, 2007.
- [101] EIA, *World Oil Market and Oil Price Chronologies*. Energy Information Administration, <http://www.eia.doe.gov>. Last access 20/07/2013.
- [102] Y. Zhang, T. Brown, G. Hu and R. Brown, “Techno-economic Analysis of Monosaccharide Production via Fast Pyrolysis of Lignocelluloses,” *Bioresource Technology*, vol. 127, pp. 358 – 365, 2013.
- [103] T. Brown, R. Thilakarathne, R. Brown and G. Hu, “Techno-economic Analysis of Biomass to Transportation Fuels and Electricity via Fast Pyrolysis and Hydroprocessing,” *Fuel*, vol. 106, pp. 463 -469, 2013.

- [104]H. Lee, J. Pinto and I. Grossmann, “Mixed-integer Linear Programming Model for Refinery Short-term Scheduling of Crude Oil Unloading with Inventory Management. *Ind. Eng. Chem. Res.*, vol. 35., no. 5, pp. 1630–1641, 1996.
- [105]I. Alhajri, Y. Saif, A. Elkamel and A. Almansoori, “Overall Integration of the Management of H₂ and CO₂ within Refinery Planning Using Rigorous Process Models,” *Chem. Eng. Comm*, vol. 200, pp. 139 – 161, 2013.

PUBLICATION LIST

- [1] Mahmoud, A and M. Shuhaimi. Systematic Methodology for Optimal Enterprise Network Design between Bio-refinery and Petroleum Refinery for the Production of Transportation Fuels. *Energy*, vol 59, pp. 1 – 10, 2013.

- [2] Mahmoud, A and M. Shuhaimi. A Systematic Approach for Co-locating Bio-refinery into an Existing Oil Refinery using MILP Model. 4th AUN/SEED-Net Regional Conference on Chemical Engineering. Kuala Lumpur, February 9-10, 2012

- [3] Mahmoud, A and M. Shuhaimi. Refinery Hydrogen Management. International Conference on Process Engineering and Advanced Materials (ICPEAM), Kuala Lumpur, convention centre, 12- 14 June, 2012.

- [4] Mahmoud, A and M. Shuhaimi. A Linearized Mixed-integer Programming Strategy for the Integration of Hydrogen Management in Refinery Operation with Materials Processing System. National Postgraduate Conference, Universiti Teknologi PETRONAS, July 2013.

APPENDIX A

BIO-REFINERY PROCESSING UNITS

A1: Feed pre-treatment and fast pyrolysis unit.

Figure A1 shows a simplified flow diagram of a pyrolysis unit, which consist of dryer followed by pyrolyser and bio-oil quenching. Biomass is dried from its moisture level of 50 wt% to 7 wt% using hot flue gases from the char combustor in a direct-contact dryer. It is then ground to approximately 2-6 mm particle size. The dried, finely ground biomass is fed to a circulating fluidized pyrolysis reactor operating at actual temperature of 520 °C. Sand is used as the fluidizing medium and the residence time is less than one second. Fast pyrolysis converts the biomass into a mixture of gases, bio-oil, and char. A cyclone at the outlet of the pyrolyser separates sand and char from the gases and liquids. The hot bio-oil vapor is rapidly quenched with cooled bio-oil and then separated from the remaining vapors. Most of the gases are recycled to the pyrolysis reactor to assist fluidization. The char and a portion of the gas are burnt to heat the circulating sand. The cooled pyrolysis oil contains about 20-25% water content.

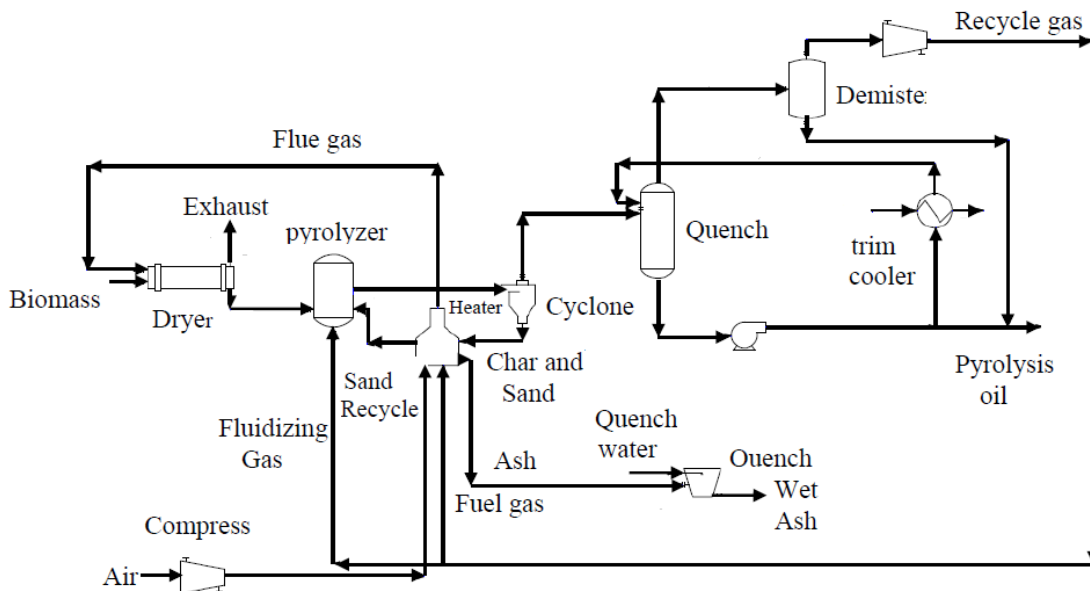


Figure A1: Flow diagram for pyrolysis unit [11]

A.2 Hydrotreating unit

Figure A2 shows a simplified flow diagram for bio-oil stabilization unit, which consists of two-stage hydrotreating unit, high pressure flash, low pressure flash and PSA unit to recover hydrogen from the off-gases. The bio-oil product from the

pyrolysis unit is pumped to high pressure, then combined with compressed hydrogen and preheated with reactor effluent. Two-stage hydrotreating unit is used to stabilize the bio-oil [34]. The product from the two-stage hydrotreating unit is separated into treated oil, wastewater, and off-gas streams using high pressure flash and low pressure flash separators. The off-gas is sent to a pressure swing adsorption (PSA) system for recovery of the hydrogen gas. The recovered hydrogen is recycled to the reactors in order to reduce the hydrogen requirement from hydrogen plant, which is more expensive than the recovered hydrogen. The low pressure gas stream from the bottom of PSA is sent to a steam reformer for hydrogen production. The treated oil is a mixture of hydrocarbons with a low level of oxygen about 2%.

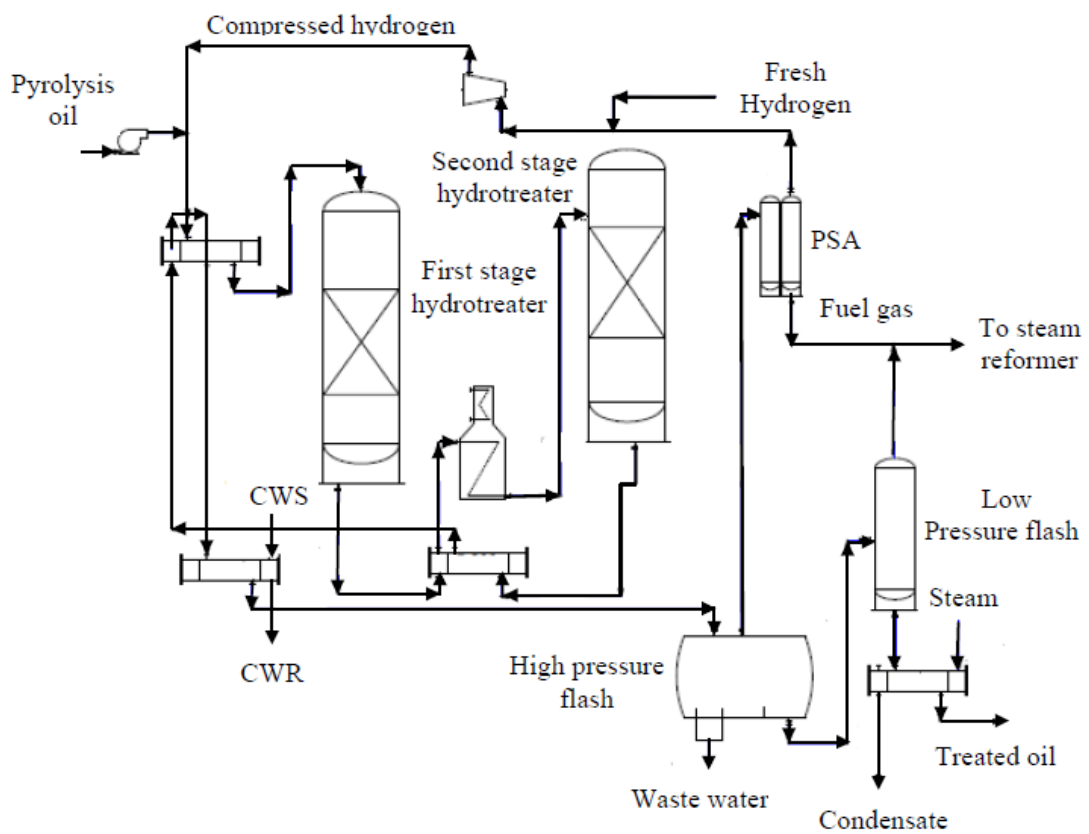


Figure A2: Flow diagram for pyrolysis oil stabilization [11].

A.3 Hydrocracking and product separation unit

Figure A3 shows a simplified flow diagram for the hydrocracking and product separation processes. The hydrotreated oil is stabilized by removing butane and lighter components in a de-butanizer column. The stable oil stream is then separated into light and heavy fractions in naphtha splitter and diesel splitter columns, respectively. The heavy fraction is sent to the hydrocracker to completely convert the oil to gasoline and diesel blend components. The product is a mixture of liquids spanning the gasoline and diesel range and some byproduct gas. The gasoline and diesel range products are separated by product splitter column. These products are

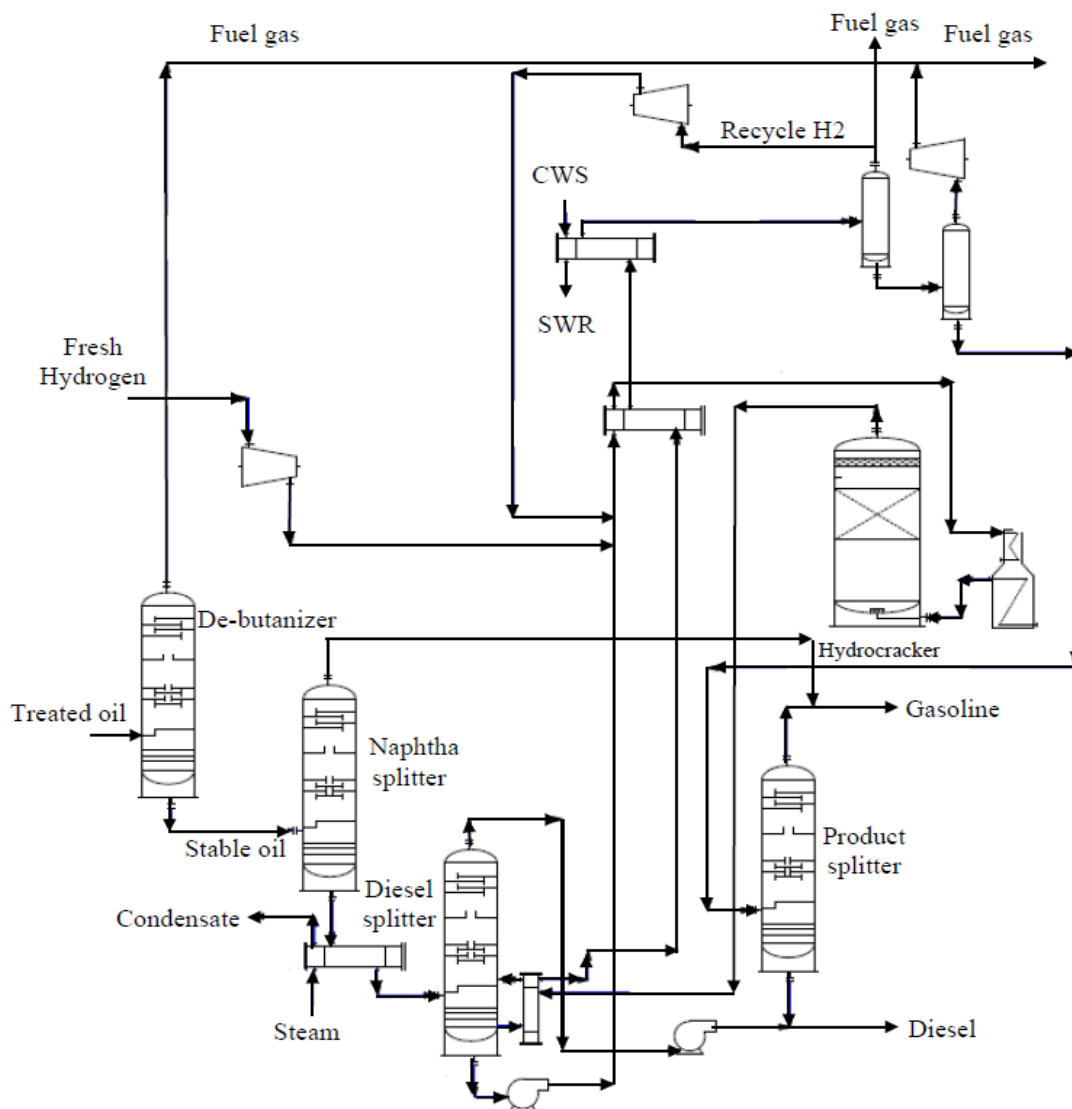


Figure A3: Flow diagram for hydrocracking and product separation [11].

suitable for blending into finished fuel [11]. The characterizations of the gasoline and diesel products are provided in Table A3.

Table A3: Characterizations of the gasoline and diesel products [11, 94]

Property	Gasoline	Diesel
SG	0.7517	0.873
Sulfur (ppm)	130	109
RON	66.4	-
RVP (psi)	11.1	-
Cetane number	-	45

A4. Hydrogen Production unit

Hydrogen is generated by steam reforming of natural gas and off-gases streams from hydrotreating and hydrocracking processes as shown in Figure A4. Some of the off-gases are compressed and mixed with makeup natural gas and sent to the hydrodesulfurization unit (HDS). Hydrogen for the HDS unit is supplied by the off-gas stream. The gas exiting the HDS unit is then mixed with superheated steam and sent to the steam reformer to produce syngas. The syngas hydrogen content is further increased by high temperature shift (HTS) reaction. After condensing out the water, the hydrogen is purified by pressure swing adsorption (PSA). The fuel gas from the bottom of PSA is recycled to the reformer burners.

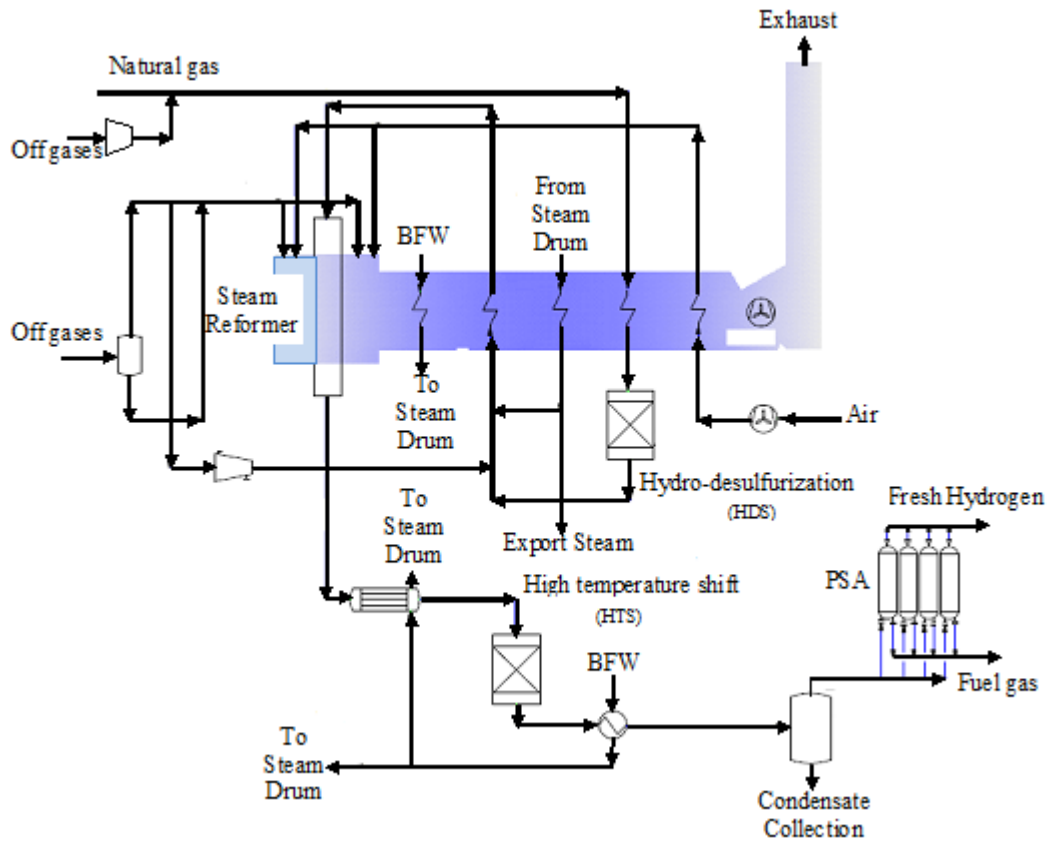


Figure A4: Flow diagram for hydrogen generation by steam reforming [11]

APPENDIX B

PETROLEUM REFINERY PROCESSING UNITS

B.1: Crude Distillation Unit

Crude distillation unit (CDU) is the first unit for the fractionation of crude oil into its' individual cuts. Figure B1 shows a simplified flow scheme of CDU, which comprise of atmospheric and vacuum distillation columns with their respective distillation products. Desalted crude feedstock is preheated in crude preheat train (CPT) by exchanging heat with the hot products coming from the CDU. The preheated crude then flows to a direct-fired heater to raise its temperature into the operating temperature of the atmospheric distillation column, 371°C. The main fractions are obtained according to specific boiling-point ranges and can be classified in order of decreasing volatility into gases, light distillates, middle distillates, gas oils, and residuum [15, 17].

Further heating of the atmospheric residue, greater than 399 °C, might form coke in the extreme and olefinic products, which are not desirable. Further vaporization and fractionation, therefore, need to be achieved at reduced pressures in a vacuum distillation unit [15, 17].

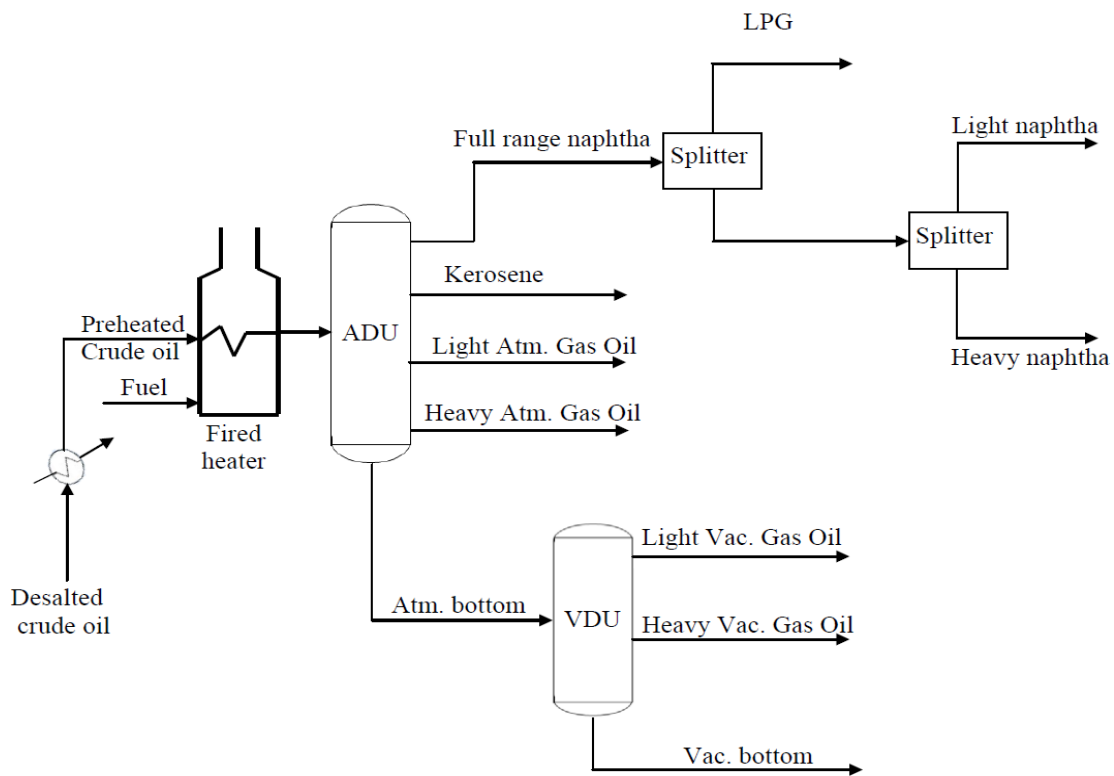


Figure B1: Simplified flow scheme of crude distillation unit [17]

B2: Hydrotreaters

Hydrotreating processes are used to remove impurities such as sulfur, nitrogen, oxygen and metals from petroleum fractions. Typically, hydrotreating is done prior to conversion processes to avoid catalyst contamination in the downstream reactors. Hydrotreating process conditions range from mild reactor conditions of as low as 2,800 kPa and 260 °C for light fractions such as naphtha to very severe conditions of up to 13,800 kPa and 427 °C for heavy fractions such as heavy gas oil and vacuum residuum [13, 15]. The amount of hydrogen required in the hydrotreating process increases significantly as the feedstock becomes heavier. Figure B2 illustrates the flow scheme for typical hydrotreating unit. Hydrocarbon feedstock is mixed with the make-up hydrogen, heated and fed to the hydrotreating reactor. The reactor effluent is separated into liquid and gas phase. The liquid stream is sent to stripper tower, where

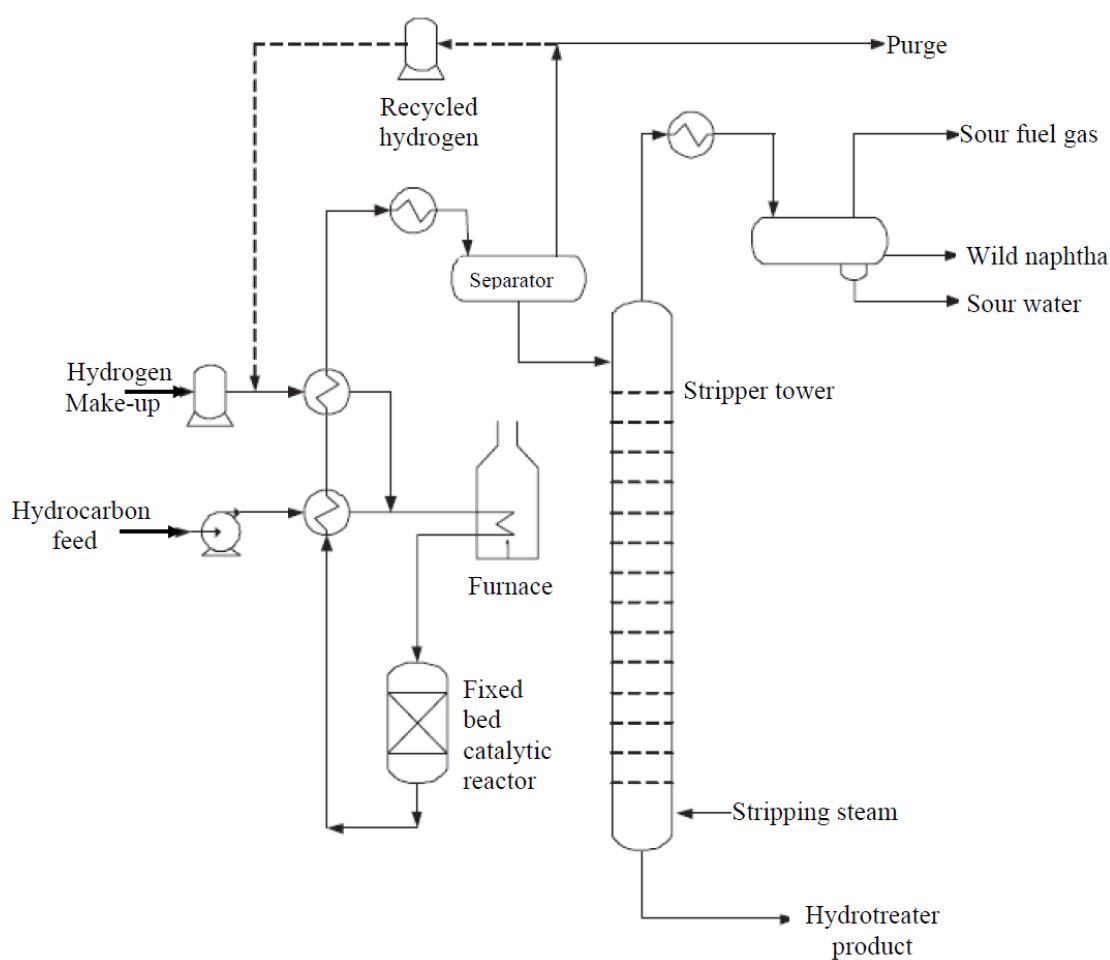


Figure B2: Catalytic hydrotreating unit flow diagram [13]

steam is used to strip the hydrogen sulfide and any naphtha and lighter boiling components generated in the reactor from the higher boiling range products. Since the resulting naphtha stream contains light ends components, it is referred to as unstabilized naphtha or wild naphtha. The stripped liquid product stream can be sent to storage tanks for additional refinery processing or finished product blending [13, 15].

B3: Hydrocrackers

Hydrocracking is the breaking down of heavy crude oil fraction into light fractions. Hydrocracking is probably the most versatile of the conversion processes. It can process a wide variety of feedstocks, including catalytic and thermally cracked oil as well as virgin gas oil of widely different boiling ranges. Hydrocracking units are configured from either a single stage or two stages of hydrocracking reactors with typical operating conditions ranging from 350 to 420 °C and from 6900 to 13,800 kPa [15, 16]. The actual temperature and pressure requirements are dependent on type of unit feeds, catalyst activity and target yields based on economics. Figure B3 shows a simplified flow scheme of hydrocracking unit comprises hydrotreating unit, two stage hydrocracking unit, high pressure separator, low pressure separator and fractionation unit. The hydrocarbon feedstock is preheated and mixed with fresh hydrogen, then pass to hydrotreater to remove the impurities from the feedstock. The treated hydrocarbon is mixed with hydrogen and pass to the first stage hydrocracker. The reactor effluent goes through heat exchangers to a high-pressure separator where the hydrogen-rich gases are separated and recycled to the reactors. The liquid product from the separator is sent to a fractionator where the C4 and lighter gases are taken off overhead, and the light and heavy naphtha, jet fuel, and diesel fuel boiling range streams are removed as liquid sidestreams. The fractionator bottom is used as feed to the second-stage reactor system [15, 16].

B4: Fluidized Catalytic Cracker

Fluidized catalytic cracking (FCC) is the most widely-used process for converting high-boiling and high-molecular weight hydrocarbon fractions of crude petroleum into more valuable products. Figure B4 shows a simplified process flow scheme of FCC

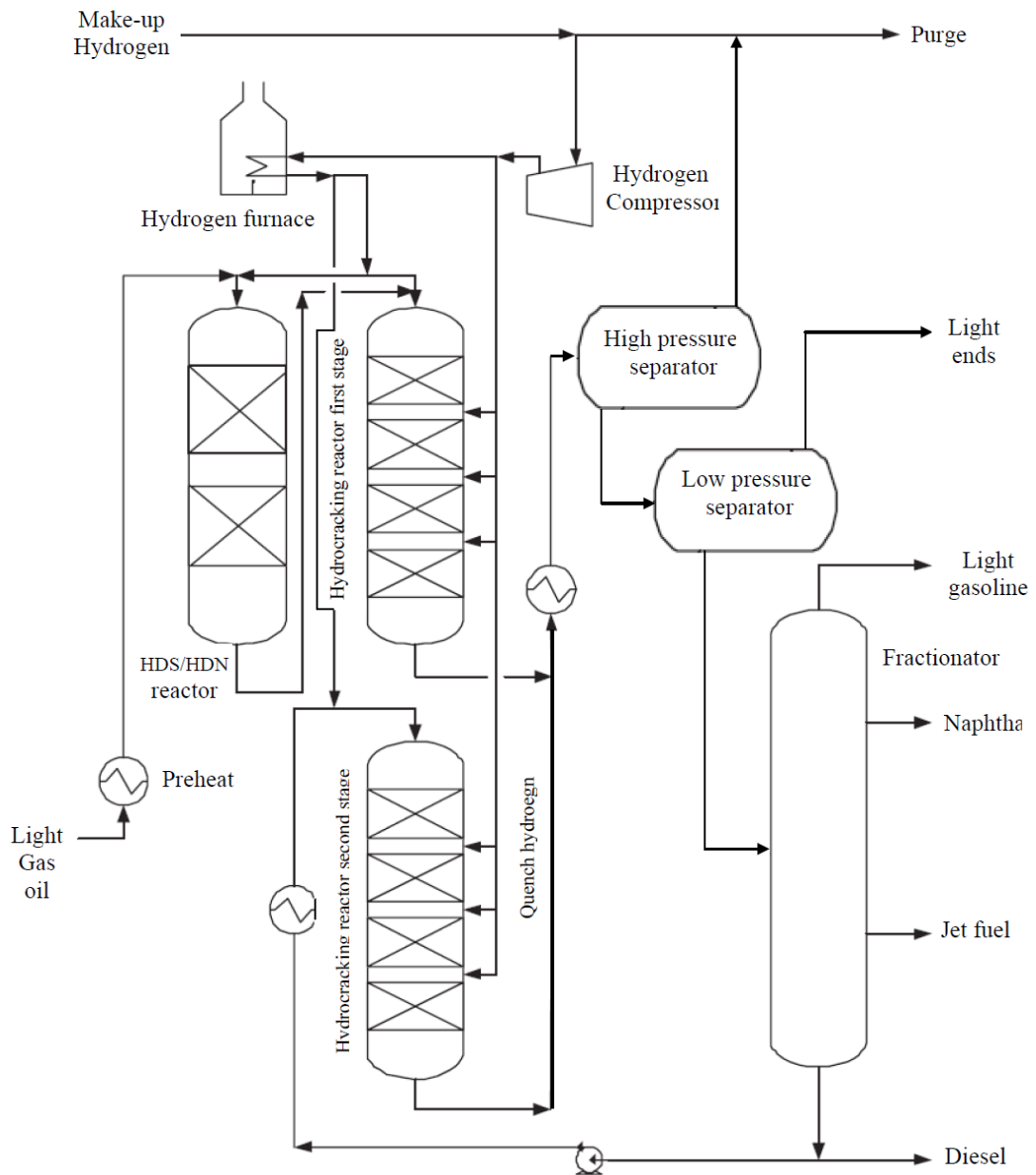


Figure B3: Simplified flow scheme of hydrocracking unit [16].

unit comprises reactor/regenerator section and fractionation section. The feedstock to an FCC is usually heavy gas oil flows from the atmospheric and vacuum distillation columns. The feedstock may be preheated, either by heat exchange or in a direct fired heater, before being mixed with the hot regenerated catalyst, Zeolite. The hot catalyst vaporizes the gas oil and heats the oil to the reactor temperature. As the cracking reaction progresses, the catalyst is progressively deactivated by the formation of coke

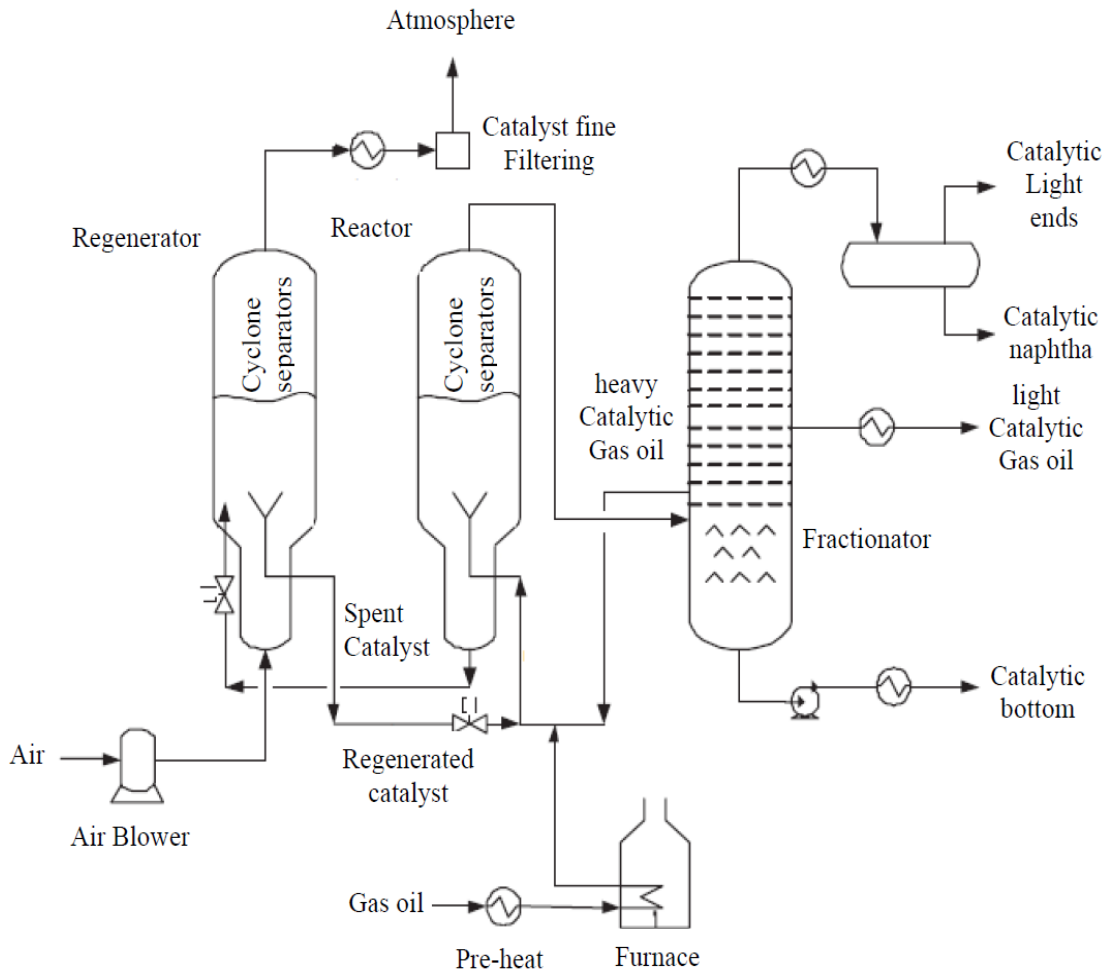


Figure B4: Fluid Catalytic Cracking Flow Diagram [15].

on the surface of the catalyst. Primary and secondary cyclone separators are utilized to separate the vaporized hydrocarbons from the catalyst. The hydrocarbons are sent to a fractionator for separation into streams having the desired boiling ranges such as catalytic lights ends, catalytic naphtha, light catalytic gas oil, heavy catalytic gas oil and catalytic bottoms. The heavy catalytic gas oil is recycled to the reactor with the unit feedstock to be converted into lower boiling components. The spent catalyst flows into the regenerator vessel where the coke is burned off by the introduction of air [15, 16].

B5: Catalytic Reformer

Catalytic reforming (CR) of low-octane virgin and cracked naphtha produces high-octane reformate for gasoline blend stocks. Figure B5 shows a simplified flow scheme

of CR unit comprises catalyst regeneration section, staged reactors and fractionation. All of the reforming catalyst in general use today contains platinum supported on an alumina base. In most cases rhenium is combined with platinum to form a more stable catalyst which permits operation at lower pressures. The reforming reactions are endothermic meaning that the reactions cool the hydrocarbons. The hydrocarbons are re-heated by direct-fired furnaces in between the subsequent reforming reactors. As a result of the very high temperatures, the catalyst becomes deactivated by the formation of coke on the catalyst which reduces the surface area available to contact with the hydrocarbons. The reactor effluents are separated in a gas liquid separator. The gas, which is rich in hydrogen, will be recycled to the reactor. The liquid product containing reformat is passed to the product stripper to separate it from the light ends [12, 15].

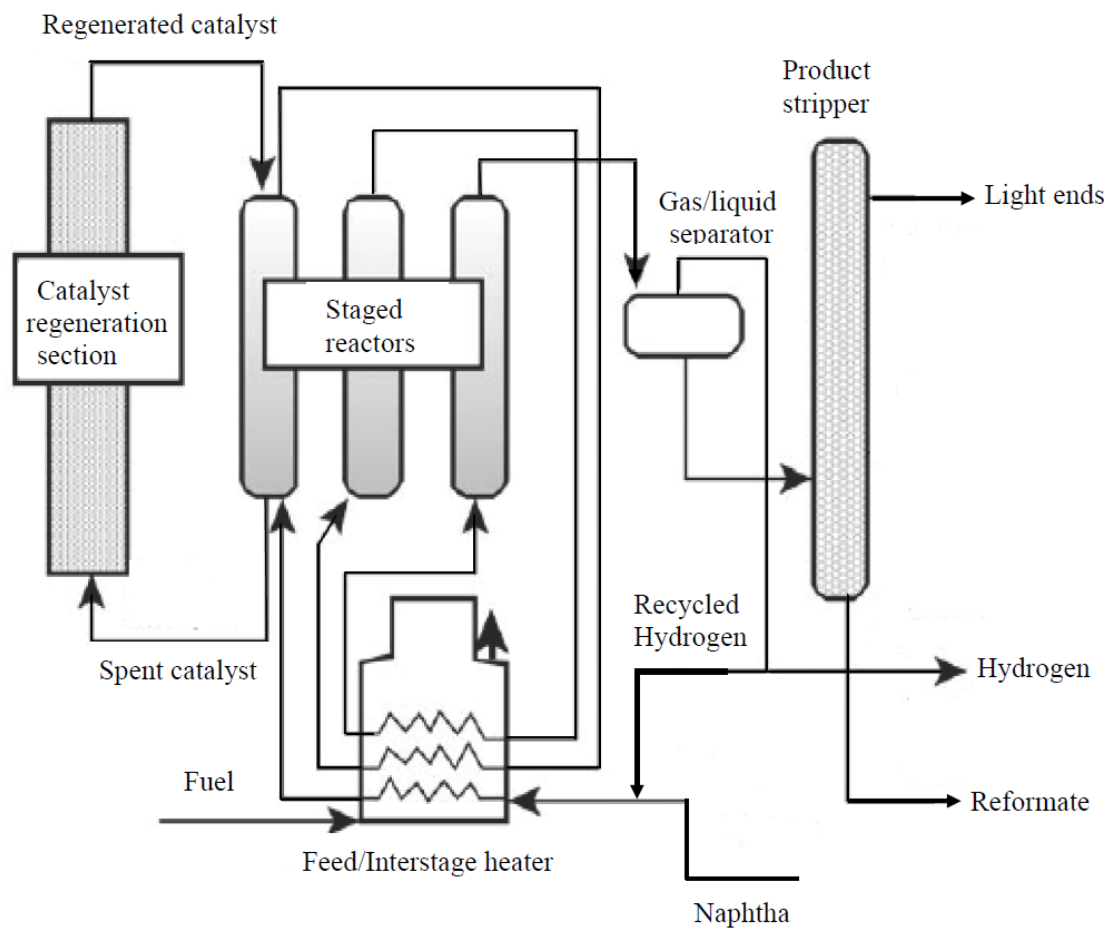


Figure B5: A simplified flow scheme of catalytic reforming unit [12].

APPENDIX C

ILLUSTRATIVE EXAMPLES

In Appendix C, simple examples are presented to illustrate the calculations of some of the models developed in the chapter of the methodology. Namely, the swing-cut model, the hydrotreating units' models, the linearized model of multiplying continuous and binary variables, the linearized model of °API property at HN region and the linearized model of calculating the power of the new compressor.

Example C1: Swing-cut model.

Figure C1 shows a part of TBP curve for Alaska crude oil. Naphtha (naph), kerosene (kero) and Diesel (dies) are separated as distillates. The IBP for naph is 32.2°C and the EBP is 193.3°C. The IBP for kero is 165.6°C and the EBP is 271.1°C. The IBP and EBP for dies are 215.6°C and 332.2°C, respectively. The base yields of naph, kero and dies are 14.7 vol%, 11.1 vol% and 17 vol%, respectively. Use the swing-cut method to maximize the yield of the more profitable fraction (kero) and calculate the new yields of naph and dies.

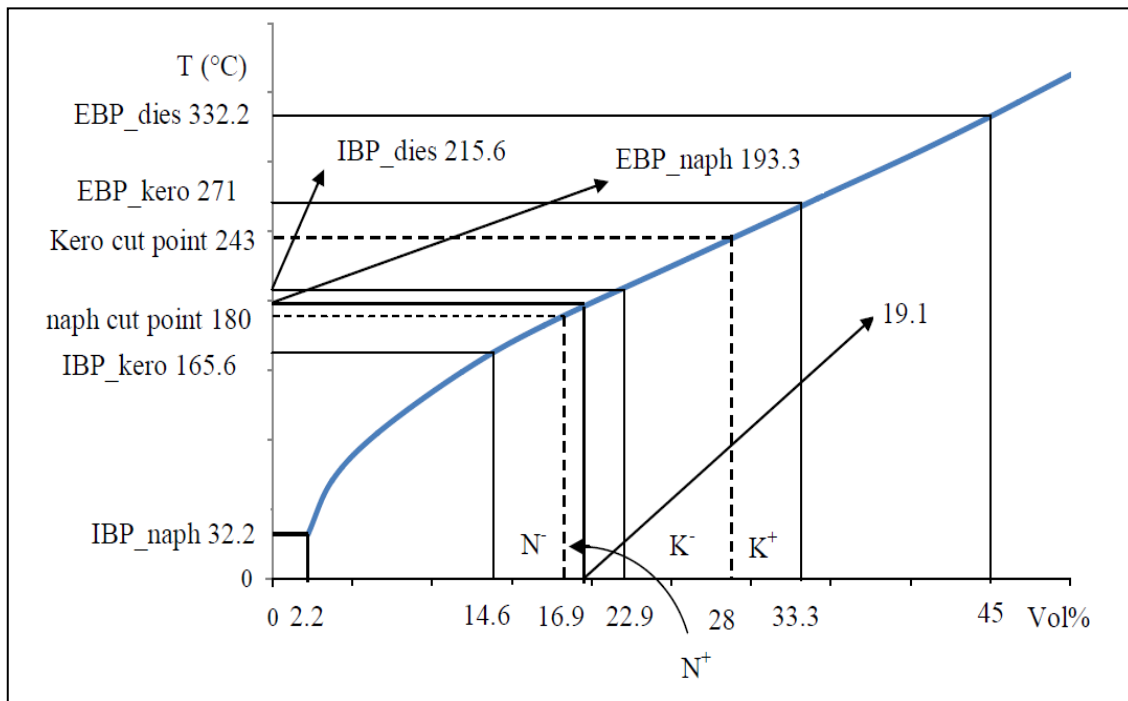


Figure C1: Cut-points and swing-cuts of a distillation fraction

Solution:

Swing cut for kero

$$\text{kero}_{\text{Base yield}} = 11.1 \text{ vol\%}$$

$$\text{kero swing-cut at IBP (naph cut point - IBP_kero), } N^- = 2.3 \text{ vol\%}$$

$$\text{kero swing-cut at EBP (EBP_kero - kero cut point), } K^+ = 5.3\%$$

New yields

$$\text{kero} = \text{kero}_{\text{Base yield}} + N^- + K^+ = 11.1 + 2.3 + 5.3 = 18.7 \text{ vol\%}$$

$$\text{naph} = \text{naph}_{\text{Base yield}} - N^- = 14.7 - 2.3 = 12.4 \text{ vol\%}$$

$$\text{dies} = \text{dies}_{\text{base yield}} - K^+ = 17 - 5.3 = 11.7 \text{ vol\%}$$

The swing-cut has increased the yield of Kerosene by 68.5%

Example C2: Hydrotreating units' models.

Gas oil fraction from CDU is sent to a hydrotreater. The properties of the gas oil are:

$$\text{SG (Specific gravity)} = 0.92$$

$$\%S \text{ (Sulfur content)} = 2.6$$

$$\%N \text{ (Nitrogen content)} = 0.09$$

$$\text{FCC1 (Volume fraction FCC stock in feed stock)} = 0.9$$

$$B \text{ (Bromine number)} = 0$$

$$K_f \text{ (Characterization factor)} = 11.87$$

Use the sub-model for GOHT to calculate the amount of hydrogen required for the hydrotreating process. Then, calculate the yield of heavy gas oil as well as the SG and %S of the hydrotreated product (TGO).

Solution:

- Hydrogen required, H_0 (Scf/bbl)
$$= 40 + 150S_f + 101.5N_f + 7(B_f)(SG_f) + 300(11.9 - K_f)(FCC1) = 447 \text{ cf/bbl}$$
 C2.1
- Hydrogen yield, H (wt%) = $\left(\frac{1}{658.29}\right)\left(\frac{H_0}{SG_f}\right) = 0.74 \text{ wt\%}$ C2.2
- Hydrogen sulfide yield, H_2S (wt%) = $0.957S_f = 2.47 \text{ wt\%}$ C2.3
- Ammonia yield, NH_3 (wt%) = $0.535N_f = 0.048 \text{ wt\%}$ C2.4
- Naphtha yield, HN (wt%) = $0.173S_f + 0.0424S_f^2 = 0.74 \text{ wt\%}$ C2.5
- Middle distillate yield, MD (wt%) = $1.418S_f + 0.432S_f^2 = 6.61 \text{ wt\%}$ C2.6

- Heavy gas oil yield, HGO (wt%) =

$$100 + H - H_2S - NH_3 - HN - MD = 90.9 \text{ wt\%} \quad \text{C2.7}$$
- Heavy gas oil specific gravity, $SG_{HGO} = SG_f - 0.025H = 0.9 \quad \text{C2.8}$
- Sulfur content of naphtha, $S_n \text{ (wt\%)} = 0.0085S_f = 0.022 \text{ wt\%} \quad \text{C2.9}$
- Sulfur content of middle distillate, $S_d \text{ (wt\%)} = 0.02S_f = 0.052 \text{ wt\%} \quad \text{C2.10}$
- Sulfur content of heavy gas oil (wt%)

$$S_{HGO} = (10S_f - (S_n)(HN) - (S_d)(MD))/HGO = 0.282 \text{ wt\%} \quad \text{C2.11}$$

Example C3: Linearized model of multiplying continuous and binary variables.

Use equation (3.57) to prove that,

If $y_d = 0$, then $C_d = 0$

If $y_d = 1$, then $C_d = \text{Mid}V_d$

In case of $y_d = 0$

Equation (3.58) $0 \leq C_d \leq \text{Mid}V_d$

Substitute $y_d = 0$ in Equation (3.59)

$$\text{Mid}V_d - \text{Mid}V_d^{up} \leq C_d \leq 0 \quad \text{C3.1}$$

From Equations (3.58) and (C3.1): $0 \leq C_d \leq 0$, therefore, C_d will be chosen to be zero.

In case of $y_d = 1$

Equation (3.58) $0 \leq C_d \leq \text{Mid}V_d$

Substitute $y_d = 1$ in Equation (3.59)

$$\text{Mid}V_d \leq C_d \leq \text{Mid}V_d^{up} \quad \text{C3.2}$$

From Equations (3.58) and (C3.2): $\text{Mid}V_d \leq C_d \leq \text{Mid}V_d$, therefore, C_d will be set equal to $\text{Mid}V_d$.

Example C4: Linearized model of °API property at HN region.

Estimate the °API property at HN region using the linearized model.

As shown in Figure 3.11, the HN Mid v% is divided into two regions. Therefore, equation (3.65) becomes

$$PV_{API} = a_{01}(MidV_1^0 * y_1) + a_{11}(MidV_1^1 * y_1) + a_{02}(MidV_2^0 * y_2) + a_{12}(MidV_2^1 * y_2) \quad C4.1$$

Substitute the HN region parameters from Table (3.4).

$$PV_{API} = 96.72 * y_1 - 7.97 * (MidV_1 * y_1) + 63.89 * y_2 - 1.08 * (MidV_2 * y_2) \quad C4.2$$

The $(MidV_1 * y_1)$ and $(MidV_2 * y_2)$ terms will be linearized using the same procedure used for linearizing Equation (3.56). Then, the application of Equation (3.60) will allow the optimizer to select only one region at a time, either $MidV_1$ or $MidV_2$.

Example C5: Linearized model for calculating the power of the new compressor.

Consider three consumers units u_1 , u_2 and u_3 with pressure requirements of 2000psi, 600psi and 350psi, respectively. A new compressor is to be installed to deliver 3 MMscfd and 5 MMscfd of gas to u_2 and u_3 , respectively. The lowest source pressure to the new compressor is 300 psi.

Determine the power requirement of the new compressor that will minimize the total annual cost.

Solution:

Pressure ratio between the new compressor and $u_1 = 6.67$

Pressure ratio between the new compressor and $u_2 = 2$

Pressure ratio between the new compressor and $u_3 = 1.17$

We assumed that each pressure ratio represents a new compressor for the three different consumers.

For installation of only one new compressor $\theta = 1$ and Equation (3.69) can be expressed as:

$$\sum_n X_n = 1 \quad C5.1$$

To minimize total annual cost, the best choice for installing a new compressor will be n_2 . This is because of its lower pressure ratio as well as its ability to deliver the gas to the consumers u_2 and u_3 . The compressor n_3 is not appropriate to deliver gas for consumer u_2 since its discharge pressure is lower than the sink of u_2 . The compressor

n_1 is able to satisfy the pressure requirement of all the consumers but its pressure ratio is higher than the compressor n_2 , hence higher power requirement. Therefore, the discharge pressure of the compressors n_1 and n_3 will be set to zero using Equation (3.70), because $X_{n1} = X_{n3} = 0$.

The power of the new compressor n_2 is calculated using Equations (3.71) and (3.72).

For $n_2 = 1$, $F_{in,n2} = 8\text{MMscfd}$, then

$$Pwr_{n2} = 22.031 * F_{in,n2} = 176.25 \text{ KW} \quad \text{C5.2}$$

APPENDIX D

PROCESSING UNITS' MODELS

D1: Naphtha hydrotreating unit model

Naphtha saturation factor, ASF

$$= 0.011 + 76N_f^2 + 0.039S_f$$

Hydrogen consumption (scf/bbl), H_0

$$= 25.0 + 70S_f + 290N_f + 6.5O_f + 28(\text{ASF})(A_f)$$

Hydrogen consumption (WT.PCT.), H

$$= \left(\frac{1}{658.29} \right) \left(\frac{H_0}{SG_f} \right)$$

Hydrogen sulfide yield (WT.PCT.), H_2S

$$= 1.063S_f$$

Ammonia yield (WT.PCT.), NH_3

$$= 1.21N_f$$

Gas yield (WT. PCT.), RG

$$= 0.25 + 0.66S_f + 7.4N_f$$

Naphtha yield (WT.PCT.), HN

$$= 100 + H - RG - NH_3 - H_2S$$

Naphtha specific gravity, SG_n

$$= SG_f / (1 + (0.001)(\text{ASF})(A_f) + (0.033)(H))$$

Sulfur content of naphtha (WT.PCT.), S_n

$$= 0.0001S_f$$

Research octane number of naphtha, RON_n

$$= RON_f - 0.33O_f + 1.5 - 0.31(\text{ASF})(A_f)$$

D2: HPI Middle distillate hydrotreating unit model

Hydrogen consumption (scf/bbl), H_0

$$= 120S_f + 159.5N_f + 8SG_fB_f + 25 + 290(\text{FCC})(11 - K_f)$$

Products yields (vol%),

$$yield_s = \sum_{h=0}^2 (a_{s,h} - b_{s,h} * FP_{DHT,SG} - c_{s,h} * FP_{DHT,S\%}) * XU_{DHT}^h$$

Products properties, API and Cetane number

Table D2: DHT Unit Model Equations coefficients

Equation	Parameter	Naphtha	Kerosene	Diesel
yield	a0	0	429E-6	1.851E-3
	b0	1.0E-3	186.872E-3	807.128E-3
	c0	0	154E-6	0.666E-3
	a1	0	7.543E-6	32.577E-6
	b1	0.40E-3	- 75.2E-6	- 324.8E-6
	c1	0	0.171E-6	0.74E-6
	a2	0	0.0	0.0
	b2	0	- 0.94E-6	- 4.06E-6
	c2	0	0	0.0
API	a0	55	7.2	- 1.8
	b0	0	1	1
	c0	12.3E-3	11.4E-6	11.4E-6
	d0	3.26E-6	4.104E-6	4.104E-6
	a1	0	0.04	0.04
	b1	0	0	0
	c1	0	0.2E-6	0.2E-6
	d1	0	4.56E-9	4.56E-9
Cetane number	a0	0	- 3.592	- 29.2
	b0	0	1.64	2
	c0	0	18.696E-6	22.8E-6
	d0	0	6.731E-6	8.208E-6
	a1	0	65.6E-3	0.08
	b1	0	0	0
	c1	0	0.328E-6	0.4E-6
	d1	0	7.478E-9	9.12E-9
Sul%	a	609.8E-3	1.0976	8.25E-6
	b	0.1	0.1	1.02E-3
	c	0.9E-3	0.9E-3	0.9E-3

$$PV_{DHT,S,P} = \sum_{h=0}^1 \left[a_s + b_s * FP_{DHT,API} + \frac{(c_s + d_s * FP_{DHT,S\%})}{FP_{DHT,SG}} \right] * XU_{DHT}^h$$

$p \in API, \text{cetane number}$

Products properties, sulfur content %

$$PV_{DHT,S,S\%} = a_s * (b_s + c_s * XU_{DHT}) * FP_{DHT,S\%}$$

D3: HPI Gas oil hydrotreating unit model

Hydrogen required, H_0 (Scf/bbl)

$$= 40 + 150S_f + 101.5N_f + 7(B_f)(SG_f) + 300(11.9 - K_f)(FCC1)$$

Hydrogen yield, H (Wt%)

$$= \left(\frac{1}{658.29} \right) \left(\frac{H_0}{SG_f} \right)$$

Hydrogen sulfide yield, H_2S (Wt%)

$$= 0.957S_f$$

Ammonia yield, NH_3 (Wt%)

$$= 0.535N_f$$

Naphtha yield, HN (Wt%)

$$= 0.173S_f + 0.0424S_f^2$$

Middle distillate yield, MD (Wt%)

$$= 1.418S_f + 0.432S_f^2$$

Heavy gas oil yield, HGO (Wt%)

$$= 100 + H - H_2S - NH_3 - HN - MD$$

Heavy gas oil specific gravity SG_{HGO}

$$= SG_f - 0.025H$$

Sulfur content of heavy gas oil, (Wt%) S_{HGO}

$$= (10S_f - (S_n)(HN) - (S_d)(MD))/HGO$$

D4: Petroleum refinery up-grading units yields

Yield wt%	FCC	FCC (VGO/BIO-OIL)	HC	CR
Hydrogen			-3.35	1.93
LPG	20.4	20	2	
Gasoline	49	48.5	5.6	
LCO	22.5	22.5		
HCO	4	3.2		
Coke	2.3	4.5		
naphtha			13.3	
Kerosene			32.9	
Diesel			43.4	
Reformate				88

D5: Bio-refinery processing units yields

Yield wt%	pyrolysis	HDT	DE-C4	NS	DS	BHC
Py-oil	76.76					
Fuel gas	11.35	10.41	4.98			
Char	11.89					
Tpy-oil		43.95				
Wst-water		45.64				
St-oil			95.02			
Naphtha				29.32		95
DS-F				70.68		
Diesel					81.14	5
HC-F					18.86	
total	100	100	100	100	100	100

APPENDIX E
EQUIPMENT COST DETAILS

Table E1: Equipment capital cost details

No	Equipment name	Original stream metric	New stream metric	Scaling unit	Size ratio	Original Equipment Cost (\$)	Base year	Scaling exp	Install factor	Scaled and installed cost in base year	Installed cost in 2011 \$	Bare Equip Cost in 2011 \$
	Pyrolysis unit											
1	Feedstock handling	500	200	tpd	4	5,570,000	2003	0.7	2.47	14,699,318	21,754,991	8,807,689
1	CFB pyrolyzer	500	200	tpd	4	3,392,000	2003	0.7	2.47	8,951,542	13,248,282	5,363,677
1	Quench	500	200	tpd	4	1,940,000	2003	0.7	2.47	5,119,691	7,577,143	3,067,669
1	Heat recovery	500	0	tpd	0	1,140,000	2003	0.7	2.47	0	0	0
1	Product recovery and storage	500	2000	tpd	4	800,000	2003	0.7	2.47	2,111,213	3,124,595	1,265,018
1	Recycle	500	2000	tpd	4	1,380,000	2003	0.7	2.47	3,641,841	5,389,926	2,182,156
1	Steam and power production	500	0	tpd	0	3,160,000	2003	0.7	2.47	0	0	0
1	Utilities	500	0	tpd	0	3,130,000	2003	0.7	2.47	0	0	0
										34,523,605	51,094,937	20,686,209
	Equipment contingency						35%				17,883,228	7,240,173
											68978165	27,926,382

Table E1: (contd)

No	Equipment name	Original stream metric	New stream metric	Scaling unit	Size ratio	Original Equipment Cost (\$)	Base year	Scaling exp	Install factor	Scaled and installed cost in base year	Installed cost in 2011 \$	Bare Equip Cost in 2011 \$
	Bio-oil up-grading											
2	Feed Booster pump	1,000	2000	tpd	2	30,000	2004	0.65	2.47	232,551	312,480	126,509
2	Feed pump	1,000	2000	tpd	2	122,000	2004	0.65	2.47	945,706	1,270,749	514,473
1	1 st stage reactor	2,038	1,959	Liq scfh	0.96	860,700	2007	0.65	2.47	2,125,929	2,409,347	975,444
1	2 nd stage reactor	2,038	1,959	Liq scfh	0.96	9,018,000	2007	0.65	2.47	19,852,131	25,243,976	10,220,233
1	2 nd stage three phase separator	174,497	161,375	Lb/h	0.92	673,300	2005	0.65	2.47	1,663,113	2,018,940	817,384
1	1 st feed/product heat exchanger	59.85	38.38	mmbtuh	0.64	647,800	2005	0.65	2.47	1,628,026	1,531,091	619,874
1	2 nd feed/product heat exchanger	33.3	1.22	mmbtuh	0.04	622,200	2005	0.65	2.47	1,537,134	228,802	92,632
1	Fired heater	8.35	40.00	mmbtuh	8.18	378,000	2004	0.65	2.47	933,660	3,473,243	1,406,171
	Air cooler	40.38	28.10	mmbtuh	0.70	228,000	2005	0.65		548,093	568,289	230,076

Table E1: (contd)

No	Equipment name	Original stream metric	New stream metric	Scaling unit	Size ratio	Original Equipment Cost (\$)	Base year	Scaling exp	Install factor	Scaled and installed cost in base year	Installed cost in 2011 \$	Bare Equip Cost in 2011 \$
	Bio-oil upgrading											
1	Product trim cooler	8.35	8.35	mmbtu/h	1.00	128,700	2005	0.65	2.47	317,889	406,034	164,386
1	PSA	10	15	mmbtu	1.50	1,750,000	2004	0.65	2.47	4,838,004	3,060,560	1,239,093
1	Product flash drum	71,462	69,520	Lb/h	0.97	38,800	2005	0.65	2.47	95,836	120,237	48,678
1	Product pump	1000	2,000	tpd	2.00	39,000	2004	0.65	2.47	151,158	406,223	164,462
1	Hydrogen compressor	2840	2,840	acfm	1.00	3,869,400	2005	0.65	2.47	9,557,418	12,207,507	4,942,311
1							subtotal				53,257,476	21,561,731
1	Equipment contingency						15%				7,988,621	3,234,259
1							total				61,246,097	24,795,990

Table E1: (contd)

No	Equipment name	Original stream metric	New stream metric	Scaling unit	Size ratio	Original Equipment Cost (\$)	Base year	Scaling exp	Install factor	Scaled and installed cost in base year	Installed cost in 2011 \$	Bare Equip Cost in 2011 \$
	Hydrocracker											
1	Debutanizer	69,495	69,495	Lb/h	1.00	55,100	2007	0.65	2.47	217,113	252,462	102,211
1	Naphtha splitter (NS)	70,500	66,028	Lb/h	0.94	183,700	2005	0.65	2.47	434,817	555,384	224,851
1	Diesel splitter (DS)	45,548	46,668	Lb/h	1.02	65,500	2005	0.65	2.47	164,360	209,934	84,993
1	Product splitter (PS)	9,680	9,694	Lb/h	1.00	123,800	2005	0.65	2.47	306,073	390,942	158,276
1	Debutanizer reboiler	11.60	11.60	mmbtu	1.00	48,600	2007	0.65	2.47	120,042	139,587	56,513
1	NS reboiler	2.90	2.90	mmbtu	1.00	27,200	2007	0.65	2.47	67,184	78,123	31,628
1	DS reboiler	4.77	10.20	mmbtu	2.14	24,900	2005	0.65	2.47	100,797	128,746	52,124
1	PS reboiler	2.63	2.63	mmbtu	1.00	22,400	2007	0.65	2.47	55,328	64,336	26,047
1	Debutanizer condenser	1.48	1.48	mmbtu	1.00	33,200	2007	0.65	2.47	82,004	95,356	38,605
1	NS condenser	5.62	5.62	mmbtu	1.00	43,200	2007	0.65	2.47	106,704	124,077	50,233

Table E1: (contd)

No	Equipment name	Original stream	New stream metric	Scaling unit	Size ratio	Original Equipment Cost (\$)	Base year	Scaling exp	Install factor	Scaled and installed cost in base year	Installed cost in 2011 \$	Bare Equip Cost in 2011 \$
	Hydrocracker											
1	DS condenser	69,495	69,495	Lb/h	1.00	55,100	2007	0.65	2.47	217,113	160,266	64,884
1	PS condenser	70,500	66,028	Lb/h	0.94	183,700	2005	0.65	2.47	434,817	227,762	92,211
1	Debutanizer reflux drum	45,548	46,668	Lb/h	1.02	65,500	2005	0.65	2.47	164,360	21,335	8,637
1	NS reflux drum	9,680	9,694	Lb/h	1.00	123,800	2005	0.65	2.47	306,073	50,877	20,597
1	DS reflux drum	11.60	11.60	mmbtu	1.00	48,600	2007	0.65	2.47	120,042	54,782	22,179
1	PS reflux drum	2.90	2.90	mmbtu	1.00	27,200	2007	0.65	2.47	67,184	35,291	14,287
1	Debutanizer feed preheater	4.77	10.20	mmbtu	2.14	24,900	2005	0.65	2.47	100,797	57,850	23,420
1	DS feed preheater	2.63	2.63	mmbtu	1.00	22,400	2007	0.65	2.47	55,328	68,116	27,577
1	Hydrocracker unit	1.48	1.48	mmbtu	1.00	33,200	2007	0.65	2.47	82,004	16,052,505	6,498,989

Table E1: (contd)

No	Equipment name	Original stream metric	New stream metric	Scaling unit	Size ratio	Original Equipment Cost (\$)	Base year	Scaling exp	Install factor	Scaled and installed cost in base year	Installed cost in 2011\$	Bare equip Cost in 2011\$
	Hydrocracker											
1	Naphtha product coller	1.4	1.45	mmbtuh	1.04	46,300	2005	0.65	2.47	116,999	149,441	60,502
1	Diesel product coller	3.1	4.93	mmbtuh	1.59	44,600	2005	0.65	2.47	148,935	190,232	77,017
1						subtotal					19,107,404	7,735,791
1	Equipment contingency					15%					2,866,110	1,160,368
1						Total					21,973,514	8,896,159

No	Equipment name	Original stream	New stream	Scaling unit	Size ratio	Original Equipment	Base year	Scaling	Install factor	Scaled and installed cost	Total investment
	Hydrogen plant										
1	Steam reformer system	24.5	34.4	Mmscfd H2	1.4	79,406,400	2011	0.65	2.47	99,005,777	97,817,707
						subtotal				99,005,777	97,817,707
	Equipment contingency					0%				0	0
						Total				99,005,777	97,817,707

Table E2: Total project investment factors

Total Project Investment Factors Total Purchased Equipment Cost (TPEC)	100%
Purchased Equipment Installation	39%
Instrumentation and Controls	26%
Piping	31%
Electrical Systems	10%
Buildings (including services)	29%
Yard Improvements	12%
Total Installed Cost (TIC)	247%
Indirect costs	
Engineering	32%
Construction	34%
Legal and Contractors Fees	23%
Project Contingency	37%
Total Indirect	126%
Total Project Investment	373%

APPENDIX F

GAMS CODE

*The following sets, parameters, tables and scalars defined are common in materials

*processing system model GAMS code and integrated model GAMS code.

* Materials-processing system GAMS code.

SETS

i Index for hydrogen source /HP, CRF, HP3/

j Index for fuel system /fuel/

k Index for existing compressor /k1, k2, k3/

u Index for hydrogen consumers /HC1, GOHT, RHT, DHT, NHT, HC2, BHDT, HC3/

n Index for new compressor /n1, n2, n3/

m Index for new purification unit /m1/

il Index for CDU and HDT products and properties /CUT, API,SG, SUL, N, nap2, ker2, dls2/

j1 Index for CDU and HDT models Equations coefficient /a0, a1, a2, b0, b1, b2, c0, c1, c2, a3, a4, a5, b3, b4, b5, c3, c4, c5, d3, d4, a31, b31, c31, d31, a41, b41, c41, d41 /

m1 Index for FCC and HC feedstocks /TGO2,TPY2,TGO3,MIX/

n1 Index for FCC and HC products /LI_GASO, NAPH, DIESEL,LPG_B, DRY_GAS, LPG, GASO,LCO, HCO, COKE, KERO/

U1 Index for processing units that incur operating costs /CDU1, VDU1,FCC1, HCK1, NHDT1, DHDT1, VHDT1, RHDT1, CRU1, PYR1, HDT1,DE-C41, NS1, DS1, PHCK1, BHCK1, PRICE1, H2P1/

O1 Index for operating cost component /S, W, P, F/

c11 Index for bio-refinery products /PY_OIL, FU_GAS, CHAR, TPY_OIL, WASTE_W, PSA_GAS, OFF_GAS, C4_FU_GAS, ST_OIL, NAPH, DS_F, DIES, HC_F, HC_NAPH, HC_DIES, HC_OFF_GAS, HC_FU_GAS/

p1 Index for bio-refinery processing units /PY, HDT, DE4, NS, DS, HC/

alias (u, v);

parameters

FHP /80/

FHP3 /50/

YHP(i) H2 producer purity

/HP 0.95

CRF 0.80

HP3 0.99/

PHP(i) H2 producer pressure

/HP 300

CRF 300

HP3 315/

CH2S(i) H2 costs

/HP 2000

CRF 0

HP3 2400/

PJ(j) pressure of the fuel

/fuel 200/

PKI(k) inlet pressure of the existing compressors

/k1 300

k2 300

K3 300/

PKO(k) outlet pressure of the existing compressor

/k1 2515

k2 2515

K3 600/

maxCP(k) maximum capacity of the existing compressor

/k1 31.5

k2 31.5

K3 31.5/

maxCP1(n) maximum capacity of the new compressor

/n1 70

n2 70

n3 70/

YH2U(u) H2 consumer hydrogen purity

/HC1 0.867

GOHT 0.836

RHT 0.826

DHT 0.749

NHT 0.727

HC2 0.958

HC3 0.958

BHDT 0.99/

CON_FAC(U) hydrogen consumption factor

/HC1 0.3468

GOHT 0.3344

RHT 0.3303

DHT 0.2995

NHT 0.2905

HC2 0.40673

HC3 0.40673

BHDT 0.59677/

PH2U(u) H2 consumer pressure

/HC1 2000

GOHT 500

RHT 600

DHT 500

NHT 300

HC2 1315

HC3 1315

BHDT 2515/

YH2V(v) H2 consumer outlet hydrogen purity

/HC1 0.80

GOHT 0.75

RHT 0.75

DHT 0.70

NHT 0.65

HC2 0.92735
 HC3 0.92735
 BHDT 0.1949/
 PH2V(v) H2 consumer outlet pressure
 /HC1 1200
 GOHT 350
 RHT 400
 DHT 350
 NHT 200
 HC2 1270
 HC3 1270
 BHDT 715/
 YPR(m) PSA product purity
 /M1 0.99/
 REC(m) PSA recovery factor
 /m1 0.9/
 PMO(m) PSA outlet pressure
 /m1 300/
 PMI(m) PSA inlet pressure
 /m1 200/
 YR(u) H2 consumer recycled hydrogen purity
 /HC1 0.80
 GOHT 0.75
 RHT 0.75
 DHT 0.70
 NHT 0.65
 HC2 0.92735
 HC3 0.92735
 BHDT 0.1949/
 PNI(n) inlet pressure of the new compressors
 /n1 300
 n2 300

n3 300/

A8(N) intercept of the new compressor power equation

/n1 4E-12

n2 -2E-12

n3 -5E-13/

B8(n) slope of the new compressor power equation

/n1 77.64

n2 67.73

n3 50.63/

*Tables

Table a1(j1, i1) CDU cut coefficients

CUT

a0 4.038444545

a1 -4.724791067E-02

a2 3.249072770E-04

a3 -2.842069071E-07

a4 8.147748945E-11 ;

Table a11(j1, i1) CDU properties coefficients

SG SUL N

a0 7.2632E-01 2.7008E-01 -8.8508E-04

a1 3.8753E-03 -2.5584E-02 3.0519E-04

a2 3.9242E-05 1.6275E-03 -2.3044E-05

a3 -1.3769E-06 -2.5941E-05 4.6110E-07

a4 9.3693E-09 1.6066E-07 6.7530E-09 ;

Table a2(j1, i1) KERO HDT products coefficients

Nap2 KER2 DLS2

a0 0 0.000429 0.001851

b0 0.001 0.186872 0.807128

c0 0 0.000154 0.000666

a1 0 0.000007543 0.000032577

b1	0.0004	0.0000752	0.3248
c1	0	0.000000171	0.00000074
a2	0	0	0
b2	0	- 0.00000094	- 0.00000406
c2	0	0	0
* SG			
a3	55	7.2	- 1.8
b3	0	1	1
c3	0.0123	0.0000114	0.000041
d3	0.00000326	0.0000041	0.0000041
a31	0	0.04	0.04
b31	0	0	0
c31	0	0.0000002	0.0000002
d31	0	0.00000000456	0.00000000456
* cetane			
a4	0	- 3.592	- 2.9
b4	0	1.64	2
c4	0	0.000018696	0.0000228
d4	0	0.000006731	0.000008208
a41	0	0.0656	0.08
b41	0	0	0
c41	0	0.000000328	0.0000004
d41	0	0.000000007478	0.00000000912
*s%			
a5	0.6098	1.0976	8.25
b5	0.1	0.1	0.00102
c5	0.0009	0.0009	0.0009

Table e1(m1, n1) FCC products

	dry_gas	lpg	gaso	lco	hco	coke
TGO3	0.018	0.204	0.490	0.225	0.040	0.032
MIX	0.020	0.200	0.485	0.225	0.032	0.045;

Table d1(m1, n1) HC products

	li_gas	naph	diesel	LPG_B	kero
TGO2	0.05609439	0.133386661	0.434556544	0.02	0.329167083'

table k1(U1, O1) utilities factors

	S	W	P	F
CDU1	10	150	0.9	0.05
VDU1	10	150	0.3	0.03
FCC1		500	6	0.1
HCK1	50	300	8	0.1
NHDT1	6	300	2	0.1
DHDT1	6	300	2	0.1
VHDT1	8	400	3	0.15
RHDT1	10	500	6	0.2
CRU1	30	400	3	0.3

* /TON

PYR1		4884	192	
HDT1	51.6	2580	30.9	1.03
DE-C41	72.4		0.14	
NS1	72.4		0.14	
DS1	72.4		0.14	
PRICE1	0.00157	0.00002	0.0534	2.5;

Table b1(c11, p1) input output coefficients

	PY	HDT	DE4	NS	DS	HC
PY_OIL	0.7676					
FU_GAS	0.1135					
CHAR	0.1189					
TPY_OIL		0.4395				
WASTE_W		0.4564				
PSA_GAS		0.1039				
OFF_GAS		0.0002				
C4_FU_GAS			0.0498			

ST_OIL 0.9502
 NAPH 0.2932
 DS_F 0.7068
 DIES 0.8114
 HC_F 0.1886
 HC_NAPH 0.95
 HC_DIES 0.05
 HC_OFF_GAS
 0.02072
 HC_FU_GAS
 0.000099;

table c(i, u)

	HC1	GOHT	RHT	DHT	NHT	HC2	BHDT	HC3
hp	0	0	0	0	0	0	0	0
crF	0	0	0	0	0	0	0	0
hp3	0	0	0	0	0	0	0	0

table h(i, k)

	k1	k2	K3
hp	1	1	1
crF	0	0	1
HP3	1	1	0;

table h1(i, N)

	N1	N2	n3
hp	1	1	1
crF	0	0	0
HP3	1	1	1 ;

table l(i, j)

	fuel
hp	0
crF	0
HP3	0;

table d(v, u)

	HC1	GOHT	RHT	DHT	NHT	HC2	BHDT
HC3							
HC1	0	1	1	1	1	0	0
0							
GOHT	0	0	0	0	1	0	0
0							
RHT	0	0	0	0	1	0	0
0							
DHT	0	0	0	0	0	0	0
NHT	0	0	0	0	0	0	0
0							
HC2	0	1	1	1	1	0	0
0							
BHDT	0	0	0	0	0	0	0
0							
HC3	0	1	1	1	1	0	0
0;							

table e(v, k)

	k1	k2	K3
HC1	0	0	0
GOHT	0	0	0
RHT	0	0	0
DHT	0	0	0
NHT	0	0	0
HC2	0	0	0
BHDT	0	0	0
HC3	0	0	0 ;

table e2(v, n)

	n1	n2	n3

HC1	0	0	0
GOHT	0	0	0
RHT	0	0	0
DHT	0	0	0
NHT	0	0	0
HC2	0	0	0
BHDT	0	0	0
HC3	0	0	0;

table r5(v, m)

	m1
HC1	1
GOHT	1
RHT	1
DHT	1
NHT	1
HC2	1
BHDT	1
HC3	1;

table q(v, j)

	fuel
HC1	0
GOHT	0
RHT	0
DHT	0
NHT	0
HC2	0
BHDT	0
HC3	0;

table f(k, u)

	HC1	GOHT	RHT	DHT	NHT	HC2	BHDT	HC3
k1	1	0	0	0	0	1	1	1

```

k2  1      1      0      0      0      0      1      1
k3  0      1      1      1      1      0      0      0;

```

table f3(m, k)

```

      k1      k2      k3
m1    1      1      1;

```

Scalar

```

LPG_CUT  LPG cut                /0.96/
F_CRUDE  crude in to the CDU    /100000/
WF       weight conversion factor /0.158827155/
B_DIES   Bromine number         /0/
FCC_DIES                /0.95/
K_DIES   characterization factor /11.83/
SG_DHDT_NAPH1          /0.759 /
SG_DHDT_KERO1          /0.843/
SG_DHDT_DIS1           /0.893/
B_VGO    bromine number         /0/
FCC_VGO  VOLUME FRACTION FCC STOCK IN FEEDSTOCK /0.45/
K_VGO    characterization factor /11.67/
SG_VGO1                /0.933/
NAPH_VGO_YIELD1        /0.00034/
N2_VGO                /0.16/
SG_DIES                /0.881/
DIS_VGO_YIELD1         /0.02348/
TGO_VGO_YIELD1         /0.96523/
SG_VGOHDT_DIS1         /0.8473/
VF        volume conversion factor /6.29615255/
SG_TGO1                /0.923/
SG_RSD1                /1.014/
SUL_RSDHDT_DIS  cetane index of treated RSD /0.78/
SG_RSDHDT_DIS  cetane index of treated RSD /0.8473/
SUL_RSDHDT_FO                /0.17 /

```

SG_RSDHDT_FO	/1.008 /
SG_GFCC_NAPH	/0.7451/
SG_GFCC_LCO	/0.925/
SG_GFCC_HCO	/1.0093/
SG_GHC_LTN	/0.669/
SG_GHC_HN	/0.7546/
SG_GHC_KERO	/0.8146/
SG_GHC_DIES	/0.8348/
SG_REFORMATE	/0.778/
RONI_SRLTN research octane number 66.4	/53.49/
RONI_REFORMATE	/66.430496/
RONI_GFCC_NAPH	/63.359/
RONI_GHC_LTN 80	/57.556/
RONI_PG octane number index PG 89	/61.462729/
RVPI_SRLTN reid vapour pressure in PSI 11.1	/20.26/
RVPI_REFORMATE	/13.45/
RVPI_GFCC_NAPH	/11.38/
RVPI_GHC_LTN	/20.26/
RVPI_PG reid vapour pressure of PG 9	/15.58845727/
SG_PG specific gravity of PG	/0.8/
SG_SRLTN1	/0.749/
SUL_REFORMATE	/0.000001/
SUL_GFCC_NAPH	/0.0084/
SUL_GHC_LTN	/0.0005/
SUL_PG sulfur of PG	/0.05/
SUL_SRLTN1	/0.0027/
CET_DHDT_DIS1	/55.376/
CET_DHDT_KERO	/44.194/
CI_GHC_DIES	/54/
CI_GFCC_LCO	/27.9/
CI_VGOHDT_DIS cetane index of treated diesel	/48.52/
CI_RSDHDT_DIS cetane index of treated RSD	/48.52/

CN_DSP	ceatne number of diesel pool	/45/
SG_DSP	diesel pool specific gravity	/0.87/
SUL_GHC_DIES		/0.0008/
SUL_GFCC_LCO		/0.34/
SUL_DSP	sulfur	/0.5/
SUL_DHDT_DIS1		/0.0010/
SUL_DHDT_KERO1		/0.262/
SUL_VGOHDT_DIS1		/0.24/
SPI_VP_KERO		/20/
SPI_DHDT_KERO		/25/
SPI_GHC_KERO		/22/
SPI_KERO		/19.2/
SG_VP_KERO		/0.85/
SG_KERO1		/0.848/
SUL_KERO1		/0.23/
SUL_GHC_KERO		/0.06/
SUL_VP_KERO		/0.25/
SG_FOP	specific gravity of fuel oil pool	/1/
SUL_FOP	sulfur of fuel oil pool	2.93 /1/
SUL_GFCC_HCO		/0.99/
SG_REF		/0.734/
H0_HN1		/30/
H0_RSD		/700/
H0_DIES1		/200/
N2_SRHN	straight run heavy naphtha nitrogen content	/0.00034/
AR_SRHN	aromatic content	/17/
OL_SRHN	olifin content	/0/
NA_SRHN	naphthene content	/38/
M_BIOMASS		/2150/
SG_NS_NAPH	SG of naphtha form naphtha spilliter	/0.7517/
SG_DS_DIES	SG diesel from diesel splitter	/0.8739/
SG_TPY1		/0.9303/

CI_DS_DIES cetane number of diesel from DS /45/
 SUL_DS_DIES sulfur content /0.0109/
 SG_MIX /0.9/
 FX_COST fixed capital cost for PYR + HDT + DE-C4 /197493.6/
 UP /2215/
 b /0.00001/
 UF /120/
 If /0/
 LNPC /200/
 a_com /163.376/
 b_com /0.1857/
 upower /2800/
 OCF /2.5/
 LHV_H2 /290/
 LHV_C4 /980/
 a_nc /115/
 b_nc /1.91/
 a_m /503.8/
 b_m /347.4/
 UPP / 7000/

variable

T;

positive variables

SRLTN_CUT, TE_SRLTN, SRHN_CUT, TE_SRHN, KERO_CUT, TE_KERO,
 DIES_CUT, TE_DIES, VGO_CUT, TE_VGO, LPG_YIELD, SRLTN_YIELD,
 SRHN_YIELD, KERO_YIELD, DIES_YIELD, VGO_YIELD, RSD_YIELD,
 T_YIELD, F_LPG, F_SRLTN, F_SRHN, F_KERO, F_DIES, F_VGO, F_RSD,
 MID_SRLTN, MID_SRHN, MID_KERO, MID_DIES, MID_VGO,
 MID_RSD, SG_SRLTN, SG_SRHN, SG_KERO, SG_DIES1, SG_VGO, SG_RSD,
 N2_KERO, N2_DIES, SUL_SRLTN, SUL_KERO, SUL_DIES, SUL_VGO,

SUL_RSD, SUL_SRHN, ASF_HN, H0_HN, H_HN, H2S_HN, NH3_HN, GAS_HN,
 HN_YIELD, SG_HN, M_SRHN, HN_MF, H0_DIES, F_DHDT_KERO,
 F_DHDT_NAPH, F_DHDT_DIS, API_DHDT_NAPH, API_DHDT_KERO,
 API_DHDT_DIS, SG_DHDT_NAPH, SG_DHDT_KERO, SG_DHDT_DIS,
 SUL_DHDT_KERO, SUL_DHDT_DIS, API_DIES, CET_DHDT_DIS,
 M_DHDT_NAPH, M_DHDT_KERO, M_DHDT_DIS, H0_VGO, H_VGO_YIELD,
 H2S_VGO_YIELD, NH3_VGO_YIELD, GAS_VGO_YIELD,
 NAPH_VGO_YIELD, DIS_VGO_YIELD, TGO_VGO_YIELD, M_VGO,
 M_VGOHDT_NAPH, M_VGOHDT_DIS, M_TGO, SG_TGO,
 SUL_VGOHDT_DIS, F_VGOHDT_DIS, F_TGO, M_RSD, M_RSDHDT_NAPH,
 M_RSDHDT_DIS, M_RSDHDT_FO, F_RSDHDT_DIS, F_RSDHDT_FO,
 HN_YIELD_DISTL, KERO_YIELD_DISTL, DIS_YIELD_DISTL,
 M_GFCC_NAPH, M_GFCC_LCO, M_GFCC_HCO, F_GFCC_NAPH,
 F_GFCC_LCO, F_GFCC_HCO, M_GHC_LTN, M_GHC_HN, M_GHC_KERO,
 M_GHC_DIES, F_GHC_LTN, F_GHC_HN, F_GHC_KERO, F_GHC_DIES,
 M_TGO3, M_TGO2, M_REF, H2_REF_WT, M_REFORMATE, F_REFORMATE,
 F_REF, M_PY_OIL, M_PY_FGAS, M_PY_CHAR, M_HDT_PY, M_HDT_WW,
 M_HDT_PSAGAS, M_HDF_OFFGAS, M_C4_FGAS, M_C4_OIL, M_TPY,
 M_TPYB, M_NS_NAPH, F_NS_NAPH, M_NS_FDIES, M_DS_DIES,
 f_DS_DIES, M_DS_FHCK, F_DS_FHCK, M_DS_FHCK1, M_DS_FHCK2,
 M_BHC_LTN, M_BHC_DIES, F_BHC_LTN, F_BHC_DIES, M_NS_NAPH1,
 M_NS_NAPH2, M_REF_B, H2_REF_WTB, M_REFORMATE_B,
 F_REFORMATE_B, F_REF_B, F_NS_NAPH1, F_NS_NAPH2, F_DS_FHCK1,
 F_DS_FHCK2, M_MIX, M_TGO1, M_TGO4, M_MIXFCC_NAPH,
 M_MIXFCC_LCO, M_MIXFCC_HCO, M_MIXFCC_COKE, F_MIXFCC_NAPH,
 F_MIXFCC_LCO, F_MIXFCC_HCO, M_PHC_LTN, M_PHC_DIES, F_PHC_LTN,
 F_PHC_DIES, VPG, MPG, A9, M_SRLTN, FDC_VGOHDT_DIS,
 FFO_VGOHDT_DIS, FDC_RSDHDT_DIS, FFO_RSDHDT_DIS,
 MDC_VGOHDT_DIS, MFO_VGOHDT_DIS, MDC_RSDHDT_DIS,
 MFO_RSDHDT_DIS, F_DHDT_KERO_D, F_DHDT_KERO_K, VDSP,
 M_DHDT_KERO_D, MDSP, VP_KERO, A6, MP_KERO, M_KERO, MP_KERO,
 M_DHDT_KERO_K, VFOP, MFOP, F_TGO2, F_TGO3, F_MIX, H2_CONSP, OC,

H2_TON, H2_SCF, RATIO, RATIO1, RATIO2, RATIO3, INDEX, INDEX1, INDEX2, INDEX3, Z11, Z12, Z13, H2_COST, RATIO21, RATIO22, RATIO23, Z21, Z22, Z23, RATIO_NS, COST_NS, INDEX21, INDEX22, INDEX23, INDEX_NS, RATIO31, RATIO32, RATIO33, Z31, Z32, Z33, RATIO_DS, COST_DS, INDEX31, INDEX32, INDEX33, INDEX_DS, RATIO41, RATIO42, RATIO43, Z41, Z42, Z43, RATIO_BHC, COST_BHC, INDEX41, INDEX42, INDEX43, INDEX_BHC, RATIO51, RATIO52, RATIO53, Z51, Z52, Z53, RATIO_RUB, COST_RUB, INDEX51, INDEX52, INDEX53, INDEX_RUB, RATIO61, RATIO62, RATIO63, Z61, Z62, Z63, RATIO_FCC, COST_FCC, INDEX61, INDEX62, INDEX63, INDEX_FCC, RATIO71, RATIO72, RATIO73, Z71, Z72, Z73, RATIO_PHC, COST_PHC, INDEX71, INDEX72, INDEX73, INDEX_PHC, RATIO81, RATIO82, RATIO83, Z81, Z82, Z83, RATIO_RUR, COST_RUR, INDEX81, INDEX82, INDEX83, INDEX_RUR, TOTAL_COST_REF, TOTAL_COST_BIO, MID_SRHN1, MID_SRHN2, Z3, MID_SRHN3, SUL_SRHN3, cons, FI(i), FIU(i, u), FIK(i, k), FIN(i, n), FIJ(i, j), PNO(n), FNU(n, u), FNK(n, k), FH2V(v), R(v), FVU(v, u), FVK(v, k), FVN(v, n), FVM(v, m), FVJ(v, j), FH2U(u), FKU(k, u), YK(k), YN(n), FKin(k), FKout(k), PWR(k), FNin(n), FMN(m, n), FNout(n), PwrN(n), FMin(m), YMin(m), FPUR(m), FRSD(m), YRSD(m), FMK(m, k), FMJ(m, j), PwrR(u), CAP_nc(n), CAP_m(m), elec, F_fuel(j), y_fu(j), OC_fuel(j), elec12, B11(j), COST_1, COST_2, COST_3, H2_TON, H2_SCF, RATIO_H2, INDEX_H2, COST_H2, RATIO_NS, INDEX_NS, COST_NS, RATIO_DS, INDEX_DS, COST_DS, RATIO_BHC, INDEX_BHC, COST_BHC, RATIO_RUB, INDEX_RUB, COST_RUB, RATIO_FCC, INDEX_FCC, COST_FCC, RATIO_PHC, INDEX_PHC, COST_PHC, RATIO_RUR, INDEX_RUR, COST_RUR, TOTAL_COST_REF, TOTAL_COST_BIO;

Integer variables

Y1, Y2, Y3, Y4, Y5, Y6, Y7, Y11, Y12, Y13, Y21, Y22, Y23, Y31, Y32, Y33, Y41, Y42, Y43, Y51, Y52, Y53, Y61, Y62, Y63, Y71, Y72, Y73, Y81, Y82, Y83, YNU(N, U), YNK(n, k), T1(n), T2(m);

Equations

OBJ,EQN1,EQN2,EQN3, EQN4, EQN5, EQN6, EQN7, EQN8, EQN9, EQN10, EQN11, EQN12, EQN13, EQN14, EQN15, EQN16, EQN17, EQN18, EQN19, EQN20, EQN21, EQN22, EQN23, EQN24, EQN25, EQN26, EQN27, EQN28, EQN29, EQN30, EQN31, EQN32, EQN33, EQN34, EQN35, EQN36, EQN37, EQN38, EQN39, EQN40, EQN41, EQN42, EQN43, EQN44, EQN45, EQN46, EQN47, EQN48, EQN49, EQN50, EQN51, EQN52, EQN53, EQN54, EQN54A, EQN54B, EQN54C, EQN54D, EQN55, EQN56, EQN57, EQN58, EQN59, EQN60, EQN61, EQN62, EQN63, EQN64, EQN65, EQN66, EQN67, EQN68, EQN69, EQN70, EQN71, EQN72, EQN73, EQN74, EQN75, EQN76, EQN77, EQN78, EQN79, EQN80, EQN81, EQN82, EQN83, EQN84, EQN85, EQN86, EQN87, EQN88, EQN89, EQN89A, EQN90, EQN91, EQN92, EQN93, EQN94, EQN95, EQN96, EQN97, EQN98, EQN99, EQN100, EQN101, EQN102, EQN103, EQN104, EQN105, EQN106, EQN107, EQN108, EQ1, EQ2, EQ3, EQ4, EQ5, EQ6, EQ7, EQ8, EQ9, EQ10, EQ11, EQ12, EQ13, EQ14, EQ15, EQ16, EQ17, EQ18, EQ19, EQ20, EQ21, EQ22, EQ23, EQ24, EQ25, EQ26, EQ27, EQ28, EQ29, EQ30, EQ31, EQ32, EQ34, EQ35, EQ36, EQ37, EQ38, EQ39, EQ40, EQ41, EQ42, EQ43, EQ44, EQ45, EQ46, EQN153, EQN154, EQN155, EQN156, EQN157, EQN158, EQN159, EQN167, EQN168, EQN169, EQN170, EQN171, EQN172, EQN173, EQN174, EQN175, EQN176, EQN177, EQN178, EQN179, EQN180, EQN181, EQN182, EQN187, EQN188, EQN189, EQN190, EQN191, EQN192, EQN193, EQN194, EQN195, EQN196, EQN197, EQN198, EQN199, EQ200, EQ201, EQ202, EQ203, EQ204, EQ205, EQ206, EQ207, EQ208, EQ209, EQ210, EQ211, EH1, EH2, EH3, EH4, EH5, EH6, EH7, EH8, EH9, EH10, EH11, EH12, EH13, EH14, EH15, EH16, EH17, EH18, EH19, EH20, EH29, EH30, EH31, EH32, EH37, EH38, EH39, EH40, EH41, EH42, EH47, EH48, EH49, EH50, EH51, EH52, EH53, EH54, EH55, EH56, EH57, EH62, EH63, EH64, EH69, EH70, EH71, EH72, EH73, EH74, EH75, EH76, EH77, EH78, EH79, EH80, EH81, EH90, EQ352, EQ353, EQ354, EQ212, EQ213, EQ214, EQ215, EQ216, EQ217, EQ218, EQ219, EQ220, EQ221, EQ222, EQ223, EQ224, EQ225, EQ226, EQ227, EQ228, EQ229, EQ230, EQ231, EQ232, EQ233,

EQ234, EQ235, EQ236, EQ237, EQ238, EQ239, EQ240, EQ241, EQ242, EQ243, EQ244, EQ245, EQ246, EQ247, EQ248, EQ249, EQ250, EQ251, EQ252, EQ253, EQ254, EQ255, EQ256, EQ257, EQ258, EQ259, EQ260, EQ261, EQ262, EQ263, EQ264, EQ265, EQ266, EQ267, EQ268, EQ269, EQ270, EQ271, EQ272, EQ273, EQ274, EQ275, EQ276, EQ277, EQ278, EQ279, EQ280, EQ281, EQ282, EQ283, EQ284, EQ285, EQ286, EQ287, EQ288, EQ289, EQ290, EQ291, EQ292, EQ293, EQ294, EQ295, EQ296, EQ297, EQ298, EQ299, EQ300, EQ301, EQ302, EQ303, EQ304, EQ305, EQ306, EQ307, EQ308, EQ309, EQ310, EQ311, EQ312, EQ313, EQ314, EQ315, EQ316, EQ317, EQ318, EQ319, EQ320, EQ321, EQ322, EQ323, EQ324, EQ325, EQ326, EQ327, EQ328, EQ329, EQ330, EQ331, EQ332, EQ333, EQ334, EQ335, EQ336, EQ337, EQ338, EQ339, EQ340, EQ341, EQ342, EQ343, EQ344, EQ345, EQ346, EQ347, EQ348, EQ349, EQ350, EQ351;

OBJ.. T =E= 0.365*122.052*VPG + 0.365*117.94*VP_KERO + 0.365*115.16*VDSP + 0.365*56.66*VFOP + 0.365*36.246*F_LPG - 0.365*OC - 0.365*sum(i, FI(i)*CH2S(i)) - 0.365*0.72*sum(k, Pwr(k)) - 0.365*0.72*sum(u, PwrR(u)) - 0.365*0.72*sum(n, PwrN(n)) + 0.365*sum(j, OC_fuel(j)) - 0.11746*sum(n, CAP_nc(n)) - 0.11746*sum(m, CAP_m(m)) - 0.15*0.11746*[sum(n, CAP_nc(n)) + sum(m, CAP_m(m))] - TOTAL_COST_REF - TOTAL_COST_BIO;

*CDU

EQN1.. SRLTN_CUT - (a1('a0','CUT') + a1('a1','CUT')*TE_SRLTN + a1('a2','CUT')*TE_SRLTN**2 + a1('a3','CUT')*TE_SRLTN**3 + a1('a4','CUT')*TE_SRLTN**4) =E= 0;

EQN2.. SRHN_CUT - (a1('a0','CUT') + a1('a1','CUT')*TE_SRHN + a1('a2','CUT')*TE_SRHN**2 + a1('a3','CUT')*TE_SRHN**3 + a1('a4','CUT')*TE_SRHN**4) =E= 0;

EQN3.. KERO_CUT - (a1('a0','CUT') + a1('a1','CUT')*TE_KERO + a1('a2','CUT')*TE_KERO**2 + a1('a3','CUT')*TE_KERO**3 + a1('a4','CUT')*TE_KERO**4) =E= 0;

EQN4.. DIES_CUT - (a1('a0','CUT') + a1('a1','CUT')*TE_DIES +
 a1('a2','CUT')*TE_DIES**2 + a1('a3','CUT')*TE_DIES**3 +
 a1('a4','CUT')*TE_DIES**4) =E= 0;
 EQN5.. VGO_CUT - (a1('a0','CUT') + a1('a1','CUT')*TE_VGO +
 a1('a2','CUT')*TE_VGO**2
 + a1('a3','CUT')*TE_VGO**3 + a1('a4','CUT')*TE_VGO**4) =E= 0;
 EQN6.. LPG_YIELD - (LPG_CUT/100) =E= 0;
 EQN7.. SRLTN_YIELD - ((SRLTN_CUT - LPG_CUT)/100) =E= 0;
 EQN8.. SRHN_YIELD - ((SRHN_CUT - SRLTN_CUT)/100) =E= 0;
 EQN9.. KERO_YIELD - ((KERO_CUT - SRHN_CUT)/100) =E= 0;
 EQN10.. DIES_YIELD - ((DIES_CUT - KERO_CUT)/100) =E= 0;
 EQN11.. VGO_YIELD - ((VGO_CUT - DIES_CUT)/100) =E= 0;
 EQN12.. RSD_YIELD - ((100 - VGO_CUT)/100) =E= 0;
 EQN13.. T_YIELD - (LPG_YIELD + SRLTN_YIELD + SRHN_YIELD +
 KERO_YIELD + DIES_YIELD + VGO_YIELD + RSD_YIELD) =E= 0;
 EQN14.. F_LPG - F_CRUDE*LPG_YIELD =E= 0;
 EQN15.. F_SRLTN - F_CRUDE*SRLTN_YIELD =E= 0;
 EQN16.. F_SRHN - F_CRUDE*SRHN_YIELD =E= 0;
 EQN17.. F_KERO - F_CRUDE*KERO_YIELD =E= 0;
 EQN18.. F_DIES - F_CRUDE*DIES_YIELD =E= 0;
 EQN19.. F_VGO - F_CRUDE*VGO_YIELD =E= 0;
 EQN20.. F_RSD - F_CRUDE*RSD_YIELD =E= 0;
 EQN21.. F_CRUDE - (F_LPG + F_SRLTN + F_SRHN + F_KERO + F_DIES +
 F_VGO + F_RSD) =E= 0;
 EQN22.. MID_SRLTN - [(SRLTN_CUT + LPG_CUT)/2] =E= 0;
 EQN23.. MID_SRHN - [(SRHN_CUT + SRLTN_CUT)/2] =E= 0;
 EQN24.. MID_KERO - [(KERO_CUT + SRHN_CUT)/2] =E= 0;
 EQN25.. MID_DIES - [(DIES_CUT + KERO_CUT)/2] =E= 0;
 EQN26.. MID_VGO - [(VGO_CUT + DIES_CUT)/2] =E= 0;
 EQN27.. MID_RSD - [(100 + VGO_CUT)/2] =E= 0;

$$\text{EQN28.. SG_SRLTN} - [\text{a11('a0','SG')} + (\text{a11('a1','SG')*(MID_SRLTN)}) + (\text{a11('a2','SG')*(MID_SRLTN)**2}) + (\text{a11('a3','SG')*(MID_SRLTN)**3}) + (\text{a11('a4','SG')*(MID_SRLTN)**4})] = \text{E}=0;$$

$$\text{EQN29.. SG_SRHN} - [\text{a11('a0','SG')} + (\text{a11('a1','SG')*(MID_SRHN)}) + (\text{a11('a2','SG')*(MID_SRHN)**2}) + (\text{a11('a3','SG')*(MID_SRHN)**3}) + (\text{a11('a4','SG')*(MID_SRHN)**4})] = \text{E}=0;$$

$$\text{EQN30.. SG_KERO} - [\text{a11('a0','SG')} + (\text{a11('a1','SG')*(MID_KERO)}) + (\text{a11('a2','SG')*(MID_KERO)**2}) + (\text{a11('a3','SG')*(MID_KERO)**3}) + (\text{a11('a4','SG')*(MID_KERO)**4})] = \text{E}=0;$$

$$\text{EQN31.. SG_DIES1} - [\text{a11('a0','SG')} + (\text{a11('a1','SG')*(MID_DIES)}) + (\text{a11('a2','SG')*(MID_DIES)**2}) + (\text{a11('a3','SG')*(MID_DIES)**3}) + (\text{a11('a4','SG')*(MID_DIES)**4})] = \text{E}=0;$$

$$\text{EQN32.. SG_VGO} - [\text{a11('a0','SG')} + (\text{a11('a1','SG')*(MID_VGO)}) + (\text{a11('a2','SG')*(MID_VGO)**2}) + (\text{a11('a3','SG')*(MID_VGO)**3}) + (\text{a11('a4','SG')*(MID_VGO)**4})] = \text{E}=0;$$

$$\text{EQN33.. SG_RSD} - [\text{a11('a0','SG')} + (\text{a11('a1','SG')*(MID_RSD)}) + (\text{a11('a2','SG')*(MID_RSD)**2}) + (\text{a11('a3','SG')*(MID_RSD)**3}) + (\text{a11('a4','SG')*(MID_RSD)**4})] = \text{E}=0;$$

$$\text{EQN34.. N2_KERO} - [\text{a11('a0','N')} + (\text{a11('a1','N')*(MID_KERO)}) + (\text{a11('a2','N')*(MID_KERO)**2}) + (\text{a11('a3','N')*(MID_KERO)**3}) + (\text{a11('a4','N')*(MID_KERO)**4})] = \text{E}=0;$$

$$\text{EQN35.. N2_DIES} - [\text{a11('a0','N')} + (\text{a11('a1','N')*(MID_DIES)}) + (\text{a11('a2','N')*(MID_DIES)**2}) + (\text{a11('a3','N')*(MID_DIES)**3}) + (\text{a11('a4','N')*(MID_DIES)**4})] = \text{E}=0;$$

$$\text{EQN36.. SUL_SRLTN} - [\text{a11('a0','SUL')} + (\text{a11('a1','SUL')*(MID_SRLTN)}) + (\text{a11('a2','SUL')*(MID_SRLTN)**2}) + (\text{a11('a3','SUL')*(MID_SRLTN)**3}) + (\text{a11('a4','SUL')*(MID_SRLTN)**4})] = \text{E}=0;$$

$$\text{EQN37.. SUL_SRHN} - [\text{a11('a0','SUL')} + (\text{a11('a1','SUL')*(MID_SRHN)}) + (\text{a11('a2','SUL')*(MID_SRHN)**2}) + (\text{a11('a3','SUL')*(MID_SRHN)**3}) + (\text{a11('a4','SUL')*(MID_SRHN)**4})] = \text{E}=0;$$

$$\text{EQN38.. SUL_DIES} - [\text{a11}('a0','SUL') + (\text{a11}('a1','SUL')*(\text{MID_DIES})) + (\text{a11}('a2','SUL')*(\text{MID_DIES})^{**2}) + (\text{a11}('a3','SUL')*(\text{MID_DIES})^{**3}) + (\text{a11}('a4','SUL')*(\text{MID_DIES})^{**4})] =E=0;$$

$$\text{EQN39.. SUL_VGO} - [\text{a11}('a0','SUL') + (\text{a11}('a1','SUL')*(\text{MID_VGO})) + (\text{a11}('a2','SUL')*(\text{MID_VGO})^{**2}) + (\text{a11}('a3','SUL')*(\text{MID_VGO})^{**3}) + (\text{a11}('a4','SUL')*(\text{MID_VGO})^{**4})] =E=0;$$

$$\text{EQN40.. SUL_RSD} - [\text{a11}('a0','SUL') + (\text{a11}('a1','SUL')*(\text{MID_RSD})) + (\text{a11}('a2','SUL')*(\text{MID_RSD})^{**2}) + (\text{a11}('a3','SUL')*(\text{MID_RSD})^{**3}) + (\text{a11}('a4','SUL')*(\text{MID_RSD})^{**4})] =E=0;$$

* Naphtha hydrotreating unit

$$\text{EQN41.. ASF_HN} - (0.011 + 76*\text{POWER}(\text{N2_SRHN}, 2) + 0.039*\text{SUL_SRHN}) =E=0;$$

$$\text{EQN42.. H0_HN} - (25 + 70*\text{SUL_SRHN} + 290*\text{N2_SRHN} + 6.5*\text{OL_SRHN} + 28*\text{ASF_HN}*\text{AR_SRHN})=E=0;$$

$$\text{EQN43.. H_HN} - (1/658.29)*(\text{H0_HN}/\text{SG_SRHN}) =E=0;$$

$$\text{EQN44.. H2S_HN} - 1.063*\text{SUL_SRHN} =E=0;$$

$$\text{EQN45.. NH3_HN} - 1.21*\text{N2_SRHN} =E=0;$$

$$\text{EQN46.. GAS_HN} - (0.25 + 0.66*\text{SUL_SRHN} + 7.4*\text{N2_SRHN}) =E=0;$$

$$\text{EQN47.. HN_YIELD}*100 =E= 100 + \text{H_HN} - \text{GAS_HN} - \text{H2S_HN} ;$$

$$\text{EQN48.. SG_HN} =E= 1.000378523*\text{SG_SRHN} - 0.149226586*\text{ASF_HN} + 0.00597639*\text{H_HN} - 0.000559111;$$

$$\text{EQN49.. F_SRHN} - [\text{M_SRHN}*(\text{VF}/\text{SG_SRHN})] =E=0;$$

$$\text{EQN50.. HN_MF} - (\text{M_SRHN}*\text{HN_YIELD}) =E=0;$$

* Diesel hydrotreating uint

$$\text{EQN51.. H0_DIES} - (120*\text{SUL_DIES} + 159.5*0.006 + 8*\text{SG_DIES}*\text{B_DIES} + 25 + 290*\text{FCC_DIES}*(11.9 - \text{K_DIES})) =E=0;$$

$$\text{EQN52.. HN_YIELD_DISTL} =E= ([(\text{a2}('a0','Nap2') + \text{a2}('b0','Nap2')*\text{SG_DIES} + \text{a2}('c0','Nap2')*\text{SUL_DIES}) + (\text{a2}('a1','Nap2') + \text{a2}('b1','Nap2')*\text{SG_DIES} + \text{a2}('c1','Nap2')*\text{SUL_DIES})*0.95 + (\text{a2}('a2','Nap2') + \text{a2}('b2','Nap2')*\text{SG_DIES} + \text{a2}('c2','Nap2')*\text{SUL_DIES})*0.9025]);$$

EQN53.. KERO_YIELD_DISTL =E= (((a2('a0','KER2') + a2('b0','KER2')*SG_DIES + a2('c0','KER2')*SUL_DIES) + (a2('a1','KER2') + a2('b1','KER2')*SG_DIES + a2('c1','KER2')*SUL_DIES)*0.95 + (a2('a2','KER2') + a2('b2','KER2')*SG_DIES + a2('c2','KER2')*SUL_DIES)]*0.9025)];

EQN54.. DIS_YIELD_DISTL =E= (((a2('a0','DLS2') + a2('b0','DLS2')*SG_DIES + a2('c0','DLS2')*SUL_DIES) + (a2('a1','DLS2') + a2('b1','DLS2')*SG_DIES + a2('c1','DLS2')*SUL_DIES)*0.95 + (a2('a2','DLS2') + a2('b2','DLS2')*SG_DIES + a2('c2','DLS2')*SUL_DIES)]*0.9025)];

EQN54A.. F_DHDT_NAPH =E= F_DIES*HN_YIELD_DISTL;

EQN54B.. F_DHDT_KERO =E= F_DIES*KERO_YIELD_DISTL;

EQN54C.. F_DHDT_DIS =E= F_DIES*DIS_YIELD_DISTL;

*EQN54A.. F_DHDT_NAPH =E= F_DIES*0.001;

*EQN54B.. F_DHDT_KERO =E= F_DIES*0.145;

*EQN54C.. F_DHDT_DIS =E= F_DIES*0.85;

EQN54D.. API_DIES =E= 56.55 - 0.669*MID_DIES ;

EQN55.. API_DHDT_NAPH =E= [(a2('a3','Nap2') + a2('b3','Nap2')*API_DIES + ((a2('c3','Nap2') + a2('d3','Nap2')*SUL_DIES)/SG_DIES)) + (a2('a31','Nap2') + a2('b31','Nap2')*API_DIES + ((a2('c31','Nap2') + a2('d31','Nap2')*SUL_DIES)/SG_DIES))*0.95] ;

EQN56.. API_DHDT_KERO =E= [(a2('a3','KER2') + a2('b3','KER2')*API_DIES + ((a2('c3','KER2') + a2('d3','KER2')*SUL_DIES)/SG_DIES)) + (a2('a31','KER2') + a2('b31','KER2')*API_DIES + ((a2('c31','KER2') + a2('d31','KER2')*SUL_DIES)/SG_DIES))*0.95] ;

EQN57.. API_DHDT_DIS =E= [(a2('a3','DLS2') + a2('b3','DLS2')*API_DIES + ((a2('c3','DLS2') + a2('d3','DLS2')*SUL_DIES)/SG_DIES)) + (a2('a31','DLS2') + a2('b31','DLS2')*API_DIES + ((a2('c31','DLS2') + a2('d31','DLS2')*SUL_DIES)/SG_DIES))*0.95] ;

EQN58.. SG_DHDT_NAPH - [141.5/(131.5 + API_DHDT_NAPH)] =E=0;

EQN59.. SG_DHDT_KERO - [141.5/(131.5 + API_DHDT_KERO)] =E=0;

EQN60.. SG_DHDT_DIS - [141.5/(131.5 + API_DHDT_DIS)] =E=0;

EQN61.. CET_DHDT_DIS =E= [(a2('a4','DLS2') + a2('b4','DLS2')*API_DIES + ((a2('c4','DLS2') + a2('d4','DLS2')*SUL_DIES)/SG_DIES)) + (a2('a41','DLS2') +

$$a2('b41','DLS2')*API_DIES + ((a2('c41','DLS2') + a2('d41','DLS2')*SUL_DIES)/SG_DIES))*0.95];$$

$$EQN62.. SUL_DHDT_KERO =E= (a2('a5','KER2')*[a2('b5','KER2') + a2('c5','KER2')*0.95]*SUL_DIES);$$

$$EQN63.. SUL_DHDT_DIS =E= (a2('a5','DLS2')*[a2('b5','DLS2') + a2('c5','DLS2')*0.95]*SUL_DIES);$$

$$EQN64.. M_DHDT_NAPH - (F_DHDT_NAPH*SG_DHDT_NAPH1*WF) =E= 0;$$

$$EQN65.. M_DHDT_KERO - (F_DHDT_KERO*SG_DHDT_KERO1*WF) =E= 0;$$

$$EQN66.. M_DHDT_DIS - (F_DHDT_DIS*SG_DHDT_DIS1*WF) =E= 0;$$

* Gas oil hydrotreating uint

$$EQN67.. H0_VGO - (40 + 150*SUL_VGO + (101.5*N2_VGO) + (7*B_VGO*SG_VGO) + (300*(11.9 - K_VGO)*FCC_VGO)) =E=0;$$

$$EQN68.. H_VGO_YIELD - [(1/658.29)*(H0_VGO/SG_VGO)] =E=0;$$

$$EQN69.. H2S_VGO_YIELD - 0.957*SUL_VGO =E=0;$$

$$EQN70.. NH3_VGO_YIELD - 0.535*N2_VGO =E=0;$$

$$EQN71.. GAS_VGO_YIELD - 0.46*H_VGO_YIELD =E=0;$$

$$EQN72.. NAPH_VGO_YIELD*100 - (0.173*SUL_VGO + 0.0424*POWER(SUL_VGO, 2)) =E=0;$$

$$EQN73.. DIS_VGO_YIELD*100 - (1.418*SUL_VGO + 0.432*POWER(SUL_VGO, 2)) =E=0;$$

$$EQN74.. TGO_VGO_YIELD*100 - (100 + H_VGO_YIELD - H2S_VGO_YIELD - NH3_VGO_YIELD - NAPH_VGO_YIELD - DIS_VGO_YIELD) =E=0;$$

$$*EQN72.. NAPH_VGO_YIELD =E= 0.00034;$$

$$*EQN73.. DIS_VGO_YIELD =E= 0.02347;$$

$$*EQN74.. TGO_VGO_YIELD =E= 0.97618;$$

$$EQN75.. M_VGO =E= F_VGO*SG_VGO1*WF;$$

$$EQN76.. M_VGOHDT_NAPH =E= M_VGO*NAPH_VGO_YIELD;$$

$$EQN77.. M_VGOHDT_DIS =E= M_VGO*DIS_VGO_YIELD ;$$

$$EQN78.. M_TGO =E= M_VGO*TGO_VGO_YIELD ;$$

$$EQN79.. SG_TGO - (SG_VGO1 - 0.025*H_VGO_YIELD) =E=0;$$

$$EQN80.. SUL_VGOHDT_DIS - 0.02*SUL_VGO =E=0;$$

EQN81.. F_VGOHDT_DIS - [M_VGOHDT_DIS*(VF/SG_VGOHDT_DIS1)] =E=0;

EQN82.. F_TGO =E= [M_TGO*(VF/SG_TGO1)] ;

* Vacuum residue hydrotreating unit

EQN83.. M_RSD =E= F_RSD*SG_RSD1*WF;

EQN84.. M_RSDHDT_NAPH =E= (M_RSD*0.00050);

EQN85.. M_RSDHDT_DIS =E= (M_RSD*0.0137);

EQN86.. M_RSDHDT_FO =E= (M_RSD*0.9857);

EQN87.. F_RSDHDT_DIS =E= [M_RSDHDT_DIS*(VF/SG_RSDHDT_DIS)] ;

EQN88.. F_RSDHDT_FO =E= [M_RSDHDT_FO*(VF/SG_RSDHDT_FO)] ;

EQN89.. M_TGO =E= M_TGO1 + M_TGO2;

EQN89A.. M_TGO1 =E= M_TGO3 + M_TGO4;

* HC yields for pure hydrocarbon (TGO2)

EQN90.. M_GHC_LTN - d1('TGO2','li_gaso')*M_TGO2 =E=0;

EQN91.. M_GHC_HN - d1('TGO2','naph')*M_TGO2 =E=0;

EQN92.. M_GHC_KERO - d1('TGO2','KERO')*M_TGO2 =E=0;

EQN93.. M_GHC_DIES - d1('TGO2','diesel')*M_TGO2 =E=0;

EQN94.. F_GHC_LTN - [M_GHC_LTN*(VF/SG_GHC_LTN)] =E=0;

EQN95.. F_GHC_HN - [M_GHC_HN*(VF/SG_GHC_HN)] =E=0;

EQN96.. F_GHC_KERO - [M_GHC_KERO*(VF/SG_GHC_KERO)] =E=0;

EQN97.. F_GHC_DIES - [M_GHC_DIES*(VF/SG_GHC_DIES)] =E=0;

* FCC yields for pure hydrocarbon (TGO3)

EQN98.. M_GFCC_NAPH - e1('TGO3','gaso')*M_TGO3 =E=0;

EQN99.. M_GFCC_LCO - e1('TGO3','lco')*M_TGO3 =E=0;

EQN100.. M_GFCC_HCO - e1('TGO3','hco')*M_TGO3 =E=0;

EQN101.. F_GFCC_NAPH - [M_GFCC_NAPH*(VF/SG_GFCC_NAPH)] =E=0;

EQN102.. F_GFCC_LCO - [M_GFCC_LCO*(VF/SG_GFCC_LCO)] =E=0;

EQN103.. F_GFCC_HCO - [M_GFCC_HCO*(VF/SG_GFCC_HCO)] =E=0;

*Catalytic reforming unit

$$\text{EQN104.. } M_{\text{REF}} - (\text{HN}_{\text{MF}} + M_{\text{DHDT_NAPH}} + M_{\text{VGOHDT_NAPH}} + M_{\text{RSDHDT_NAPH}} + M_{\text{GHC_HN}} + M_{\text{NS_NAPH2}}) = E = 0;$$

$$\text{EQN105.. } H2_{\text{REF_WT}} - M_{\text{REF}} * 0.0193 = E = 0;$$

$$\text{EQN106.. } M_{\text{REFORMATE}} - (0.88 * M_{\text{REF}}) = E = 0;$$

$$\text{EQN107.. } F_{\text{REFORMATE}} = E = [M_{\text{REFORMATE}} * (\text{VF}/\text{SG}_{\text{REFORMATE}})];$$

$$\text{EQN108.. } M_{\text{REF}} - (F_{\text{REF}} * \text{SG}_{\text{REF}} * \text{WF}) = E = 0;$$

* Pyrolysis unit

$$\text{EQ1.. } M_{\text{PY_OIL}} - b1(\text{'PY_OIL'}, \text{'PY'}) * M_{\text{BIOMASS}} = E = 0;$$

$$\text{EQ2.. } M_{\text{PY_FGAS}} - b1(\text{'FU_GAS'}, \text{'PY'}) * M_{\text{BIOMASS}} = E = 0;$$

$$\text{EQ3.. } M_{\text{PY_CHAR}} - b1(\text{'CHAR'}, \text{'PY'}) * M_{\text{BIOMASS}} = E = 0;$$

*Pyrolysis oil hydrotreating unit

$$\text{EQ4.. } M_{\text{HDT_PY}} - b1(\text{'TPY_OIL'}, \text{'HDT'}) * (M_{\text{PY_OIL}} + (0.0429 * M_{\text{PY_OIL}})) = E = 0;$$

$$\text{EQ5.. } M_{\text{HDT_WW}} - b1(\text{'WASTE_W'}, \text{'HDT'}) * (M_{\text{PY_OIL}} + (0.0429 * M_{\text{PY_OIL}})) = E = 0;$$

$$\text{EQ6.. } M_{\text{HDT_PSAGAS}} - b1(\text{'PSA_GAS'}, \text{'HDT'}) * (M_{\text{PY_OIL}} + (0.0429 * M_{\text{PY_OIL}})) = E = 0;$$

$$\text{EQ7.. } M_{\text{HDF_OFFGAS}} - b1(\text{'OFF_GAS'}, \text{'HDT'}) * (M_{\text{PY_OIL}} + (0.0429 * M_{\text{PY_OIL}})) = E = 0;$$

*De-butanizer

$$\text{EQ8.. } M_{\text{C4_FGAS}} - b1(\text{'C4_FU_GAS'}, \text{'DE4'}) * M_{\text{HDT_PY}} = E = 0;$$

$$\text{EQ9.. } M_{\text{C4_OIL}} - b1(\text{'ST_OIL'}, \text{'DE4'}) * M_{\text{HDT_PY}} = E = 0;$$

$$\text{EQ10.. } M_{\text{C4_OIL}} - M_{\text{TPY}} - M_{\text{TPYB}} = E = 0;$$

*Naphtha splitter

$$\text{EQ11.. } M_{\text{NS_NAPH}} - b1(\text{'NAPH'}, \text{'NS'}) * M_{\text{TPYB}} = E = 0;$$

$$\text{EQ12.. } F_{\text{NS_NAPH}} - [M_{\text{NS_NAPH}} * (\text{VF}/\text{SG}_{\text{NS_NAPH}})] = E = 0;$$

$$\text{EQ13.. } M_{\text{NS_FDIES}} - b1(\text{'DS_F'}, \text{'NS'}) * M_{\text{TPYB}} = E = 0;$$

*Diesel splitter

$$\text{EQ14.. M_DS_DIES} - \text{b1('DIES','DS')} * \text{M_NS_FDIES} = \text{E}=0;$$

$$\text{EQ15.. F_DS_DIES} - [\text{M_DS_DIES} * (\text{VF}/\text{SG_DS_DIES})] = \text{E}=0;$$

$$\text{EQ16.. M_DS_FHCK} - \text{b1('HC_F','DS')} * \text{M_NS_FDIES} = \text{E}=0;$$

$$\text{EQ17.. F_DS_FHCK} - [\text{M_DS_FHCK} * (\text{VF}/\text{SG_TPY1})] = \text{E}=0;$$

*Bio-refinery HC unit

$$\text{EQ18.. M_DS_FHCK} - \text{M_DS_FHCK1} - \text{M_DS_FHCK2} = \text{E}=0;$$

$$\text{EQ19.. M_BHC_LTN} - \text{b1('HC_NAPH','HC')} * (\text{M_DS_FHCK1}) = \text{E}=0;$$

$$\text{EQ20.. M_BHC_DIES} - \text{b1('HC_DIES','HC')} * (\text{M_DS_FHCK1}) = \text{E}=0;$$

$$\text{EQ21.. M_BHC_LTN} - (\text{F_BHC_LTN} * \text{SG_GHC_LTN} * \text{WF}) = \text{E}=0;$$

$$\text{EQ22.. M_BHC_DIES} - (\text{F_BHC_DIES} * \text{SG_GHC_DIES} * \text{WF}) = \text{E}=0;$$

*Bio-refinery catalytic reforming unit

$$\text{EQ23.. M_NS_NAPH} = \text{E}= \text{M_NS_NAPH1} + \text{M_NS_NAPH2};$$

$$\text{EQ24.. M_REF_B} - \text{M_NS_NAPH1} = \text{E}=0;$$

$$\text{EQ25.. H2_REF_WTB} - \text{M_REF_B} * 0.0193 = \text{E}=0;$$

$$\text{EQ26.. M_REFORMATE_B} - (0.88 * \text{M_REF_B}) = \text{E}=0;$$

$$\text{EQ27.. M_REFORMATE_B} - (\text{F_REFORMATE_B} * \text{SG_REFORMATE} * \text{WF}) = \text{E}=0;$$

$$\text{EQ28.. M_REF_B} - (\text{F_REF_B} * \text{SG_REF} * \text{WF}) = \text{E}=0;$$

$$\text{EQ29.. M_NS_NAPH1} - (\text{F_NS_NAPH1} * \text{SG_NS_NAPH} * \text{WF}) = \text{E}=0;$$

$$\text{EQ30.. M_NS_NAPH2} - (\text{F_NS_NAPH2} * \text{SG_NS_NAPH} * \text{WF}) = \text{E}=0;$$

$$\text{EQ31.. M_DS_FHCK1} - (\text{F_DS_FHCK1} * \text{SG_TPY1} * \text{WF}) = \text{E}=0;$$

$$\text{EQ32.. M_DS_FHCK2} - (\text{F_DS_FHCK2} * \text{SG_TPY1} * \text{WF}) = \text{E}=0;$$

$$\text{EQ34.. M_TPY} - 0.25 * \text{M_TGO4} = \text{E}=0;$$

$$\text{EQ35.. M_MIX} - \text{M_TPY} - \text{M_TGO4} = \text{E}=0;$$

* FCC yield for mix stream

$$\text{EQ36.. M_MIXFCC_NAPH} - \text{e1('MIX','gaso')} * \text{M_MIX} = \text{E}=0;$$

$$\text{EQ37.. M_MIXFCC_LCO} - \text{e1('MIX','lco')} * \text{M_MIX} = \text{E}=0;$$

$$\text{EQ38.. M_MIXFCC_HCO} - \text{e1('MIX','hco')} * \text{M_MIX} = \text{E}=0;$$

$$\text{EQ39.. M_MIXFCC_COKE} - \text{e1('MIX','coke')} * \text{M_MIX} = \text{E}=0;$$

EQ40.. M_MIXFCC_NAPH - [F_MIXFCC_NAPH*SG_GFCC_NAPH*WF] =E=0;
 EQ41.. M_MIXFCC_LCO - [F_MIXFCC_LCO*SG_GFCC_LCO*WF] =E=0;
 EQ42.. M_MIXFCC_HCO - [F_MIXFCC_HCO*SG_GFCC_HCO*WF] =E=0;

*Petroleum refinery HC unit yields for pure bio-oil

EQ43.. M_PHC_LTN - b1('HC_NAPH','HC')*(M_DS_FHCK2) =E=0;
 EQ44.. M_PHC_DIES - b1('HC_DIES','HC')*(M_DS_FHCK2) =E=0;
 EQ45.. M_PHC_LTN - (F_PHC_LTN*SG_GHC_LTN*WF) =E=0;
 EQ46.. M_PHC_DIES - (F_PHC_DIES*SG_GHC_DIES*WF) =E=0;

*BLENDING

EQN153.. VPG - F_SRLTN - F_REFORMATE - F_GFCC_NAPH - F_GHC_LTN
 - F_MIXFCC_NAPH - F_PHC_LTN - F_REFORMATE_B - F_BHC_LTN =E=0;

EQN154.. RONI_SRLTN*F_SRLTN + RONI_REFORMATE*F_REFORMATE +
 RONI_GFCC_NAPH*F_GFCC_NAPH + RONI_GHC_LTN*F_GHC_LTN +
 RONI_GFCC_NAPH*F_MIXFCC_NAPH + RONI_GHC_LTN*F_PHC_LTN +
 RONI_REFORMATE*F_REFORMATE_B + RONI_GHC_LTN*F_BHC_LTN -
 RONI_PG*VPG =G=0;

EQN155.. RVPI_SRLTN*F_SRLTN + RVPI_REFORMATE*F_REFORMATE +
 RVPI_GFCC_NAPH*F_GFCC_NAPH + RVPI_GHC_LTN*F_GHC_LTN +
 RVPI_GFCC_NAPH*F_MIXFCC_NAPH + RVPI_GHC_LTN*F_PHC_LTN +
 RVPI_REFORMATE*F_REFORMATE_B + RVPI_GHC_LTN*F_BHC_LTN -
 RVPI_PG*VPG =L=0;

EQN156.. SG_SRLTN*F_SRLTN + SG_REFORMATE*F_REFORMATE +
 SG_GFCC_NAPH*F_GFCC_NAPH + SG_GHC_LTN*F_GHC_LTN +
 SG_GFCC_NAPH*F_MIXFCC_NAPH + SG_GHC_LTN*F_PHC_LTN +
 SG_REFORMATE*F_REFORMATE_B + SG_GHC_LTN*F_BHC_LTN -
 SG_PG*VPG =L=0;

EQN157.. M_SRLTN =E= SG_SRLTN*F_SRLTN*WF;

EQN158.. MPG - M_SRLTN - M_REFORMATE - M_GFCC_NAPH -
 M_GHC_LTN - M_MIXFCC_NAPH - M_PHC_LTN - M_REFORMATE_B -
 M_BHC_LTN =E=0;

$$\begin{aligned} \text{EQN159.. } & \text{SUL_SRLTN1*M_SRLTN} + \text{SUL_REFORMATE*M_REFORMATE} + \\ & \text{SUL_GFCC_NAPH*M_GFCC_NAPH} + \text{SUL_GHC_LTN*M_GHC_LTN} + \\ & \text{SUL_GFCC_NAPH*M_MIXFCC_NAPH} + \text{SUL_GHC_LTN*M_PHC_LTN} + \\ & \text{SUL_REFORMATE*M_REFORMATE_B} + \text{SUL_GHC_LTN*M_BHC_LTN} - \\ & \text{SUL_PG*MPG} =L=0; \end{aligned}$$

$$\text{EQN167.. } F_VGOHDT_DIS - FDC_VGOHDT_DIS - FFO_VGOHDT_DIS =E=0;$$

$$\text{EQN168.. } F_RSDHDT_DIS - FDC_RSDHDT_DIS - FFO_RSDHDT_DIS =E=0;$$

$$\begin{aligned} \text{EQN169.. } & \text{MDC_VGOHDT_DIS} - \\ & (\text{FDC_VGOHDT_DIS*SG_VGOHDT_DIS1*WF}) =E=0; \end{aligned}$$

$$\begin{aligned} \text{EQN170.. } & \text{MFO_VGOHDT_DIS} - (\text{FFO_VGOHDT_DIS*SG_VGOHDT_DIS1*WF}) \\ & =E=0; \end{aligned}$$

$$\begin{aligned} \text{EQN171.. } & \text{MDC_RSDHDT_DIS} - (\text{FDC_RSDHDT_DIS*SG_RSDHDT_DIS*WF}) \\ & =E=0; \end{aligned}$$

$$\begin{aligned} \text{EQN172.. } & \text{MFO_RSDHDT_DIS} - (\text{FFO_RSDHDT_DIS*SG_RSDHDT_DIS*WF}) \\ & =E=0; \end{aligned}$$

$$\text{EQN173.. } F_DHDT_KERO - F_DHDT_KERO_D - F_DHDT_KERO_K =E=0;$$

$$\begin{aligned} \text{EQN174.. } & \text{VDSP} - F_DHDT_DIS - F_DHDT_KERO_D - F_GHC_DIES - \\ & F_GFCC_LCO - FDC_VGOHDT_DIS - FDC_RSDHDT_DIS - F_MIXFCC_LCO - \\ & F_PHC_DIES - F_BHC_DIES - F_DS_DIES =E=0; \end{aligned}$$

$$\begin{aligned} \text{EQN175.. } & \text{CET_DHDT_DIS1*F_DHDT_DIS} + \\ & \text{CET_DHDT_KERO*F_DHDT_KERO_D} + \text{CI_GHC_DIES*F_GHC_DIES} + \\ & \text{CI_GFCC_LCO*F_GFCC_LCO} + \text{CI_VGOHDT_DIS*FDC_VGOHDT_DIS} + \\ & \text{CI_RSDHDT_DIS*FDC_RSDHDT_DIS} + \text{CI_GFCC_LCO*F_MIXFCC_LCO} + \\ & \text{CI_GHC_DIES*F_PHC_DIES} + \text{CI_GHC_DIES*F_BHC_DIES} + \\ & \text{CI_DS_DIES*F_DS_DIES} - \text{CN_DSP*VDSP} =G=0; \end{aligned}$$

$$\begin{aligned} \text{EQN176.. } & \text{SG_DHDT_DIS1*F_DHDT_DIS} + \\ & \text{SG_DHDT_KERO1*F_DHDT_KERO_D} + \text{SG_GHC_DIES*F_GHC_DIES} + \\ & \text{SG_GFCC_LCO*F_GFCC_LCO} + \text{SG_VGOHDT_DIS1*FDC_VGOHDT_DIS} + \\ & \text{SG_RSDHDT_DIS*FDC_RSDHDT_DIS} + \text{SG_GFCC_LCO*F_MIXFCC_LCO} + \\ & \text{SG_GHC_DIES*F_PHC_DIES} + \text{SG_GHC_DIES*F_BHC_DIES} + \\ & \text{SG_DS_DIES*F_DS_DIES} - \text{SG_DSP*VDSP} =L=0; \end{aligned}$$

$$\text{EQN177.. } M_{\text{DHDT_KERO_D}} - (F_{\text{DHDT_KERO_D}} * SG_{\text{DHDT_KERO1}} * WF) = E=0;$$

$$\text{EQN178.. } MDSP - M_{\text{DHDT_DIS}} - M_{\text{DHDT_KERO_D}} - M_{\text{GHC_DIES}} - M_{\text{GFCC_LCO}} - MDC_{\text{VGOHDT_DIS}} - MDC_{\text{RSDHDT_DIS}} - M_{\text{MIXFCC_LCO}} - M_{\text{PHC_DIES}} - M_{\text{BHC_DIES}} - M_{\text{DS_DIES}} = E=0;$$

$$\begin{aligned} \text{EQN179..} \quad & \text{SUL}_{\text{DHDT_DIS1}} * M_{\text{DHDT_DIS}} + \\ & \text{SUL}_{\text{DHDT_KERO1}} * M_{\text{DHDT_KERO_D}} + \text{SUL}_{\text{GHC_DIES}} * M_{\text{GHC_DIES}} + \\ & \text{SUL}_{\text{GFCC_LCO}} * M_{\text{GFCC_LCO}} + \text{SUL}_{\text{VGOHDT_DIS1}} * MDC_{\text{VGOHDT_DIS}} \\ & + \text{SUL}_{\text{RSDHDT_DIS}} * MDC_{\text{RSDHDT_DIS}} + \\ & \text{SUL}_{\text{GFCC_LCO}} * M_{\text{MIXFCC_LCO}} + \text{SUL}_{\text{GHC_DIES}} * M_{\text{PHC_DIES}} + \\ & \text{SUL}_{\text{GHC_DIES}} * M_{\text{BHC_DIES}} + \text{SUL}_{\text{DS_DIES}} * M_{\text{DS_DIES}} - \\ & \text{SUL}_{\text{DSP}} * MDSP = L=0; \end{aligned}$$

$$\text{EQN180.. } VP_{\text{KERO}} - F_{\text{KERO}} - F_{\text{DHDT_KERO_K}} - F_{\text{GHC_KERO}} = E=0;$$

$$\text{EQN181.. } SPI_{\text{KERO}} * F_{\text{KERO}} + SPI_{\text{DHDT_KERO}} * F_{\text{DHDT_KERO_K}} + SPI_{\text{GHC_KERO}} * F_{\text{GHC_KERO}} - SPI_{\text{VP_KERO}} * VP_{\text{KERO}} = G=0;$$

$$\text{EQN182.. } SG_{\text{KERO}} * F_{\text{KERO}} + SG_{\text{DHDT_KERO1}} * F_{\text{DHDT_KERO_K}} + SG_{\text{GHC_KERO}} * F_{\text{GHC_KERO}} - SG_{\text{VP_KERO}} * VP_{\text{KERO}} = L=0;$$

$$\text{EQN187.. } M_{\text{KERO}} - (F_{\text{KERO}} * SG_{\text{KERO1}} * WF) = E=0;$$

$$\text{EQN188.. } M_{\text{DHDT_KERO_K}} - (F_{\text{DHDT_KERO_K}} * SG_{\text{DHDT_KERO1}} * WF) = E=0;$$

$$\text{EQN189.. } MP_{\text{KERO}} - M_{\text{KERO}} - M_{\text{DHDT_KERO_K}} - M_{\text{GHC_KERO}} = E=0;$$

$$\text{EQN190.. } \text{SUL}_{\text{KERO1}} * M_{\text{KERO}} + \text{SUL}_{\text{DHDT_KERO1}} * M_{\text{DHDT_KERO_K}} + \text{SUL}_{\text{GHC_KERO}} * M_{\text{GHC_KERO}} - \text{SUL}_{\text{VP_KERO}} * MP_{\text{KERO}} = L=0;$$

$$\text{EQN191.. } VFOP - F_{\text{RSDHDT_FO}} - FFO_{\text{RSDHDT_DIS}} - FFO_{\text{VGOHDT_DIS}} - F_{\text{GFCC_HCO}} - F_{\text{MIXFCC_HCO}} = E=0;$$

$$\text{EQN192.. } MFOP - M_{\text{RSDHDT_FO}} - MFO_{\text{RSDHDT_DIS}} - MFO_{\text{VGOHDT_DIS}} - M_{\text{GFCC_HCO}} - M_{\text{MIXFCC_HCO}} = E=0;$$

$$\begin{aligned} \text{EQN193..} \quad & \text{SG}_{\text{RSDHDT_FO}} * F_{\text{RSDHDT_FO}} + \\ & \text{SG}_{\text{RSDHDT_DIS}} * FFO_{\text{RSDHDT_DIS}} + \\ & \text{SG}_{\text{VGOHDT_DIS1}} * FFO_{\text{VGOHDT_DIS}} + \text{SG}_{\text{GFCC_HCO}} * F_{\text{GFCC_HCO}} + \\ & \text{SG}_{\text{GFCC_HCO}} * F_{\text{MIXFCC_HCO}} - \text{SG}_{\text{FOP}} * VFOP = L=0; \end{aligned}$$

EQN194.. SUL_RSDHDT_FO*M_RSDHDT_FO +
 SUL_RSDHDT_DIS*MFO_RSDHDT_DIS +
 SUL_VGOHDT_DIS1*MFO_VGOHDT_DIS + SUL_GFCC_HCO*M_GFCC_HCO
 + SUL_GFCC_HCO*M_MIXFCC_HCO - SUL_FOP*MFOP =1=0;
 EQN195.. F_TGO3 - [M_TGO3*(VF/SG_TGO1)] =E=0;
 EQN196.. F_TGO2 - [M_TGO2*(VF/SG_TGO1)] =E=0;
 EQN197.. F_MIX - [M_MIX*(VF/SG_MIX)] =E=0;
 EQN198.. H2_CONSP =E= [0.95*(F_SRHN*H0_HN1)/1000000] +
 [0.95*(F_DIES*H0_DIES1)/1000000] + [0.95*(F_RSD*H0_RSD)/1000000] +
 [0.95*(F_VGO*439)/1000000] + 0.95*0.012241*M_TGO2*0.4178 +
 0.99*0.1249*M_DS_FHCK1*0.4178 + 0.99*0.04287*M_PY_OIL*0.4178 +
 0.99*0.1249*M_DS_FHCK2*0.4178 - 0.4178*H2_REF_WT*0.8;

*Operating cost

EQN199.. OC - (0.009*F_CRUDE + F_SRLTN + F_SRHN + F_KERO +
 F_DIES)*K1('CDU1', 'S')*K1('PRICE1','S') - (0.009*F_CRUDE + F_SRLTN +
 F_SRHN + F_KERO + F_DIES)*K1('CDU1', 'W')*K1('PRICE1','W') -
 (0.009*F_CRUDE + F_SRLTN + F_SRHN + F_KERO + F_DIES)*K1('CDU1',
 'P')*K1('PRICE1','P') - (0.009*F_CRUDE + F_SRLTN + F_SRHN + F_KERO +
 F_DIES)*K1('CDU1', 'F')*K1('PRICE1','F') - (F_VGO + F_RSD)*K1('VDU1',
 'S')*K1('PRICE1','S') - (F_VGO + F_RSD)*K1('VDU1', 'W')*K1('PRICE1','W') -
 (F_VGO + F_RSD)*K1('VDU1', 'P')*K1('PRICE1','P') - (F_VGO +
 F_RSD)*K1('VDU1', 'F')*K1('PRICE1','F') - (F_SRHN)*K1('NHDT1',
 'S')*K1('PRICE1','S') - (F_SRHN)*K1('NHDT1', 'W')*K1('PRICE1','W') -
 (F_SRHN)*K1('NHDT1', 'P')*K1('PRICE1','P') - (F_SRHN)*K1('NHDT1',
 'F')*K1('PRICE1','F') - (F_DIES)*K1('DHDT1', 'S')*K1('PRICE1','S') -
 (F_DIES)*K1('DHDT1', 'W')*K1('PRICE1','W') - (F_DIES)*K1('DHDT1',
 'P')*K1('PRICE1','P') - (F_DIES)*K1('DHDT1', 'F')*K1('PRICE1','F') -
 (F_VGO)*K1('VHDT1', 'S')*K1('PRICE1','S') - (F_VGO)*K1('VHDT1',
 'W')*K1('PRICE1','W') - (F_VGO)*K1('VHDT1', 'P')*K1('PRICE1','P') -
 (F_VGO)*K1('VHDT1', 'F')*K1('PRICE1','F') - (F_RSD)*K1('RHDT1',
 'S')*K1('PRICE1','S') - (F_RSD)*K1('RHDT1', 'W')*K1('PRICE1','W') -

(F_RSD)*K1('RHDT1', 'P')*K1('PRICE1','P') - (F_RSD)*K1('RHDT1',
'F')*K1('PRICE1','F') - (F_REF)*K1('CRU1', 'S')*K1('PRICE1','S') -
(F_REF)*K1('CRU1', 'W')*K1('PRICE1','W') - (F_REF)*K1('CRU1',
'P')*K1('PRICE1','P') - (F_REF)*K1('CRU1', 'F')*K1('PRICE1','F') -
(F_REF_B)*K1('CRU1', 'S')*K1('PRICE1','S') - (F_REF_B)*K1('CRU1',
'W')*K1('PRICE1','W') - (F_REF_B)*K1('CRU1', 'P')*K1('PRICE1','P') -
(F_REF_B)*K1('CRU1', 'F')*K1('PRICE1','F') - (F_TGO3)*K1('FCC1',
'S')*K1('PRICE1','S') - (F_TGO3)*K1('FCC1', 'W')*K1('PRICE1','W') -
(F_TGO3)*K1('FCC1', 'P')*K1('PRICE1','P') - (F_TGO3)*K1('FCC1',
'F')*K1('PRICE1','F') - (F_MIX)*K1('FCC1', 'S')*K1('PRICE1','S') -
(F_MIX)*K1('FCC1', 'W')*K1('PRICE1','W') - (F_MIX)*K1('FCC1',
'P')*K1('PRICE1','P') - (F_MIX)*K1('FCC1', 'F')*K1('PRICE1','F') -
(F_TGO2)*K1('HCK1', 'S')*K1('PRICE1','S') - (F_TGO2)*K1('HCK1',
'P')*K1('PRICE1','P') - (F_TGO2)*K1('HCK1', 'W')*K1('PRICE1','W') -
(F_TGO2)*K1('HCK1','F')*K1('PRICE1','F') - (F_DS_FHCK1)*K1('BHCK1',
'S')*K1('PRICE1','S') - (F_DS_FHCK1)*K1('BHCK1', 'W')*K1('PRICE1','W') -
(F_DS_FHCK1)*K1('BHCK1', 'P')*K1('PRICE1','P') -
(F_DS_FHCK1)*K1('BHCK1', 'F')*K1('PRICE1','F') -
(F_DS_FHCK2)*K1('BHCK1', 'S')*K1('PRICE1','S') -
(F_DS_FHCK2)*K1('BHCK1', 'W')*K1('PRICE1','W') -
(F_DS_FHCK2)*K1('BHCK1', 'P')*K1('PRICE1','P') -
(F_DS_FHCK2)*K1('BHCK1', 'F')*K1('PRICE1','F') - (M_BIOMASS)*K1('PYR1',
'P')*K1('PRICE1','P') - (M_BIOMASS)*K1('PYR1', 'W')*K1('PRICE1','W') -
(M_PY_OIL)*K1('HDT1', 'S')*K1('PRICE1','S') - (M_PY_OIL)*K1('HDT1',
'W')*K1('PRICE1','W') - (M_PY_OIL)*K1('HDT1','P')*K1('PRICE1','P') -
(M_PY_OIL)*K1('HDT1', 'F')*K1('PRICE1','F') - (M_HDT_PY)*K1('DE-C41',
'S')*K1('PRICE1','S') - (M_HDT_PY)*K1('DE-C41', 'P')*K1('PRICE1','P') -
(M_TPYB)*K1('NS1', 'S')*K1('PRICE1','S') - (M_TPYB)*K1('NS1',
'P')*K1('PRICE1','P') - (M_NS_FDIES)*K1('DS1', 'S')*K1('PRICE1','S') -
(M_NS_FDIES)*K1('DS1', 'P')*K1('PRICE1','P') - 92.02*F_CRUDE -
83*M_BIOMASS =E=0;

*integration logic constraints

$$\text{EQ200.. } Y1 + Y2 =E= 1;$$

$$\text{EQ201.. } M_TPY - Y1*M_TPY.UP =L=0;$$

$$\text{EQ202.. } M_TPYB - Y2*M_TPYB.UP =L=0;$$

$$\text{EQ203.. } Y3 + Y4 =E=1;$$

$$\text{EQ204.. } M_DS_FHCK2 - y3*M_DS_FHCK2.UP =L=0;$$

$$\text{EQ205.. } M_TGO2 - Y4*M_TGO2.UP =L=0;$$

$$\text{EQ206.. } Y5 + Y6 =L=1;$$

$$\text{EQ207.. } M_NS_NAPH1 - y5*M_NS_NAPH1.UP =L=0;$$

$$\text{EQ208.. } M_NS_NAPH2 - y6*M_NS_NAPH2.UP =L=0;$$

$$\text{EQ209.. } Y1 + Y7 =E= 1;$$

$$\text{EQ210.. } M_TPY - Y1*M_TPY.UP =L=0;$$

$$\text{EQ211.. } M_TGO3 - Y7*M_TGO3.UP =L=0;$$

$$\text{EH1(u).. } \text{cons('NHT')} =E= [(F_SRHN*H0_HN1)/1000000];$$

$$\text{EH2(u).. } \text{cons('DHT')} =E= [(F_DIES*H0_DIES1)/1000000];$$

$$\text{EH3(u).. } \text{cons('RHT')} =E= [(F_RSD*H0_RSD)/1000000];$$

$$\text{EH4(u).. } \text{cons('GOHT')} =E= [(F_VGO*439)/1000000];$$

$$\text{EH5(U).. } \text{Cons('HC1')} =E= 0.012241*M_TGO2;$$

$$\text{EH6(U).. } \text{Cons('HC2')} =E= 0.04267*M_DS_FHCK1;$$

$$\text{EH7(U).. } \text{Cons('BHDT')} =E= 0.016056812*M_PY_OIL;$$

$$\text{EH8(U).. } \text{Cons('HC3')} =E= 0.04267*M_DS_FHCK2;$$

*hydrogen network balance

$$\text{EH9(i).. } FI(i) =E= \text{sum}(u, FIU(i, u)*c(i, u)) + \text{sum}(k, FIK(i, k)*h(i, k)) + \text{sum}(n, FIN(i, n)*h1(i, N)) + \text{sum}(j, FIJ(i, j)*l(i, j));$$

$$\text{EH10(n, u).. } UP*(YNU(n, u) - 1) =l= (PNO(n) - PH2U(u));$$

$$\text{EH11(n, u).. } YNU(n, u)*UP - b =g= (PNO(n) - PH2U(u));$$

$$\text{EH12(n, u).. } FNU(n, u) - YNU(n, u)*UF =l= 0;$$

$$\text{EH13(n, k).. } UP*(YNK(n, k) - 1) =l= (PNO(n) - PKI(k));$$

$$\text{EH14(n, k).. } YNK(n, k)*UP - b =g= (PNO(n) - PKI(k));$$

$$\text{EH15(n, k).. } FNK(n, k) - YNK(n, k)*UF =l= 0;$$

EH16(V).. FH2V(v) =E= R(v) + sum(u, FVU(v, u)*d(v, u)) + sum(k, FVK(v, k)*e(v, k)) + sum(n, FVN(v, n)*e2(v, n)) + sum(m, FVM(v, m)*r5(v, m)) + sum(j, FVJ(v, j)*q(v, j));

EH17(U).. FH2U(u) =E= cons(u)/CON_FAC(U) ;

EH18(u).. FH2V(u)*YH2V(u) =E= FH2U(u)*YH2U(u) - cons(u);

EH19(u).. FH2U(u) =E= R(u) + sum(i, FIU(i, u)*c(i, u)) + sum(v, FVU(v, u)*d(v, u)) + sum(k, FKU(k, u)*f(k, u)) + sum(n, FNU(n, u));

EH20(u).. FH2U(u)*YH2U(u) =E= R(u)*YR(u) + sum(i, FIU(i, u)*c(i, u)*YHP(i)) + sum(v, FVU(v, u)*d(v, u)*YH2V(v)) + sum(K, FKU(K, U)*f(k, u)*YK(k)) + sum(N, FNU(N, U)*YN(N));

EH29(k).. FKIn(k) =E= sum(i, FIK(i, k)*h(i, k)) + sum(v, FVK(v, k)*e(v, k)) + sum(n, FNK(n, k)) + sum(m, FMK(m, k)*f3(m, k));

EH30(k).. FKout(k) =E= sum(u, FKU(k, u)*f(k, u));

EH31(k).. FKIn(k) =E= FKout(k);

EH32(k).. FKIn(k)*YK(k) =E= sum(i, FIK(i, k)*h(i, k)*YHP(i)) + sum(v, FVK(v, k)*e(v, k)*YH2V(v)) + sum(N, FNK(N, K)*YN(N)) + sum(m, FMK(m, k)*YPR(m)*f3(m, k));

EH37(k).. FKIn(k) =E= maxCP(k);

EH38(k).. PWR(k) =E= a_com*[[PKO(k)/PKI(k)]**b_com - 1]*FKIn(k);

EH39(n).. FNin(n) =E= sum(i, FIN(i, n)*h1(i, N)) + sum(v, FVN(v, n)*e2(v, n)) + sum(m, FMN(m, n));

EH40(n).. FNout(n) =E= sum(u, FNU(n, u)) + sum(k, FNK(n, k));

EH41(n).. FNin(n) =E= FNout(n);

EH42(n).. FNin(n)*YN(n) =E= sum(i, FIN(i, n)*h1(i, N)*YHP(i)) + sum(v, FVN(v, n)*e2(v, n)*YH2V(v)) + sum(m, FMN(m, n)*YPR(m));

EH47(n).. FNin(n) =L= maxCP1(n);

EH48(n).. UP*(T1(n) - 1) + LNPC =L= (PNO(n) - PNI(N));

EH49(n).. T1(n)*UP + LNPC - b =G= (PNO(n) - PNI(N));

EH50(n).. FNin(n) - T1(n)* FNin.UP(n) =l= 0;

EH51(n).. FNin(n) - T1(n)* FNin.LO(n) =g= 0;

EH52(n).. PwrN(n) - a_com*[[PNO(n) /PNI(n)]**b_com - 1]*FNin(n) - (1 - T1(n))*upp =l= 0;

EH53(n).. $PwrN(n) - a_com * [(PNO(n) / PNI(n))]^{b_com - 1} * FNin(n) - (T1(n) - 1) * upp = g = 0;$
 EH54(n).. $PwrN(n) - T1(n) * upp = l = 0;$
 EH55.. $SUM(N, T1(N)) = e = 2;$
 EH56(m).. $FMin(m) = E = \text{sum}(v, FVM(v, m) * r5(v, m));$
 EH57(m).. $FMin(m) * YMin(m) = E = \text{sum}(v, FVM(v, m) * r5(v, m) * YH2V(v));$
 EH62(m).. $FPUR(m) * YPR(m) = E = FMin(m) * YMin(m) * 0.9;$
 EH63(m).. $FMin(m) = E = FPUR(m) + FRSD(m);$
 EH64(m).. $FRSD(m) * YRSD(m) = E = FMin(m) * YMin(m) * 0.1;$
 EH69(m).. $FPUR(m) = E = \text{sum}(k, FMK(m, k) * f3(m, k)) + \text{sum}(n, FMN(m, n));$
 EH70(m).. $FRSD(m) = e = \text{sum}(j, FMJ(m, j));$
 EH71(m).. $FMin(m) - T2(m) * FMin.UP(m) = l = 0;$
 EH72(m).. $FMin(m) - T2(m) * FMin.LO(m) = g = 0;$
 EH73(i).. $FI('HP') = E = FHP;$
 EH74(i).. $FI('CRF') = e = 0.417776 * (H2_REF_WT + H2_REF_WTB);$
 EH75(i).. $FI('HP3') = L = FHP3;$
 EH76(u).. $PwrR(u) = e = a_com * [(PH2U(u) / PH2V(u))]^{b_com - 1} * R(u);$
 EH77(N).. $CAP_nc(n) = e = (a_nc * T1(n) + b_nc * PwrN(n));$
 EH78(m).. $CAP_m(m) = e = (a_m * T2(m) + b_m * FMin(m));$
 EH79.. $elec = e = 0.72 * [\text{sum}(k, Pwr(k)) + \text{sum}(n, PwrN(n)) + \text{sum}(u, PwrR(u))];$
 EH80(j).. $F_fuel(j) = E = \text{sum}(m, FMJ(m, j));$
 EH81(j).. $F_fuel(j) * y_fu(j) = E = \text{sum}(m, FMJ(m, j) * YRSD(m));$
 EH90(j).. $OC_fuel(j) = e = OCF * F_fuel(j) * ((LHV_H2 * y_fu(j)) + LHV_C4 * (1 - y_fu(j)));$
 EQ352.. $COST_1 = E = \text{sum}(i, FI(i) * CH2S(i));$
 EQ353.. $COST_2 = E = 0.72 * [\text{sum}(k, Pwr(k)) + \text{sum}(n, PwrN(n)) + \text{sum}(u, PwrR(u))];$
 ;
 EQ354.. $COST_3 = E = \text{sum}(j, OC_fuel(j));$

*Capital costs

EQ212.. $H2_TON = [(0.0429 * M_PY_OIL) + (0.1249 * M_DS_FHCK1) + (0.1249 * M_DS_FHCK2)] = E = 0;$

EQ213.. $H2_SCF - 0.417776 * H2_TON = E = 0$;
 EQ214.. $RATIO = E = (H2_SCF / 24.5)$;
 EQ215.. $RATIO = E = Z11 + Z12 + Z13$;
 EQ216.. $RATIO1 - RATIO1.UP * (1 - Y11) = L = Z11$;
 EQ217.. $Z11 = L = RATIO1.UP * Y11$;
 EQ218.. $Z11 = L = RATIO1$;
 EQ219.. $RATIO2 - RATIO2.UP * (1 - Y12) = L = Z12$;
 EQ220.. $Z12 = L = RATIO2.UP * Y12$;
 EQ221.. $Z12 = L = RATIO2$;
 EQ222.. $RATIO3 - RATIO3.UP * (1 - Y13) = L = Z13$;
 EQ223.. $Z13 = L = RATIO3.UP * Y13$;
 EQ224.. $Z13 = L = RATIO3$;
 EQ225.. $Y11 + Y12 + Y13 = L = 1$;
 EQ226.. $INDEX1 = E = 1.088 * Z11 + 0.123 * Y11$;
 EQ227.. $INDEX2 = E = 0.729 * Z12 + 0.273 * Y12$;
 EQ228.. $INDEX3 = E = 0.476 * Z13 + 0.595 * Y13$;
 EQ229.. $INDEX = E = INDEX1 + INDEX2 + INDEX3$;
 EQ230.. $H2_COST = E = 79406 * INDEX$;
 EQ231.. $RATIO_NS = E = M_TPYB / 718.77$;
 EQ232.. $RATIO_NS = E = Z21 + Z22 + Z23$;
 EQ233.. $RATIO21 - RATIO21.UP * (1 - Y21) = L = Z21$;
 EQ234.. $Z21 = L = RATIO21.UP * Y21$;
 EQ235.. $Z21 = L = RATIO21$;
 EQ236.. $RATIO22 - RATIO22.UP * (1 - Y22) = L = Z22$;
 EQ237.. $Z22 = L = RATIO22.UP * Y22$;
 EQ238.. $Z22 = L = RATIO22$;
 EQ239.. $RATIO23 - RATIO23.UP * (1 - Y23) = L = Z23$;
 EQ240.. $Z23 = L = RATIO23.UP * Y23$;
 EQ241.. $Z23 = L = RATIO23$;
 EQ242.. $Y21 + Y22 + Y23 = L = 1$;
 EQ243.. $INDEX21 = E = 1.088 * Z21 + 0.123 * Y21$;
 EQ244.. $INDEX22 = E = 0.729 * Z22 + 0.273 * Y22$;

EQ245.. INDEX23 =E= 0.476*Z23 + 0.595*Y23;
 EQ246.. INDEX_NS =E= INDEX21 + INDEX22 + INDEX23;
 EQ247.. COST_NS =E= 1404*INDEX_NS;
 EQ248.. RATIO_DS =E= M_NS_FDIES/508.027;
 EQ249.. RATIO_DS =E= Z31 + Z32 + Z33;
 EQ250.. RATIO31 - RATIO31.UP*(1-Y31) =L= Z31;
 EQ251.. Z31 =L= RATIO31.UP*Y31;
 EQ252.. Z31 =L= RATIO31;
 EQ253.. RATIO32 - RATIO32.UP*(1-Y32) =L= Z32;
 EQ254.. Z32 =L= RATIO32.UP*Y32;
 EQ255.. Z32 =L= RATIO32;
 EQ256.. RATIO33 - RATIO33.UP*(1-Y33) =L= Z33;
 EQ257.. Z33 =L= RATIO33.UP*Y33;
 EQ258.. Z33 =L= RATIO33;
 EQ259.. Y31 + Y32 + Y33 =L= 1;
 EQ260.. INDEX31 =E= 1.088*Z31 + 0.123*Y31;
 EQ261.. INDEX32 =E= 0.729*Z32 + 0.273*Y32;
 EQ262.. INDEX33 =E= 0.476*Z33 + 0.595*Y33;
 EQ263.. INDEX_DS =E= INDEX31 + INDEX32 + INDEX33;
 EQ264.. COST_DS =E= 1080*INDEX_DS;
 EQ265.. RATIO_BHC =E= M_DS_FHCK1/95.814;
 EQ266.. RATIO_BHC =E= Z41 + Z42 + Z43;
 EQ267.. RATIO41 - RATIO41.UP*(1-Y41) =L= Z41;
 EQ268.. Z41 =L= RATIO41.UP*Y41;
 EQ269.. Z41 =L= RATIO41;
 EQ270.. RATIO42 - RATIO42.UP*(1-Y42) =L= Z42;
 EQ271.. Z42 =L= RATIO42.UP*Y42;
 EQ272.. Z42 =L= RATIO42;
 EQ273.. RATIO43 - RATIO43.UP*(1-Y43) =L= Z43;
 EQ274.. Z43 =L= RATIO43.UP*Y43;
 EQ275.. Z43 =L= RATIO43;
 EQ276.. Y41 + Y42 + Y43 =L= 1;

EQ277.. INDEX41 =E= 1.088*Z41 + 0.123*Y41;
 EQ278.. INDEX42 =E= 0.729*Z42 + 0.273*Y42;
 EQ279.. INDEX43 =E= 0.476*Z43 + 0.595*Y43;
 EQ280.. INDEX_BHC =E= INDEX41 + INDEX42 + INDEX43;
 EQ281.. COST_BHC =E= 29476*INDEX_BHC;
 EQ282.. RATIO_RUB =E= M_NS_NAPH1/210.743;
 EQ283.. RATIO_RUB =E= Z51 + Z52 + Z53;
 EQ284.. RATIO51 - RATIO51.UP*(1-Y51) =L= Z51;
 EQ285.. Z51 =L= RATIO51.UP*Y51;
 EQ286.. Z51 =L= RATIO51;
 EQ287.. RATIO52 - RATIO52.UP*(1-Y52) =L= Z52;
 EQ288.. Z52 =L= RATIO52.UP*Y52;
 EQ289.. Z52 =L= RATIO52;
 EQ290.. RATIO53 - RATIO53.UP*(1-Y53) =L= Z53;
 EQ291.. Z53 =L= RATIO53.UP*Y53;
 EQ292.. Z53 =L= RATIO53;
 EQ293.. Y51 + Y52 + Y53 =L= 1;
 EQ294.. INDEX51 =E= 1.088*Z51 + 0.123*Y51;
 EQ295.. INDEX52 =E= 0.729*Z52 + 0.273*Y52;
 EQ296.. INDEX53 =E= 0.476*Z53 + 0.595*Y53;
 EQ297.. INDEX_RUB =E= INDEX51 + INDEX52 + INDEX53;
 EQ298.. COST_RUB =E= 18896*INDEX_RUB;
 EQ299.. RATIO_FCC =E= M_TPY/718.77;
 EQ300.. RATIO_FCC =E= Z61 + Z62 + Z63;
 EQ301.. RATIO61 - RATIO61.UP*(1-Y61) =L= Z61;
 EQ302.. Z61 =L= RATIO61.UP*Y61;
 EQ303.. Z61 =L= RATIO61;
 EQ304.. RATIO62 - RATIO62.UP*(1-Y62) =L= Z62;
 EQ305.. Z62 =L= RATIO62.UP*Y62;
 EQ306.. Z62 =L= RATIO62;
 EQ307.. RATIO63 - RATIO63.UP*(1-Y63) =L= Z63;
 EQ308.. Z63 =L= RATIO63.UP*Y63;

EQ309.. $Z63 = L = \text{RATIO63}$;
 EQ310.. $Y61 + Y62 + Y63 = L = 1$;
 EQ311.. $\text{INDEX61} = E = 1.088 * Z61 + 0.123 * Y61$;
 EQ312.. $\text{INDEX62} = E = 0.729 * Z62 + 0.273 * Y62$;
 EQ313.. $\text{INDEX63} = E = 0.476 * Z63 + 0.595 * Y63$;
 EQ314.. $\text{INDEX_FCC} = E = \text{INDEX61} + \text{INDEX62} + \text{INDEX63}$;
 EQ315.. $\text{COST_FCC} = E = 86869 * \text{INDEX_FCC}$;
 EQ316.. $\text{RATIO_PHC} = E = \text{M_DS_FHCK2} / 95.814$;
 EQ317.. $\text{RATIO_PHC} = E = Z71 + Z72 + Z73$;
 EQ318.. $\text{RATIO71} - \text{RATIO71.UP} * (1 - Y71) = L = Z71$;
 EQ319.. $Z71 = L = \text{RATIO71.UP} * Y71$;
 EQ320.. $Z71 = L = \text{RATIO71}$;
 EQ321.. $\text{RATIO72} - \text{RATIO72.UP} * (1 - Y72) = L = Z72$;
 EQ322.. $Z72 = L = \text{RATIO72.UP} * Y72$;
 EQ323.. $Z72 = L = \text{RATIO72}$;
 EQ324.. $\text{RATIO73} - \text{RATIO73.UP} * (1 - Y73) = L = Z73$;
 EQ325.. $Z73 = L = \text{RATIO73.UP} * Y73$;
 EQ326.. $Z73 = L = \text{RATIO73}$;
 EQ327.. $Y71 + Y72 + Y73 = L = 1$;
 EQ328.. $\text{INDEX71} = E = 1.088 * Z71 + 0.123 * Y71$;
 EQ329.. $\text{INDEX72} = E = 0.729 * Z72 + 0.273 * Y72$;
 EQ330.. $\text{INDEX73} = E = 0.476 * Z73 + 0.595 * Y73$;
 EQ331.. $\text{INDEX_PHC} = E = \text{INDEX71} + \text{INDEX72} + \text{INDEX73}$;
 EQ332.. $\text{COST_PHC} = E = 29476 * \text{INDEX_PHC}$;
 EQ333.. $\text{RATIO_RUR} = E = \text{M_NS_NAPH2} / 210.743$;
 EQ334.. $\text{RATIO_RUR} = E = Z81 + Z82 + Z83$;
 EQ335.. $\text{RATIO81} - \text{RATIO81.UP} * (1 - Y81) = L = Z81$;
 EQ336.. $Z81 = L = \text{RATIO81.UP} * Y81$;
 EQ337.. $Z81 = L = \text{RATIO81}$;
 EQ338.. $\text{RATIO82} - \text{RATIO82.UP} * (1 - Y82) = L = Z82$;
 EQ339.. $Z82 = L = \text{RATIO82.UP} * Y82$;
 EQ340.. $Z82 = L = \text{RATIO82}$;

EQ341.. $RATIO83 - RATIO83.UP*(1-Y83) =L= Z83$;
 EQ342.. $Z83 =L= RATIO83.UP*Y83$;
 EQ343.. $Z83 =L= RATIO83$;
 EQ344.. $Y81 + Y82 + Y83 =L= 1$;
 EQ345.. $INDEX81 =E= 1.088*Z81 + 0.123*Y81$;
 EQ346.. $INDEX82 =E= 0.729*Z82 + 0.273*Y82$;
 EQ347.. $INDEX83 =E= 0.476*Z83 + 0.595*Y83$;
 EQ348.. $INDEX_RUR =E= INDEX81 + INDEX82 + INDEX83$;
 EQ349.. $COST_RUR =E= 18896*INDEX_RUR$;
 EQ350.. $TOTAL_COST_REF =E= 0.11746*[COST_FCC*y1 + COST_PHC*y2 + COST_RUR*y2]$;
 EQ351.. $TOTAL_COST_BIO =E= 0.11746*[H2_COST + COST_NS + COST_DS + COST_BHC + COST_RUB + FX_COST]$;

FNin.lo("n1") = 15;
 FNin.lo("n3") = 3;
 FNin.lo("n2") = 0;
 FNin.up(n) = 47;
 FMin.LO(m)= 10;
 FMin.up(m)= 150;
 YN.LO(N)= 0.90;
 YN.up(N)= 0.99;
 YN.lo('n1') = 0.99;
 YN.up('N1')= 0.99;
 R.fx('BHDT') = 0;
 PNO.up('n1') = 2515;
 PNO.up('n2') = 2000;
 PNO.up('n3') = 1315;
 YK.LO(K)= 0.85;
 YK.up(K)= 0.95;
 YK.lo("K3")= 0.8;
 YK.up("K3")= 0.95;

YMin.lo(m) = 0.1;
YMin.up(m) = 0.8;
FRSD.LO(m) = 0;
FRSD.UP(m) = 120;
YRSD.lo(m) = 0;
YRSD.UP(m) = 0.8;
F_fuel.LO(j) = 0.01;
F_fuel.UP(j) = 120;
y_fu.LO(j) = 0;
y_fu.up(j) = 0.8;
FMJ.LO(m, j) = 0;
FMJ.up(m, j) = 120;
FKU.LO(K, U) = 0;
FKU.up(K, U) = 31.5;
FNU.LO(N, U) = 0;
FNU.up(N, U) = 60;
FNK.LO(N, K) = 0;
FNK.UP(N, K) = 60;
FKin.LO(k) = 0;
FKin.UP(k) = 31.5;
RATIO81.LO = 0;
RATIO81.UP = 0.4;
RATIO82.LO = 0.401;
RATIO82.UP = 1.1;
RATIO83.LO = 1.101;
RATIO83.UP = 4;
RATIO71.LO = 0;
RATIO71.UP = 0.4;
RATIO72.LO = 0.401;
RATIO72.UP = 1.1;
RATIO73.LO = 1.101;
RATIO73.UP = 4;

RATIO61.LO = 0;
RATIO61.UP = 0.4;
RATIO62.LO = 0.401;
RATIO62.UP = 1.1;
RATIO63.LO = 1.101;
RATIO63.UP = 4;
RATIO51.LO = 0.001;
RATIO51.UP = 0.4;
RATIO52.LO = 0.401;
RATIO52.UP = 1.1;
RATIO53.LO = 1.101;
RATIO53.UP = 4;
RATIO41.LO = 0;
RATIO41.UP = 0.4;
RATIO42.LO = 0.401;
RATIO42.UP = 1.1;
RATIO43.LO = 1.101;
RATIO43.UP = 4;
RATIO31.LO = 0;
RATIO31.UP = 0.4;
RATIO32.LO = 0.401;
RATIO32.UP = 1.1;
RATIO33.LO = 1.101;
RATIO33.UP = 4;
RATIO21.LO = 0;
RATIO21.UP = 0.4;
RATIO22.LO = 0.41;
RATIO22.UP = 1.1;
RATIO23.LO = 1.11;
RATIO23.UP = 4;
RATIO1.LO = 0;
RATIO1.UP = 0.4;

RATIO2.LO = 0.41;
RATIO2.UP = 1.1;
RATIO3.LO = 1.11;
RATIO3.UP = 4;
M_TGO3.UP = 3665 ;
M_TGO2.UP = 3665 ;
M_DS_FHCK2.UP = 95.9;
M_NS_NAPH1.UP = 210.8;
M_NS_NAPH2.UP = 210.8;
M_TPY.UP = 720;
M_TPYB.UP = 720;
F_TGO2.UP = 25000;
F_TGO3.up = 25000;
VPG.LO = 27500;
VP_KERO.LO = 25000;
VDSP.LO = 25000;
VFOP.lo = 18000;
F_REF.up = 20000;
SG_TGO.LO = 0.01;
SG_VGO.LO = 0.01;
SG_SRHN.LO = 0.01;
TE_SRLTN.LO = 90;
TE_SRLTN.UP =220;
TE_SRHN.LO = 180;
TE_SRHN.UP = 380;
TE_KERO.LO = 330;
TE_KERO.UP = 520;
TE_DIES.LO = 420;
TE_DIES.UP = 630;
TE_VGO.LO = 610;
TE_VGO.UP = 1050;

```
model oil_refinery /all/;  
option iterlim = 500000;  
solve oil_refinery using MINLP maximize T;
```

* Linearized integrated model GAMS code

OBJ.. profit =E= 0.365*122.052*VPG + 0.365*117.94*VP_KERO +
.365*115.16*VDSP + 0.365*56.66*VFOP + 0.365*36.246*F_LPG - 0.365*OC -
0.365*sum(i, FI(i)*CH2S(i)) - 0.365*0.72*sum(k, Pwr(k)) - 0.365*0.72*sum(u,
PwrR(u)) - 0.365*0.72*sum(n, PwrN(n)) + 0.365*sum(j, OC_fuel(j)) -
0.11746*sum(n, CAP_nc(n)) - 0.11746*sum(m, CAP_m(m)) -
0.15*0.11746*[sum(n, CAP_nc(n)) + sum(m, CAP_m(m))] - TOTAL_COST_REF -
TOTAL_COST_BIO;

*CDU

EQN1.. SRLTN_CUT =E= 0.088351*TE_SRLTN - 12.653;
EQN2.. SRHN_CUT =E= 0.088351*TE_SRHN - 12.653;
EQN3.. KERO_CUT =E= 0.088351*TE_KERO - 12.653;
EQN4.. DIES_CUT =E= 0.088351*TE_DIES - 12.653;
EQN5.. VGO_CUT =E= 0.0888*TE_VGO - 12.653;
EQN6.. LPG_YIELD - (LPG_CUT/100) =E= 0;
EQN7.. SRLTN_YIELD - ((SRLTN_CUT - LPG_CUT)/100) =E= 0;
EQN8.. SRHN_YIELD - ((SRHN_CUT - SRLTN_CUT)/100) =E= 0;
EQN9.. KERO_YIELD - ((KERO_CUT - SRHN_CUT)/100) =E= 0;
EQN10.. DIES_YIELD - ((DIES_CUT - KERO_CUT)/100) =E= 0;
EQN11.. VGO_YIELD - ((VGO_CUT - DIES_CUT)/100) =E= 0;
EQN12.. RSD_YIELD - ((100 - VGO_CUT)/100) =E= 0;
EQN13.. T_YIELD - (LPG_YIELD + SRLTN_YIELD + SRHN_YIELD +
KERO_YIELD + DIES_YIELD + VGO_YIELD + RSD_YIELD) =E= 0;
EQN14.. F_LPG - F_CRUDE*LPG_YIELD =E= 0;
EQN15.. F_SRLTN - F_CRUDE*SRLTN_YIELD =E= 0;
EQN16.. F_SRHN - F_CRUDE*SRHN_YIELD =E= 0;
EQN17.. F_KERO - F_CRUDE*KERO_YIELD =E= 0;
EQN18.. F_DIES - F_CRUDE*DIES_YIELD =E= 0;
EQN19.. F_VGO - F_CRUDE*VGO_YIELD =E= 0;
EQN20.. F_RSD - F_CRUDE*RSD_YIELD =E= 0;
EQN22.. MID_SRLTN - [(SRLTN_CUT + LPG_CUT)/2] =E= 0;

EQN23.. MID_SRHN - [(SRHN_CUT + SRLTN_CUT)/2] =E= 0;
 EQN24.. MID_KERO - [(KERO_CUT + SRHN_CUT)/2] =E= 0;
 EQN25.. MID_DIES - [(DIES_CUT + KERO_CUT)/2] =E= 0;
 EQN26.. MID_VGO - [(VGO_CUT + DIES_CUT)/2] =E= 0;
 EQN27.. MID_RSD - [(100 + VGO_CUT)/2] =E= 0;
 EQN28.. SG_SRLTN =E= 0.003*MID_SRLTN + 0.726;
 EQN29.. SG_SRHN =E= 0.003*MID_SRHN + 0.726;
 EQN30.. SG_KERO =E= 0.003*MID_KERO + 0.726;
 EQN31.. SG_DIES1 =E= 0.003*MID_DIES + 0.726;
 EQN32.. SG_VGO =E= 0.003*MID_VGO + 0.726;
 EQN33.. SG_RSD =E= 0.003*MID_RSD + 0.726;
 EQN34.. N2_KERO =E= 0.000187*MID_KERO - 0.00243;
 EQN35.. N2_DIES =E= 0.000612*MID_DIES - 0.013;
 EQN38.. SUL_SRLTN =E= 0.000213*MID_SRLTN + 0.0015;
 EQN39.. SUL_KERO =E= 0.0217*MID_KERO - 0.28;
 EQN40.. SUL_DIES =E= 0.0243*MID_DIES - 0.342;
 EQN41.. SUL_VGO =E= 0.0216*MID_VGO - 0.258;
 EQN42.. SUL_RSD =E= 0.0627*MID_RSD - 2.86;
 EQN43.. MID_SRHN =E= Z1 + Z2 + Z3;
 EQN44.. MID_SRHN1 - MID_SRHN1.UP*(1-Y10)=L= Z1;
 EQN45.. Z1=L= MID_SRHN1.UP*Y10;
 EQN46.. Z1 =L= MID_SRHN1;
 EQN47.. MID_SRHN2 - MID_SRHN2.UP*(1-Y20)=L= Z2;
 EQN48.. Z2=L= MID_SRHN2.UP*Y20;
 EQN49.. Z2 =L= MID_SRHN2;
 EQN49A.. MID_SRHN3 - MID_SRHN3.UP*(1-Y30)=L= Z3;
 EQN49B.. Z3=L= MID_SRHN3.UP*Y30;
 EQN49C.. Z3 =L= MID_SRHN3;
 EQN50.. Y10 + Y20 + Y30 =E= 1;
 EQN51.. SUL_SRHN1 =E= 0.000934*Z1 - 0.00223*Y10;
 EQN52.. SUL_SRHN2 =E= 0.0275*Z2 - 0.019*Y20;
 EQN52A.. SUL_SRHN3 =E= 0.0136*Z3 - 0.163*Y30;

$$\text{EQN52B.. SUL_SRHN} = \text{E} = \text{SUL_SRHN1} + \text{SUL_SRHN2} + \text{SUL_SRHN3};$$

* Naphtha hydrotreating unit

$$\text{EQN53.. ASF_HN} = \text{E} = 0.039 * \text{SUL_SRHN} + 0.011;$$

$$\text{EQN54.. H0_HN} = \text{E} = 25 + 70 * \text{SUL_SRHN} + 372.4 * \text{ASF_HN};$$

$$\text{EQN55.. H_HN} = \text{E} = 0.0020772 * \text{H0_HN} - 0.087850957 * \text{SG_SRHN} + 0.066467779;$$

$$\text{EQN56.. H2S_HN} = \text{E} = 1.063 * \text{SUL_SRHN} + 0.11206 ;$$

$$\text{EQN57.. GAS_HN} = \text{E} = 0.25 + 0.66 * \text{SUL_SRHN} ;$$

$$\text{EQN58.. HN_YIELD} = \text{E} = 100 + \text{H_HN} - \text{GAS_HN} - \text{H2S_HN};$$

$$\text{EQN59.. SG_HN} = \text{E} = 1.000378523 * \text{SG_SRHN} - 0.149226586 * \text{ASF_HN} + 0.00597639 * \text{H_HN} - 0.000559111;$$

$$\text{EQN61.. M_SRHN/WF} = \text{G} = \text{F_SRHN.LO} * \text{SG_SRHN} + \text{F_SRHN} * \text{SG_SRHN.LO} - \text{F_SRHN.LO} * \text{SG_SRHN.LO};$$

$$\text{EQN62.. M_SRHN/WF} = \text{G} = \text{F_SRHN.UP} * \text{SG_SRHN} + \text{F_SRHN} * \text{SG_SRHN.UP} - \text{F_SRHN.UP} * \text{SG_SRHN.UP};$$

$$\text{EQN63.. M_SRHN/WF} = \text{L} = \text{F_SRHN.LO} * \text{SG_SRHN} + \text{F_SRHN} * \text{SG_SRHN.UP} - \text{F_SRHN.LO} * \text{SG_SRHN.UP};$$

$$\text{EQN64.. M_SRHN/WF} = \text{L} = \text{F_SRHN.UP} * \text{SG_SRHN} + \text{F_SRHN} * \text{SG_SRHN.LO} - \text{F_SRHN.UP} * \text{SG_SRHN.LO};$$

$$\text{EQN66.. } 100 * \text{HN_MF} = \text{G} = \text{M_SRHN.LO} * \text{HN_YIELD} + \text{M_SRHN} * \text{HN_YIELD.LO} - \text{M_SRHN.LO} * \text{HN_YIELD.LO};$$

$$\text{EQN67.. } 100 * \text{HN_MF} = \text{G} = \text{M_SRHN.UP} * \text{HN_YIELD} + \text{M_SRHN} * \text{HN_YIELD.UP} - \text{M_SRHN.UP} * \text{HN_YIELD.UP};$$

$$\text{EQN68.. } 100 * \text{HN_MF} = \text{L} = \text{M_SRHN.LO} * \text{HN_YIELD} + \text{M_SRHN} * \text{HN_YIELD.UP} - \text{M_SRHN.LO} * \text{HN_YIELD.UP};$$

$$\text{EQN69.. } 100 * \text{HN_MF} = \text{L} = \text{M_SRHN.UP} * \text{HN_YIELD} + \text{M_SRHN} * \text{HN_YIELD.LO} - \text{M_SRHN.UP} * \text{HN_YIELD.LO};$$

* Diesel hydrotreating unit

$$\text{EQN70.. H0_DIES} - (120 * \text{SUL_DIES} + 159.5 * \text{N2_DIES} + 8 * \text{SG_DIES} * \text{B_DIES} + 25 + 290 * \text{FCC_DIES} * (11.9 - \text{K_DIES})) = \text{E} = 0;$$

EQN71.. HN_YIELD_DISTL =E= (((a2('a0','Nap2') + a2('b0','Nap2')*SG_DIES + a2('c0','Nap2')*SUL_DIES) + (a2('a1','Nap2') + a2('b1','Nap2')*SG_DIES + a2('c1','Nap2')*SUL_DIES)*0.95 + (a2('a2','Nap2') + a2('b2','Nap2')*SG_DIES + a2('c2','Nap2')*SUL_DIES)]*0.9025]);

EQN72.. KERO_YIELD_DISTL =E= (((a2('a0','KER2') + a2('b0','KER2')*SG_DIES + a2('c0','KER2')*SUL_DIES) + (a2('a1','KER2') + a2('b1','KER2')*SG_DIES + a2('c1','KER2')*SUL_DIES)*0.95 + (a2('a2','KER2') + a2('b2','KER2')*SG_DIES + a2('c2','KER2')*SUL_DIES)]*0.9025]);

EQN73.. DIS_YIELD_DISTL =E= (((a2('a0','DLS2') + a2('b0','DLS2')*SG_DIES + a2('c0','DLS2')*SUL_DIES) + (a2('a1','DLS2') + a2('b1','DLS2')*SG_DIES + a2('c1','DLS2')*SUL_DIES)*0.95 + (a2('a2','DLS2') + a2('b2','DLS2')*SG_DIES + a2('c2','DLS2')*SUL_DIES)]*0.9025]);

*EQN71.. HN_YIELD_DISTL =E= 0.001;

*EQN72.. KERO_YIELD_DISTL =E= 0.145;

*EQN73.. DIS_YIELD_DISTL =E= 0.84;

EQN73A.. API_DIES =E= 56.55 - 0.669*MID_DIES ;

EQN74.. API_DHDT_NAPH =E= 0.270698692*API_DIES - 0.000153438*SUL_DIES + 54.69512*SG_DIES ;

EQN75.. API_DHDT_KERO =E= 1.0356053*API_DIES + 0.000014369*SUL_DIES + 7.196331548*SG_DIES;

EQN76.. API_DHDT_DIS =E= 0.991333*API_DIES + 0.0000176457*SUL_DIES - 1.75184*SG_DIES;

EQN77.. SG_DHDT_NAPH =E= 1.0087 - 0.004*API_DHDT_NAPH ;

EQN78.. SG_DHDT_KERO =E= 1.0087 - 0.004*API_DHDT_KERO;

EQN79.. SG_DHDT_DIS =E= 1.0087 - 0.004*API_DHDT_DIS;

EQN80.. CET_DHDT_DIS =E= 1.986108497*API_DIES + 1.0162E-05*SUL_DIES - 2.807718365*SG_DIES;

EQN81.. SUL_DHDT_KERO =E= (a2('a5','KER2')*[a2('b5','KER2') + a2('c5','KER2')*0.95]*SUL_DIES);

EQN82.. SUL_DHDT_DIS =E= (a2('a5','DLS2')*[a2('b5','DLS2') + a2('c5','DLS2')*0.95]*SUL_DIES);

*EQN83.. F_DHDT_NAPH =E= F_DIES*HN_YIELD_DISTL;

EQN83.. F_DHDT_NAPH =G= F_DIES.LO*HN_YIELD_DISTL +
 F_DIES*HN_YIELD_DISTL.LO - F_DIES.LO*HN_YIELD_DISTL.LO;
 EQN84.. F_DHDT_NAPH =G= F_DIES.UP*HN_YIELD_DISTL +
 F_DIES*HN_YIELD_DISTL.UP - F_DIES.UP*HN_YIELD_DISTL.UP;
 EQN85.. F_DHDT_NAPH =L= F_DIES.LO*HN_YIELD_DISTL +
 F_DIES*HN_YIELD_DISTL.UP - F_DIES.LO*HN_YIELD_DISTL.UP;
 EQN86.. F_DHDT_NAPH =L= F_DIES.UP*HN_YIELD_DISTL +
 F_DIES*HN_YIELD_DISTL.LO - F_DIES.UP*HN_YIELD_DISTL.LO;
 *EQN83.. F_DHDT_DIS =E= F_DIES*DIS_YIELD_DISTL
 EQN87.. F_DHDT_DIS =G= F_DIES.LO*DIS_YIELD_DISTL +
 F_DIES*DIS_YIELD_DISTL.LO - F_DIES.LO*DIS_YIELD_DISTL.LO;
 EQN88.. F_DHDT_DIS =G= F_DIES.UP*DIS_YIELD_DISTL +
 F_DIES*DIS_YIELD_DISTL.UP - F_DIES.UP*DIS_YIELD_DISTL.UP;
 EQN89.. F_DHDT_DIS =L= F_DIES.LO*DIS_YIELD_DISTL +
 F_DIES*DIS_YIELD_DISTL.UP - F_DIES.LO*DIS_YIELD_DISTL.UP;
 EQN90.. F_DHDT_DIS =L= F_DIES.UP*DIS_YIELD_DISTL +
 F_DIES*DIS_YIELD_DISTL.LO - F_DIES.UP*DIS_YIELD_DISTL.LO;
 *EQN91.. F_DHDT_KERO =E= F_DIES*KERO_YIELD_DISTL;
 EQN91.. F_DHDT_KERO =G= F_DIES.LO*KERO_YIELD_DISTL +
 F_DIES*KERO_YIELD_DISTL.LO - F_DIES.LO*KERO_YIELD_DISTL.LO;
 EQN92.. F_DHDT_KERO =G= F_DIES.UP*KERO_YIELD_DISTL +
 F_DIES*KERO_YIELD_DISTL.UP - F_DIES.UP*KERO_YIELD_DISTL.UP;
 EQN93.. F_DHDT_KERO =L= F_DIES.LO*KERO_YIELD_DISTL +
 F_DIES*KERO_YIELD_DISTL.UP - F_DIES.LO*KERO_YIELD_DISTL.UP;
 EQN94.. F_DHDT_KERO =L= F_DIES.UP*KERO_YIELD_DISTL +
 F_DIES*KERO_YIELD_DISTL.LO - F_DIES.UP*KERO_YIELD_DISTL.LO;
 EQN95.. M_DHDT_NAPH =E= (F_DHDT_NAPH*SG_DHDT_NAPH1*WF) ;
 EQN96.. M_DHDT_KERO=E= (F_DHDT_KERO*SG_DHDT_KERO1*WF) ;
 EQN97.. M_DHDT_DIS =E= (F_DHDT_DIS*SG_DHDT_DIS1*WF) ;

* Gas oil hydrotreating uint

EQN98.. $H0_VGO - (40 + 150*SUL_VGO + (101.5*N2_VGO) + (7*B_VGO*SG_VGO) + (300*(11.9 - K_VGO)*FCC_VGO)) =E=0;$
 EQN99.. $H_VGO_YIELD =E= 0.001322558*H0_VGO + 0.082714288*SG_VGO;$
 EQN100.. $H2S_VGO_YIELD - 0.957*SUL_VGO =E=0;$
 EQN101.. $NH3_VGO_YIELD - 0.535*N2_VGO =E=0;$
 EQN102.. $GAS_VGO_YIELD - 0.46*H_VGO_YIELD =E=0;$
 EQN103.. $NAPH_VGO_YIELD =E= 0.244120435*SUL_VGO - 0.02800077;$
 EQN104.. $DIS_VGO_YIELD =E= 2.142623295*SUL_VGO - 0.285290863;$
 EQN105.. $TGO_VGO_YIELD - (100 + H_VGO_YIELD - H2S_VGO_YIELD - NH3_VGO_YIELD - NAPH_VGO_YIELD - DIS_VGO_YIELD) =E=0;$
 *EQN103.. $NAPH_VGO_YIELD =E= 0.00034;$
 *EQN104.. $DIS_VGO_YIELD =E= 0.02348;$
 *EQN105.. $TGO_VGO_YIELD =E= 0.97618;$
 EQN106.. $M_VGO =E= F_VGO*SG_VGO1*WF;$
 EQN107.. $M_VGOHDT_NAPH =G= M_VGO.LO*NAPH_VGO_YIELD + M_VGO*NAPH_VGO_YIELD.LO - M_VGO.LO*NAPH_VGO_YIELD.LO;$
 EQN108.. $M_VGOHDT_NAPH =G= M_VGO.UP*NAPH_VGO_YIELD + M_VGO*NAPH_VGO_YIELD.UP - M_VGO.UP*NAPH_VGO_YIELD.UP;$
 EQN109.. $M_VGOHDT_NAPH =L= M_VGO.LO*NAPH_VGO_YIELD + M_VGO*NAPH_VGO_YIELD.UP - M_VGO.LO*NAPH_VGO_YIELD.UP;$
 EQN110.. $M_VGOHDT_NAPH =L= M_VGO.UP*NAPH_VGO_YIELD + M_VGO*NAPH_VGO_YIELD.LO - M_VGO.UP*NAPH_VGO_YIELD.LO;$
 EQN111.. $M_VGOHDT_DIS =G= M_VGO.LO*DIS_VGO_YIELD + M_VGO*DIS_VGO_YIELD.LO - M_VGO.LO*DIS_VGO_YIELD.LO;$
 EQN112.. $M_VGOHDT_DIS =G= M_VGO.UP*DIS_VGO_YIELD + M_VGO*DIS_VGO_YIELD.UP - M_VGO.UP*DIS_VGO_YIELD.UP;$
 EQN113.. $M_VGOHDT_DIS =L= M_VGO.LO*DIS_VGO_YIELD + M_VGO*DIS_VGO_YIELD.UP - M_VGO.LO*DIS_VGO_YIELD.UP;$
 EQN114.. $M_VGOHDT_DIS =L= M_VGO.UP*DIS_VGO_YIELD + M_VGO*DIS_VGO_YIELD.LO - M_VGO.UP*DIS_VGO_YIELD.LO;$
 EQN115.. $M_TGO =G= M_VGO.LO*TGO_VGO_YIELD + M_VGO*TGO_VGO_YIELD.LO - M_VGO.LO*TGO_VGO_YIELD.LO;$

EQN116.. M_TGO =G= M_VGO.UP*TGO_VGO_YIELD +
 M_VGO*TGO_VGO_YIELD.UP - M_VGO.UP*TGO_VGO_YIELD.UP;
 EQN117.. M_TGO =L= M_VGO.LO*TGO_VGO_YIELD +
 M_VGO*TGO_VGO_YIELD.UP - M_VGO.LO*TGO_VGO_YIELD.UP;
 EQN118.. M_TGO =L= M_VGO.UP*TGO_VGO_YIELD +
 M_VGO*TGO_VGO_YIELD.LO - M_VGO.UP*TGO_VGO_YIELD.LO;
 EQN119.. SG_TGO =E= (SG_VGO1 - 0.025*H_VGO_YIELD);
 EQN120.. SUL_VGO_NAPH - 0.0085*SUL_VGO =E=0;
 EQN121.. SUL_VGOHDT_DIS - 0.02*SUL_VGO =E=0;
 EQN122.. SUL_TGO - [(10*SUL_VGO -
 SUL_VGO_NAPH*NAPH_VGO_YIELD1 -
 SUL_VGOHDT_DIS*DIS_VGO_YIELD1)/100*TGO_VGO_YIELD1] =E=0;
 EQN123.. F_VGOHDT_DIS - [M_VGOHDT_DIS*(VF/SG_VGOHDT_DIS1)]
 =E=0;
 EQN124.. F_TGO =E= [M_TGO*(VF/SG_TGO1)] ;

* Vacuum residue hydrotreating unit

EQN125.. M_RSD =E= F_RSD*SG_RSD1*WF;
 EQN126.. M_RSDHDT_NAPH =E= (M_RSD*0.00060);
 EQN127.. M_RSDHDT_DIS =E= (M_RSD*0.0137);
 EQN128.. M_RSDHDT_FO =E= (M_RSD*0.9857);
 EQN129.. F_RSDHDT_DIS =E= [M_RSDHDT_DIS*(VF/SG_RSDHDT_DIS)] ;
 EQN130.. F_RSDHDT_FO =E= [M_RSDHDT_FO*(VF/SG_RSDHDT_FO)] ;
 EQN131.. M_TGO =E= M_TGO1 + M_TGO2;

* FCC yield for pure hydrocarbon (TGO3)

EQN133.. M_GFCC_NAPH - e1('TGO3','gaso')*M_TGO3 =E=0;
 EQN134.. M_GFCC_LCO - e1('TGO3','lco')*M_TGO3 =E=0;
 EQN135.. M_GFCC_HCO - e1('TGO3','hco')*M_TGO3 =E=0;
 EQN136.. M_GFCC_COKE - e1('TGO3','coke')*M_TGO3 =E=0;
 EQN137.. M_GFCC_LPG - e1('TGO3','lpg')*M_TGO3 =E=0;
 EQN138.. F_GFCC_NAPH - [M_GFCC_NAPH*(VF/SG_GFCC_NAPH)] =E=0;

EQN139.. F_GFCC_LCO - [M_GFCC_LCO*(VF/SG_GFCC_LCO)] =E=0;
EQN140.. F_GFCC_HCO - [M_GFCC_HCO*(VF/SG_GFCC_HCO)] =E=0;

* HCK yield for pure hydrocarbon (TGO2)

EQN141.. M_GHC_LTN - d1('TGO2','li_gasol')*M_TGO2 =E=0;
EQN142.. M_GHC_HN - d1('TGO2','naph')*M_TGO2 =E=0;
EQN143.. M_GHC_KERO - d1('TGO2','KERO')*M_TGO2 =E=0;
EQN144.. M_GHC_DIES - d1('TGO2','diesel')*M_TGO2 =E=0;
EQN145.. F_GHC_LTN - [M_GHC_LTN*(VF/SG_GHC_LTN)] =E=0;
EQN146.. F_GHC_HN - [M_GHC_HN*(VF/SG_GHC_HN)] =E=0;
EQN147.. F_GHC_KERO - [M_GHC_KERO*(VF/SG_GHC_KERO)] =E=0;
EQN148.. F_GHC_DIES - [M_GHC_DIES*(VF/SG_GHC_DIES)] =E=0;

*Catalytic reforming unit

EQN149.. M_REF - (HN_MF + M_DHDT_NAPH + M_VGOHDT_NAPH +
M_RSDHDT_NAPH + M_GHC_HN + M_NS_NAPH2) =E=0;
EQN150.. H2_REF_WT - M_REF*0.0193 =E=0;
EQN151.. M_REFORMATE - (0.88*M_REF) =E=0;
EQN152.. F_REFORMATE =E= [M_REFORMATE*(VF/SG_REFORMATE)] ;
EQN152A.. M_REF - (F_REF*SG_REF*WF) =E=0;

* Pyrolysis unit

EQ1.. M_PY_OIL - b1('PY_OIL','PY')*M_BIOMASS =E= 0;
EQ2.. M_PY_FGAS - b1('FU_GAS','PY')*M_BIOMASS =E= 0;
EQ3.. M_PY_CHAR - b1('CHAR','PY')*M_BIOMASS =E= 0;

*Pyrolysis oil hydrotreating unit

EQ4.. M_HDT_PY - b1('TPY_OIL','HDT')*(M_PY_OIL + (0.0429*M_PY_OIL))
=E=0;
EQ5.. M_HDT_WW - b1('WASTE_W','HDT')*(M_PY_OIL +
(0.0429*M_PY_OIL)) =E=0;

$$\text{EQ6.. } M_{\text{HDT_PSAGAS}} - b1(\text{'PSA_GAS','HDT'}) * (M_{\text{PY_OIL}} + (0.0429 * M_{\text{PY_OIL}})) = E = 0;$$

$$\text{EQ7.. } M_{\text{HDF_OFFGAS}} - b1(\text{'OFF_GAS','HDT'}) * (M_{\text{PY_OIL}} + (0.0429 * M_{\text{PY_OIL}})) = E = 0;$$

*De-butanizer

$$\text{EQ8.. } M_{\text{C4_FGAS}} - b1(\text{'C4_FU_GAS','DE4'}) * M_{\text{HDT_PY}} = E = 0;$$

$$\text{EQ9.. } M_{\text{C4_OIL}} - b1(\text{'ST_OIL','DE4'}) * M_{\text{HDT_PY}} = E = 0;$$

$$\text{EQ10.. } M_{\text{C4_OIL}} - M_{\text{TPY}} - M_{\text{TPYB}} = E = 0;$$

* Naphtha splitter

$$\text{EQ11.. } M_{\text{NS_NAPH}} - b1(\text{'NAPH','NS'}) * M_{\text{TPYB}} = E = 0;$$

$$\text{EQ12.. } F_{\text{NS_NAPH}} - [M_{\text{NS_NAPH}} * (VF/SG_{\text{NS_NAPH}})] = E = 0;$$

$$\text{EQ13.. } M_{\text{NS_FDIES}} - b1(\text{'DS_F','NS'}) * M_{\text{TPYB}} = E = 0;$$

* Diesel splitter

$$\text{EQ14.. } M_{\text{DS_DIES}} - b1(\text{'DIES','DS'}) * M_{\text{NS_FDIES}} = E = 0;$$

$$\text{EQ15.. } F_{\text{DS_DIES}} - [M_{\text{DS_DIES}} * (VF/SG_{\text{DS_DIES}})] = E = 0;$$

$$\text{EQ16.. } M_{\text{DS_FHCK}} - b1(\text{'HC_F','DS'}) * M_{\text{NS_FDIES}} = E = 0;$$

$$\text{EQ17.. } F_{\text{DS_FHCK}} - [M_{\text{DS_FHCK}} * (VF/SG_{\text{TPY1}})] = E = 0;$$

* Bio-refinery hydrocracker

$$\text{EQ18.. } M_{\text{DS_FHCK}} - M_{\text{DS_FHCK1}} - M_{\text{DS_FHCK2}} = E = 0;$$

$$\text{EQ19.. } M_{\text{BHC_LTN}} - b1(\text{'HC_NAPH','HC'}) * (M_{\text{DS_FHCK1}}) = E = 0;$$

$$\text{EQ20.. } M_{\text{BHC_DIES}} - b1(\text{'HC_DIES','HC'}) * (M_{\text{DS_FHCK1}}) = E = 0;$$

$$\text{EQ21.. } M_{\text{BHC_LTN}} - (F_{\text{BHC_LTN}} * SG_{\text{GHC_LTN}} * WF) = E = 0;$$

$$\text{EQ22.. } M_{\text{BHC_DIES}} - (F_{\text{BHC_DIES}} * SG_{\text{GHC_DIES}} * WF) = E = 0;$$

* Bio-refinery catalytic reforming unit

$$\text{EQ23.. } M_{\text{NS_NAPH}} = E = M_{\text{NS_NAPH1}} + M_{\text{NS_NAPH2}};$$

$$\text{EQ24.. } M_{\text{REF_B}} - M_{\text{NS_NAPH1}} = E = 0;$$

$$\text{EQ25.. } H2_{\text{REF_WTB}} - M_{\text{REF_B}} * 0.0193 = E = 0;$$

EQ26.. M_REFORMATE_B - (0.88*M_REF_B) =E=0;
 EQ27.. M_REFORMATE_B - (F_REFORMATE_B*SG_REFORMATE*WF) =E=0;
 EQ28.. M_REF_B - (F_REF_B*SG_REF*WF) =E=0;
 EQ29.. M_NS_NAPH1 - (F_NS_NAPH1*SG_NS_NAPH*WF) =E=0;
 EQ30.. M_NS_NAPH2 - (F_NS_NAPH2*SG_NS_NAPH*WF) =E=0;
 EQ31.. M_DS_FHCK1 - (F_DS_FHCK1*SG_TPY1*WF) =E=0;
 EQ32.. M_DS_FHCK2 - (F_DS_FHCK2*SG_TPY1*WF) =E=0;
 EQ33.. M_TGO1 - M_TGO3 - M_TGO4 =E=0;
 EQ34.. M_TPY - 0.25*M_TGO4 =E=0;
 EQ35.. M_MIX - M_TPY - M_TGO4 =E=0;

* FCC yield for mix (MIX)

EQ36.. M_MIXFCC_NAPH - e1('MIX','gaso')*M_MIX =E=0;
 EQ37.. M_MIXFCC_LCO - e1('MIX','lco')*M_MIX =E=0;
 EQ38.. M_MIXFCC_HCO - e1('MIX','hco')*M_MIX =E=0;
 EQ39.. M_MIXFCC_COKE - e1('MIX','coke')*M_MIX =E=0;
 EQ40.. M_MIXFCC_NAPH - [F_MIXFCC_NAPH*SG_GFCC_NAPH*WF] =E=0;
 EQ41.. M_MIXFCC_LCO - [F_MIXFCC_LCO*SG_GFCC_LCO*WF] =E=0;
 EQ42.. M_MIXFCC_HCO - [F_MIXFCC_HCO*SG_GFCC_HCO*WF] =E=0;

* Bio-refinery hydrocracker

EQ43.. M_PHC_LTN - b1('HC_NAPH','HC')*(M_DS_FHCK2) =E=0;
 EQ44.. M_PHC_DIES - b1('HC_DIES','HC')*(M_DS_FHCK2) =E=0;
 EQ45.. M_PHC_LTN - (F_PHC_LTN*SG_GHC_LTN*WF) =E=0;
 EQ46.. M_PHC_DIES - (F_PHC_DIES*SG_GHC_DIES*WF) =E=0;

*BLENDING

EQN153.. VPG - F_SRLTN - F_REFORMATE - F_GFCC_NAPH - F_GHC_LTN
 - F_MIXFCC_NAPH - F_PHC_LTN - F_REFORMATE_B - F_BHC_LTN =E=0;
 EQN154.. RONI_SRLTN*F_SRLTN + RONI_REFORMATE*F_REFORMATE +
 RONI_GFCC_NAPH*F_GFCC_NAPH + RONI_GHC_LTN*F_GHC_LTN +

$$\begin{aligned} & \text{RONI_GFCC_NAPH*F_MIXFCC_NAPH} + \text{RONI_GHC_LTN*F_PHC_LTN} + \\ & \text{RONI_REFORMATE*F_REFORMATE_B} + \text{RONI_GHC_LTN*F_BHC_LTN} - \\ & \text{RONI_PG*VPG} =G=0; \end{aligned}$$

$$\begin{aligned} \text{EQN155..} & \text{RVPI_SRLTN*F_SRLTN} + \text{RVPI_REFORMATE*F_REFORMATE} + \\ & \text{RVPI_GFCC_NAPH*F_GFCC_NAPH} + \text{RVPI_GHC_LTN*F_GHC_LTN} + \\ & \text{RVPI_GFCC_NAPH*F_MIXFCC_NAPH} + \text{RVPI_GHC_LTN*F_PHC_LTN} + \\ & \text{RVPI_REFORMATE*F_REFORMATE_B} + \text{RVPI_GHC_LTN*F_BHC_LTN} - \\ & \text{RVPI_PG*VPG} =L=0; \end{aligned}$$

$$\begin{aligned} \text{EQN156..} & \text{A9} + \text{SG_REFORMATE*F_REFORMATE} + \\ & \text{SG_GFCC_NAPH*F_GFCC_NAPH} + \text{SG_GHC_LTN*F_GHC_LTN} + \\ & \text{SG_GFCC_NAPH*F_MIXFCC_NAPH} + \text{SG_GHC_LTN*F_PHC_LTN} + \\ & \text{SG_REFORMATE*F_REFORMATE_B} + \text{SG_GHC_LTN*F_BHC_LTN} - \\ & \text{SG_PG*VPG} =L=0; \end{aligned}$$

$$\begin{aligned} \text{EQN157..} & \text{A9} =G= \text{SG_SRLTN.LO*F_SRLTN} + \text{SG_SRLTN*F_SRLTN.LO} - \\ & \text{SG_SRLTN.LO*F_SRLTN.LO}; \end{aligned}$$

$$\begin{aligned} \text{EQN158..} & \text{A9} =G= \text{SG_SRLTN.UP*F_SRLTN} + \text{SG_SRLTN*F_SRLTN.UP} - \\ & \text{SG_SRLTN.UP*F_SRLTN.UP}; \end{aligned}$$

$$\begin{aligned} \text{EQN159..} & \text{A9} =L= \text{SG_SRLTN.LO*F_SRLTN} + \text{SG_SRLTN*F_SRLTN.UP} - \\ & \text{SG_SRLTN.LO*F_SRLTN.UP}; \end{aligned}$$

$$\begin{aligned} \text{EQN160..} & \text{A9} =L= \text{SG_SRLTN.UP*F_SRLTN} + \text{SG_SRLTN*F_SRLTN.LO} - \\ & \text{SG_SRLTN.UP*F_SRLTN.LO}; \end{aligned}$$

$$\begin{aligned} \text{EQN161..} & \text{M_SRLTN/WF} =G= \text{SG_SRLTN.LO*F_SRLTN} + \\ & \text{SG_SRLTN*F_SRLTN.LO} - \text{SG_SRLTN.LO*F_SRLTN.LO}; \end{aligned}$$

$$\begin{aligned} \text{EQN162..} & \text{M_SRLTN/WF} =G= \text{SG_SRLTN.UP*F_SRLTN} + \\ & \text{SG_SRLTN*F_SRLTN.UP} - \text{SG_SRLTN.UP*F_SRLTN.UP}; \end{aligned}$$

$$\begin{aligned} \text{EQN163..} & \text{M_SRLTN/WF} =L= \text{SG_SRLTN.LO*F_SRLTN} + \\ & \text{SG_SRLTN*F_SRLTN.UP} - \text{SG_SRLTN.LO*F_SRLTN.UP}; \end{aligned}$$

$$\begin{aligned} \text{EQN164..} & \text{M_SRLTN/WF} =L= \text{SG_SRLTN.UP*F_SRLTN} + \\ & \text{SG_SRLTN*F_SRLTN.LO} - \text{SG_SRLTN.UP*F_SRLTN.LO}; \end{aligned}$$

$$\begin{aligned} \text{EQN165..} & \text{MPG} - \text{M_SRLTN} - \text{M_REFORMATE} - \text{M_GFCC_NAPH} - \\ & \text{M_GHC_LTN} - \text{M_MIXFCC_NAPH} - \text{M_PHC_LTN} - \text{M_REFORMATE_B} - \\ & \text{M_BHC_LTN} =E=0; \end{aligned}$$

$$\begin{aligned} \text{EQN166.. } & \text{SUL_SRLTN1*M_SRLTN} + \text{SUL_REFORMATE*M_REFORMATE} + \\ & \text{SUL_GFCC_NAPH*M_GFCC_NAPH} + \text{SUL_GHC_LTN*M_GHC_LTN} + \\ & \text{SUL_GFCC_NAPH*M_MIXFCC_NAPH} + \text{SUL_GHC_LTN*M_PHC_LTN} + \\ & \text{SUL_REFORMATE*M_REFORMATE_B} + \text{SUL_GHC_LTN*M_BHC_LTN} - \\ & \text{SUL_PG*MPG} =L=0; \end{aligned}$$

$$\text{EQN167.. } \text{F_VGOHDT_DIS} - \text{FDC_VGOHDT_DIS} - \text{FFO_VGOHDT_DIS} =E=0;$$

$$\text{EQN168.. } \text{F_RSDHDT_DIS} - \text{FDC_RSDHDT_DIS} - \text{FFO_RSDHDT_DIS} =E=0;$$

$$\begin{aligned} \text{EQN169.. } & \text{MDC_VGOHDT_DIS} - \\ & (\text{FDC_VGOHDT_DIS*SG_VGOHDT_DIS1*WF}) =E=0; \end{aligned}$$

$$\begin{aligned} \text{EQN170.. } & \text{MFO_VGOHDT_DIS} - (\text{FFO_VGOHDT_DIS*SG_VGOHDT_DIS1*WF}) \\ & =E=0; \end{aligned}$$

$$\begin{aligned} \text{EQN171.. } & \text{MDC_RSDHDT_DIS} - (\text{FDC_RSDHDT_DIS*SG_RSDHDT_DIS*WF}) \\ & =E=0; \end{aligned}$$

$$\begin{aligned} \text{EQN172.. } & \text{MFO_RSDHDT_DIS} - (\text{FFO_RSDHDT_DIS*SG_RSDHDT_DIS*WF}) \\ & =E=0; \end{aligned}$$

$$\text{EQN173.. } \text{F_DHDT_KERO} - \text{F_DHDT_KERO_D} - \text{F_DHDT_KERO_K} =E=0;$$

$$\begin{aligned} \text{EQN174.. } & \text{VDSP} - \text{F_DHDT_DIS} - \text{F_DHDT_KERO_D} - \text{F_GHC_DIES} - \\ & \text{F_GFCC_LCO} - \text{FDC_VGOHDT_DIS} - \text{FDC_RSDHDT_DIS} - \text{F_MIXFCC_LCO} - \\ & \text{F_PHC_DIES} - \text{F_BHC_DIES} - \text{F_DS_DIES} =E=0; \end{aligned}$$

$$\begin{aligned} \text{EQN175.. } & \text{CET_DHDT_DIS1*F_DHDT_DIS} + \\ & \text{CET_DHDT_KERO*F_DHDT_KERO_D} + \text{CI_GHC_DIES*F_GHC_DIES} + \\ & \text{CI_GFCC_LCO*F_GFCC_LCO} + \text{CI_VGOHDT_DIS*FDC_VGOHDT_DIS} + \\ & \text{CI_RSDHDT_DIS*FDC_RSDHDT_DIS} + \text{CI_GFCC_LCO*F_MIXFCC_LCO} + \\ & \text{CI_GHC_DIES*F_PHC_DIES} + \text{CI_GHC_DIES*F_BHC_DIES} + \\ & \text{CI_DS_DIES*F_DS_DIES} - \text{CN_DSP*VDSP} =G=0; \end{aligned}$$

$$\begin{aligned} \text{EQN176.. } & \text{SG_DHDT_DIS1*F_DHDT_DIS} + \\ & \text{SG_DHDT_KERO1*F_DHDT_KERO_D} + \text{SG_GHC_DIES*F_GHC_DIES} + \\ & \text{SG_GFCC_LCO*F_GFCC_LCO} + \text{SG_VGOHDT_DIS1*FDC_VGOHDT_DIS} + \\ & \text{SG_RSDHDT_DIS*FDC_RSDHDT_DIS} + \text{SG_GFCC_LCO*F_MIXFCC_LCO} + \\ & \text{SG_GHC_DIES*F_PHC_DIES} + \text{SG_GHC_DIES*F_BHC_DIES} + \\ & \text{SG_DS_DIES*F_DS_DIES} - \text{SG_DSP*VDSP} =L=0; \end{aligned}$$

EQN177.. $M_DHDT_KERO_D - (F_DHDT_KERO_D * SG_DHDT_KERO1 * WF) = E = 0;$
 EQN178.. $MDSP - M_DHDT_DIS - M_DHDT_KERO_D - M_GHC_DIES - M_GFCC_LCO - MDC_VGOHDT_DIS - MDC_RSDHDT_DIS - M_MIXFCC_LCO - M_PHC_DIES - M_BHC_DIES - M_DS_DIES = E = 0;$
 EQN179.. $SUL_DHDT_DIS1 * M_DHDT_DIS + SUL_DHDT_KERO1 * M_DHDT_KERO_D + SUL_GHC_DIES * M_GHC_DIES + SUL_GFCC_LCO * M_GFCC_LCO + SUL_VGOHDT_DIS1 * MDC_VGOHDT_DIS + SUL_RSDHDT_DIS * MDC_RSDHDT_DIS + SUL_GFCC_LCO * M_MIXFCC_LCO + SUL_GHC_DIES * M_PHC_DIES + SUL_GHC_DIES * M_BHC_DIES + SUL_DS_DIES * M_DS_DIES - SUL_DSP * MDSP = L = 0;$
 EQN180.. $VP_KERO - F_KERO - F_DHDT_KERO_K - F_GHC_KERO = E = 0;$
 EQN181.. $SPI_KERO * F_KERO + SPI_DHDT_KERO * F_DHDT_KERO_K + SPI_GHC_KERO * F_GHC_KERO - SPI_VP_KERO * VP_KERO = G = 0;$
 EQN182.. $A6 + SG_DHDT_KERO1 * F_DHDT_KERO_K + SG_GHC_KERO * F_GHC_KERO - SG_VP_KERO * VP_KERO = L = 0;$
 EQN183.. $A6 = G = SG_KERO.LO * F_KERO + SG_KERO * F_KERO.LO - SG_KERO.LO * F_KERO.LO;$
 EQN184.. $A6 = G = SG_KERO.UP * F_KERO + SG_KERO * F_KERO.UP - SG_KERO.UP * F_KERO.UP;$
 EQN185.. $A6 = G = SG_KERO.LO * F_KERO + SG_KERO * F_KERO.UP - SG_KERO.LO * F_KERO.UP;$
 EQN186.. $A6 = G = SG_KERO.UP * F_KERO + SG_KERO * F_KERO.LO - SG_KERO.UP * F_KERO.LO;$
 EQN187.. $M_KERO - (F_KERO * SG_KERO1 * WF) = E = 0;$
 EQN188.. $M_DHDT_KERO_K - (F_DHDT_KERO_K * SG_DHDT_KERO1 * WF) = E = 0;$
 EQN189.. $MP_KERO - M_KERO - M_DHDT_KERO_K - M_GHC_KERO = E = 0;$
 EQN190.. $SUL_KERO1 * M_KERO + SUL_DHDT_KERO1 * M_DHDT_KERO_K + SUL_GHC_KERO * M_GHC_KERO - SUL_VP_KERO * MP_KERO = L = 0;$

EQN191.. VFOP - F_RSDHDT_FO - FFO_RSDHDT_DIS - FFO_VGOHDT_DIS - F_GFCC_HCO - F_MIXFCC_HCO =E=0;

EQN192.. MFOP - M_RSDHDT_FO - MFO_RSDHDT_DIS - MFO_VGOHDT_DIS - M_GFCC_HCO - M_MIXFCC_HCO =E=0;

EQN193.. SG_RSDHDT_FO*F_RSDHDT_FO + SG_RSDHDT_DIS*FFO_RSDHDT_DIS + SG_VGOHDT_DIS1*FFO_VGOHDT_DIS + SG_GFCC_HCO*F_GFCC_HCO + SG_GFCC_HCO*F_MIXFCC_HCO - SG_FOP*VFOP =L=0;

EQN194.. SUL_RSDHDT_FO*M_RSDHDT_FO + SUL_RSDHDT_DIS*MFO_RSDHDT_DIS + SUL_VGOHDT_DIS1*MFO_VGOHDT_DIS + SUL_GFCC_HCO*M_GFCC_HCO + SUL_GFCC_HCO*M_MIXFCC_HCO - SUL_FOP*MFOP =I=0;

EQN195.. F_TGO3 - [M_TGO3*(VF/SG_TGO1)] =E=0;

EQN196.. F_TGO2 - [M_TGO2*(VF/SG_TGO1)] =E=0;

EQN197.. F_MIX - [M_MIX*(VF/SG_MIX)] =E=0;

EQN198.. H2_CONSP =E= [(F_SRHN*H0_HN1)/1000000] + [(F_DIES*H0_DIES1)/1000000] + [(F_RSD*H0_RSD)/1000000] + [(F_VGO*439)/1000000] + 0.012241*M_TGO2 + 0.0522*M_DS_FHCK1 + 0.0179*M_PY_OIL + 0.0522*M_DS_FHCK2 - 0.417776*H2_REF_WT;

*Operating cost

EQN199.. OC - (0.009*F_CRUDE + F_SRLTN + F_SRHN + F_KERO + F_DIES)*K1('CDU1', 'S')*K1('PRICE1','S') - (0.009*F_CRUDE + F_SRLTN + F_SRHN + F_KERO + F_DIES)*K1('CDU1', 'W')*K1('PRICE1','W') - (0.009*F_CRUDE + F_SRLTN + F_SRHN + F_KERO + F_DIES)*K1('CDU1', 'P')*K1('PRICE1','P') - (0.009*F_CRUDE + F_SRLTN + F_SRHN + F_KERO + F_DIES)*K1('CDU1', 'F')*K1('PRICE1','F') - (F_VGO + F_RSD)*K1('VDU1', 'S')*K1('PRICE1','S') - (F_VGO + F_RSD)*K1('VDU1', 'W')*K1('PRICE1','W') - (F_VGO + F_RSD)*K1('VDU1', 'P')*K1('PRICE1','P') - (F_VGO + F_RSD)*K1('VDU1', 'F')*K1('PRICE1','F') - (F_SRHN)*K1('NHDT1', 'S')*K1('PRICE1','S') - (F_SRHN)*K1('NHDT1', 'W')*K1('PRICE1','W') -

(F_SRHN)*K1('NHDT1', 'P')*K1('PRICE1','P') - (F_SRHN)*K1('NHDT1',
'F')*K1('PRICE1','F') - (F_DIES)*K1('DHDT1', 'S')*K1('PRICE1','S') -
(F_DIES)*K1('DHDT1', 'W')*K1('PRICE1','W') - (F_DIES)*K1('DHDT1',
'P')*K1('PRICE1','P') - (F_DIES)*K1('DHDT1', 'F')*K1('PRICE1','F') -
(F_VGO)*K1('VHDT1', 'S')*K1('PRICE1','S') - (F_VGO)*K1('VHDT1',
'W')*K1('PRICE1','W') - (F_VGO)*K1('VHDT1', 'P')*K1('PRICE1','P') -
(F_VGO)*K1('VHDT1', 'F')*K1('PRICE1','F') - (F_RSD)*K1('RHDT1',
'S')*K1('PRICE1','S') - (F_RSD)*K1('RHDT1', 'W')*K1('PRICE1','W') -
(F_RSD)*K1('RHDT1', 'P')*K1('PRICE1','P') - (F_RSD)*K1('RHDT1',
'F')*K1('PRICE1','F') - (F_REF)*K1('CRU1', 'S')*K1('PRICE1','S') -
(F_REF)*K1('CRU1', 'W')*K1('PRICE1','W') - (F_REF)*K1('CRU1',
'P')*K1('PRICE1','P') - (F_REF)*K1('CRU1', 'F')*K1('PRICE1','F') -
(F_REF_B)*K1('CRU1', 'S')*K1('PRICE1','S') - (F_REF_B)*K1('CRU1',
'W')*K1('PRICE1','W') - (F_REF_B)*K1('CRU1', 'P')*K1('PRICE1','P') -
(F_REF_B)*K1('CRU1', 'F')*K1('PRICE1','F') - (F_TGO3)*K1('FCC1',
'S')*K1('PRICE1','S') - (F_TGO3)*K1('FCC1', 'W')*K1('PRICE1','W') -
(F_TGO3)*K1('FCC1', 'P')*K1('PRICE1','P') - (F_TGO3)*K1('FCC1',
'F')*K1('PRICE1','F') - (F_MIX)*K1('FCC1', 'S')*K1('PRICE1','S') -
(F_MIX)*K1('FCC1', 'W')*K1('PRICE1','W') - (F_MIX)*K1('FCC1',
'P')*K1('PRICE1','P') - (F_MIX)*K1('FCC1', 'F')*K1('PRICE1','F') -
(F_TGO2)*K1('HCK1', 'S')*K1('PRICE1','S') - (F_TGO2)*K1('HCK1',
'P')*K1('PRICE1','P') - (F_TGO2)*K1('HCK1', 'W')*K1('PRICE1','W') -
(F_TGO2)*K1('HCK1', 'F')*K1('PRICE1','F') - (F_DS_FHCK1)*K1('BHCK1',
'S')*K1('PRICE1','S') - (F_DS_FHCK1)*K1('BHCK1', 'W')*K1('PRICE1','W') -
(F_DS_FHCK1)*K1('BHCK1', 'P')*K1('PRICE1','P') -
(F_DS_FHCK1)*K1('BHCK1', 'F')*K1('PRICE1','F') -
(F_DS_FHCK2)*K1('BHCK1', 'S')*K1('PRICE1','S') -
(F_DS_FHCK2)*K1('BHCK1', 'W')*K1('PRICE1','W') -
(F_DS_FHCK2)*K1('BHCK1', 'P')*K1('PRICE1','P') -
(F_DS_FHCK2)*K1('BHCK1', 'F')*K1('PRICE1','F') - (M_BIOMASS)*K1('PYR1',
'P')*K1('PRICE1','P') - (M_BIOMASS)*K1('PYR1', 'W')*K1('PRICE1','W') -
(M_PY_OIL)*K1('HDT1', 'S')*K1('PRICE1','S') - (M_PY_OIL)*K1('HDT1',

'W')*K1('PRICE1','W') - (M_PY_OIL)*K1('HDT1', 'P')*K1('PRICE1','P') -
(M_PY_OIL)*K1('HDT1', 'F')*K1('PRICE1','F') - (M_HDT_PY)*K1('DE-C41',
'S')*K1('PRICE1','S') - (M_HDT_PY)*K1('DE-C41', 'P')*K1('PRICE1','P') -
(M_TPYB)*K1('NS1', 'S')*K1('PRICE1','S') - (M_TPYB)*K1('NS1',
'P')*K1('PRICE1','P') - (M_NS_FDIES)*K1('DS1', 'S')*K1('PRICE1','S') -
(M_NS_FDIES)*K1('DS1', 'P')*K1('PRICE1','P') - 92.02*F_CRUDE -
83*M_BIOMASS =E=0;

*integration logic constraints

EQ200.. Y1 + Y2 =E= 1;
EQ201.. M_TPY - Y1*M_TPY.UP =L=0;
EQ202.. M_TPYB - Y2*M_TPYB.UP =L=0;
EQ203.. Y3 + Y4 =E=1;
EQ204.. M_DS_FHCK2 - y3*M_DS_FHCK2.UP =L=0;
EQ205.. M_TGO2 - Y4*M_TGO2.UP =L=0;
EQ206.. Y5 + Y6 =L=1;
EQ207.. M_NS_NAPH1 - y5*M_NS_NAPH1.UP =L=0;
EQ208.. M_NS_NAPH2 - y6*M_NS_NAPH2.UP =L=0;
EQ209.. Y1 + Y7 =E= 1;
EQ210.. M_TPY - Y1*M_TPY.UP =L=0;
EQ211.. M_TGO3 - Y7*M_TGO3.UP =L=0;

*capital costs

EQ212.. H2_TON - [(0.0429*M_PY_OIL) + (0.1249*M_DS_FHCK1) +
(0.1249*M_DS_FHCK2)] =E= 0;
EQ213.. H2_SCF - 0.417776*H2_TON =E= 0;
EQ214.. RATIO =E= (H2_SCF/24.5);
EQ215.. RATIO =E= Z11 + Z12 + Z13;
EQ216.. RATIO1 - RATIO1.UP*(1-Y11) =L= Z11;
EQ217.. Z11=L= RATIO1.UP*Y11;
EQ218.. Z11 =L= RATIO1;
EQ219.. RATIO2 - RATIO2.UP*(1-Y12)=L= Z12;

EQ220.. $Z12=L= \text{RATIO2.UP} * Y12;$
 EQ221.. $Z12 =L= \text{RATIO2};$
 EQ222.. $\text{RATIO3} - \text{RATIO3.UP} * (1-Y13)=L= Z13;$
 EQ223.. $Z13=L= \text{RATIO3.UP} * Y13;$
 EQ224.. $Z13 =L= \text{RATIO3};$
 EQ225.. $Y11 + Y12 + Y13 =L= 1;$
 EQ226.. $\text{INDEX1} =E= 1.088 * Z11 + 0.123 * Y11;$
 EQ227.. $\text{INDEX2} =E= 0.729 * Z12 + 0.273 * Y12;$
 EQ228.. $\text{INDEX3} =E= 0.476 * Z13 + 0.595 * Y13;$
 EQ229.. $\text{INDEX} =E= \text{INDEX1} + \text{INDEX2} + \text{INDEX3};$
 EQ230.. $\text{H2_COST} =E= 79406 * \text{INDEX};$
 EQ231.. $\text{RATIO_NS} =E= \text{M_TPYB} / 718.77;$
 EQ232.. $\text{RATIO_NS} =E= Z21 + Z22 + Z23;$
 EQ233.. $\text{RATIO21} - \text{RATIO21.UP} * (1-Y21) =L= Z21;$
 EQ234.. $Z21=L= \text{RATIO21.UP} * Y21;$
 EQ235.. $Z21 =L= \text{RATIO21};$
 EQ236.. $\text{RATIO22} - \text{RATIO22.UP} * (1-Y22) =L= Z22;$
 EQ237.. $Z22=L= \text{RATIO22.UP} * Y22;$
 EQ238.. $Z22 =L= \text{RATIO22};$
 EQ239.. $\text{RATIO23} - \text{RATIO23.UP} * (1-Y23) =L= Z23;$
 EQ240.. $Z23=L= \text{RATIO23.UP} * Y23;$
 EQ241.. $Z23 =L= \text{RATIO23};$
 EQ242.. $Y21 + Y22 + Y23 =L= 1;$
 EQ243.. $\text{INDEX21} =E= 1.088 * Z21 + 0.123 * Y21;$
 EQ244.. $\text{INDEX22} =E= 0.729 * Z22 + 0.273 * Y22;$
 EQ245.. $\text{INDEX23} =E= 0.476 * Z23 + 0.595 * Y23;$
 EQ246.. $\text{INDEX_NS} =E= \text{INDEX21} + \text{INDEX22} + \text{INDEX23};$
 EQ247.. $\text{COST_NS} =E= 1404 * \text{INDEX_NS};$
 EQ248.. $\text{RATIO_DS} =E= \text{M_NS_FDIES} / 508.027;$
 EQ249.. $\text{RATIO_DS} =E= Z31 + Z32 + Z33;$
 EQ250.. $\text{RATIO31} - \text{RATIO31.UP} * (1-Y31) =L= Z31;$
 EQ251.. $Z31 =L= \text{RATIO31.UP} * Y31;$

EQ252.. $Z31 = L = \text{RATIO31}$;
 EQ253.. $\text{RATIO32} - \text{RATIO32} \cdot \text{UP} \cdot (1 - Y32) = L = Z32$;
 EQ254.. $Z32 = L = \text{RATIO32} \cdot \text{UP} \cdot Y32$;
 EQ255.. $Z32 = L = \text{RATIO32}$;
 EQ256.. $\text{RATIO33} - \text{RATIO33} \cdot \text{UP} \cdot (1 - Y33) = L = Z33$;
 EQ257.. $Z33 = L = \text{RATIO33} \cdot \text{UP} \cdot Y33$;
 EQ258.. $Z33 = L = \text{RATIO33}$;
 EQ259.. $Y31 + Y32 + Y33 = L = 1$;
 EQ260.. $\text{INDEX31} = E = 1.088 \cdot Z31 + 0.123 \cdot Y31$;
 EQ261.. $\text{INDEX32} = E = 0.729 \cdot Z32 + 0.273 \cdot Y32$;
 EQ262.. $\text{INDEX33} = E = 0.476 \cdot Z33 + 0.595 \cdot Y33$;
 EQ263.. $\text{INDEX_DS} = E = \text{INDEX31} + \text{INDEX32} + \text{INDEX33}$;
 EQ264.. $\text{COST_DS} = E = 1080 \cdot \text{INDEX_DS}$;
 EQ265.. $\text{RATIO_BHC} = E = \text{M_DS_FHCK1} / 95.814$;
 EQ266.. $\text{RATIO_BHC} = E = Z41 + Z42 + Z43$;
 EQ267.. $\text{RATIO41} - \text{RATIO41} \cdot \text{UP} \cdot (1 - Y41) = L = Z41$;
 EQ268.. $Z41 = L = \text{RATIO41} \cdot \text{UP} \cdot Y41$;
 EQ269.. $Z41 = L = \text{RATIO41}$;
 EQ270.. $\text{RATIO42} - \text{RATIO42} \cdot \text{UP} \cdot (1 - Y42) = L = Z42$;
 EQ271.. $Z42 = L = \text{RATIO42} \cdot \text{UP} \cdot Y42$;
 EQ272.. $Z42 = L = \text{RATIO42}$;
 EQ273.. $\text{RATIO43} - \text{RATIO43} \cdot \text{UP} \cdot (1 - Y43) = L = Z43$;
 EQ274.. $Z43 = L = \text{RATIO43} \cdot \text{UP} \cdot Y43$;
 EQ275.. $Z43 = L = \text{RATIO43}$;
 EQ276.. $Y41 + Y42 + Y43 = L = 1$;
 EQ277.. $\text{INDEX41} = E = 1.088 \cdot Z41 + 0.123 \cdot Y41$;
 EQ278.. $\text{INDEX42} = E = 0.729 \cdot Z42 + 0.273 \cdot Y42$;
 EQ279.. $\text{INDEX43} = E = 0.476 \cdot Z43 + 0.595 \cdot Y43$;
 EQ280.. $\text{INDEX_BHC} = E = \text{INDEX41} + \text{INDEX42} + \text{INDEX43}$;
 EQ281.. $\text{COST_BHC} = E = 29476 \cdot \text{INDEX_BHC}$;
 EQ282.. $\text{RATIO_RUB} = E = \text{M_NS_NAPH1} / 210.743$;
 EQ283.. $\text{RATIO_RUB} = E = Z51 + Z52 + Z53$;

EQ284.. $\text{RATIO51} - \text{RATIO51}.\text{UP}*(1-\text{Y51}) = \text{L} = \text{Z51}$;
 EQ285.. $\text{Z51} = \text{L} = \text{RATIO51}.\text{UP}*\text{Y51}$;
 EQ286.. $\text{Z51} = \text{L} = \text{RATIO51}$;
 EQ287.. $\text{RATIO52} - \text{RATIO52}.\text{UP}*(1-\text{Y52}) = \text{L} = \text{Z52}$;
 EQ288.. $\text{Z52} = \text{L} = \text{RATIO52}.\text{UP}*\text{Y52}$;
 EQ289.. $\text{Z52} = \text{L} = \text{RATIO52}$;
 EQ290.. $\text{RATIO53} - \text{RATIO53}.\text{UP}*(1-\text{Y53}) = \text{L} = \text{Z53}$;
 EQ291.. $\text{Z53} = \text{L} = \text{RATIO53}.\text{UP}*\text{Y53}$;
 EQ292.. $\text{Z53} = \text{L} = \text{RATIO53}$;
 EQ293.. $\text{Y51} + \text{Y52} + \text{Y53} = \text{L} = 1$;
 EQ294.. $\text{INDEX51} = \text{E} = 1.088*\text{Z51} + 0.123*\text{Y51}$;
 EQ295.. $\text{INDEX52} = \text{E} = 0.729*\text{Z52} + 0.273*\text{Y52}$;
 EQ296.. $\text{INDEX53} = \text{E} = 0.476*\text{Z53} + 0.595*\text{Y53}$;
 EQ297.. $\text{INDEX_RUB} = \text{E} = \text{INDEX51} + \text{INDEX52} + \text{INDEX53}$;
 EQ298.. $\text{COST_RUB} = \text{E} = 18896*\text{INDEX_RUB}$;
 EQ299.. $\text{RATIO_FCC} = \text{E} = \text{M_TPY}/718.77$;
 EQ300.. $\text{RATIO_FCC} = \text{E} = \text{Z61} + \text{Z62} + \text{Z63}$;
 EQ301.. $\text{RATIO61} - \text{RATIO61}.\text{UP}*(1-\text{Y61}) = \text{L} = \text{Z61}$;
 EQ302.. $\text{Z61} = \text{L} = \text{RATIO61}.\text{UP}*\text{Y61}$;
 EQ303.. $\text{Z61} = \text{L} = \text{RATIO61}$;
 EQ304.. $\text{RATIO62} - \text{RATIO62}.\text{UP}*(1-\text{Y62}) = \text{L} = \text{Z62}$;
 EQ305.. $\text{Z62} = \text{L} = \text{RATIO62}.\text{UP}*\text{Y62}$;
 EQ306.. $\text{Z62} = \text{L} = \text{RATIO62}$;
 EQ307.. $\text{RATIO63} - \text{RATIO63}.\text{UP}*(1-\text{Y63}) = \text{L} = \text{Z63}$;
 EQ308.. $\text{Z63} = \text{L} = \text{RATIO63}.\text{UP}*\text{Y63}$;
 EQ309.. $\text{Z63} = \text{L} = \text{RATIO63}$;
 EQ310.. $\text{Y61} + \text{Y62} + \text{Y63} = \text{L} = 1$;
 EQ311.. $\text{INDEX61} = \text{E} = 1.088*\text{Z61} + 0.123*\text{Y61}$;
 EQ312.. $\text{INDEX62} = \text{E} = 0.729*\text{Z62} + 0.273*\text{Y62}$;
 EQ313.. $\text{INDEX63} = \text{E} = 0.476*\text{Z63} + 0.595*\text{Y63}$;
 EQ314.. $\text{INDEX_FCC} = \text{E} = \text{INDEX61} + \text{INDEX62} + \text{INDEX63}$;
 EQ315.. $\text{COST_FCC} = \text{E} = 86869*\text{INDEX_FCC}$;

EQ316.. $RATIO_PHC = E = M_DS_FHCK2/95.814;$
 EQ317.. $RATIO_PHC = E = Z71 + Z72 + Z73;$
 EQ318.. $RATIO71 - RATIO71.UP*(1-Y71) = L = Z71;$
 EQ319.. $Z71 = L = RATIO71.UP*Y71;$
 EQ320.. $Z71 = L = RATIO71;$
 EQ321.. $RATIO72 - RATIO72.UP*(1-Y72) = L = Z72;$
 EQ322.. $Z72 = L = RATIO72.UP*Y72;$
 EQ323.. $Z72 = L = RATIO72;$
 EQ324.. $RATIO73 - RATIO73.UP*(1-Y73) = L = Z73;$
 EQ325.. $Z73 = L = RATIO73.UP*Y73;$
 EQ326.. $Z73 = L = RATIO73;$
 EQ327.. $Y71 + Y72 + Y73 = L = 1;$
 EQ328.. $INDEX71 = E = 1.088*Z71 + 0.123*Y71;$
 EQ329.. $INDEX72 = E = 0.729*Z72 + 0.273*Y72;$
 EQ330.. $INDEX73 = E = 0.476*Z73 + 0.595*Y73;$
 EQ331.. $INDEX_PHC = E = INDEX71 + INDEX72 + INDEX73;$
 EQ332.. $COST_PHC = E = 29476*INDEX_PHC;$
 EQ333.. $RATIO_RUR = E = M_NS_NAPH2/210.743;$
 EQ334.. $RATIO_RUR = E = Z81 + Z82 + Z83;$
 EQ335.. $RATIO81 - RATIO81.UP*(1-Y81) = L = Z81;$
 EQ336.. $Z81 = L = RATIO81.UP*Y81;$
 EQ337.. $Z81 = L = RATIO81;$
 EQ338.. $RATIO82 - RATIO82.UP*(1-Y82) = L = Z82;$
 EQ339.. $Z82 = L = RATIO82.UP*Y82;$
 EQ340.. $Z82 = L = RATIO82;$
 EQ341.. $RATIO83 - RATIO83.UP*(1-Y83) = L = Z83;$
 EQ342.. $Z83 = L = RATIO83.UP*Y83;$
 EQ343.. $Z83 = L = RATIO83;$
 EQ344.. $Y81 + Y82 + Y83 = L = 1;$
 EQ345.. $INDEX81 = E = 1.088*Z81 + 0.123*Y81;$
 EQ346.. $INDEX82 = E = 0.729*Z82 + 0.273*Y82;$
 EQ347.. $INDEX83 = E = 0.476*Z83 + 0.595*Y83;$

EQ348.. INDEX_RUR =E= INDEX81 + INDEX82 + INDEX83;
 EQ349.. COST_RUR =E= 18896*INDEX_RUR;
 EQ350.. TOTAL_COST_REF =E= 0.11746*[COST_FCC*y1 + COST_PHC*y2 +
 COST_RUR*y2];
 EQ351.. TOTAL_COST_BIO =E= 0.11746*[H2_COST + COST_NS + COST_DS +
 COST_BHC + COST_RUB + FX_COST];
 EH1(u).. cons('NHT') =E= [(F_SRHN*H0_HN1)/1000000];
 EH2(u).. cons('DHT') =E= [(F_DIES*H0_DIES1)/1000000];
 EH3(u).. cons('RHT') =E= [(F_RSD*H0_RSD)/1000000];
 EH4(u).. cons('GOHT') =E= [(F_VGO*439)/1000000];
 EH5(U).. Cons('HC1') =E= 0.012241*M_TGO2;
 EH6(U).. Cons('HC2') =E= 0.04267*M_DS_FHCK1;
 EH7(U).. Cons('BHDT') =E= 0.016056812*M_PY_OIL;
 EH8(U).. Cons('HC3') =E= 0.04267*M_DS_FHCK2;

*hydrogen network balance

EH9(i).. FI(i) =E= sum(u, FIU(i, u)*c(i, u)) + sum(k, FIK(i, k)*h(i, k)) + sum(n,
 FIN(i, n)*h1(i, N)) + sum(j, FIJ(i, j)*l(i, j));
 EH10(n, u).. UP*(YNU(n, u) - 1) =l= (PNO(n) - PH2U(u));
 EH11(n, u).. YNU(n, u)*UP - b =g= (PNO(n) - PH2U(u));
 EH12(n, u).. FNU(n, u) - YNU(n, u)*UF =l= 0;
 EH13(n, k).. UP*(YNK(n, k) - 1) =l= (PNO(n) - PKI(k));
 EH14(n, k).. YNK(n, k)*UP - b =g= (PNO(n) - PKI(k));
 EH15(n, k).. FNK(n, k) - YNK(n, k)*UF =l= 0;
 EH16(V).. FH2V(v) =E= R(v) + sum(u, FVU(v, u)*d(v, u)) + sum(k, FVK(v, k)*e(v,
 k)) + sum(n, FVN(v, n)*e2(v, n)) + sum(m, FVM(v, m)*r5(v, m)) + sum(j, FVJ(v,
 j)*q(v, j));
 EH17(U).. FH2U(u) =E= cons(u)/CON_FAC(U) ;
 EH18(u).. FH2V(u)*YH2V(u) =E= FH2U(u)*YH2U(u) - cons(u);
 EH19(u).. FH2U(u) =E= R(u) + sum(i, FIU(i, u)*c(i, u)) + sum(v, FVU(v, u)*d(v, u))
 + sum(k, Fku(k, u)*f(k, u)) + sum(n, FNU(n, u));

EH20(u).. $FH2U(u)*YH2U(u) =E= R(u)*YR(u) + \text{sum}(i, FIU(i, u)*c(i, u)*YHP(i)) + \text{sum}(v, FVU(v, u)*d(v, u)*YH2V(v)) + \text{SUM}(K, a5(u)*f(k, u)) + a7(u);$

EH21(U).. $\text{SUM}(K, a5(u)*f(k, u)) =G= \text{sum}(K, FKU.LO(K, U)*f(k, u)*YK(k)) + \text{sum}(k, FKU(k, u)*f(k, u)*YK.lo(k)) - \text{sum}(k, FKU.LO(K, U)*f(k, u)*yk.lo(k));$

EH22(U).. $\text{SUM}(K, a5(u)*f(k, u)) =G= \text{sum}(K, FKU.UP(K, U)*f(k, u)*YK(k)) + \text{sum}(k, FKU(k, u)*f(k, u)*YK.UP(k)) - \text{sum}(k, FKU.UP(K, U)*f(k, u)*yk.UP(k));$

EH23(U).. $\text{SUM}(K, a5(u)*f(k, u)) =L= \text{sum}(K, FKU.LO(K, U)*f(k, u)*YK(k)) + \text{sum}(k, FKU(k, u)*f(k, u)*YK.UP(k)) - \text{sum}(k, FKU.LO(K, U)*f(k, u)*yk.UP(k));$

EH24(U).. $\text{SUM}(K, a5(u)*f(k, u)) =L= \text{sum}(K, FKU.UP(K, U)*f(k, u)*YK(k)) + \text{sum}(k, FKU(k, u)*f(k, u)*YK.LO(k)) - \text{sum}(k, FKU.UP(K, U)*f(k, u)*yk.LO(k));$

EH25(U).. $a7(u) =G= \text{sum}(N, FNU.LO(N, U)*YN(N)) + \text{sum}(N, FNU(N, u)*YN.lo(N)) - \text{sum}(N, FNU.LO(N, U)*yN.lo(N));$

EH26(U).. $a7(u) =G= \text{sum}(N, FNU.UP(N, U)*YN(N)) + \text{sum}(N, FNU(N, u)*YN.UP(N)) - \text{sum}(N, FNU.UP(N, U)*yN.UP(N));$

EH27(U).. $a7(u) =L= \text{sum}(N, FNU.LO(N, U)*YN(N)) + \text{sum}(N, FNU(N, u)*YN.UP(N)) - \text{sum}(N, FNU.LO(N, U)*yN.UP(N));$

EH28(U).. $a7(u) =L= \text{sum}(N, FNU.UP(N, U)*YN(N)) + \text{sum}(N, FNU(N, u)*YN.LO(N)) - \text{sum}(N, FNU.UP(N, U)*yN.LO(N));$

EH29(k).. $FKin(k) =E= \text{sum}(i, FIK(i, k)*h(i, k)) + \text{sum}(v, FVK(v, k)*e(v, k)) + \text{sum}(n, FNK(n, k)) + \text{sum}(m, FMK(m, k)*f3(m, k));$

EH30(k).. $FKout(k) =E= \text{sum}(u, FKU(k, u)*f(k, u));$

EH31(k).. $FKin(k) =E= FKout(k);$

EH32(k).. $B5(k) =E= \text{sum}(i, FIK(i, k)*h(i, k)*YHP(i)) + \text{sum}(v, FVK(v, k)*e(v, k)*YH2V(v)) + B15(k) + \text{sum}(m, FMK(m, k)*YPR(m)*f3(m, k));$

EH33(k).. $B5(k) =G= FKin.LO(k)*YK(k) + FKin(k)*yk.lo(k) - FKin.LO(k)*yk.lo(k);$

EH34(k).. $B5(k) =G= FKin.UP(k)*YK(k) + FKin(k)*yk.UP(k) - FKin.UP(k)*yk.UP(k);$

EH35(k).. $B5(k) =L= FKin.LO(k)*YK(k) + FKin(k)*yk.UP(k) - FKin.LO(k)*yk.UP(k);$

EH36(k).. $B5(k) =L= FKin.UP(k)*YK(k) + FKin(k)*yk.lo(k) - FKin.UP(k)*yk.lo(k);$

EHA1(K).. $B15(K) =G= \text{sum}(N, FNK.LO(N, K)*YN(N)) + \text{sum}(N, FNK(N, K)*YN.lo(N)) - \text{sum}(N, FNK.LO(N, K)*yN.lo(N));$

EHA2(K).. B15(K) =G= $\sum(N, FNK.UP(N, K)*YN(N)) + \sum(N, FNK(N, K)*YN.UP(N)) - \sum(N, FNK.UP(N, K)*yN.UP(N));$
 EHA3(K).. B15(K) =L= $\sum(N, FNK.LO(N, K)*YN(N)) + \sum(N, FNK(N, K)*YN.UP(N)) - \sum(N, FNK.LO(N, K)*yN.UP(N));$
 EHA4(K).. B15(K) =L= $\sum(N, FNK.UP(N, K)*YN(N)) + \sum(N, FNK(N, K)*YN.lo(N)) - \sum(N, FNK.UP(N, K)*yN.lo(N));$
 EH37(k).. FKIn(k) =e= maxCP(k);
 EH38(k).. PWR(k) =E= a_com*[[PKO(k)/PKI(k)]**b_com - 1]*FKIn(k);
 EH39(n).. FNin(n) =E= $\sum(i, FIN(i, n)*h1(i, N)) + \sum(v, FVN(v, n)*e2(v, n)) + \sum(m, FMN(m, n));$
 EH40(n).. FNout(n) =E= $\sum(u, FNU(n, u)) + \sum(k, FNK(n, k));$
 EH41(n).. FNin(n) =E= FNout(n);
 EH42(n).. B6(N) =E= $\sum(i, FIN(i, n)*h1(i, N)*YHP(i)) + \sum(v, FVN(v, n)*e2(v, n)*YH2V(v)) + \sum(m, FMN(m, n)*YPR(m));$
 EH43(n).. B6(n) =G= $FNin.LO(n)*YN(n) + FNin(n)*yn.lo(n) - FNin.LO(n)*yn.lo(n);$
 EH44(n).. B6(n) =G= $FNin.UP(n)*YN(n) + FNin(n)*yn.UP(n) - FNin.UP(n)*yn.UP(n);$
 EH45(n).. B6(n) =L= $FNin.LO(n)*YN(n) + FNin(n)*yn.UP(n) - FNin.LO(n)*yn.UP(n);$
 EH46(n).. B6(n) =L= $FNin.UP(n)*YN(n) + FNin(n)*yn.lo(n) - FNin.UP(n)*yn.lo(n);$
 EH47(n).. FNin(n) =L= maxCP1(n);
 EH48(n).. $UP*(T1(n) - 1) + LNPC =L= (PNO(n) - PNI(N));$
 EH49(n).. $T1(n)*UP + LNPC - b =G= (PNO(n) - PNI(N));$
 EH50(n).. $FNin(n) - T1(n)*FNin.UP(n) =l= 0;$
 EH51(n).. $FNin(n) - T1(n)*FNin.LO(n) =g= 0;$
 EH52(N).. $PwrN(n) - (A8(N) + B8(N)*FNin(n)) - (1 - T1(n))*upp =l= 0;$
 EH53(N).. $PWRN(N) - (A8(N) + B8(N)*FNin(n)) - (T1(n) - 1)*upp =G= 0;$
 EH54(n).. $PwrN(n) - T1(n)*UPP =l= 0;$
 EH55.. $SUM(N, T1(N)) =e= 2;$
 EH56(m).. $FMin(m) =E= \sum(v, FVM(v, m)*r5(v, m));$
 EH57(m).. $B7(m) =E= \sum(v, FVM(v, m)*r5(v, m)*YH2V(v));$

EH58(m).. B7(m) =G= FMin.lo(m)*YMin(m) + FMin(m)*YMin.lo(m) -
 FMin.LO(m)*YMin.lo(m);
 EH59(m).. B7(m) =G= FMin.UP(m)*YMin(m) + FMin(m)*YMin.UP(m) -
 FMin.UP(m)*YMin.UP(m);
 EH60(m).. B7(m) =L= FMin.LO(m)*YMin(m) + FMin(m)*YMin.UP(m) -
 FMin.LO(m)*YMin.UP(m);
 EH61(m).. B7(m) =L= FMin.UP(m)*YMin(m) + FMin(m)*YMin.lo(m) -
 FMin.UP(m)*YMin.lo(m);
 EH62(m).. FPUR(m)*YPR(m) =E= B7(m)*0.9;
 EH63(m).. FMin(m) =E= FPUR(m) + FRSD(m);
 *EH64(m).. FRSD(m)*YRSD(m) =E= FMin(m)*YMin(m)*0.1;
 EH64(m).. B9(M) =E= B7(m)*0.1;
 EH65(m).. B9(M) =G= FRSD.lo(m)*YRSD(m) + FRSD(m)*YRSD.lo(m) -
 FRSD.LO(m)*YRSD.lo(m);
 EH66(m).. B9(M) =G= FRSD.UP(m)*YRSD(m) + FRSD(m)*YRSD.UP(m) -
 FRSD.UP(m)*YRSD.UP(m);
 EH67(m).. B9(M) =L= FRSD.lo(m)*YRSD(m) + FRSD(m)*YRSD.UP(m) -
 FRSD.LO(m)*YRSD.UP(m);
 EH68(m).. B9(M) =L= FRSD.UP(m)*YRSD(m) + FRSD(m)*YRSD.lo(m) -
 FRSD.UP(m)*YRSD.lo(m);
 EH69(m).. FPUR(m) =E= sum(k, FMK(m, k)*f3(m, k)) + sum(n, FMN(m, n));
 EH70(m).. FRSD(m) =e= sum(j, FMJ(m, j));
 EH71(m).. FMin(m) - T2(m)*FMin.UP(m) =l= 0;
 EH72(m).. FMin(m) - T2(m)*FMin.LO(m) =g= 0;
 EH73(i).. FI('HP') =E= FHP;
 EH74(i).. FI('CRF') =E= 0.417776*(H2_REF_WT + H2_REF_WTB);
 EH75(i).. FI('HP3') =L= FHP3;
 EH76(u).. PwrR(u) =e= a_com*[[PH2U(u)/PH2V(u)]**b_com - 1]*R(u);
 EH77(N).. CAP_nc(n) =e= (a_nc*T1(n) + b_nc*PwrN(n)) ;
 EH78(m).. CAP_m(m) =e= (a_m*T2(m) + b_m*FMin(m)) ;
 EH79.. elec =e= 0.72*[sum(k, Pwr(k)) + sum(n, PwrN(n)) + sum(u, PwrR(u))];

$$\text{EH80(j).. } F_fuel(j) =E= \text{sum(m, FMJ(m, j))} + \text{sum(i, FIJ(i, j)*l(i, j))} + \text{sum(v, FVJ(v, j)*q(v, j));}$$

$$\text{EH81(j).. } B11(j) =E= B12(j) + \text{sum(i, FIJ(i, j)*l(i, j)*YHP(i))} + \text{sum(v, FVJ(v, j)*q(v, j)*YH2V(v));}$$

$$\text{EH82(J).. } B11(j) =G= F_fuel.LO(j)*y_fu(j) + F_fuel(j)*y_fu.LO(j) - F_fuel.LO(j)*y_fu.LO(j);$$

$$\text{EH83(J).. } B11(j) =G= F_fuel.UP(j)*y_fu(j) + F_fuel(j)*y_fu.UP(j) - F_fuel.UP(j)*y_fu.UP(j);$$

$$\text{EH84(J).. } B11(j) =L= F_fuel.LO(j)*y_fu(j) + F_fuel(j)*y_fu.UP(j) - F_fuel.LO(j)*y_fu.UP(j);$$

$$\text{EH85(J).. } B11(j) =L= F_fuel.UP(j)*y_fu(j) + F_fuel(j)*y_fu.LO(j) - F_fuel.UP(j)*y_fu.LO(j);$$

$$\text{EH86(j).. } B12(j) =G= \text{sum(m, FMJ.LO(m, j)*YRSD(m))} + \text{sum(m, FMJ(m, j)*YRSD.lo(m))} - \text{sum(m, FMJ.LO(m, j)*YRSD.lo(m));}$$

$$\text{EH87(j).. } B12(j) =G= \text{sum(m, FMJ.UP(m, j)*YRSD(m))} + \text{sum(m, FMJ(m, j)*YRSD.UP(m))} - \text{sum(m, FMJ.UP(m, j)*YRSD.UP(m))};$$

$$\text{EH88(j).. } B12(j) =L= \text{sum(m, FMJ.LO(m, j)*YRSD(m))} + \text{sum(m, FMJ(m, j)*YRSD.UP(m))} - \text{sum(m, FMJ.LO(m, j)*YRSD.UP(m))};$$

$$\text{EH89(j).. } B12(j) =L= \text{sum(m, FMJ.UP(m, j)*YRSD(m))} + \text{sum(m, FMJ(m, j)*YRSD.lo(m))} - \text{sum(m, FMJ.UP(m, j)*YRSD.LO(m))};$$

$$\text{EH90(j).. } OC_fuel(j) =E= OCF*LHV_H2*B11(j) + OCF*LHV_C4*F_fuel(j) - OCF*LHV_C4*B11(j);$$

$$M_TPY.UP = 718.8;$$

$$M_TPYB.UP = 718.8;$$

$$FMin.LO(m)= 10;$$

$$FMin.up(m)= 150;$$

$$YN.LO(N)= 0.90;$$

$$YN.up(N)= 0.99;$$

$$YN.lo('n1') = 0.99;$$

YN.up('N1')= 0.99;
R.fx('BHDT') = 0;
PNO.up('n1') = 2515;
PNO.up('n2') = 2000;
PNO.up('n3') = 1315;
YK.LO(K)= 0.85;
YK.up(K)= 0.95;
YK.lo("K3")= 0.8;
YK.up("K3")= 0.95;
FNin.LO(n) = 0;
FNin.up(n) = 60;
YMin.lo(m) = 0.1;
YMin.up(m) = 0.8;
FRSD.LO(m) = 0;
FRSD.UP(m) = 120;
YRSD.lo(m) = 0;
YRSD.UP(m) = 0.8;
F_fuel.LO(j) = 0;
F_fuel.UP(j) = 120;
y_fu.LO(j) = 0.01;
y_fu.up(j) = 0.8;
FMJ.LO(m, j) = 0;
FMJ.up(m, j) = 120;
FKU.LO(K, U) = 0;
FKU.up(K, U) = 31.5;
FNU.LO(N, U) = 0;
FNU.up(N, U) = 60;
FNK.LO(N, K) = 0;
FNK.UP(N, K) = 60;
FKin.LO(k) = 0;
FKin.UP(k) = 31.5;
RATIO81.LO = 0;

RATIO81.UP = 0.4;
RATIO82.LO = 0.401;
RATIO82.UP = 1.1;
RATIO83.LO = 1.101;
RATIO83.UP = 4;
RATIO71.LO = 0;
RATIO71.UP = 0.4;
RATIO72.LO = 0.401;
RATIO72.UP = 1.1;
RATIO73.LO = 1.101;
RATIO73.UP = 4;
RATIO61.LO = 0;
RATIO61.UP = 0.4;
RATIO62.LO = 0.401;
RATIO62.UP = 1.1;
RATIO63.LO = 1.101;
RATIO63.UP = 4;
RATIO51.LO = 0.001;
RATIO51.UP = 0.4;
RATIO52.LO = 0.401;
RATIO52.UP = 1.1;
RATIO53.LO = 1.101;
RATIO53.UP = 4;
RATIO41.LO = 0;
RATIO41.UP = 0.4;
RATIO42.LO = 0.401;
RATIO42.UP = 1.1;
RATIO43.LO = 1.101;
RATIO43.UP = 4;
RATIO31.LO = 0;
RATIO31.UP = 0.4;
RATIO32.LO = 0.401;

RATIO32.UP = 1.1;
RATIO33.LO = 1.101;
RATIO33.UP = 4;
RATIO21.LO = 0;
RATIO21.UP = 0.4;
RATIO22.LO = 0.41;
RATIO22.UP = 1.1;
RATIO23.LO = 1.11;
RATIO23.UP = 4;
RATIO1.LO = 0;
RATIO1.UP = 0.4;
RATIO2.LO = 0.41;
RATIO2.UP = 1.1;
RATIO3.LO = 1.11;
RATIO3.UP = 4;
M_TGO3.UP = 3665 ;
M_TGO2.UP = 3665 ;
M_DS_FHCK2.UP = 95.9;
M_NS_NAPH1.UP = 210.8;
M_NS_NAPH2.UP = 210.8;
M_TPY.UP = 718.9;
M_TPYB.UP = 718.9;
F_TGO2.UP = 25000;
F_TGO3.up = 25000;
VPG.LO = 25000;
VP_KERO.LO = 25000;
VDSP.LO = 25000;
VFOP.lo = 18000;
F_REF.up =20000;
F_KERO.LO = 0;
F_KERO.UP = 29920;
SG_KERO.LO = 0.72;

SG_KERO.UP = 0.848;
F_SRLTN.LO = 0;
F_SRLTN.UP = 5750;
SG_SRLTN.LO = 0;
SG_SRLTN.UP = 0.749;
TGO_VGO_YIELD.LO = 0.96523;
TGO_VGO_YIELD.UP = 0.97618;
DIS_VGO_YIELD.LO = 0.02348;
DIS_VGO_YIELD.UP = 0.02348;
NAPH_VGO_YIELD.LO = 0.00034;
NAPH_VGO_YIELD.UP = 0.00034;
M_VGO.LO = 0;
M_VGO.UP = 7370;
KERO_YIELD_DISTL.LO = 0.01;
KERO_YIELD_DISTL.UP = 0.145;
DIS_YIELD_DISTL.LO = 0.8;
DIS_YIELD_DISTL.UP = 0.844;
F_DIES.LO = 0;
F_DIES.UP = 26400;
HN_YIELD_DISTL.LO = 0.001;
HN_YIELD_DISTL.UP = 0.001;
M_SRHN.LO = 0;
M_SRHN.UP = 2300;
HN_YIELD.LO = 99;
HN_YIELD.UP = 99.6;
F_SRHN.LO = 0;
F_SRHN.UP = 19360;
SG_SRHN.LO = 0.734781;
SG_SRHN.UP = 0.788 ;
MID_SRHN1.LO = 5.17;
MID_SRHN1.UP = 9.24;
MID_SRHN2.LO = 9.241;

```
MID_SRHN2.UP = 13.19;  
MID_SRHN3.LO = 13.191;  
MID_SRHN3.UP = 15.1064;  
TE_SRLTN.LO = 90;  
TE_SRLTN.UP = 220;  
TE_SRHN.LO = 180;  
TE_SRHN.UP = 380;  
TE_KERO.LO = 330;  
TE_KERO.UP = 520;  
TE_DIES.LO = 420;  
TE_DIES.UP = 630;  
TE_VGO.LO = 610;  
TE_VGO.up = 1050;
```

```
model oil_refinery /all/;  
oil_refinery.nodlim = 5000;  
OPTION ITERLIM = 50000;  
solve oil_refinery using MIP maximize profit;
```

